UNIVERSITY OF Southampton

The synthesis of birefringent chromophores for optoelectronic applications

School of Chemistry and Chemical Engineering/Zepler Institute

Faculty of Engineering and Physical Sciences

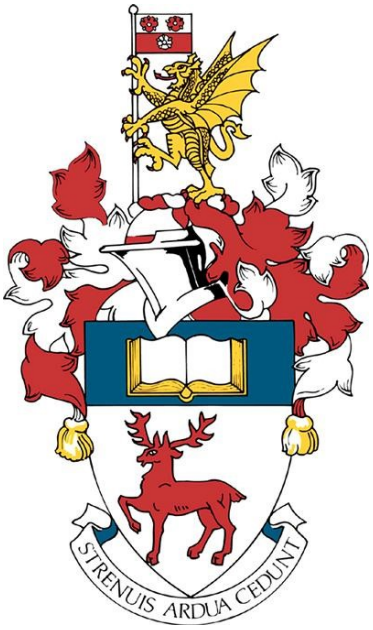

Jodie Violet Henningway (https://orcid.org/0000-0001-6688-1726)

Supervised by Assoc. Prof. Ramon Rios and Assoc. Prof. Frederic Gardes

Thesis for the award of Doctor of Philosiphy – 08/11/2024

Abstract

Birefringence is a property of a material, whereby the change in refractive index is linearly proportional to the applied electric field. Birefringent materials can therefore be used to modulate light, both in a singular Pockels cell or a more complex system such as a Mach-Zehnder interferometer (MZI). Organic birefringent chromophores can be polymerised and poled in order to maintain their dipole. Such polymers have been reported to have electro-optic coefficients (r_{33}) of over 10 times that of the industry standard for an MZI. This thesis reports synthetic routes to a previously reported chromophore bearing a substituted furan ring as the electron-withdrawing group, and three novel chromophores with BODIPY-based withdrawing groups, ready for polymerisation and subsequent optoelectronic testing. Syntheses towards additional novel BODIPY-based chromophores and side-chain modified chromophores bearing a triazole and amine side chain are also attempted.

Table of contents

Declaration of authorship

I, JODIE VIOLET HENNINGWAY

declare that this thesis and the work presented in it are my own and has been generated by me as the result of my own original research.

The synthesis of birefringent chromophores for optoelectronic applications

I confirm that:

1. This work was done wholly or mainly while in candidature for a research degree at this University;

2. Where any part of this thesis has previously been submitted for a degree or any other qualification at this University or any other institution, this has been clearly stated;

3. Where I have consulted the published work of others, this is always clearly attributed;

4. Where I have quoted from the work of others, the source is always given. With the exception of such quotations, this thesis is entirely my own work;

5. I have acknowledged all main sources of help;

6. Where the thesis is based on work done by myself jointly with others, I have made clear exactly what was done by others and what I have contributed myself;

7. None of this work has been published before submission.

Signed: ……

Date: ……

Acknowledgements

I would first like to thank, my primary supervisor, Prof. Ramon Rios, for his invaluable support and guidance throughout my project. I am also immensely grateful that he has been so very understanding when it has come to my, at best, appalling health. I would like to thank my secondary supervisor, Prof. Frederic Gardes, for his help with the physical applications of my research, as I have never claimed to be a physicist. I would also like to thank Prof. David Harrowven for taking me into his group upon Ramon's departure. Being adopted into the 'Harroven home for unwanted chemists' was the first time at Southampton that I truly felt like I was part of a research group, or a community if you will. Thanks also go to Neil and Julie for their NMR and MS guidance respectively.

I would like to thank Marta, who helped me settle into the lab when I first arrived at the University of Southampton. Although she moved on to bigger and better things soon after my arrival, she taught me so much in such a short time. I would like to thank all the members of the groups whom I have shared a lab, office space and group meetings with over the years for their company and fun: Baker, Baud, Goldup, Harroven, Linclau, Stulz and Thompson. Special shout-outs go to: Jo, for being an unstoppable force of positivity; Tina, for putting up with my unbearable screeching that I call singing; and David, for all the morning coffees and gossip.

I would like to thank my close friends; Bestie Millie, Mark and Charlotte for being my support system over what has been a difficult 4 years, and James and Meg for making me feel welcome in Southampton. Finally, I would like to thank my brother Carl for his unconditional love and support.

When the wind's against you, remember this insight: that's the optimal condition for birds to take flight. Now the wind's against you, don't give up the fight. – Enter Shikari

List of abbreviations

Ac	Acetate
AIBN	Azobisisobutyronitrile
APC	Amorphopus polycarbonate
aq.	Aqueous solution
atm	Atmosphere (unit of pressure)
BINOL	1,1'-Bi-2-naphthol
Boc	*tertiary*-butyloxycarbonyl
BODIPY	Boron-dipyrromethene
Bu	Butyl
DANS	*N*,*N*-dimethyl-4,4-aminonitrostilbene
CD	Circular dichroism
COSY	Correlated spectroscopy
CPL	Circularly polarised luminescence
dba	Dibenzylideneacetone
DCE	1,2-Dichloroethane
DDQ	2,3-Dichloro-5,6-dicyano-1,4-benzoquinone
DIBAL	Diisobutylaluminium hydride
DMAP	4-Dimethylaminopyridine
DMF	Dimethylformahyde
DMSO	Dimethyl sulfoxide
DPPA	Diphenylphosphoryl azide
e.e.	Enantiomeric excess
eq.	Equivalents

ESI	Electrospray ionisation
Et	Ethyl
h	Hour(s)
HPLC	High-performance liquid chromatography
IC	Integrated circuit
IPA	*iso*-propyl alcohol
^{i}Pr	*iso*-propyl
IR	Infrared
LDA	Lithium diisopropylamine
LCMS	Liquid chromatography-mass spectrometry
MBH	Morita–Baylis–Hillman
Me	Methyl
min	Minute(s)
MS	Mass spectrometry
MZI	Mach-Zehnder inferometer
n-Bu	Normal-butyl (straight chain)
NLO	Nonlinear optical
NMR	Nuclear magnetic resonance
NOESY	Nuclear overhauser effect spectroscopy
PC	Polycarbonate
PET	Photoinduced electron transfer
Ph	Phenyl
pK_a	Acid dissociation constant
PMMA	Poly(methyl methacrylate)chromophore

RCA	Radio Corporation of America
R_f	Retention factor
ROS	Reactive oxygen species
RT	Room temperature
r_{33}	Electro-optic coefficient
Sp. gr.	Specific gravity
TBAF	Tetra-n-butylammonium fluoride
TBDMS	*tertiary*-butyldimethylsilyl
t-Bu	*tertiary*-butyl
TFA	Trifluoro acetic acid
T_g	Glass transition temperature
THF	Tetrahydrofuran
TIC	Total ion chromatogram
TLC	Thin layer chromatography
T_m	Melting temperature
t_r	Retention time
uHPLC	Ultra high-performance liquid chromatography
λ_{abs}	Wavelength of the absorbtion maxima
λ_{em}	Wavelength of the emission (fluorescence) maxima
Φ_f	Quantum yield

Chapter 1: Introduction

1.1 Photonics

1.1.1 The electro-optic effect

The electro-optic effect is the change in the properties of a molecule or material in response to a change in the electric field. The refractive index of a material is defined in Equation 1. As n → 1, the speed of light across the material approaches that of the speed of light through a vacuum.

$$n = \frac{c}{v}$$

Equation 1: The definition of the refractive index of a material where n is the refractive index, c is the speed of light in a vacuum and v is the phase velocity of the material.

The Kerr effect can be derived to describe that the change in the refractive index is proportional to the square of the electric field.[1]

$$P_{NL}(\omega) = \frac{3}{4}\varepsilon_0\chi^{(3)}(\omega_l)|E(\omega_l)|^2E(\omega_l)$$

Equation 2: Kerr's effect describes the intensity dependence of the refractive index. Polarisation (P_{NL}) is proportional to the cube of the electric field $E(\omega_l)$ where ε is the permittivity and χ is the susceptibility.[2]

Pockels' effect describes the change in the refractive index that is linearly proportional to the electric field.[3] All materials display the Kerr effect, whereas only a small number of crystalline solids display Pockels' effect. Materials that show Pockel's effect are known as birefringent or birefractive.[4] The change in the refractive index of a birefringent material can be approximated using Equation 3. The larger the electro-optic coefficient (r_{33}), the larger the change in the refractive index (Δn) will be upon the application of an electric field.[5]

$$\Delta n = \frac{1}{2}n^3 r_{33}E_{\hat{z}}(\omega_l)$$

Equation 3: Approximation for the change in refractive index (n) upon the application of an electric field $E(\omega_l)$ along the z-axis where r_{33} is the electro-optic coefficient that is constant for materials and has a unit of pm V^{-1}.

1.1.2 Optical modulation

Optical modulation is the variation of a property of visible light. This is most often achieved using the intensity of the light or the phase through which the light travels (waveguide).[6] The most common waveguides consist of silicon and are insulated by either silicon nitride (Si_3N_4) or silicon dioxide (SiO_2). The simplest phase modulator consists of a singular Pockels cell (a

single birefringent crystal that is sandwiched between electrodes); when a current is passed through the crystal, the phase delay will be modulated, creating a signal.[7] A more sophisticated example is a Mach-Zehnder interferometer (MZI) modulator (Figure 1). Here, the light source is split into two paths, on one of the paths the phase of light is modulated by a Pockels' cell, when the two beams recombine at the output there will be a series of constructive and destructive interference, thus enabling the transmission of data.[8] For a material to be suitable as a device's Pockel's cell, a large Δn is desirable, so that good interference can be obtained. A prerequisite to this is a large electro-optic coefficient.

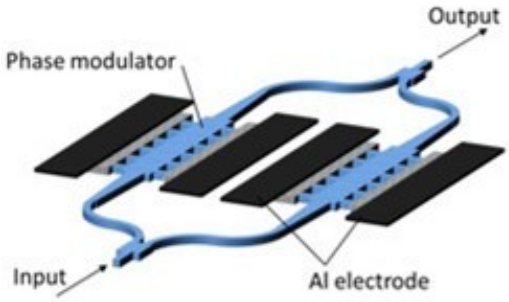

Figure 1: Diagram of a Mach-Zehnder interferometer (MZI) modulator taken from the paper reported by Inoue et al..[8]

The current standard of material for Pockels cells in modulators is Lithium Niobate ($LiNbO_3$), which has an electro-optic coefficient of 30.8 pm V^{-1}.[9] The concept of an electro-optic polymer was first reported by Jen *et al.* who reported electro-optic coefficients of over 10 times that of Lithium Niobate's.[10,11]

1.1.3 Electro-optic polymers

An electro-optic monomer is designed with a donor and acceptor electron moiety that connect over a π-conjugated bridge.[12] If monomers were to be deposited onto a device, the monomers would orient themselves isotropically (randomly), thus cancelling the overall dipole (Figure 2A). Since an overall dipole is desired, monomers are designed with a rigid structure, polymerised and then poled (Figure 2B).

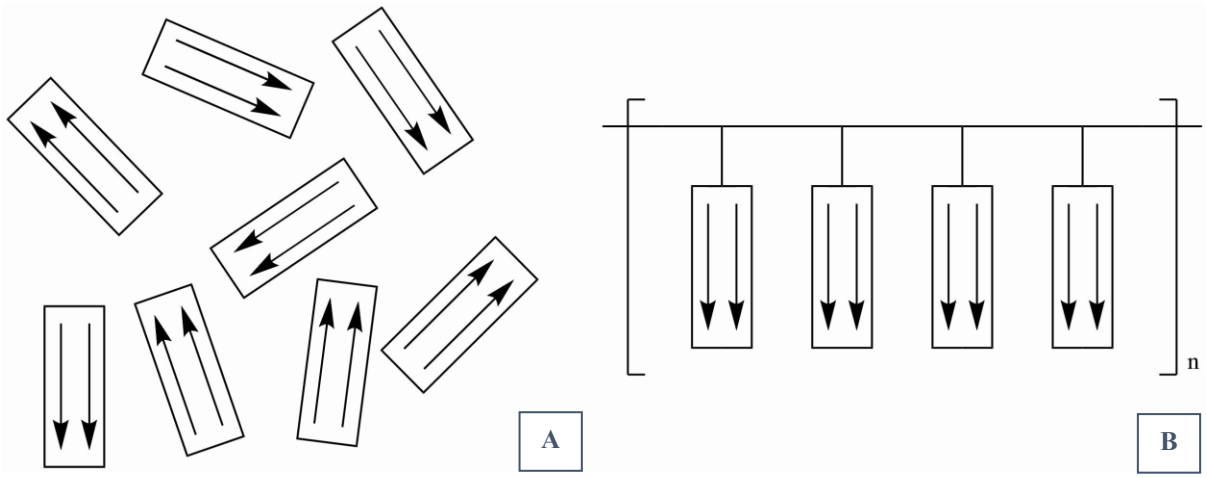

*Figure 2: A schematic diagram of: **A** Monomer molecules orientated randomly after deposition onto a device; **B** Monomers on a side-chain electro-optic polymer molecule with perfectly aligned dipoles.*

Poling (forced dipole orientation) can be achieved through a variety of different techniques. Electrode poling was the first method of achieving a forced dipole;[12,13] but the method is still used for the fabrication of modern electronic devices.[14,15] Electrode poling uses an applied electric field stronger than that of the coercive field, to achieve the desired orientation of dipoles. Instead of forcing dipole orientation, it is possible to synthesise intramolecular bonding moieties into the monomer, thus encouraging the spontaneous alignment of dipoles within the polymer.[16]

Monomers can be integrated into a polymer chain in several ways, which is illustrated in Figure 3.[7,17] In a main-chain polymer (Figure 3A), monomers are tightly packed providing much rigidity to the structure of the polymer. In a guest-host polymer (Figure 3B), the chromophore molecules are only mixed in with the polymer as opposed to being incorporated into the chain, this will give a more malleable structure that becomes more difficult to pole. In a crosslinked polymer (Figure 3C), monomers are polymerised from both ends, further increasing the rigidity. In a side-chain polymer (Figure 3D), monomers are polymerised from one end, this type of structure has some rigidity, depending on the structure of the chromophore, but is the most stable. In a dendrimer (Figure 3E), the polymer can display rigidity, but it is very difficult to pole because, within the molecule, the chromophore dipoles can be oriented in any direction.

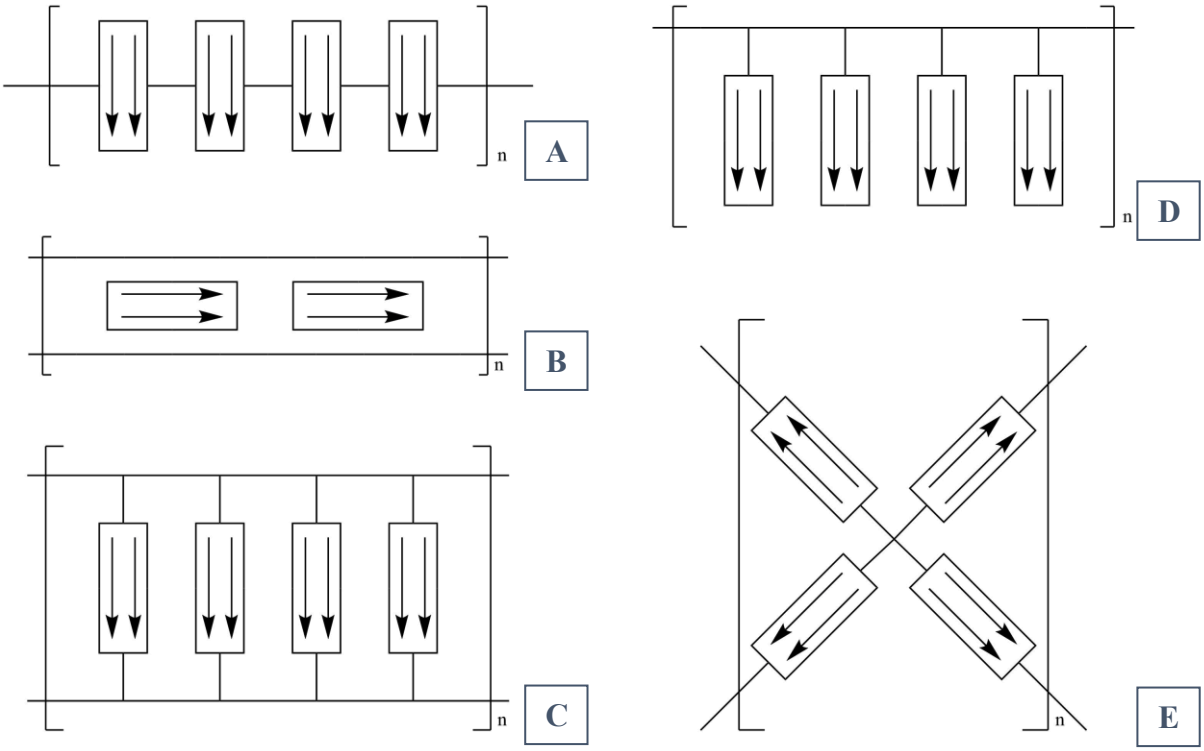

*Figure 3: A Schematic diagram of: **A** A main-chain electro-optic polymer; **B** A Guest-Host electro-optic polymer; **C** A crosslinked electro-optic polymer; **D** A side-chain electro-optic polymer; **E** A dendrimer electro-optic polymer.*[7,17]

1.1.4 Desired properties of electro-optic polymers

Along with the rigidity of the polymer and the electro-optic coefficient (r_{33}), there are a few other important characteristics that are desired for an electro-optic polymer. The first of which is its glass transition temperature (T_g). The glass transition temperature is defined as the temperature at which a polymer goes from a glass-like state to a rubber-like state.[18] This is different to the melting temperature (T_m) where the polymer becomes a liquid.[18] These transition temperatures represent the temperature at which these transitions begin to occur, however, the full transition occurs over a temperature range. When integrated into a device, the polymer will be subject to very high temperatures. If the temperature were to exceed the glass transition temperature, and the polymer was to transition to its rubber-like state, the optical activity of the material would be affected.

The optical loss of a material essentially describes its efficiency as a waveguide. When passing through a medium, light is both absorbed and scattered which weakens the optical signal.[19] There are ways to minimise optical losses over a device, such as ensuring connections are secure and operating at cryogenic temperatures.[20,21] These measures, however, do not directly combat the problem but rather reduce any further loss. Instead, it is more efficient to design a material with low optical loss in the first place.

In a device fabrication process, material compatibility must be taken into consideration. For example: a silicon-based integrated circuit (IC) production line does not mix well with III-V material systems (such as GaAs), owing to cross-contamination;[22] or the H_2O_2 component in the RCA (Radio Corporation of America) cleaning solutions, that are widely used in silicon wafer cleaning, can attack reactive moieties in organic compounds doped throughout the semiconductor.[23,24] If a birefringent polymer is going to be integrated into a device then it must be compatible with the fabrication processes.

1.2 Monomer designs of birefringent chromophores

1.2.1 π-bridges

In theory, any π-conjugated bridge will allow for a fully conjugated molecule, and bridges as simple as a double bond or an aromatic ring are seen as the bridge within birefringent molecules.[12,25] *N*,*N*-Dimethyl-4,4-aminonitrostilbene (DANS) **1** is one such chromophore with an *E* double bond connecting an *N*,*N*-dimethylaniline donating group to a nitrobenzene withdrawing group.[12] When dispersed (30% by weight) in PMMA, DANS **1** has an electro-optic coefficient of 13 pm V^{-1}.[26]

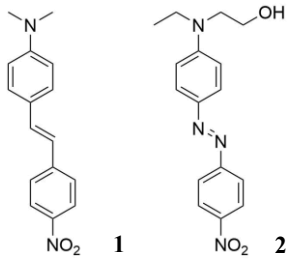

*Figure 4: Structures of: N,N-dimethyl-4,4-aminonitrostilbene (DANS) **1**, N-Ethyl-N-(2-hydroxyethyl)-4-(4-nitrophenylazo)aniline (Disperse Red) **2**.*

N-Ethyl-*N*-(2-hydroxyethyl)-4-(4-nitrophenylazo)aniline (Disperse Red) **2** has a very similar structure to that of DANS, the difference being the ethyl(2-hydroxyethyl)amino moiety in the place of the dimethylamine and the azo-bridge. This 2-(ethylamino)ethanol moiety is seen regularly throughout synthetic birefringent polymers as a method of attachment to a polymerisable monomer such as methyl methacrylate by an esterification reaction with methacryloyl chloride. When dispersed (10% by weight) in PMMA, Disperse Red **2** has an electro-optic coefficient of 0.8 pm V^{-1}.[27] The change to the azo-bridge moiety is seen to decrease the electro-optic coefficient, indicating that the *E* carbon-carbon bond gives better electron transfer between the donating and withdrawing groups.

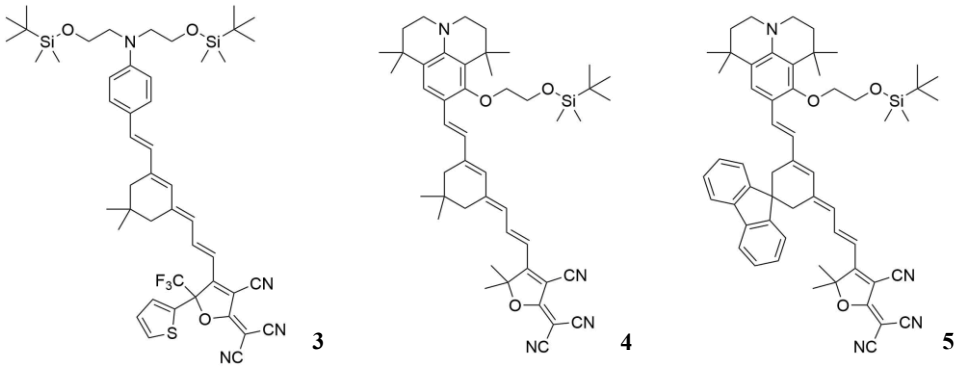

*Figure 5: Structures of chromophores **3**, **4** and **5** that contain an isophorone-based π-bridge.*[10,28]

Seen regularly throughout more recently devised birefringent polymers are 5,5-dimethylcyclohex-2-ene bridges because of the increased rigidity compared to a conjugated chain. When dispersed (~25% by weight) in APC, **3** showed an electro-optic coefficient of 107 pm V^{-1}.[10] When dispersed (30% by weight) in PMMA, **4** has an electro-optic coefficient of 130 pm V^{-1}.[28] When the dimethyl group on the isophorone-based bridge was substituted for a fluorene moiety **5**, the electro-optic coefficient increased to 240 pm V^{-1} (30% weight in PMMA) and the thermal decomposition temperature also increased.[28] These are >10× increases compared to DANS, which is owing to the extensively conjugated π-systems in these molecules. Between **3**, **4** and **5** it has been theorised that the ring-fused amine within the julolidinyl group allows for better π-overlap between the nitrogen lone-pair/p-orbital with the phenyl ring.[29]

As well as dimethyl cyclohexene, dimethyl bicyclohexene and dimethyl cyclopentene have been studied as bridges, however, they have been seen to show reduced electro-optic coefficients in comparison to the isophorone-based bridge.[30]

1.2.2 Withdrawing groups

In the withdrawing region of the chromophore, lots of variation in structure can be observed. The nitrophenyl ring in **1** and **2** (Figure 4) would be a simpler example, but more complex withdrawing moieties are seen much more frequently.[27,31] Chromophore **6** features a substituted isoxazole ring as its withdrawing group. When dispersed (10% by weight) in PMMA, **6** has an electro-optic coefficient of 5.0 pm V^{-1}.[27] Chromophore **7** contains a diethylthiobarbituric acid withdrawing group. When dispersed (10% by weight) in PMMA, **7** has an electro-optic coefficient of 6.0 pm V^{-1}.[27] Chromophore **8** features a substituted benzothiophene withdrawing group. When dispersed (20% by weight) in PC, **8** has an electro-optic coefficient of 55 pm V^{-1}.[9] Finally, chromophore **9** contains a substituted indane withdrawing group. When dispersed (20% by weight) in PMMA, **9** displayed an electro-optic coefficient of 17.3 pm V^{-1}.[32]

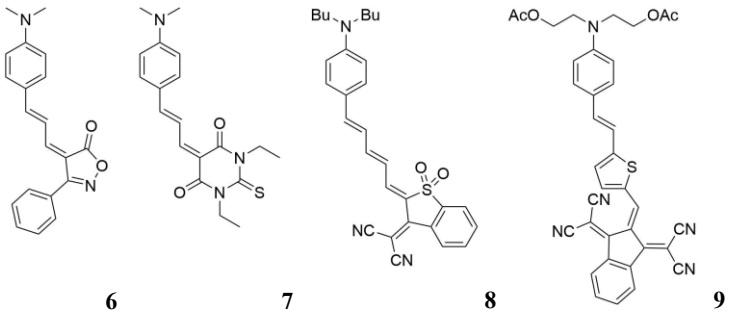

*Figure 6: Structures of chromophores **6**, **7**, **8** and **9** that display a variety of electron-withdrawing groups.*[9,27,32]

Although lots of variety is reported in this region, the one withdrawing group that does appear regularly is a malononitrile-substituted furan ring (Figure 7). Here, He *et al.* have synthesised R_1 and R_2 to be: phenyl rings (substituted and non-substituted); thiophene rings; trifluoromethyl groups; and spirocyclic attachments of a fluorene moiety and cyclohexane derivatives.[31]

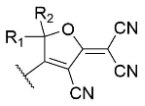

Figure 7: Structure of the furan-based withdrawing group, with two 'R-groups' that have been seen to incorporate, but are not limited to: phenyl-rings (with and without substitutions), thiophene rings, trifluoromethyl groups, and spirocyclic fluorene moieties.[10,31]

1.2.3 Donating groups

As previously mentioned, ethyl(2-hydroxyethyl)amino moieties are seen frequently throughout electro-optic polymers, both because it facilitates easy attachment to a polymerisable monomer and also because of its donatable lone pair. Beyond that specific amine, of the chromophores that have been covered so far (**1** to **9**), all have amine-based donating groups. There are very few examples of non-amine-based donating groups in NLO chromophores, but a few (**10** to **12**) are shown in Figure 8.[33–35] Of which, only **11** has a reported electro-optic coefficient of 25 pm V^{-1} (20% by weight in APC).[34]

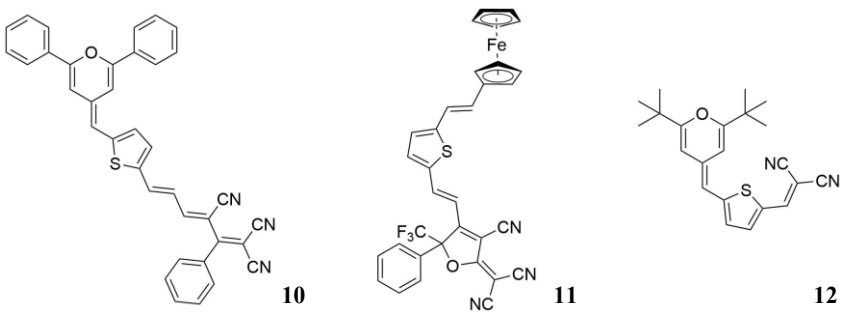

*Figure 8: Structures of chromophores **10**, **11** and **12** that contain donating groups not based upon amines.*[33–35]

1.3 An introduction to BODIPY chemistry

1.3.1 Structure of BODIPY and its derivatives

Boron-dipyrromethene (BODIPY) **13** is a highly fluorescent dye. The syntheses of BODIPY derivatives have been reported since 1968.[36] The core structure of BODIPY is based on that of *s*-indacene. Boron has 3 valence electrons; its 4 bonds within the BODIPY structure give it a full valence shell and thus a formal negative charge. BODIPY is, however, an overall neutral molecule, with the positive charge being delocalised around the rings, between the two nitrogen atoms.

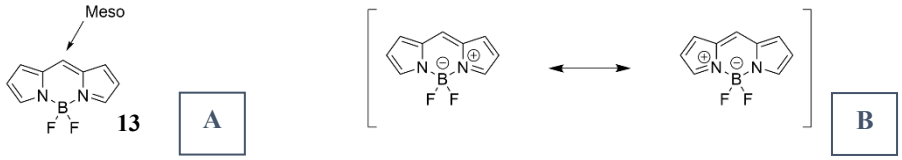

*Figure 9: **A** Structure of BODIPY **13**, with the meso-position identified. **B** Resonance structures of BODIPY **13**.*[37]

The BODIPY core is more often seen with substitutions. Owing to the electron-withdrawing effects of the BF_2 moiety, a double bond α to the *meso*-position is activated similarly to that of an α,β-unsaturated carbonyl compound and therefore prone to nucleophilic attack. This activity has been explored by Arroyo *et al.*.[38] Michael additions and several palladium-catalysed hydrogenations were tested, examples of which are shown in Figure 10.

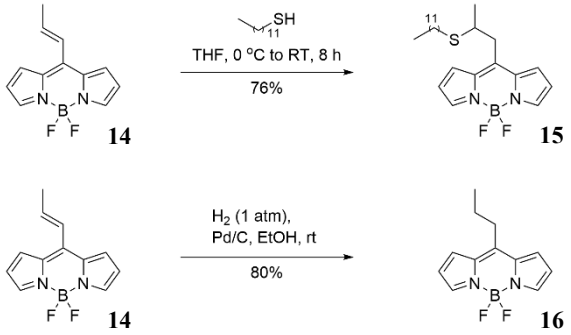

Figure 10: Reactions exploring the reactivity of a double bond at the meso-position of a BODIPY reported by Arroyo et al.. The Michael addition gave a 76% yield and the Palladium catalysed hydrogenation gave an 80% yield.[38]

The activation of this double bond, along with the high fluorescence of the BODIPY core, can be used to detect hydrogen peroxide levels in cells.[39] Hydrogen peroxide reacts with the double bond α to the *meso*-position in **17** by nucleophilic addition and oxidation, which stops the photoinduced electron transfer (PET) between the malononitrile and the BODIPY core, thus increasing the fluorescent emissions.

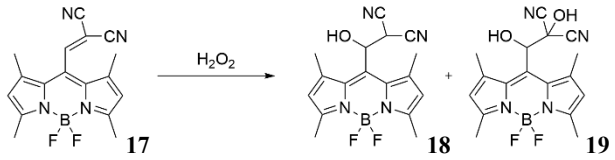

*Figure 11: Reaction of a meso-substituted BODIPY with hydrogen peroxide. **17** can be used to detect hydrogen peroxide levels in cells.*[39]

Chrial BODIPYs are of particular interest owing to their circularly polarised luminescence (CPL).[40–43] Chirality can be introduced by using the activated *meso*-double bond. Guerrero-Corella *et al.* have demonstrated this with a [4+2] cycloaddition using a range of dieneyls, one such reaction is shown in Figure 12A, this example gave a 92% yield with 98% e.e..[44] Meazza *et al.* on the other hand, used Lewis bases to deprotonate an αH to the *meso*-position allowing it to react with electrophilic Morita–Baylis–Hillman (MBH) carbonates, an example of which is shown in Figure 12B.[45] BODIPY **27** has an λ_{abs} of 504 nm, an λ_{em} of 515 nm and a Φ_f of 0.99 in $CHCl_3$.[45]

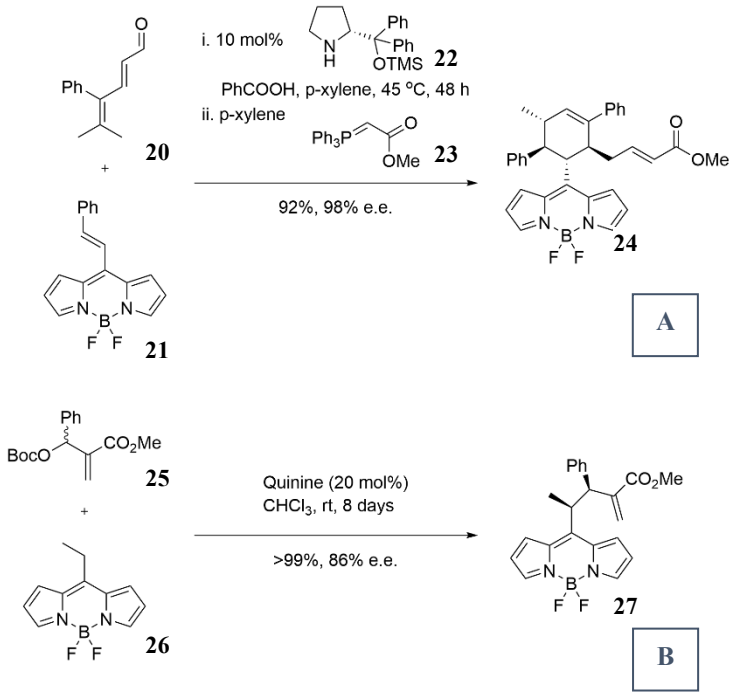

*Figure 12: **A** An enantioselective cycloaddition reaction between BODIPY **21** and dieneyl **20**, utilising the activation of a double bond at the meso-position of a BODIPY.*[44] ***B** An enantioselective addition of an MBH carbonate **25** to BODIPY **26** utilising the acidic proton α to the meso-position.*[45]

BODIPYs with substitutions around the pyrrole rings have been widely studied. Adding alkyl groups here can be used to fine-tune the fluorescence properties of the molecule. BODIPY derivatives **28** to **33**, shown in Figure 13 with varying numbers of alkyl group substitutions have their UV-absorption and emission maxima, and quantum yields shown in Table 1.[46–49] The trends seen are that the higher the number of substitutions, the more red-shifted the

maxima will be, and that substitutions in the *meso*-position do not produce effects so prominent.

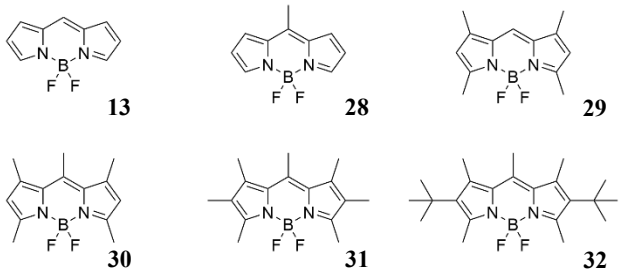

*Figure 13: Structures of BODIPY derivatives **13** and **28** to **32** whose UV-absorption and emission maxima, and quantum yields are shown in Table 1.*

*Table 1: UV-absorption and emission maxima, and quantum yields for BODIPY derivatives **13** and **28** to **32**.*[46–49]

	Solvent	λ_{abs}	λ_{em}	Φ_f
13	MeOH	497 nm	505 nm	0.96
28	MeOH	494 nm	503 nm	1.00
29	EtOH	503 nm	510 nm	0.99
30	MeOH	493 nm	503 nm	0.99
31	EtOH	517 nm	534 nm	0.70
32	EtOH	525 nm	557 nm	0.77

Many of the reported BODIPY derivates have the BF_2 moiety in the 5-position, however, there are some with substitutions on the boron, BODIPY derivatives **33** to **38** are shown in Figure 14 and those with reported UV-absorption data are shown in Table 2.[50–54] Absorption data has not been reported for **36** (probably owing to its stability) nor for **37**. **33** and **34** have symmetrical aryl groups on the boron centre.[53] Wang *et al.* reported a synthesis of BODIPY derivates with only one substitution at the boron centre, including **35** with one phenyl substitution.[52] Chloro substitutions can be made on the boron centre such as in **36** which although less stable than the fluoro-BODIPY derivates, can be synthesised and then used *in situ* to increase the reactivity of the boron, allowing for further substitutions.[43,50,51] **37** is one such derivative that can be synthesised using a chloro-substituted BODIPY as an intermediate that can be reacted with a Grignard reagent in CH_2Cl_2.[51] Although **38** also possesses alkyl chains on the boron centre, it can be synthesised with butyl lithium in THF.[54]

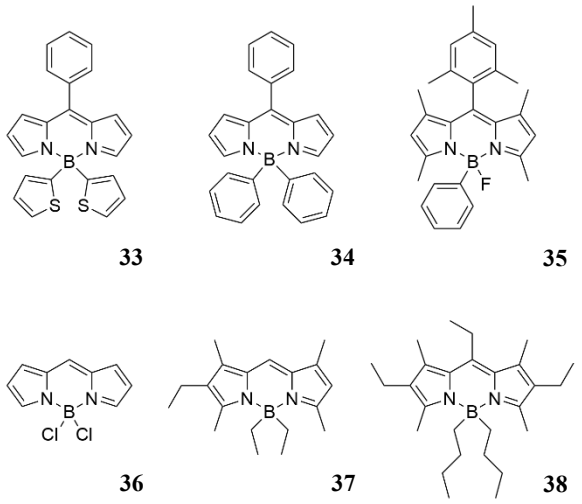

*Figure 14: Structures of BODIPY derivatives **33** to **38**, all with substitutions at the 5-position, on the boron.*[50–54]

*Table 2: UV-absorption and emission maxima, and quantum yields for BODIPY derivatives **33**, **34**, **35**, and **36**.*[52–54]

	Solvent	λ_{abs}	λ_{em}	Φ_f
33	Toluene	503 nm	523 nm	0.22
34	Toluene	501 nm	520 nm	0.19
35	CH_2Cl_2	501 nm	512 nm	0.94
36	CH_2Cl_2	527 nm	538 nm	0.95

Chirality can be introduced at the boron centre with axial and helical chirality, once again presenting CPL. Zhang *et al.* synthesised enantiopure axial chiral BODIPYs **39R** and **39S** by activating a fluoro-BODIPY with aluminium chloride *in situ* allowing for the addition of *R*/*S*-BINOL.[43] **39R** has an λ_{abs} of 580 nm, an λ_{em} of 618 nm and a Φ_f of 0.58 in a 10% CH_2Cl_2 in hexane mixture.[43] **39R** and **39S** showed mirror images in the CD and CPL spectra.[43] Clarke *et al*. synthesised racemates of helically chiral BODIPYs which were separable by chiral HPLC including **40P** and **40M**.[42] The racemate has an λ_{abs} of 637 nm and a Φ_f of 0.25 in CH_2Cl_2.[42] **40P** and **40M** showed mirror images in the CD and CPL spectra.[42]

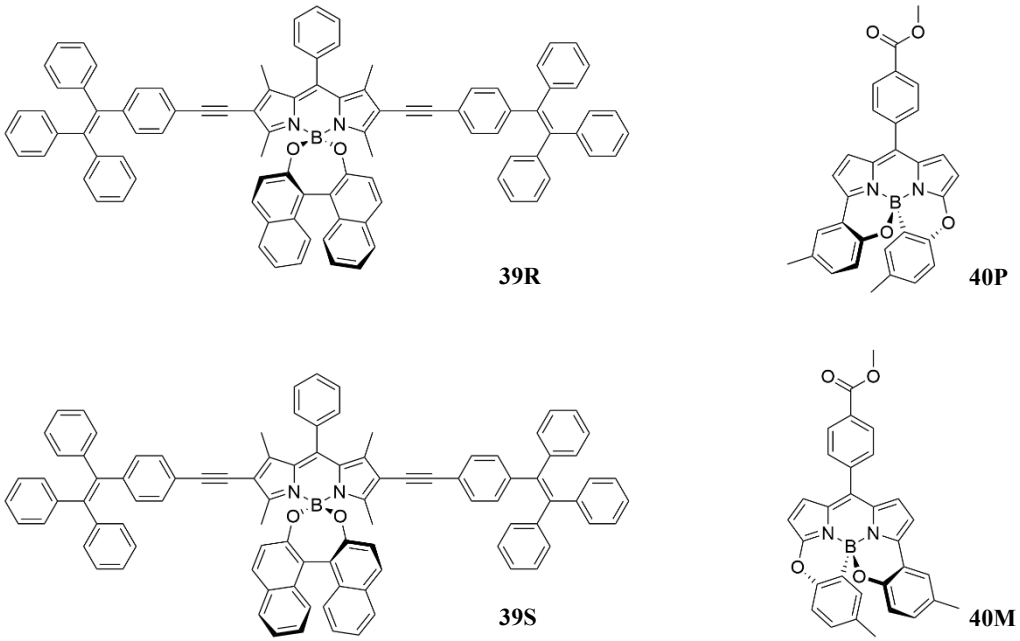

*Figure 15: Structures of **39R** and **39S** which show axial chirality, and **40P** and **40M** which show helical chirality.*[42,43]

1.3.2 Applications of BODIPY derivatives

The fluorescent properties of BODIPYs make them useful tools within cell imaging.[40,55–59] Patalag *et al.* synthesised a library of GlycoBODIPYs, with a range of monosaccharides, disaccharides and trisaccharides at the *meso*-position.[56] One such example of a disaccharide is **41** which has an λ_{abs} of 508 nm, an λ_{em} of 520 nm and a Φ_f of 0.89 in MeOH.[56] The addition of the glycan moieties increased the solubility in water, thus decreasing aggregation in the cellular studies while the fluorescence capabilities were preserved.[56]

Ray *et al.* synthesised BODIPY derivates with substituted ethane-1,2-diamine moieties at the boron centre.[60] Upon further functionalisation, with a click-chemistry cycloaddition to a lysosomal probe, **42** strongly co-localised with Lysotracker™ Red after short incubation times.[40] **42** has an λ_{abs} of 525 nm, an λ_{em} of 544 nm and a Φ_f of 0.88 in MeOH.[40]

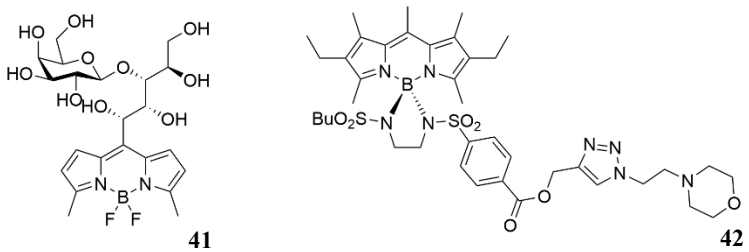

*Figure 16: Structures of **41** and **42** which have uses within cell imaging.*[40,56]

Owing to their fluorescent ability to emit light, BODIPYs have also found uses within photocatalysis.[61–66] Pantaine *et al.* used **43** to catalyse the synthesis of 1,4-naphthoquinone-derived polycycles.[66] Fischer *et al.* also used **43** as a catalyst but instead for asymmetric

hydroxylations of indane derivatives.[64] **43** has an λ_{abs} of 532 nm and a Φ_f of 0.72 in MeOH.[61] Furthering BODIPY derivatives' ability to act as a photocatalyst, research is emerging into their prospective use as a photosensitizer.[62,63,67,68] Upon excitation, a photosensitizer can generate a reactive oxygen species (ROS) which can induce apoptosis or necrosis in cells.[69] Zhang *et al.* observed cell uptake then ROS generation and subsequently cell death from aggregates of **44** when exposed to light irradiation.[67] **44** has an λ_{abs} of 592 nm and an λ_{em} of 667 nm in H_2O.[67]

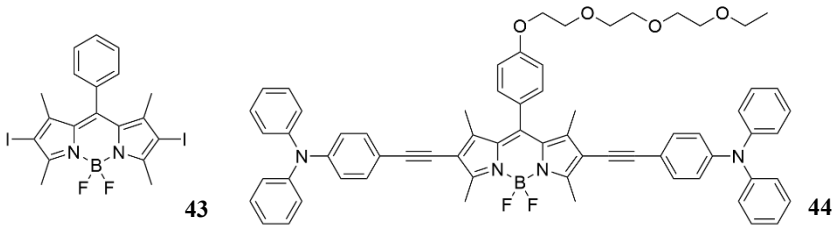

*Figure 17: Structures of **43** and **44**. **43** has been used in photocatalysis and **44** can act as a photosensitizer in cells.*[61,64,66,67]

1.4 Project aims

At the beginning of this project, it was set out to attempt to synthesise a variety of electro-optic polymers. Owing to the time lost as a result of COVID-19 and my poor health, the effects were mitigated by aiming to synthesise a variety of electro-optic chromophores instead. The chromophores could be polymerised and then have their electro-optic coefficients tested as a part of a future project.

To begin with, a previously known chromophore would be synthesised, to act as a control in optoelectronic testing. Chromophore **49** was chosen as the first target molecule because of its incorporation of common groups, high polarizability and stable glass-like structure.[30] Polymer **45** has an electro-optic coefficient of 78 pm V^{-1}.[30]

After this, novel structures could be devised and synthesised with the goal being to improve the physical properties, such as: increasing the glass transition temperature; increasing the electro-optic coefficient; increasing the rigidity; increasing the polarisability; decreasing the optical loss; and increasing the compatibility of the polymer with common waveguides, allowing better integration into optoelectronic devices.

Possible changes could be made in: the π-bridge region of the monomer, by elongating the π-bridge or making modifications to the isophorone-based bridge by adding side chains (Figure 18); electron-withdrawing region of the monomer, such as changing the two 'R-groups' shown in Figure 7, or replacing the region entirely with another electron-withdrawing moiety such as a BODIPY;[45] the electron-donating region of the monomer, such as using a pyrrole or ether in the place of the secondary amine; and also the integration of the monomer into the polymer (Figure 3).

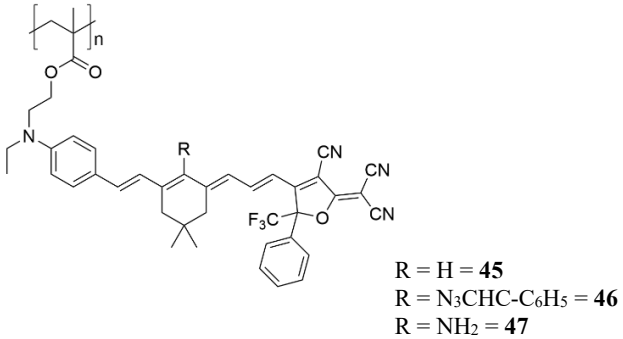

R = H = **45**
R = $N_3CHC\text{-}C_6H_5$ = **46**
R = NH_2 = **47**

*Figure 18: Generic structure of a modified electro-optic polymer, based on polymer **45**, with an R-group modification on the isophorone-based π-bridge.*

Chapter 2: Results and Discussion

2.1 The synthesis of chromophore **49**

Since chromophore **49** is a reported compound, the synthetic route reported by Espinar-Barranco et al. would be followed, proceeded by the deprotection of the alcohol, addition of methacryloyl chloride then a polymerisation step (Scheme 1, Scheme 2 and Scheme 3).[70] The synthesis includes 12 steps total with a longest-linear sequence of 9 steps.

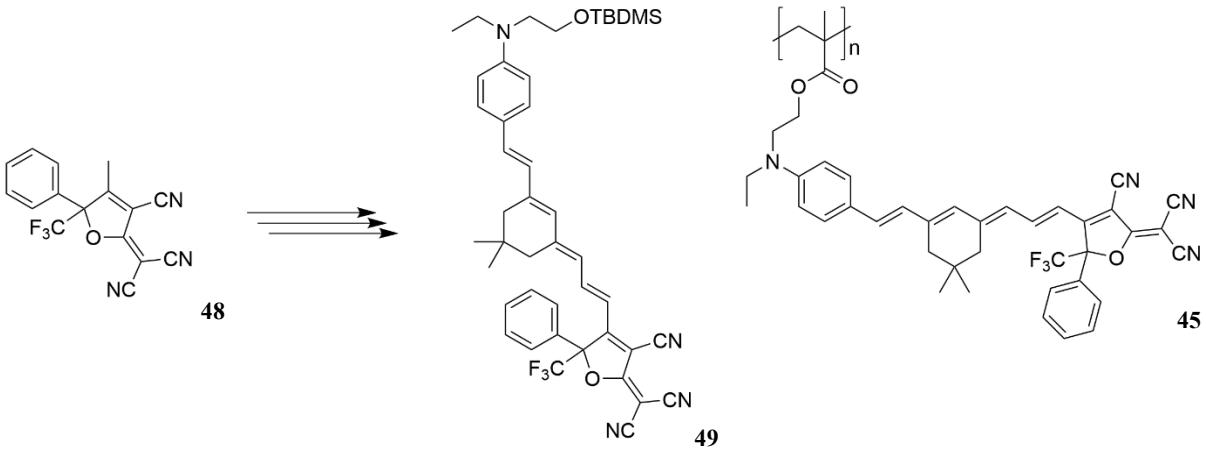

*Figure 19: Structures of five-membered ring **48**, chromophore **49** and polymer **45**.*

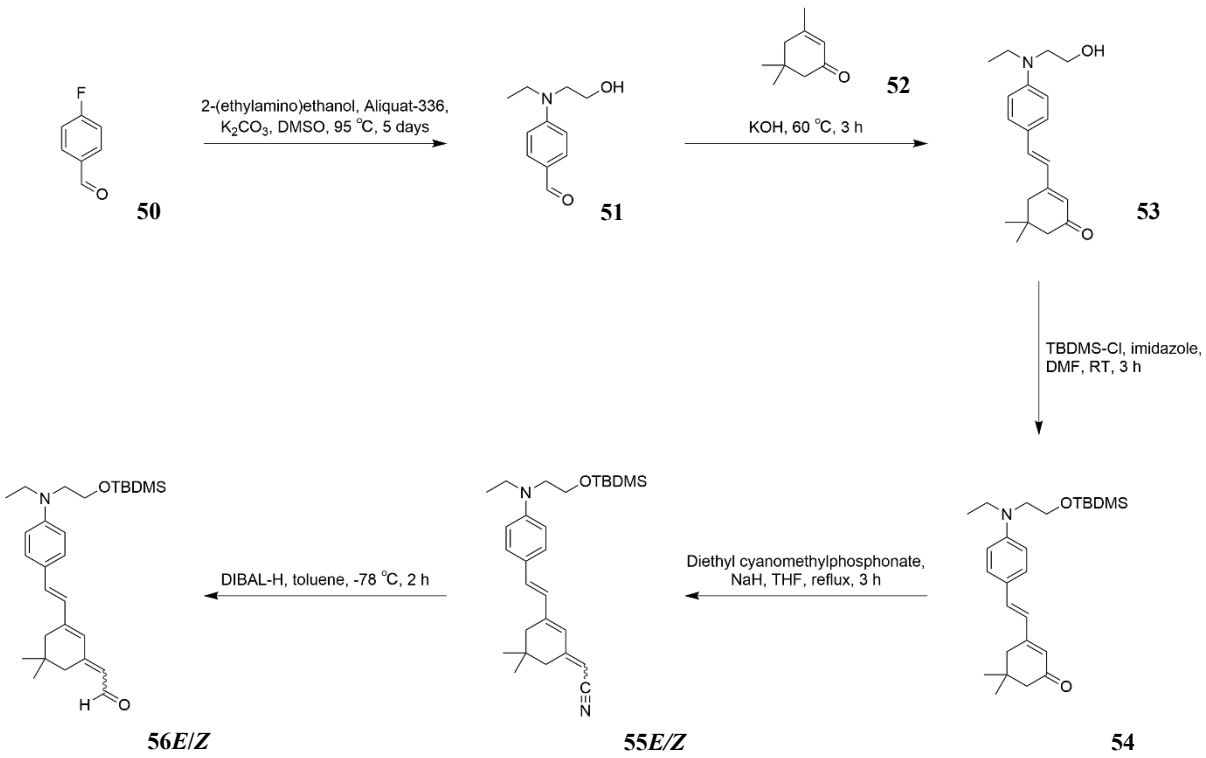

*Scheme 1: Proposed synthesis of polymer **45**, part 1.*

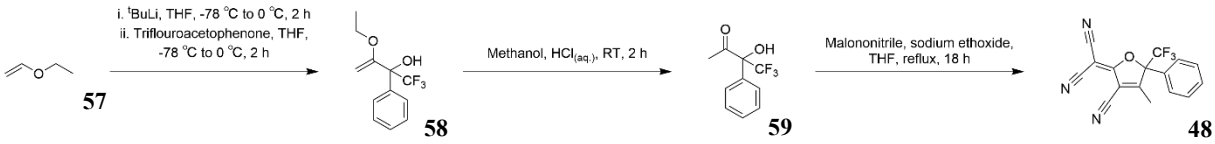

*Scheme 2: Proposed synthesis of polymer **45**, part 2.*

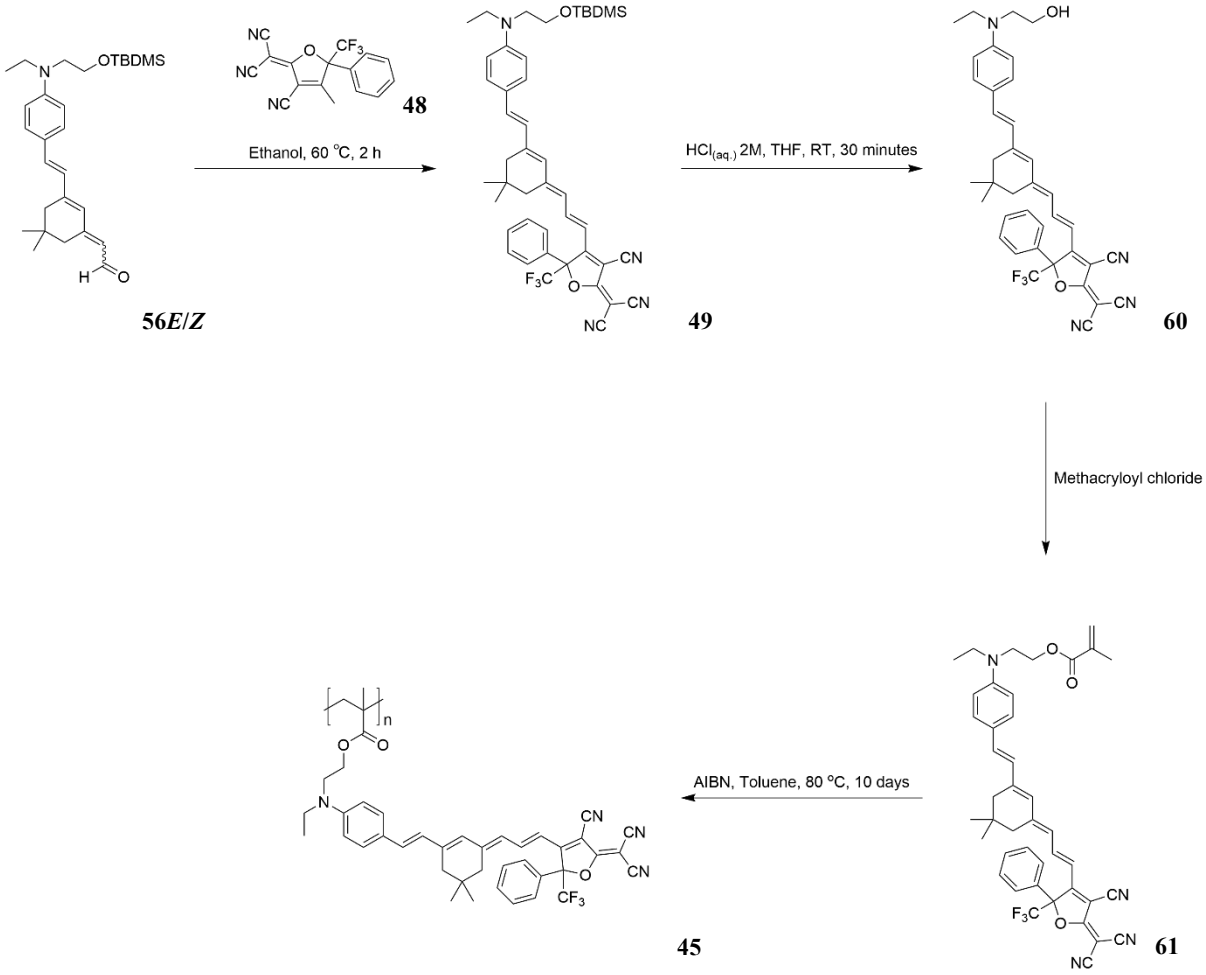

*Scheme 3: Proposed synthesis of polymer **45**, part 3.*

The first step in the synthesis of chromophore **45** is an aromatic substitution (Figure 20), which was executed with yields of up to 94%.[71] In the NMR spectrum of the product, even after column chromatography, an impurity peak at 4.24 ppm was often seen. It was realised that despite the amount of this impurity present, any trace of this would cause the following aldol condensation reaction to fail to proceed. After testing a variety of column conditions, this impurity was isolated and subsequently characterised. It was deduced to be 3,8-diethyl-1,6,3,8-dioxadiazecane-2,7-dione **63** (Figure 21) which was being produced as a side reaction of the 2-(ethylamino)ethanol **62** and the carbonate ions.

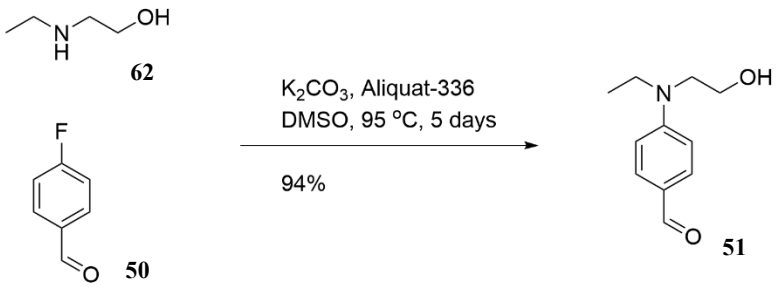

*Figure 20: Step 1 in the synthesis of polymer **45**, an aromatic substitution reaction with amine **62** and substituted benzaldehyde **50** to afford aldehyde **51**.*

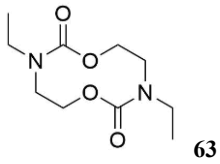

*Figure 21: Structure of 3,8-diethyl-1,6,3,8-dioxadiazecane-2,7-dione **63**. The ^{1}H NMR spectrum can be seen in Appendix 103.*

The second step was a solventless aldol condensation reaction (Figure 22) which, even after removing any trace of **63**, tended to be highly capricious. A selection of test reactions was completed to attempt to improve the efficacy, using varying amounts of base and isophorone **52**.

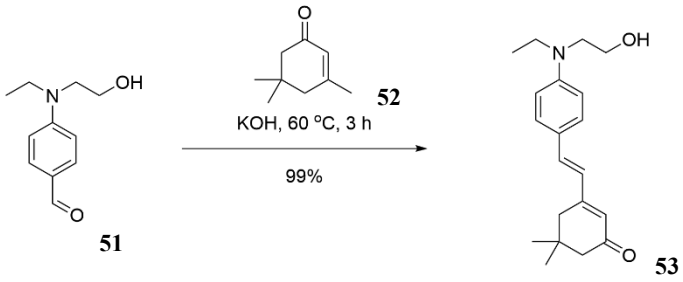

*Figure 22: Step 2 in the synthesis of polymer **45**, a solventless aldol condensation reaction between aldehyde **51** and isophorone **52** to afford ketone **53**.*

The results of these experiments are shown in Table 3. The conditions that were previously reported in the literature were mimicked with 1.2 eq. of isophorone and 1.0 eq. of potassium hydroxide.[72] These equivalents produced the lowest conversion, although the difference in conversion between reactions 0.8 equivalents and 1 equivalents was only 2%. Nevertheless, increasing either the equivalents of the potassium hydroxide to 1.2 or the equivalents of isophorone to 1.5 saw increases to 99% and 97% in the conversion to product respectively. From this point onwards, the reaction conditions using 1.2 equivalents of potassium hydroxide and 1.2 equivalents of isophorone used in the synthesis of chromophore **49**.

*Table 3: Conversion of starting material aldehyde **51** to product ketone **53** as measured by ^{1}H NMR spectrum integrations of the Ar(CH)-m-N protons in the crude reaction mixture.*

Eq. of isophorone 52	Eq. of potassium hydroxide	Conversion to product
1.2	0.8	16%
1.2	1	14%
1.2	1.2	99%
1.5	1.0	97%

The third step was a trivial silyl protection of the alcohol group (Figure 23), which at first produced fair yields.[73] After increasing the equivalents of *tert*-butyldimethylsilylchloride from 1.2 to 2.4 the yields increased to up to 84%. It was theorised that this was owing to the reagent being slightly old.

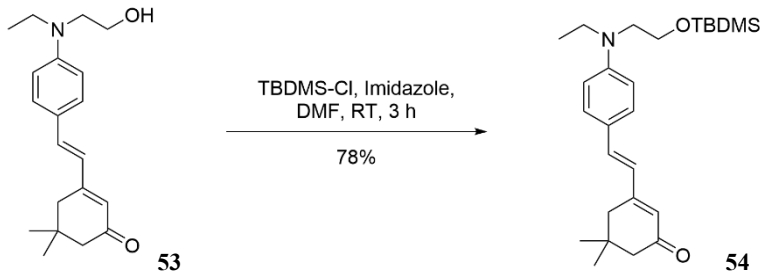

*Figure 23: Step 3 in the synthesis of polymer **45**, a protection of the alcohol group on ketone **53** with a tert-butyldimethylsilyl moiety to afford protected ketone **53**.*

The fourth step was a Horner-Wadsworth-Emmons reaction (Figure 24) that was reported in the literature to synthesise a 50:50 mixture of inseparable E/Z isomers.[30] A 57:43 (E:Z) ratio between the isomers calculated from the integrations of the NC-CH peaks at 5.06 and 4.89 ppm respectively (Appendix 10). As previously mentioned, these isomers were inseparable by column chromatography but would be separable in a later step so the mixture would be carried forward. Yields of up to 70% were observed for **55*E*/*Z***.

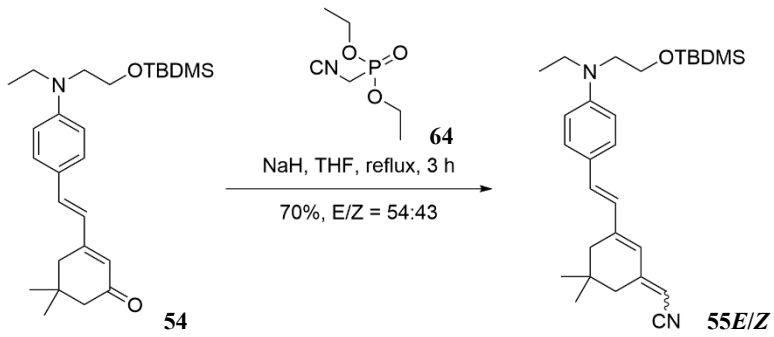

*Figure 24: Step 4 in the synthesis of polymer **45**, a Horner-Wadsworth-Emmons reaction between protected ketone **53** and diethyl cyanomethylphosphonate **64** to afford nitriles **55E** and **55Z**.*

The fifth step was a DIBAL reduction of the nitrile to an aldehyde (Figure 25).[74] Yields of up to 69% were observed. Here a 70:30 (E:Z) ratio was seen, calculated with ^{1}H NMR spectrum

integrations of the isomers, that remained inseparable by column chromatography. The isomeric ratio had changed from 57:43 over this step.

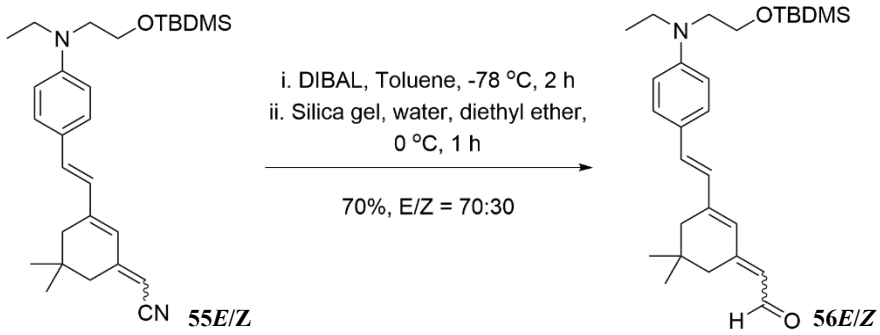

*Figure 25: Step 5 in the synthesis of polymer **45**, a DIBAL reduction of nitriles **55E** and **55Z** to afford aldehydes **56E** and **56Z**.*

Assignment of the mixture of E and Z isomers was assisted by 2D NMR experiments. Nuclear overhauser effect spectroscopy (NOESY) can be used to detect through-space interactions of protons. NOE peaks highlighted in red in Figure 26 show the interaction between -CO*H* (*E*) and HOC-CH-C-CH_2 (*E*). NOE peaks highlighted in blue in Figure 26 show the interaction between -CO*H* (*Z*) and HOC-CH-C-C*H* (*Z*).

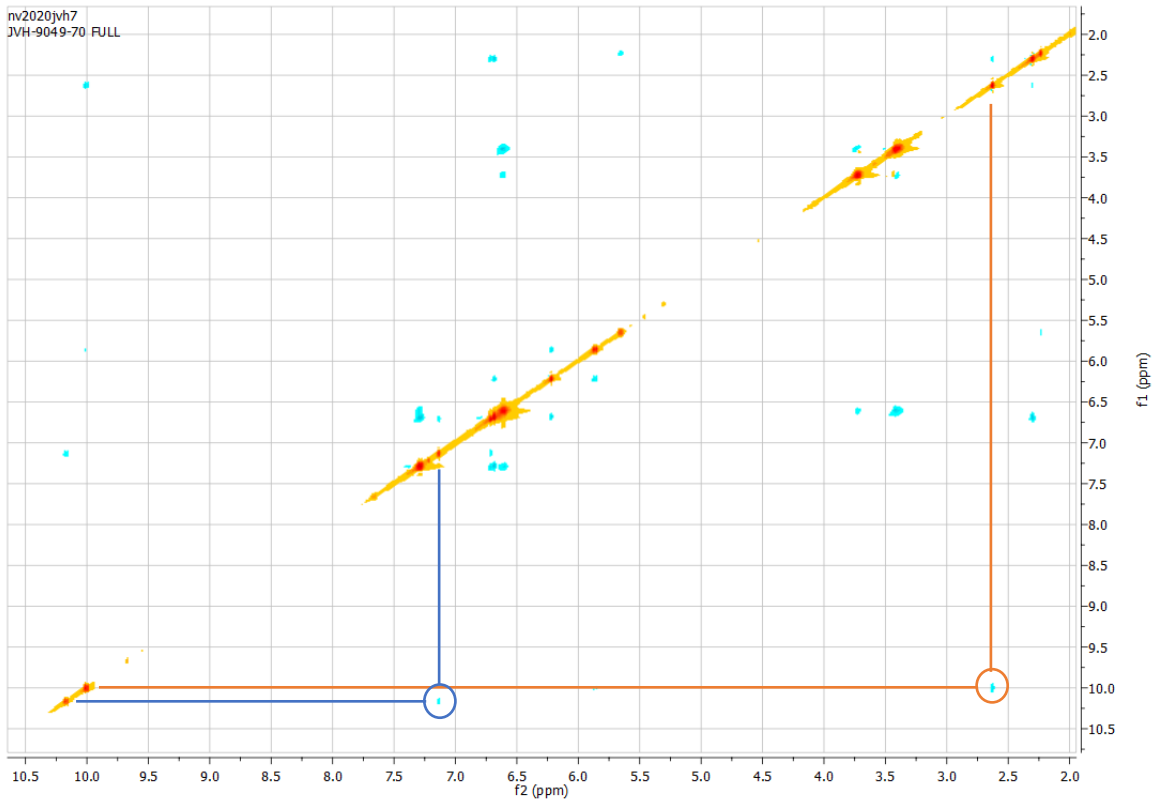

*Figure 26: Snapshot of the NOESY spectrum for mixed aldehydes **56E** and **56Z** with the relevant NOE -CO*H *and HOC-CH-C-C*H_2 *or HOC-CH-C-CH interactions highlighted in red and blue respectively.*

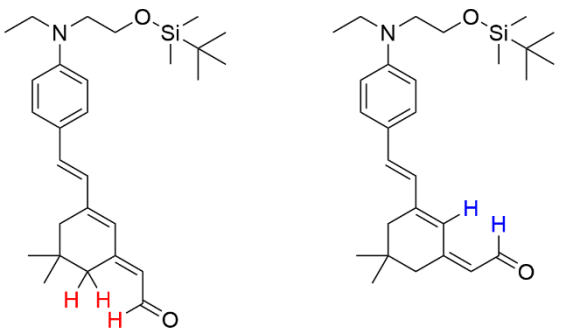

56*E* **56*Z***

*Figure 27: Structures of aldehydes **56E** and **56Z** with the protons that show NOE interactions highlighted in red and blue respectively.*

^{1}H – ^{1}H correlation spectroscopy (COSY) can be used to detect proton interactions through bonds. Knowing the exact assignments for the separate -CO*H* peaks allowed for the use of COSY to differentiate between the HOC-C*H* peaks for **56*E*** and **56*Z*** as 5.91 and 5.70 respectively.

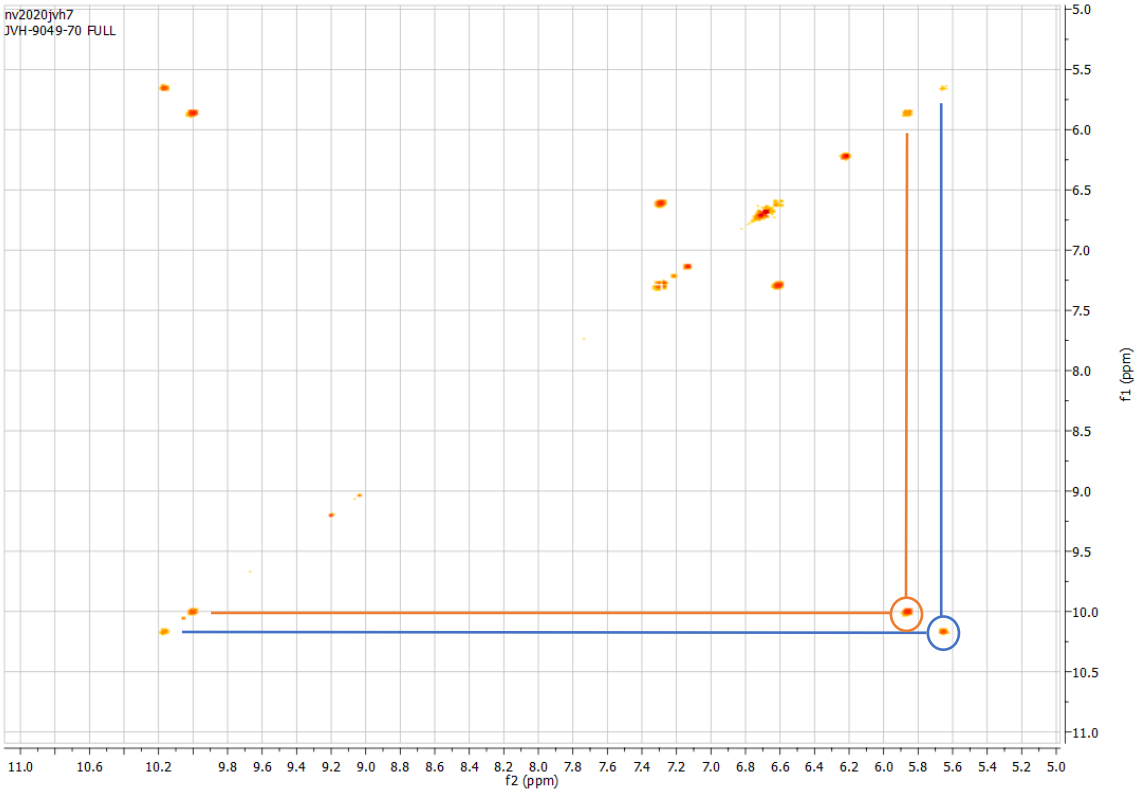

*Figure 28: Snapshot of the COSY spectrum for mixed aldehydes **56E** and **56Z** with the relevant COSY -COH and HOC-CH interactions highlighted in red and blue respectively.*

Peaks for the C(C*H*$_3$)$_2$, HOC-CH-C-C*H*$_2$ and C*H*$_2$-C(CH$_2$)$_3$ peaks can be assigned using their integration values. Additional COSY interactions can also be seen between the HOC-C*H* (*E*) and HOC-CH-C-C*H*$_2$ (*E*) peaks and HOC-CH-C-C*H* (*E*) and C*H*$_2$-C(CH$_2$)$_3$ (*E*) peaks, but these interactions are not seen in the *Z* isomer.

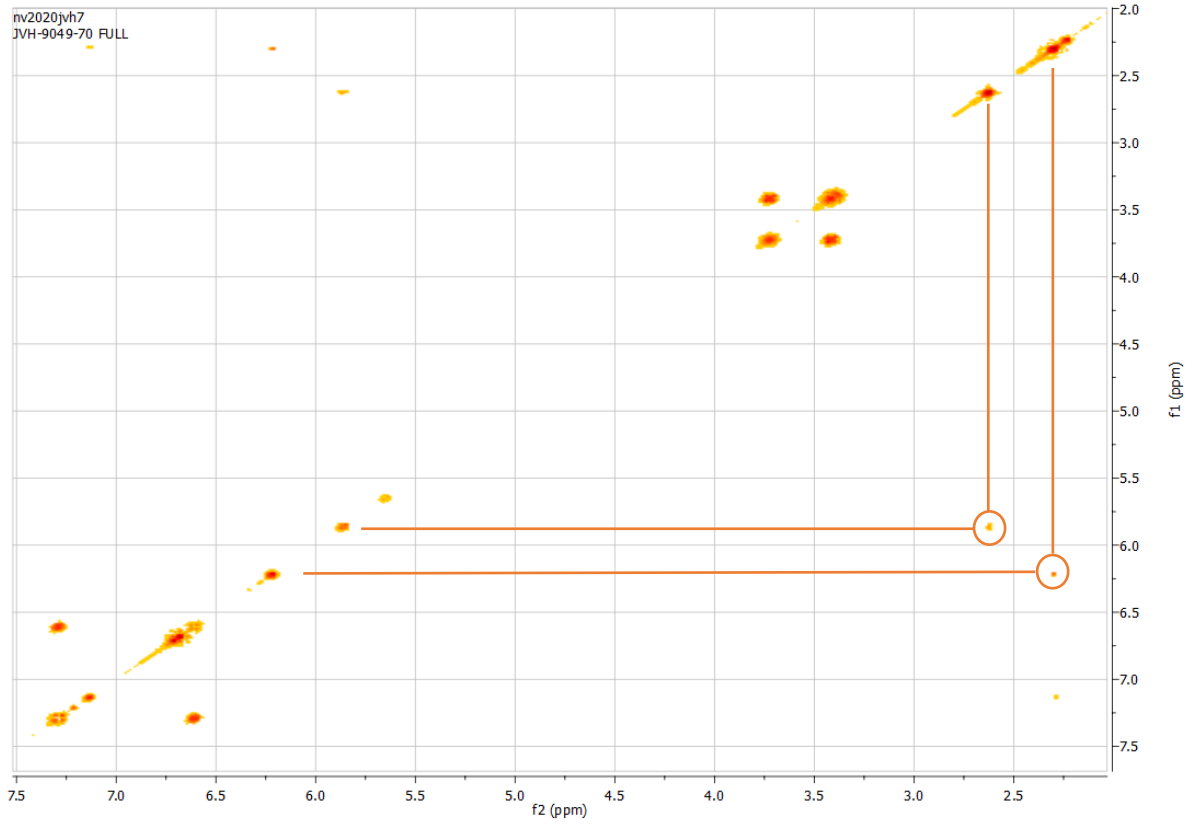

*Figure 29: Snapshot of the COSY spectrum for mixed aldehydes **56E** and **56Z** with the relevant COSY HOC-CH (E) and HOC-CH-C-CH$_2$ (E) interaction and HOC-CH-C-CH (E) and CH$_2$-C(CH$_2$)$_3$ (E) interaction highlighted.*

In parallel to the synthesis of **56*E*/*Z***, the synthesis of the five-membered ring **48** was to be carried out. First in this synthesis is a base-induced nucleophilic addition of ethyl vinyl ether **57** to 4,4,4-trifluoroacetophenone **54** (Scheme 4).[75]

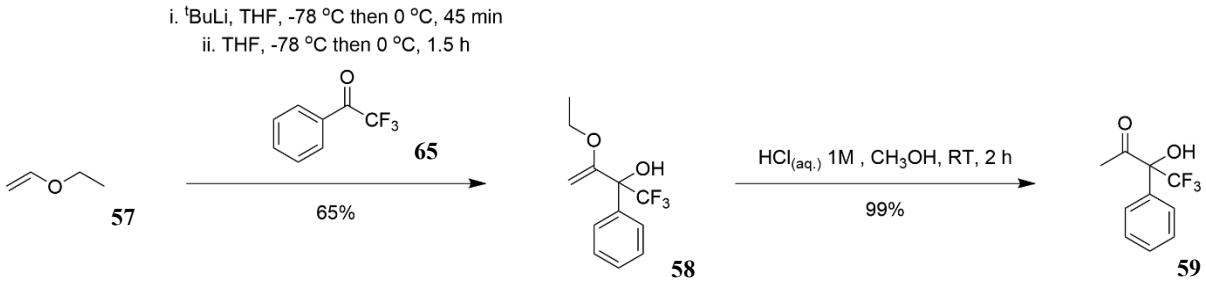

*Scheme 4: Steps 1 and 2 of the synthesis of the five-membered ring **48**.*

This addition was followed by an acid-catalysed elimination reaction that did not require purification between steps, however, purification of the alkene intermediate **58** was carried out on one occasion for characterisation purposes. Over the two steps, yields of up to 77% of **59** were observed. On the occasion the two steps were carried out separately, yields of 65% and 99% were attained respectively.

The next step in the synthesis of the five-membered ring **48**, was the condensation of **59** with malononitrile **66** (Figure 30).[31]

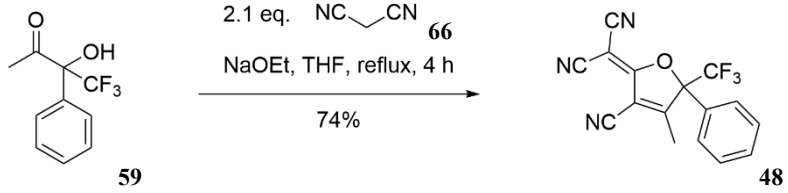

*Figure 30: Step 3 in the synthesis of the five-membered ring **48**, a condensation reaction between ketone **59** and malononitrile **66** to five-membered ring **48**.*

The literature reports using lithium ethoxide (0.05 eq.) in THF to afford **48** with a 26% yield.[31] When these conditions were reproduced, only trace amounts of **48** was detected by NMR. Upon changing the solvent to anhydrous ethanol, yields of up to 74% were observed. **48** contains a chiral centre but to check the mixture was racemic, a specific rotation ($[\alpha]_D$) measurement was performed and no rotation was observed thus proving the mixture is racemic. Chirality, and thus the rotation of light, is undesirable in an electro-optic polymer as the rotating light may not fit within the waveguide and could cause undesired interference.

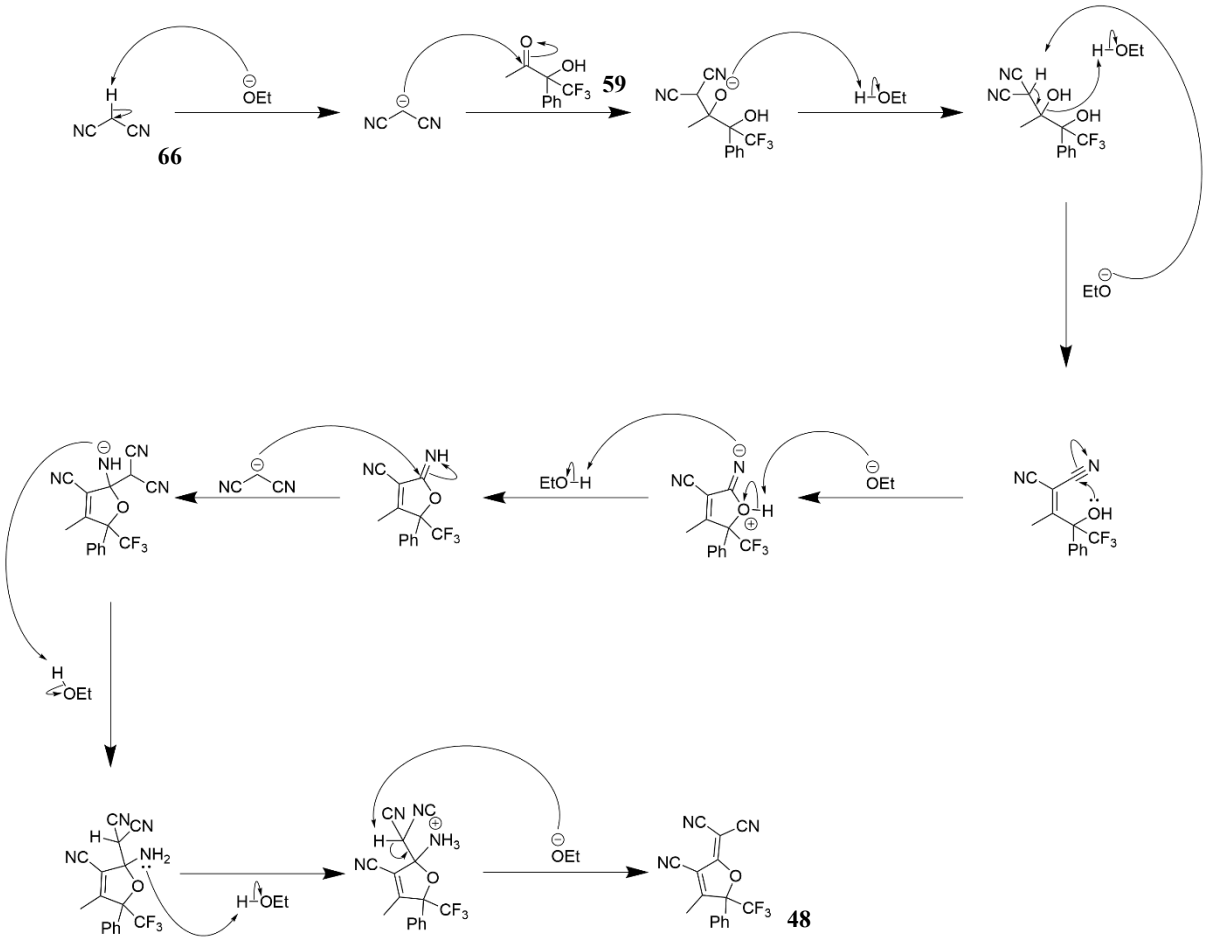

*Figure 31: Mechanism for the condensation of ketone **59** with malononitrile **66** to afford five-membered ring **48**. Reaction conditions: **59** (1.0 eq.), malononitrile **66** (2.1 eq.), sodium ethoxide (21% weight in ethanol, 0.05 eq.), anhydrous ethanol, reflux, 4 hours.*

The ninth overall step in the synthesis of polymer **45** was the condensation of the acceptor moiety with the donor and π-bridge (Figure 32). The procedure reported by J. Luo *et al.* was followed.[74]

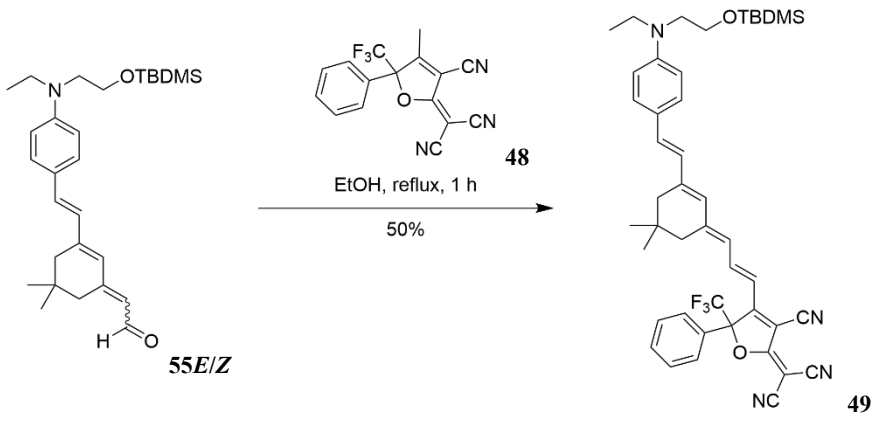

*Figure 32: Step 9 overall in the synthesis of polymer **45**. Aldehyde **55E/Z** were condensed with five-membered ring **48** to afford chromophore **49**.*

Reagents **56*E*/*Z*** and **48** were stirred in ethanol at reflux for 1 hour. In the first two attempts at this reaction, two spots were visible by thin layer chromatography (TLC) and separable by column chromatography. However, when characterising the addition product, the two CH_2 peaks from the isophorone π-bridge (usually seen within the 2.5 – 2 ppm region of the spectra) were not visible in the ^{1}H NMR spectrum (Appendix 106). The possible structure of this molecule was not able to be identified, nor how such a product might occur in such mild conditions. Upon lowering the temperature to 60 °C, the desired product was formed, with HRMS and NMR spectroscopy confirming the product. The *E* and *Z* isomers became separable at this step, with yields of up to 50% for the desired *E* isomer. Although the *Z* isomer could be seen by TLC, the isolated yield (<1mg) was inadequate for complete characterisation.

The tenth step in the synthesis of polymer **45** was the deprotection of the silyl group from the alcohol moiety on chromophore **49**. The procedure used by Espinar-Barranco *et al.* was followed.[70] $HCl_{(aq.)}$ (2M solution) was used, and although it did successfully deprotect the alcohol most of the material decomposed in the acidic solution. It is unclear why the more commonly used silyl deprotection reagent, TBAF, was not used for this deprotection; it could be tested before proceeding with this reaction on a larger scale. A yield of 11% of deprotected-chromophore **60** was achieved.

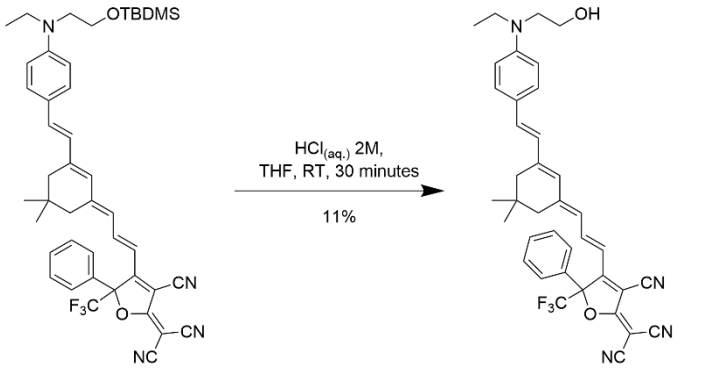

49 **60**

*Figure 33: Step 10 in the overall synthesis of polymer **45**. A silyl deprotection of chromophore **49** afforded chromophore **60**.*

Upon the synthesis of the deprotected chromophore **60**, it was decided to focus on the synthesis of novel chromophores before attempting the connection to methacryloyl chloride and subsequent polymerisation to afford polymer **45**. It was decided that focusing on novel molecules would be the best use of the time available, after much was lost due to the ongoing effects of COVID-19, in an attempt to mitigate some of the effects.

2.2 The synthesis towards side chain-modified electro-optic polymers using isophorone derivatives as the π-bridge

2.2.1 The synthetic route towards chromophore **79**

Upon the completion of the synthesis of chromophore **49**, possible modifications were considered. As discussed in 1.4 Project aims, the first set of modifications would be within the π-bridge region of the molecule, replacing the conjugated hydrogen atom from the isophorone bridge of **49** with an R-group, as shown in Figure 18. It was hoped that by incorporating R-groups with intramolecular bonding capabilities (hydrogen bonding/π-π stacking) would increase the rigidity, increase the T_g and increase the r_{33} of the polymer. Ideally, isophorone derivatives would be synthesised and then used in the same procedures as those in the synthesis of chromophore **49**. After looking at what isophorone derivatives were commercially available, it was decided that isophorone oxide **67** would be a good starting point for our modifications to be synthesised from, owing to its ability to undergo nucleophilic substitution reactions. A selection of previously reported reactions from isophorone oxide **67** are shown in Figure 34. It was decided that the azide **73**, enol **74** and primary amine **75** would be good targets.

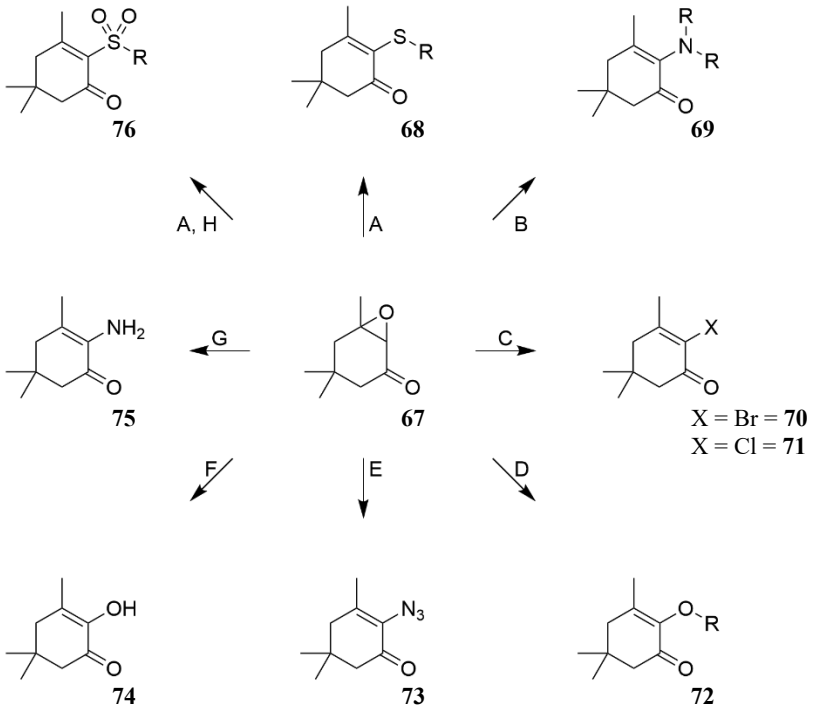

*Figure 34: Possible reactions of isophorone oxide **67**, reported in the literature.*[76–81] *Reaction conditions: **A** Aqueous base, thiol; **B** Secondary amine, methanol, water, heat; **C** 1-Carboxymethyl-3-methyl-3H-imidazole-1-ium bromide/chloride, heat; **D** aqueous R-OH, heat; **E** 1-Carboxyethyl-3-methyl-3H-imidazole-1-ium azide, heat; **F** Sulphuric acid, silica gel, acetic acid, heat; **G** Aqueous ammonia, irradiation (sonication), heat; **H** acetic acid, hydrogen peroxide.*

The first isophorone modification attempted was the azide **73**, with the hope that it could be followed by a click chemistry azide-alkyne cycloaddition, forming a 1,2,3-triazole, thus increasing the π-system into the R-group, increasing the π-π stacking between monomers. It was also hoped that the side chain would increase the rigidity of the electro-optic polymer thus increasing the r_{33}. The procedure to synthesise isophorone azide **73** reported by Mizuno *et al.* was followed and yields of up to 98% were obtained (Figure 35).[81]

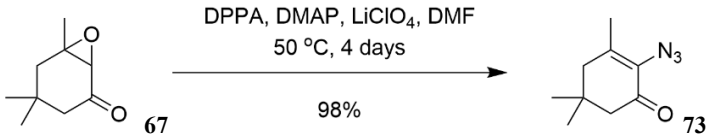

*Figure 35: Reaction of isophorone oxide **73** to form isophorone azide **73**, reported by Mizuno et al..*[81]

To achieve the additional conjugation a click chemistry azide-alkyne cycloaddition to form a 1,2,3-triazole (Figure 36) was carried out. To begin with, the conditions reported by Himo *et al.* were followed, using 1 mol% of Cu(II)SO_4 with 10 mol% sodium-*L*-ascorbate in a 50:50 solution of H_2O:^{t}BuOH. Phenylacetylene **77** was chosen as the first alkyne owing to its simple structure, allowing us to test a triazole-based side chain. This made the next target molecules, chromophore **79** and polymer **46**. It would also be possible to use alkynes with substituted arenes that could introduce hydrogen bonding into the polymer, increasing both the rigidity and the polarisability.

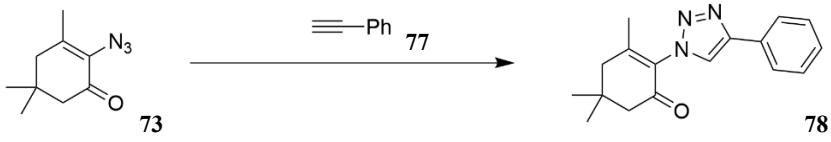

*Figure 36: Generic reaction scheme showing a click chemistry azide-alkyne cycloaddition between isophorone azide **73** and phenylacetylene **77** to form 1,2,3-triazole **78**.*

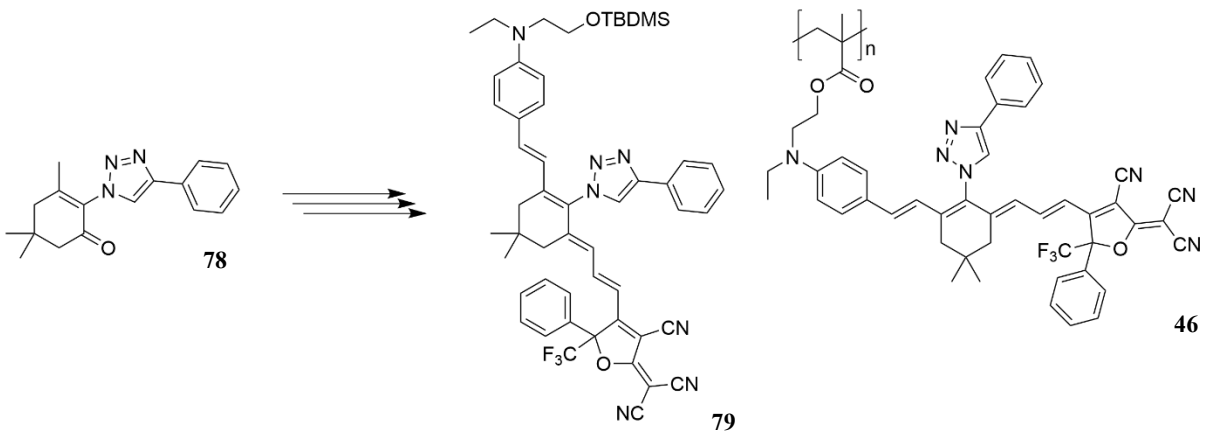

*Figure 37: Structures of isophorone triazole **78**, chromophore **79** and polymer **46**.*

Although some product was observed in the crude ^{1}H NMR, the conversion was estimated to be 7%, with mostly starting material left in the resulting reaction mixture. After increasing, the mol% of the catalyst, the temperature and the reaction time (as shown in Table 4), using 10% of Cu(II)SO_4 at 100 °C for 12 hours produced complete conversion to product, with no starting material alkyne C*H* peak visible in the crude ^{1}H NMR.

*Table 4: Conversion of phenylacetylene **77** to 1,2,3-triazole **78** as measured by ^{1}H NMR spectrum integrations of the alkyne CH peak and the triazole CH peak in the crude reaction mixtures.*

mol% Cu(II)SO_4 Catalyst	**Temperature**	**Time**	**% Conversion to product (Measured by crude NMR)**
1	RT	12 h	7
1	RT	36 h	11
2	RT	12 h	9
10	RT	60 h	29
10	50 °C	12 h	18
10	100 °C	12 h	100

An aldol condensation reaction between aldehyde **51** and the 1,2,3-triazole **78** (Figure 38) was attempted next. The first attempt at this reaction followed the procedure developed for the synthesis of chromophore **49**. Because the triazole isophorone derivative **78** was now a solid, it was powdered with the potassium hydroxide, and the two solids were stirred together before the addition of the aldehyde **51**. This method saw no traces of product in the crude ^{1}H NMR. After this, other similar reported aldol procedures were followed, to no avail.[30,70–74,80,82] In all of these attempts, no products of any kind were detected, only the starting materials were seen in the crude ^{1}H NMR spectra of the resulting reaction mixtures.

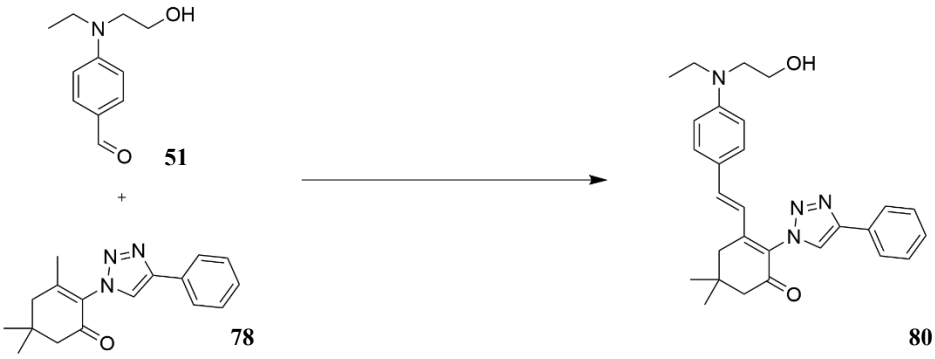

*Figure 38: Generic scheme showing an aldol condensation reaction between aldehyde **51** and 1,2,3-triazole **78** to produce ketone **80**.*

At this point, it was decided to do a series of test reactions varying the solvents, temperatures and reagents. Analytical TLC was used to detect the presence of **80** and integration of starting material and product Ar(C*H*)-*o*-N peaks in the crude ^{1}H NMR were used to determine the conversion. Owing to the high fluorescence of triazole **80**, it was very easily detected by analytical TLC, using UV to visualise the spots. Even when clearly visible by analytical TLC, product peaks were not always visible in the crude ^{1}H NMR spectra, in these cases, only its presence is reported instead of the percentage conversion. Percentage conversions are reported where available. All reactions were left to stir for 16 h, overnight. Table 5 shows the first set of reactions, which were completed at room temperature. Diethyl ether proved to be the best solvent at room temperature, with product detected by TLC when using all three of the reaction conditions tested. Using Conditions III in diethyl ether a conversion of 16% product was achieved. Conditions I produced the best results at room temperature, with all solvents producing some amount of product. It was also noted that there were solubility issues using conditions II in water.

*Table 5: Table depicting if the presence of product **80** was detected in reaction mixtures by analytical TLC. All reactions were left at room temperature for 16 hours, overnight.*

Solvent	**Conditions I (RT)** **78** (1.2 eq.), **51** (1.0 eq.) and NaOEt (2.2 eq)	**Conditions II (RT)** **78** (1.2 eq.), **51** (1.0 eq.), KOH (2.2 eq.) and Aliquat-336 (0.05 eq.)	**Conditions III (RT)** **78** (1.2 eq.), **51** (1.0 eq.), $LiClO_4$ (1.0 eq.) and NaOEt (1.2 eq.)
Ethanol	Yes	No	No
Methanol	Yes	Yes	No
THF	Yes	No	No
Diethyl ether	Yes	Yes	Yes (16%)
Water	Yes	No	No

The temperature was then increased to 50 °C for the best-performing reaction conditions (diethyl ether was excluded owing to its boiling temperature being at 35 °C). Table 6 shows the results of these reactions, with the two best-yielding reactions from the room temperature reactions continuing to yield product at the increased temperature. There was however no significant increase in yield for these reactions. Conditions I in methanol produced an 18% conversion to product. Conditions I in THF at 50 °C still did not produce enough product to be detectable by ^{1}H NMR. Increasing the temperature of conditions II in water did improve the solubility of the starting materials, however, product was only detectable by analytical TLC.

*Table 6: Table depicting if the presence of product **80** was detected in reaction mixtures by analytical TLC. All reactions were left at 50 °C for 16 hours, overnight. Diethyl ether was not applicable at this temperature because it boils at 35 °C.*

Solvent	**Conditions I (50 °C)** **78** (1.2 eq.), **51** (1.0 eq.) and NaOEt (2.2 eq)	**Conditions II (50 °C)** **78** (1.2 eq.), **51** (1.0 eq.) and Aliquat-336 (0.05 eq.)	**Conditions III (50 °C)** **78** (1.2 eq.), **51** (1.0 eq.), $LiClO_4$ (1.0 eq.) and NaOEt (1.2 eq.)
Ethanol			
Methanol	Yes (18%)		
THF	Yes		
Diethyl ether	n/a	n/a	n/a
Water		Yes	

Next, reflux conditions were tested. Conditions I were not tested at this temperature after the conversion did not increase between room temperature and 50 °C. Table 7 shows the results of the tested reflux reactions. Conditions I in methanol and diethyl ether did not yield any product, but instead, a complex mixture was seen by ^{1}H NMR. Conditions III in diethyl ether did produce product but with a 14% conversion, 4% lower than at room temperature.

*Table 7: Table depicting if the presence of product **80** was detected in reaction mixtures by analytical TLC. All reactions were left at their respective reflux temperatures for 16 hours, overnight.*

Solvent	**Conditions I (reflux)** **78** (1.2 eq.), **51** (1.0 eq.) and NaOEt (2.2 eq)	**Conditions II (reflux)** **78** (1.2 eq.), **51** (1.0 eq.), KOH (2.2 eq.) and Aliquat-336 (0.05 eq.)	**Conditions III (reflux)** **78** (1.2 eq.), **51** (1.0 eq.), $LiClO_4$ (1.0 eq.) and NaOEt (1.2 eq.).
Ethanol			
Methanol	No		
THF			
Diethyl ether	No		Yes (14%)
Water			

After seeing no significant improvements by increasing the temperature to reflux, a new set of conditions was designed, combining the increased sodium ethoxide from conditions I and the lithium perchlorate from conditions III. Conditions IV: **78** (1.2 eq.) was dissolved in solvent (35 mg mL^{-1}) to which NaOEt (2.2 eq.) was added and the solution was stirred for 30 minutes. **51** (1.0 eq.) and $LiClO_4$ (1.0 eq.) were added then the reaction mixture was stirred for 16 hours, overnight. In methanol at 50 °C, no conversion to product was observed. In diethyl ether at room temperature, these conditions produced a 25% conversion to product,

which was the highest seen so far. The crude ^{1}H NMR spectrum for this reaction can be seen in Appendix 105. The complete characterisation for **80** can also be found in the experimental details (**3.14**).

An aldol condensation reaction using isophorone azide **73** instead of the click product **78** was also attempted (Figure 39) using Conditions IV, but upon the addition of the sodium ethoxide, effervescence was observed and no starting material **73** or product **84** was detected in the resulting reaction mixture. Although starting material **51** was still visible, the starting material **73** had become a complex mixture.

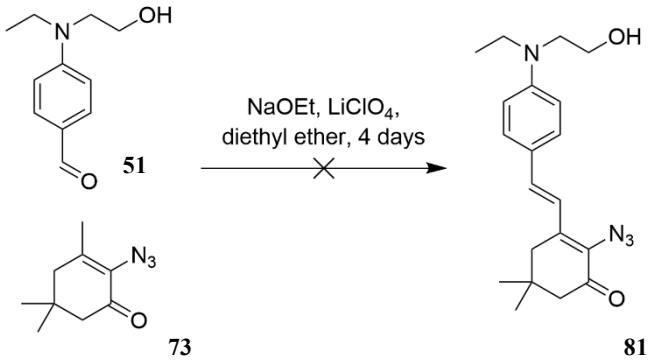

*Figure 39: Generic reaction scheme showing an aldol condensation reaction between aldehyde **51** and isophorone azide **73** to produce ketone **81**.*

Although the yield of **80** was increased to 25%, the poor yield was discouraging enough to decide to pursue other chromophores.

2.2.2 The synthetic route towards chromophore **82**

The second isophorone modification to be attempted was the amine **75**, thus making our next target molecules chromophore **82** and polymer **47**. This would give us an amine moiety in the side chain of the electro-optic polymer **47**. Having hydrogen bonding between monomers could increase the rigidity of the electro-optic polymer. To further increase the rigidity, secondary and tertiary amines could also be synthesised and tested.

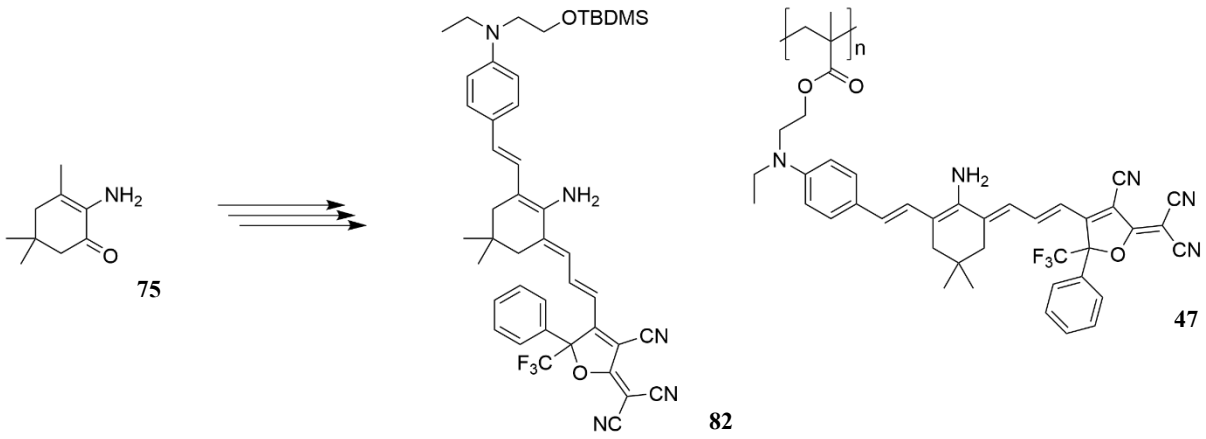

*Figure 40: Structures of isophorone amine **75**, chromophore **82** and polymer **47**.*

There is a reported procedure directly from isophorone oxide **67** to isophorone amine **75**.[79] However, it uses aqueous ammonia (sp. gr. 0.88), which gives off hazardous fumes. This, coupled with our excellent yields synthesising isophorone azide **73**, made us consider an alternative route to isophorone amine **75** via isophorone azide **73**, utilising a Staudinger reaction.

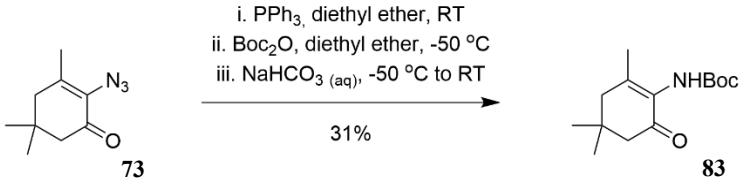

*Figure 41: Reaction of isophorone azide **73** with triphenylphosphine followed by a boc protection to boc-protected isophorone amine **83**.*

The Staudinger reaction was immediately followed by a boc protection of the amine as it was worried the amine would interfere with the subsequent reactions. The procedure reported by Afonso was followed.[83] Yields of up to 31% were achieved with **83** being the minor product. The major product was tentatively assigned as conjugated imine **84**, based on the two C*H* peaks at 5.10 and 4.86 ppm seen in the ^{1}H NMR spectrum (Appendix 104), however, the LCMS peak did not agree with this (m/z = 263) and full characterisation was not attempted. Although the yield for **83** was poor, it was satisfactory enough to continue, to see if there could be a more successful aldol condensation reaction, before optimising the Staudinger reaction at a later stage.

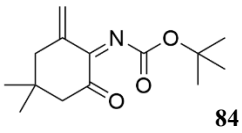

*Figure 42: Structure of the very tentatively assigned conjugated imine **84**, the tentatively assigned major product of the Staudinger reaction of isophorone azide **73** followed by a boc protection. The ^{1}H NMR spectrum can be seen in Appendix 104.*

The reaction conditions developed for the synthesis of triazole **80** were tested on the aldol condensation reaction between **83** and **51**. No product **85** was detected by ^{1}H NMR or LCMS. Thoerising that a stronger base might be the answer, an aldol procedure using LDA was followed.[84] As before, no product was detected by ^{1}H NMR or LCMS. Next, the LDA procedure was modified, instead of using n-BuLi (1.1 eq.) with diisopropylamine (1.1 eq.) to form LDA (1.1 eq.), solely *t*-BuLi (1.1 eq) was used as the base. Similarly to the previous attempts, no product was detected by ^{1}H NMR or LCMS.

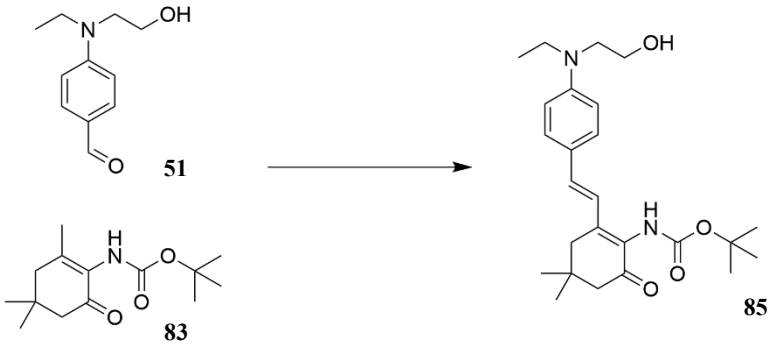

*Figure 43: Generic reaction scheme showing an aldol condensation reaction between aldehyde **51** and boc-protected isophorone amine **83** to produce ketone **85**.*

Seeing as the aldol condensation reaction was consistently troublesome across all of the isophorone derivatives tested so far, it was theorised that changing the aldehyde might improve the yields. Seeing as the amino aldehyde **51** was synthesised from fluoro-aldehyde **50** this would be an easy option to test and would change the electronics of the π-conjugated system, potentially improving the yields. Similarly, the alcohol group would next be protected, so protecting it before the aldol condensation reaction might change the solubility enough to increase the yields. To begin with, aldehyde **86** was synthesised from aldehyde **51** using the same protection conditions as for the synthesis of **51**. Yields of up to 94% were achieved.

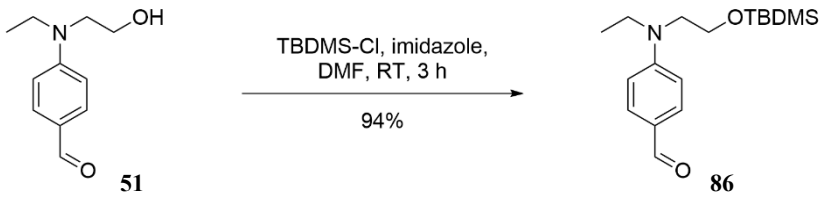

*Figure 44: Protection of aldehyde **51** with a tert-butyldimethylsilyl moiety to afford aldehyde **86**.*

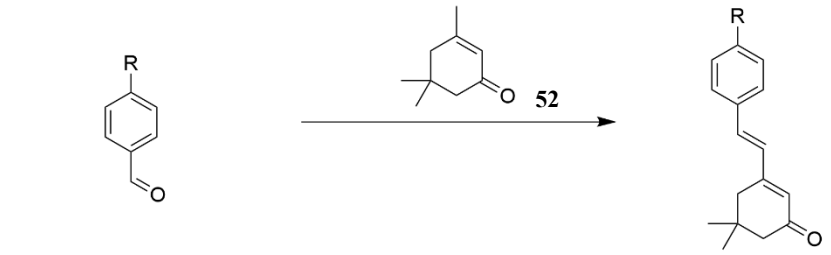

R = F = **50**
R = N(CH_2CH_3)(CH_2CH_2OH) = **51**
R = N(CH_2CH_3)($CH_2CH_2OTBDMS$) = **86**

R = F = **87**
R = N(CH_2CH_3)(CH_2CH_2OH) = **53**
R = N(CH_2CH_3)($CH_2CH_2OTBDMS$) = **54**

*Figure 45: Generic reaction scheme showing an aldol condensation reaction between para-substituted aldehydes **50**, **51** and **86** and isophorone **52** to afford **87**, **53** and **54** respectively.*

Isophorone **52** was used for the testing owing to its commercial availability and low price. Tests were also carried out on **51** as a control. The favourable conditions for the aldol condensation reaction from **78** and **51** to **80** were used (**52** (1.2 eq.) was dissolved in solvent (35 mg mL^{-1}) to which NaOEt (2.2 eq.) was added and the solution was stirred for 30 minutes. The respective aldehyde (1.0 eq.) and $LiClO_4$ (1.0 eq.) were added then the reaction mixture was stirred for 16 hours, overnight). Products **53** and **54** were extracted into $CHCl_3$ and **87** was extracted into ethyl acetate. There were slight differences in the conversions between using **51** and **86**. The highest conversion for both was using 2.2 eq. of sodium ethoxide in THF (15% and 16% respectively). For aldehyde **50**, however, there was only traces of the starting material left in the reaction mixtures across all the tests. An unexpected challenge was that there were two products visible in the crude NMRs. The ratios between these mixed products were measured using integrations of the ^1H NMR spectrum peaks at 7.47 ppm and 7.33 ppm respectively. When an LCMS was taken, only one major peak was observed in the TIC, with a m/z peak at 245 $[M+H]^+$ corresponding to the desired condensed product.

*Table 8: Table depicting the percentage conversion (measured by ^1H NMR) of para-substituted aldehyde starting material to product for the aldol condensation reaction shown in Figure 45. Conditions kept consistent across the reactions: respective aldehyde (1.0 eq.) isophorone **52** (1.2 eq.), $LiClO_4$ (1.0 eq.), RT, 16 h.*

Reaction conditions	**R = F** **50 → 87**	**R = N(CH_2CH_3)(CH_2CH_2OH)** **51 → 53**	**R = N(CH_2CH_3)($CH_2CH_2OSi(CH_3)_2(C(CH_3)_3)$)** **86 → 54**
1.2 eq. NaOEt, diethyl ether	No starting material was detected. Two products were observed. 54:46	6% conversion	No product detected
1.2 eq. NaOEt, THF	Traces of starting material were detected. Two products were observed. 54:46	No product detected	No product detected
2.2 eq. NaOEt, THF	No starting material was detected. Two products were observed. 54:46	15% conversion	16% conversion
2.2 eq. NaOEt, diethyl ether	No starting material was detected. Two products were observed. 58:42	No product detected	12% conversion

The reaction from aldehyde **50** to fluoro-aldol product **87** was scaled up for purification, using 2.2 eq. of NaOEt in diethyl ether. Only one UV-visible product spot was observed by TLC and similarly, only one product was successfully isolated by column chromatography. The desired aldol product **87** was isolated with a 51% yield. It is possible that the additional products that were visible in the crude NMR, were the aldol products before condensation. The conditions in the LCMS run and silica could have then proceeded to condense the bond and eliminating a water molecule. An acidic/basic work up could be added in future to encourage complete condensation of the product.

Equipped with a potential alternative route to the chromophores, next was to see if an aromatic substitution reaction would proceed on the aldol product **87**, replacing the fluoro moiety with the substituted amine.

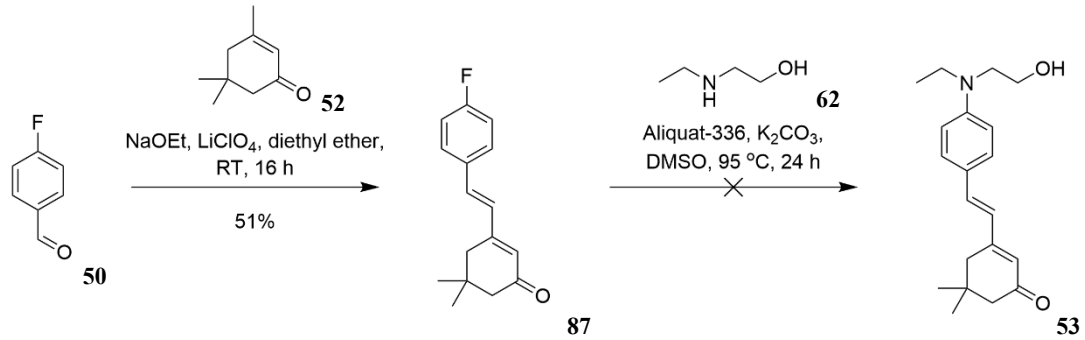

*Scheme 5: Reaction scheme showing a potential alternative route to ketone **53**. First an aldol condensation reaction between aldehyde **50** and isophorone **52**, before an aromatic substitution reaction where 2-(ethylamino)ethanol **62** replaces the fluoro moiety.*

The reaction conditions were copied from the synthesis of aldehyde **51**. The reaction was left to stir for 24 hours then a sample was taken from the reaction mixture for LCMS analysis. Disappointingly, no reaction was detected. Although the aromatic substitution would usually be left for 4 days, some product would be detectable after this time so the reaction was abandoned and the starting material reisolated.

Returning to the aldol condensation reactions between aldehyde **51** and boc-protected isophorone amine **83** to produce ketone **85**, shown in Figure 43, with what seemed like little progress having been made except the knowledge that protecting the alcohol before the aldol condensation reaction would have similar chances of succeeding, the procedure reported by Jin *et al.* was followed as it has similar starting material.[82] Three UV-visible product spots were seen by analytical TLC, their structures are theorised in Figure 46. Traces of products were visible by crude ^{1}H NMR. However, nothing could be isolated by column chromatography.

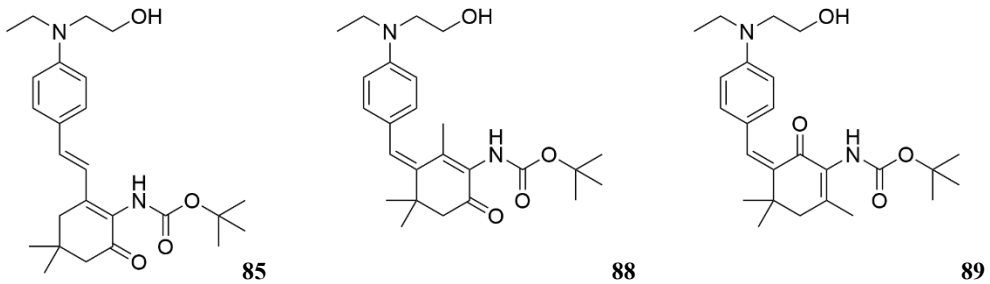

*Figure 46: Three possible products from the aldol condensation reaction between aldehyde **51** and boc-protected isophorone amine **83**: **85**, **88**, and **89**. Reaction conditions: **51** (1.0 eq.), N,N-diethyltrimethylsilylamine (1.4 eq.), lithium perchlorate (0.85 eq.), **83** (1.0 eq.), THF, RT, 3 hours.*

As mentioned in Section 2.2.1, trace products of the highly fluorescent compounds can be very visible by analytical TLC, but the concentrations would be undetectable by NMR spectroscopy. It was decided to try these conditions with the protected aldehyde **86**.

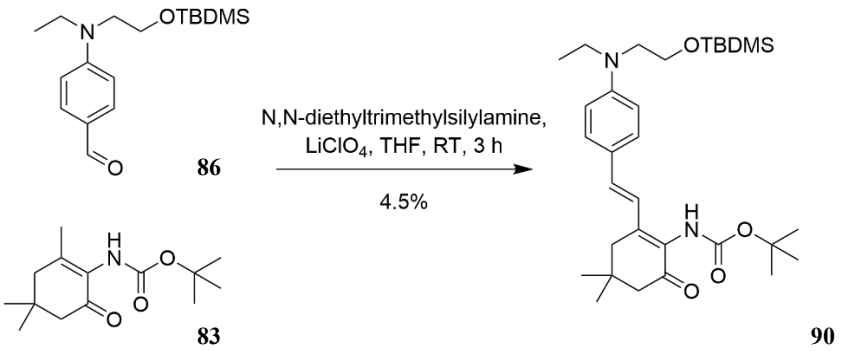

*Figure 47: Generic reaction scheme showing an aldol condensation reaction between aldehyde **86** and boc-protected isophorone amine **83** to produce ketone **90**.*

Similarly, three product peaks were visible by TLC. LCMS showed all three peaks (t_r = 5.34, 6.64 and 7.02, using the 10-minute run) possessed the same mass, m/z = 543 $[M+H]^+$, which matches the desired product. Three possible products (**90**, **95**, **96**) were theorised, which are shown in Figure 48. Column chromatography successfully isolated and characterised the desired product **90** with a yield of 4.5%. The characteristic doublet peaks of N-Ar-C*H*-CH and N-Ar-CH-C*H* would only be present in **90**. The other two products were visible in trace amounts in the post-column ^{1}H NMR spectrum, but were impure. After a second column, the additional products had decomposed and were no longer visible by ^{1}H NMR.

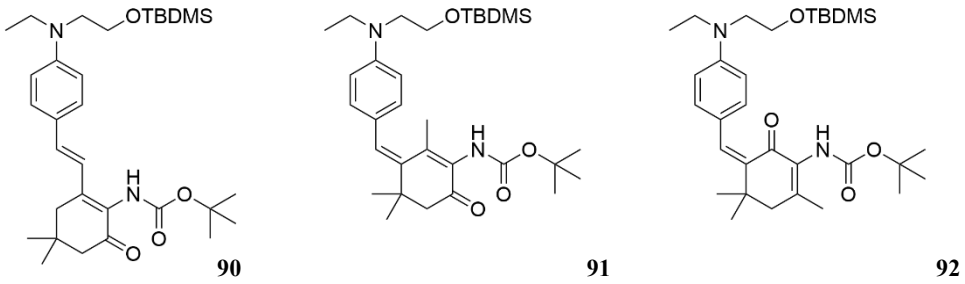

*Figure 48: Three possible products from the aldol condensation reaction between aldehyde **86** and boc-protected isophorone amine **83**: **90**, **91**, and **92**. Reaction conditions: **86** (1.0 eq.), N,N-diethyltrimethylsilylamine (1.4 eq.), lithium perchlorate (0.85 eq.), **83** (1.0 eq.), THF, RT, 3 hours.*

If this reaction were to be scaled up using aldehyde **86**, purification of the alternative products could be reattempted, taking into consideration their stability, and subsequently characterised. However, seeing as now there was not only extremely poor yields but also multiple and competing aldol products, it was decided that entirely different chromophore modifications should be considered.

2.3 The synthesis towards electro-optic polymers with BODIPY derivatives as the electron-withdrawing group

2.3.1 The synthesis of chromophore **94**

Owing to the lack of success in developing a synthesis to a novel side chain-modified chromophore, modifications in the withdrawing group were considered. BODIPY derivatives have strong withdrawing capabilities for substitutions in the *meso*-positon and therefore could make an excellent withdrawing group within an electro-optic polymer. BODIPY derivatives with groups in the 3- and 7-positions can be synthesised in a one-pot procedure, albeit in poor yields. The first BODIPY chosen was **93**, owing to the ease of its synthesis, making the next target molecules chromophore **94** and polymer **95**.

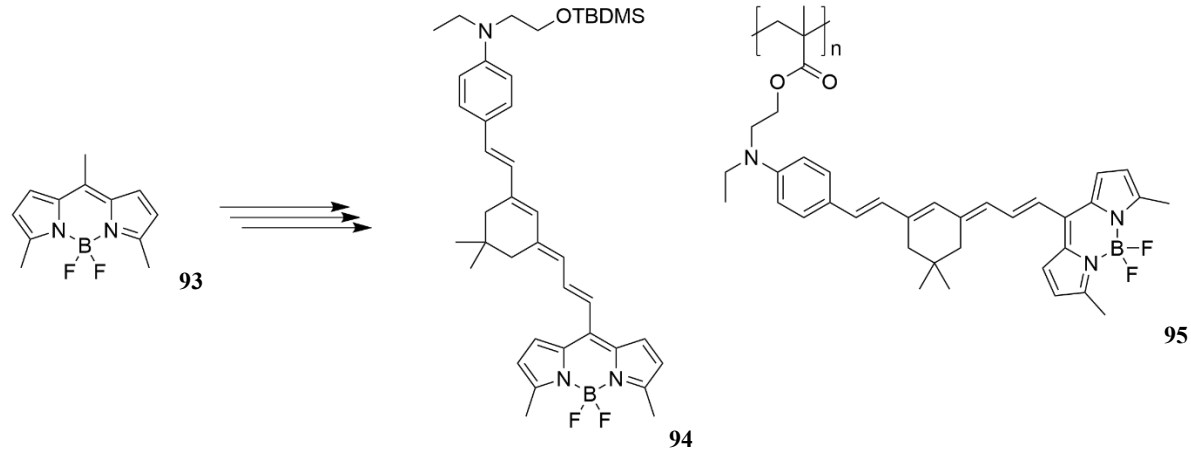

*Figure 49: Structures of BODIPY **93**, chromophore **94** and polymer **95**.*

The procedure by Macias-Contreras *et al.* was followed; a one-pot procedure condensing 2-methyl pyrrole **126** with acetyl chloride **96** followed by the complexation of the fluoroborate yielding BODIPY **93** (Figure 50).[85] A yield of 6% of **93** was achieved. Although this yield is very poor, the ease of a one-pot synthesis and convenient purification provided sufficient material to proceed.

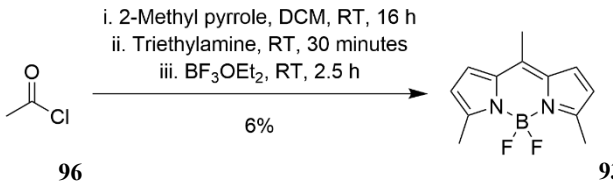

*Figure 50: One-pot BODIPY synthesis of BODIPY **93** from 2-methyl pyrrole **126** and acetyl chloride **96**.*

It was decided to follow the procedure reported by Palao *et al.* for a Knoevenagel condensation between aldehyde **56*E*/*Z*** and BODIPY **93,** owing to its similar reagents.[86] The first attempt at this reaction (Figure 51) was done on a 44 µmol scale in order to test the reaction, while 2 products were visible by TLC there was not enough product to be able to

characterise it. Most of the aldehyde starting material **56*E*/*Z*** had decomposed under the conditions, while the BODIPY **93** remained in the crude reaction mixture. The reaction was done a second time on a 308 µmol scale, and while only 3 nmol (2 mg) of product was isolated with a 1% yield, it was enough for complete characterisation.

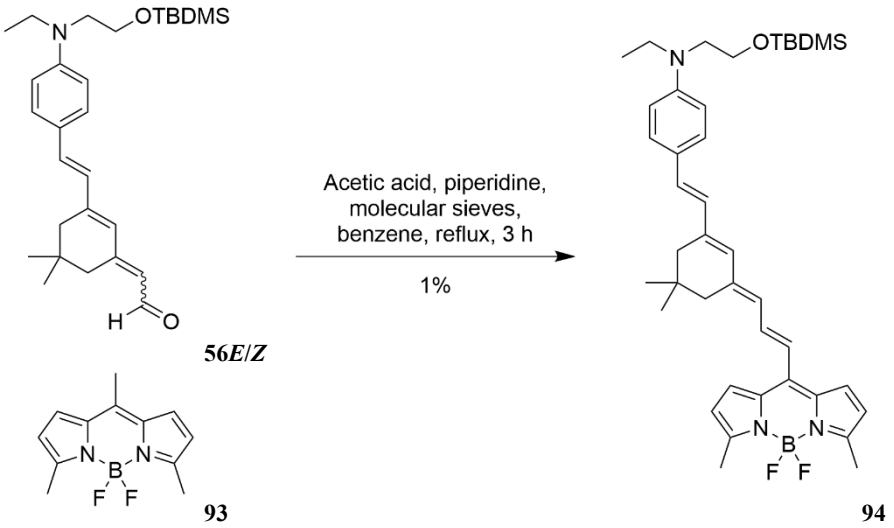

*Figure 51: Knoevenagel condensation reaction between aldehyde **56E/Z** and BODIPY **93** to afford chromophore **94**.*

After the first success at a novel chromophore, it was decided to focus on synthesising other chromophores with BODIPY derivatives as the withdrawing group.

2.3.2 The synthesis of chromophore **96**

The next BODIPY to be synthesised was BODIPY **28** giving us the target molecules chromophore **96** and polymer **97**. The synthesis of the unsubstituted BODIPY **28** is composed of 4 steps, and the synthetic route to **28** is shown in Scheme 6.[87–89]

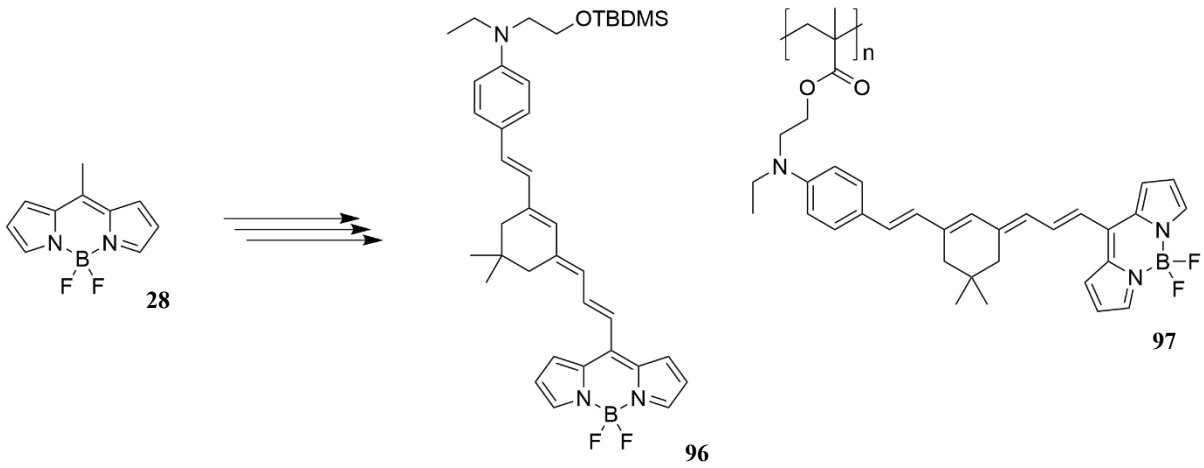

*Figure 52: Structures of BODIPY **28**, chromophore **96** and polymer **97**.*

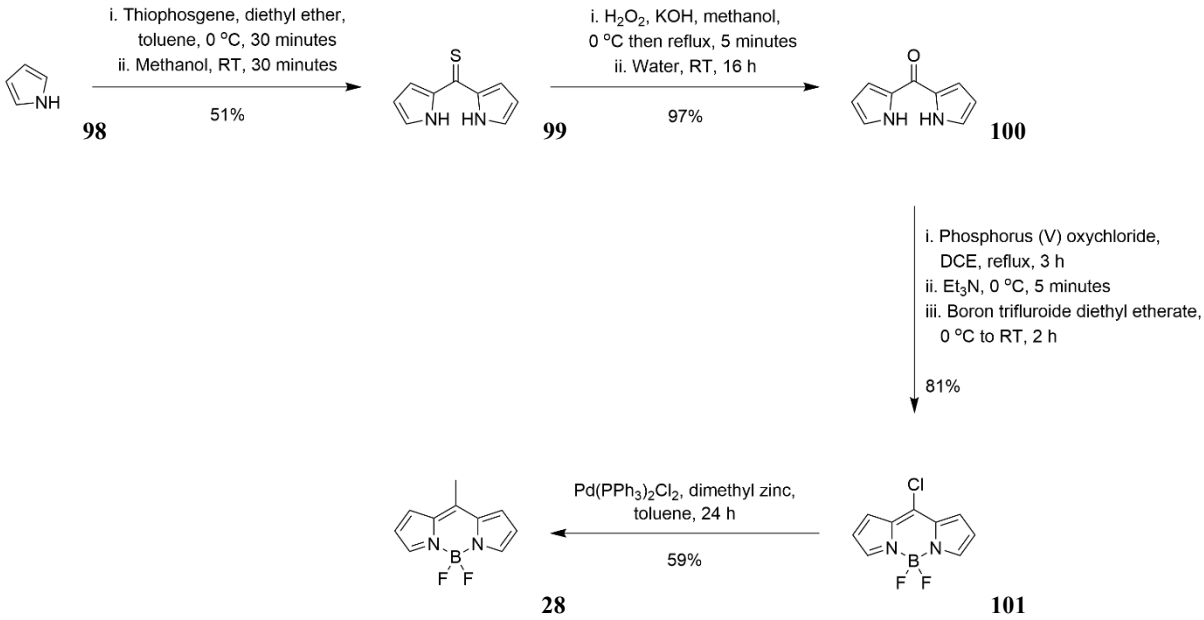

*Scheme 6: Synthetic route to BODIPY **28**.*

To begin the synthesis of BODIPY **28** is a two-consecutive addition-elimination reaction of pyrrole **98** on thiophosgene **102 (**Figure 53**)** to give thione **99** in a fair yield of 51%.

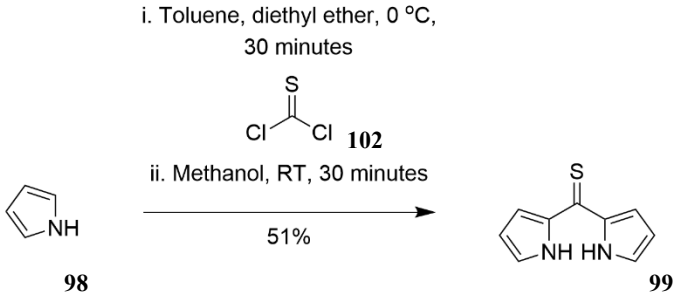

*Figure 53: Step 1 in the synthesis of BODIPY **28**. Two consecutive addition-elimination reactions of pyrrole **98** on thiophosgene **102** to afford thione **99**.*

Next in the synthesis of BODIPY **28** was the conversion of the thione moiety to a ketone using hydrogen peroxide and base. Excellent yields of up to 97% were achieved.

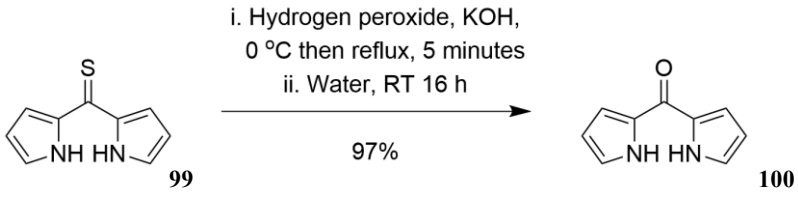

*Figure 54: Step 2 in the synthesis of BODIPY **28**.*

To complete the core of the unsubstituted BODIPY **28**, ketone **100** was reacted with phosphorous (V) oxychloride followed by complexation of the fluoroborate yielding BODIPY **101** (Figure 55). Very good yields of up to 81% were achieved when working on a smaller scale. Yields lowered to 40-50% when working on a gram scale.

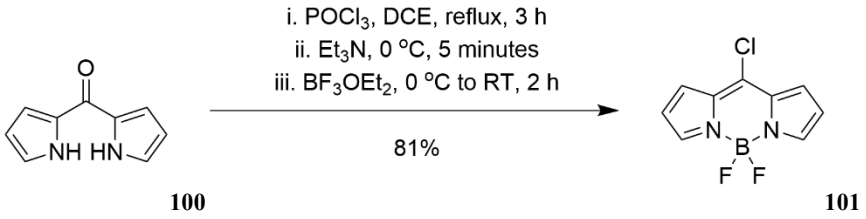

*Figure 55: Step 3 in the synthesis of BODIPY **28**.*

To add the slightly acidic methyl group to BODIPY **101**, a Negishi coupling reaction between **101** and dimethyl zinc in the presence of $Pd(PPh_3)_2Cl_2$ gave a yield of 59% of BODIPY **28**.

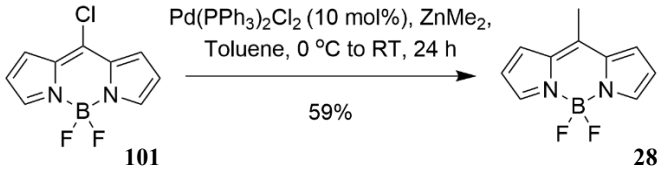

*Figure 56: Step 4 in the synthesis of BODIPY **28**. A Negishi coupling between BODIPY **101** and dimethyl zinc to afford BODIPY **28**.*

With the BODIPY **28** in hand, how to connect it was the next challenge. Although the Knoevenagel condensation reaction used in the synthesis of chromophore **94** did produce product, the conditions were unfavourable for the aldehyde starting material **56*E*/*Z*** which mostly decomposed in the acidic conditions. Milder conditions were considered. The conditions from the connection step of aldehyde **56*E*/*Z*** with **48** were tested, but with the addition of varying equivalents of sodium ethoxide (Table 9), as it was expected basic conditions would assist the reaction.

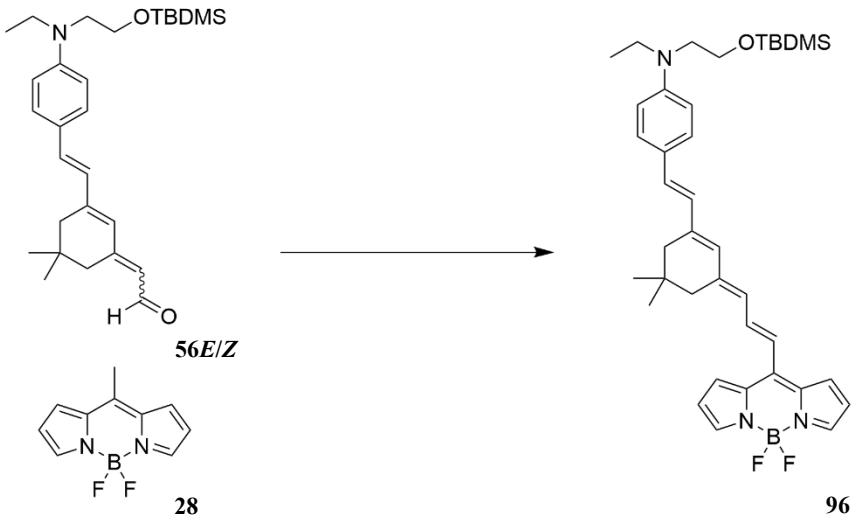

*Figure 57: Generic reaction scheme showing the reaction between aldehyde **56E/Z** and BODIPY **28** to form chromophore **96**.*

*Table 9: Table depicting the presence of product detected in reaction mixtures for the reaction between **56E/Z** and **28** to produce chromophore **96** using varied temperatures and equivalents of sodium ethoxide. All reactions were left for 5 hours and done on a 44 µmol scale. The presence of product was detected by LCMS.*

Reaction Conditions	**0.0 eq. NaOEt**	**0.1 eq. NaOEt**	**0.5 eq. NaOEt**	**1.0 eq. NaOEt**
RT	Trace products detected	No product detected	No product detected	No product detected
50 °C	Product detected	Trace products detected	Trace products detected	No product detected
Reflux	Product detected	Trace products detected		

Surprisingly, using 0.0 eq. of sodium ethoxide produced the best conversion over all of the temperatures. The reactions at 0.5 and 1.0 eq. of sodium ethoxide were excluded to not waste starting material, as it had become clear that the reactions with lower equivalents of base were performing better. Although the product was clearly visible in the LCMS TIC for 0.0 eq. of sodium ethoxide at 50 °C and reflux, the conversion was so minimal that it could not be measured using ^{1}H NMR integration values. Purification was attempted, but the minimal product made it difficult to purify. This reaction could be scaled up in order to reattempt purification, but it was decided against, instead to try different conditions.

Given the Knoevenagel condensation reaction between aldehyde **56*E*/*Z*** and BODIPY **93** did produce enough product for characterisation, it was decided to try a different one with milder conditions. Given that the chromophores had shown instability in acidic conditions both in the deprotection step of protected chromophore **49** to deprotected chromophore **60** and in the Knovenagel between aldehyde **56*E*/*Z*** and BODIPY **93** to form chromophore **94**, the Knovenagel procedure without acid reported by Conlon *et al.* was followed.[90] To begin with, aldehyde **56*E*/*Z*** and BODIPY **28** were dissolved in anhydrous IPA stirred together with 1.2 eq. of piperidine at reflux for 16 hours, overnight. The LCMS showed a complex mixture of products that did not contain the desired product. The temperature was lowered to 50 °C and the reagents were stirred for 4 hours. While product was seen in the LCMS TIC of the reaction mixture after 30 minutes, no product was detected after the 4 hours was complete and the solvent was removed in *vacuo*. After the reaction was put on again but only left for 30 minutes in total and an aqueous work up added, product was detected in the crude LCMS TIC. After column chromatography, a yield of 7% of **96** was achieved.

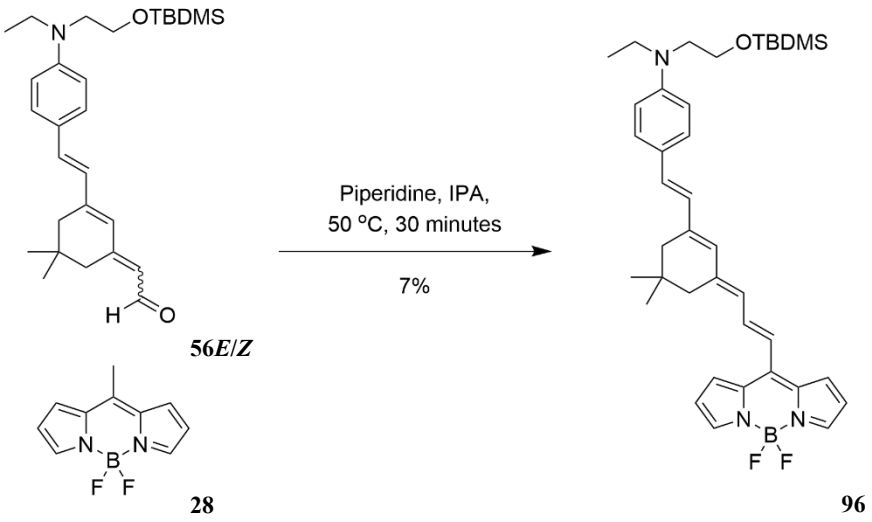

*Figure 58: Reaction between BODIPY **28** and aldehyde **56E/Z** to form chromophore **96**.*

2.3.3 The synthesis of chromophore **104**

The next BODIPY derivative to be synthesised was BODIPY **103** which possesses ethyl instead of methyl groups in the 3- and 7-positions. Thus, the next target molecules would be chromophore **104** and polymer **105**.

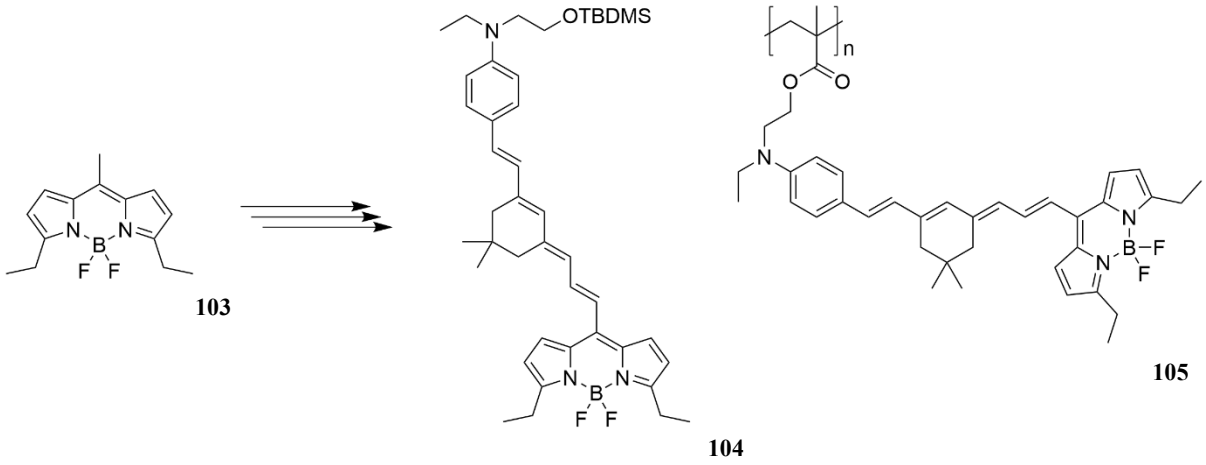

*Figure 59: Structures of BODIPY **103**, chromophore **104** and polymer **105**.*

In order to synthesise BODIPY **103**, the one-pot procedure used to synthesise BODIPY **93** could be used again. Unlike 2-methyl pyrrole **126**, 2-ethyl pyrrole **107** is not commercially available. It can be synthesised by the reduction of 2-acetyl pyrrole **106** using $LiAlH_4$. The procedure reported by Kancharla *et al*. was followed, using lithium aluminium hydride to reduce the ketone on 2-acetyl pyrrole.[91] Fair yields of up to 53% were achieved.

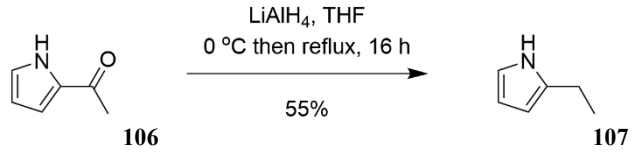

*Figure 60: Reduction of 2-acetyl pyrrole **106** to form 2-ethyl pyrrole **107**.*[91]

This time, for the one-pot procedure for the synthesis of 3,7-substituted BODIPY derivatives, it was theorised that instead of adding the pyrrole derivative dropwise to the stirring solution of acetyl chloride **96**, adding **96** dropwise to the stirring solution of the pyrrole derivative could produce higher yields owing to the difference in reactivity of the reagents. When adding the 2-ethyl pyrrole **107** dropwise to the stirring solution of acetyl chloride **96** a yield of 7% was achieved. When adding the acetyl chloride **96** dropwise to the stirring solution of 2-ethyl pyrrole **107** a yield of 12% was achieved.

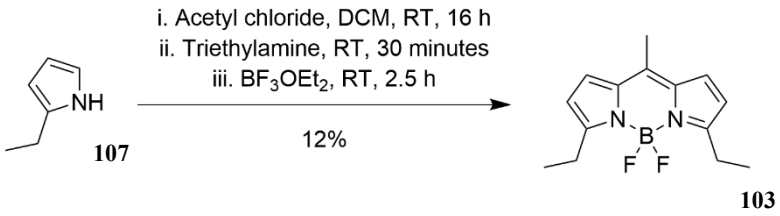

*Figure 61: One-pot BODIPY synthesis of BODIPY **103** from 2-ethyl pyrrole **107** and acetyl chloride **96**.*

Next, the Knoevenagel conditions developed in the synthesis of chromophore **96** were used on the new BODIPY derivative **103** producing a yield of 13% of **104**.

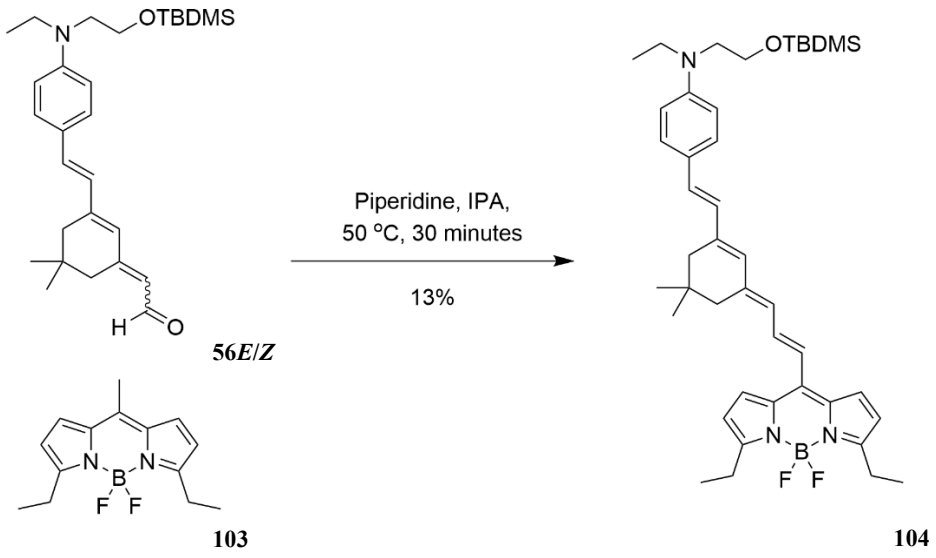

*Figure 62: Knoevenagel condensation reaction between aldehyde **56E/Z** and BODIPY **103** to form chromophore **104**.*

2.3.4 The synthetic route towards other chromophores with BODIPY derivatives as the electron-withdrawing group

Now that chromophores **94**, **96** and **104** with BODIPYs **28**, **93** and **103** as the withdrawing groups had been synthesised, it was set out to attempt to change the methyl group at the *meso*-position, thus elongating the π-bridge. Increasing the bridge could increase the polarisability or electro-optic coefficient by increasing the length of the dipole created upon the application of the electric field. The moieties in the *meso*-position would have to be π-conjugated and have a mildly acidic methyl group. The suitable groups decided upon were *p*-toluyl and *trans*-CH_3-CH=CH-. The target toluyl chromophores **111**, **112** and **113** and polymers **114**, **115** and **116** are shown in Figure 63 and the target *trans*-CH_3-CH=CH-chromophores **119**, **120** and **121** and polymers **122**, **123** and **124** are shown in Figure 64.

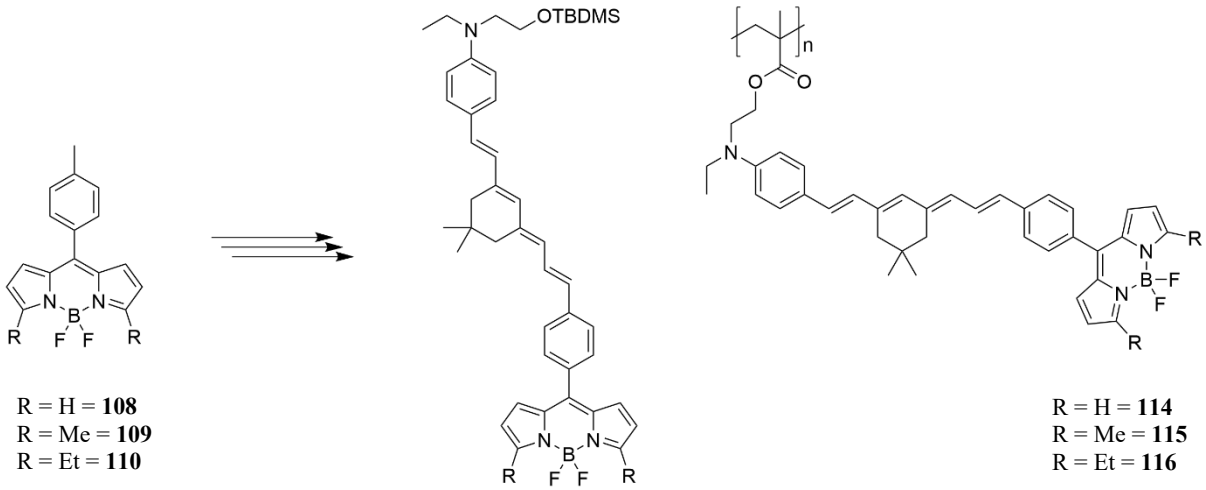

*Figure 63: Structures of BODIPYs **108**, **109** and **110**, chromophores **111**, **112** and **113** and polymers **114**, **115** and **116**.*

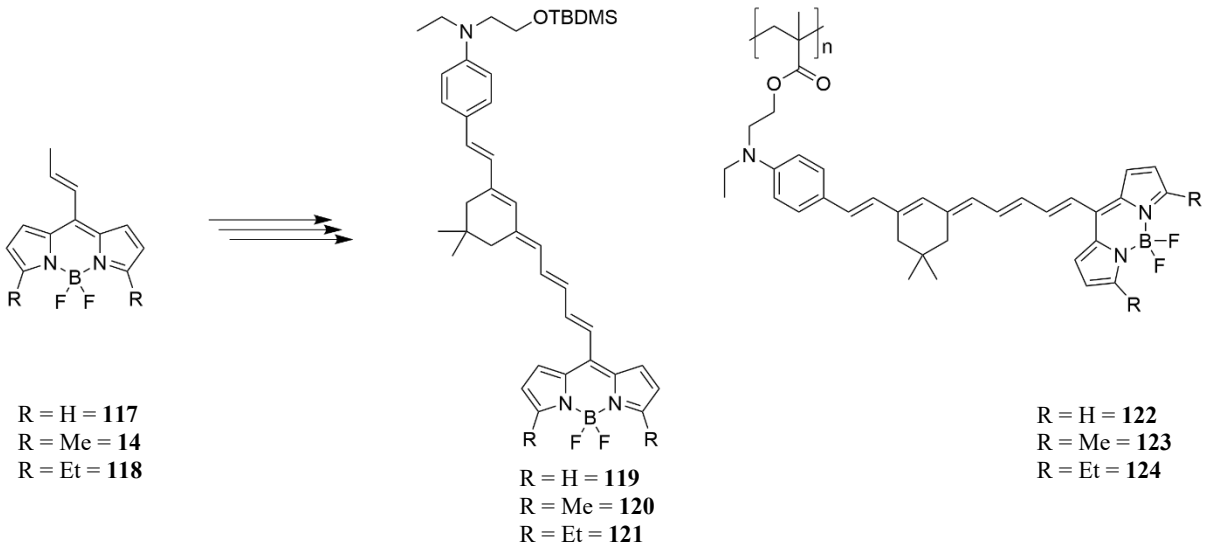

*Figure 64: Structures of BODIPYs **117**, **14** and **118**, chromophores **119**, **120** and **121** and polymers **122**, **123** and **124**.*

The next BODIPY derivatives synthesised were **109** and **110**. BODIPY **108** with hydrogen atoms in the 3- and 7-positions, similar to that of BODIPY **28**, would require a longer synthetic route. BODIPYs **108**, **109** and **110** are known compounds, although their reported syntheses use different reagents.[92–94] BODIPY **108** has been reported by Kaur *et al.* synthesised from 4-methyl benzaldehyde and pyrrole **98** with a yield of 70%.[92] BODIPY **109** has been reported by Chen *et al.* synthesised from 4-methyl benzaldehyde and 2-methyl pyrrole **126** with a yield of 27%.[93] BODIPY **110** has been reported by Duran-Sampedro *et al*. from BODIPY **127** by a Negishi coupling with dimethyl zinc with a yield of 73%.[94]

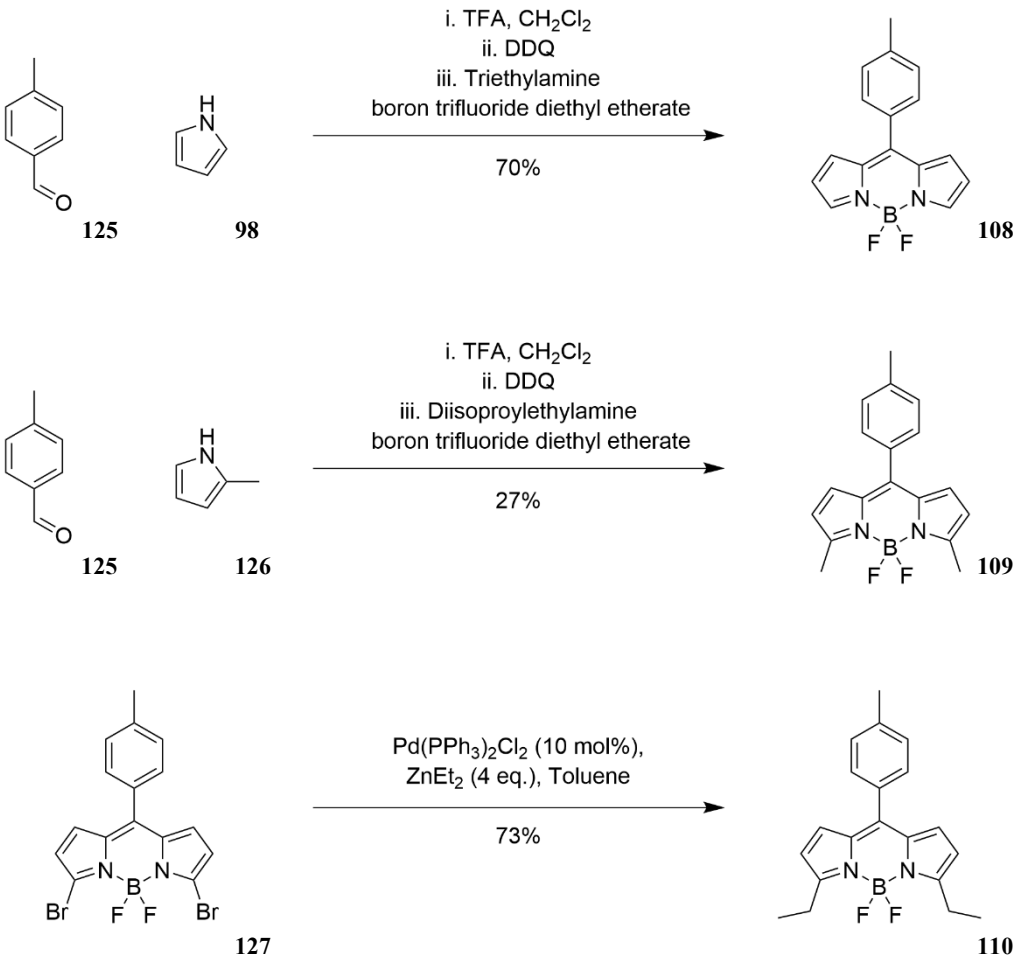

*Figure 65: Reported syntheses for BODIPYs **108**, **109** and **110**.*[92–94]

The one-pot procedure from BODIPYs **93** and **103** was followed with slight modifications. Again, it was hoped that by adding the more reactive acid chloride into a stirring solution of the pyrrole derivative (instead of adding the pyrrole derivative into the stirring solution of acid chloride), the yields would be improved. When the 2-methyl pyrrole **126** was added dropwise to a stirring solution of *p*-toluyl chloride, a yield of 0.5% of **109** was achieved. When the *p*-toluyl chloride was added to a stirring solution of 2-methyl pyrrole **126**, a yield of 10% of **109** was achieved. When the 2-ethyl pyrrole **107** was added dropwise to a stirring solution of *p*-toluyl chloride, a yield of 0.5% of **110** was achieved. When the *p*-toluyl chloride was added to a stirring solution of 2-ethyl pyrrole **107**, a yield of 10% of **110** was achieved.

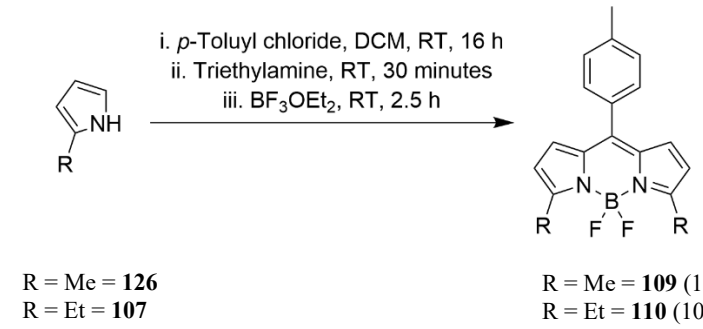

R = Me = **126**
R = Et = **107**

R = Me = **109** (10%)
R = Et = **110** (10%)

*Figure 66: Synthesis of BODIPY **109** and BODIPY **110** from 2-methyl pyrrole **126** and 2-ethyl pyrrole **107** respectively with p-toluyl chloride.*

When it came to the Knoevenagel condensations, the conditions from the synthesis of chromophores **96** and **104** were followed. No products were seen by TLC after 30 minutes so the reactions were left for 5 hours in total. Still, no products were seen by TLC or LCMS. Presumably, the lack of reaction would be owing to the *p*-toluyl methyl group having a higher pK_a than that of the methyl groups α to the *meso*-position in BODIPY derivatives **28**, **93** and **103**. Other Knoevenagel condensation conditions would need to be tested for these reactions.

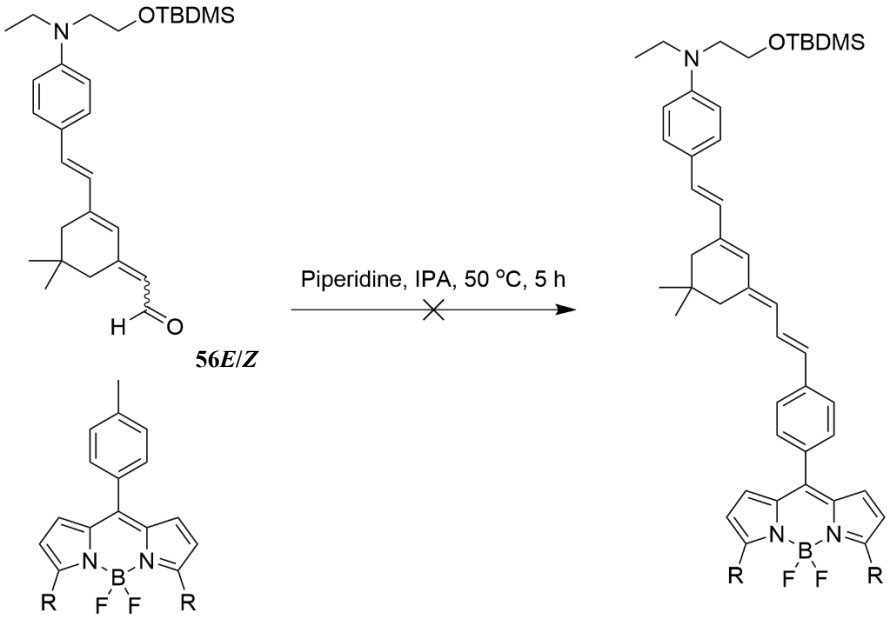

R = H = **108**
R = Me = **109**
R = Et = **110**

R = H = **111**
R = Me = **112**
R = Et = **113**

*Figure 67: Proposed reaction to chromophores **111**, **112** and **113** from aldehyde **56E/Z** and BODIPYs **108**, **109** and **110** respectively.*

The next BODIPYs to be synthesised were with *trans*-CH_3CH=CH- in the *meso*-position. Again the one-pot BODIPY synthesis conditions were used, adding the crotonoyl chloride to the stirring solution of the respective pyrrole. Upon the completion of the reactions, neither of the desired product masses for **14** or **118** were detected by LCMS, although small amounts of BODIPY-looking products were visible by TLC. BODIPY compounds are characteristically

very bright compounds (often orange-red), that are very fluorescent (often yellow-green) under UV light. After column chromatography, the BODIPY products that were isolated were found to be those with methyl groups in the *meso*-position, **93** (3% yield) and **103** (0.6% yield) respectively. As discussed in Section 1.3.1, a double bond in the *meso*-position is activated.

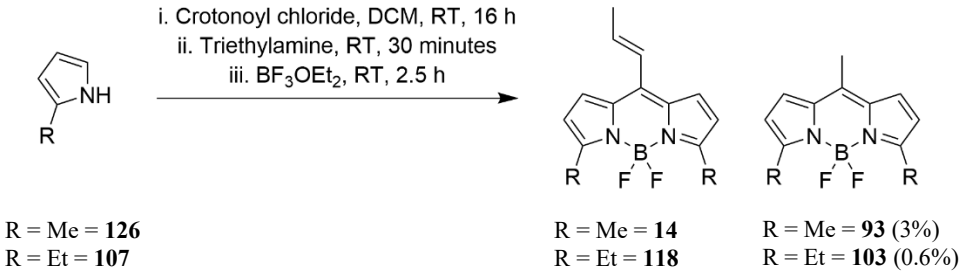

R = Me = **126**
R = Et = **107**

R = Me = **14**
R = Et = **118**

R = Me = **93** (3%)
R = Et = **103** (0.6%)

*Figure 68: Proposed reaction to synthesise BODIPYs **14** and **118** that was shown to produce trace amounts of BODIPYs **93** and **103** respectively.*

BODIPY derivatives with *trans*-CH_3CH=CH- groups have been reported, but with longer preparations, comparable to that of BODIPY **28**.[38,95] **14**, **117** and **118** could be synthesised by this method and then the Knoevenagel condensations tested.

2.4 Conclusions and Future Work

So far, the chromophore **49** has been synthesised, and a deprotection completed, but the addition of the methacryloyl moiety and subsequent polymerisation steps have yet to be completed. The overall percentage yield achieved for chromophore **49** was 12% with respect to the 4-fluorobenzaldehyde **50**.

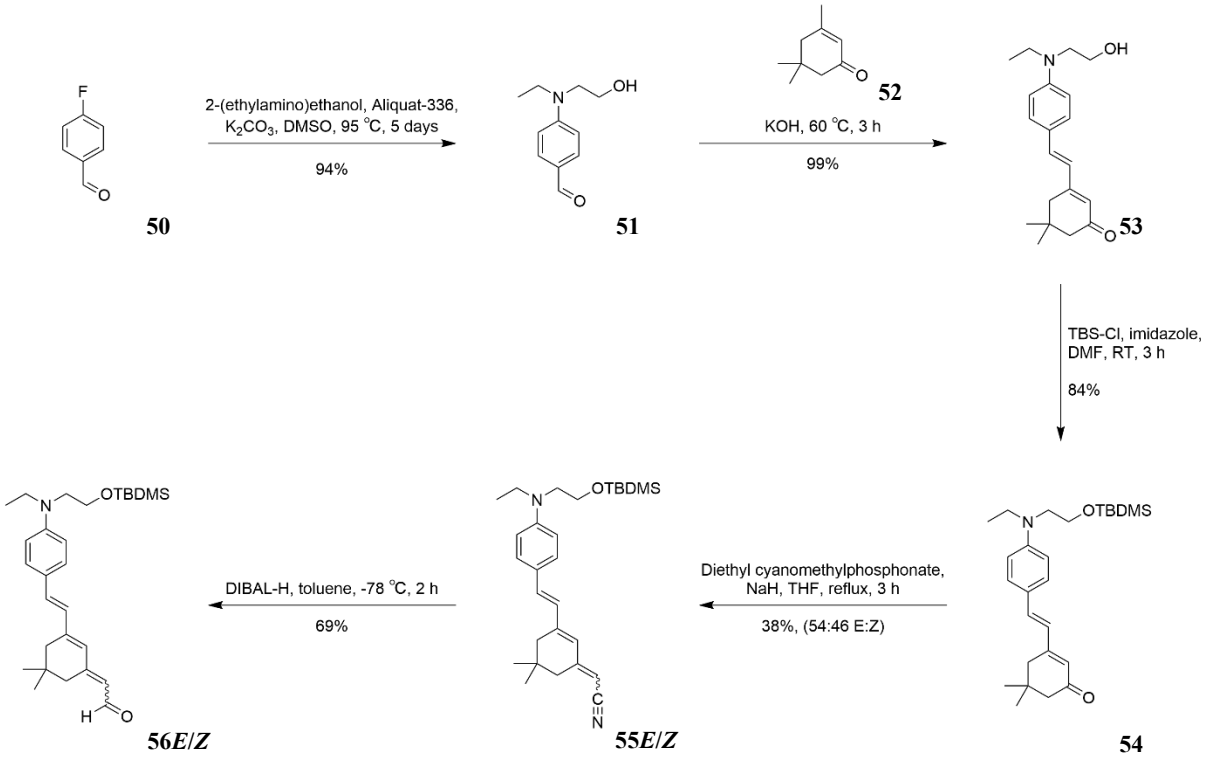

*Scheme 7: Reaction scheme for the partial synthesis of polymer **45** including yields, part 1.*

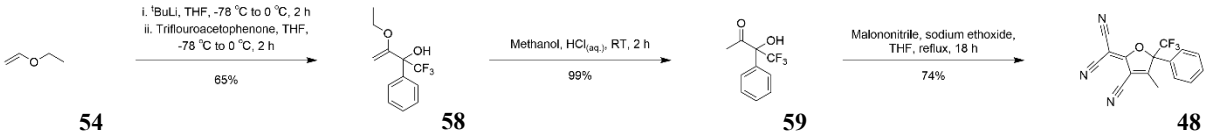

*Scheme 8: Reaction scheme for the partial synthesis of polymer **45** including yields, part 2.*

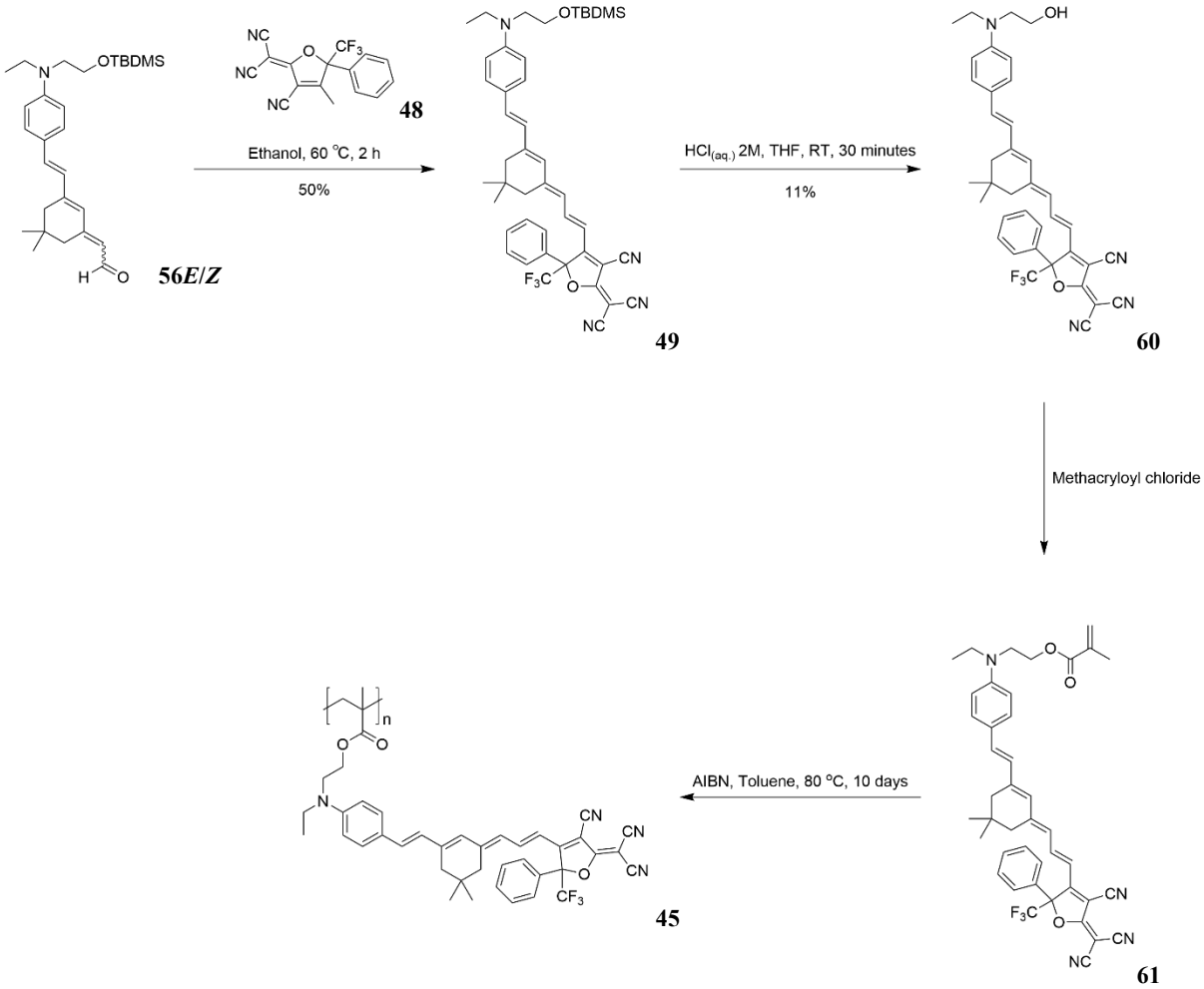

*Scheme 9: Reaction scheme for the partial synthesis of polymer **45** including yields, part 3.*

A synthetic route towards chromophore **79** was begun, up to aldol product **80**. Ideally, more work to increase the percentage yield of the aldol condensation reaction would be carried out and then the product carried forward to complete the synthesis of polymer **46**.

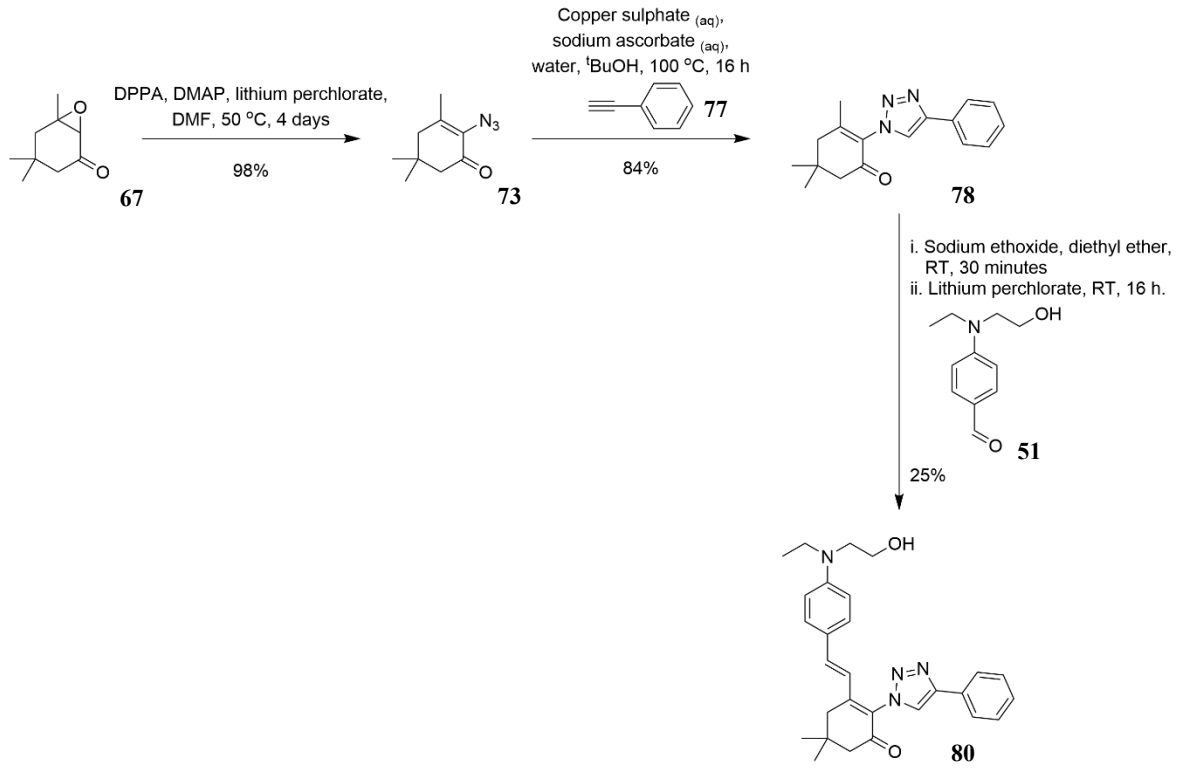

*Scheme 10: Reaction scheme for the partial synthesis of polymer **79** including yields.*

A synthetic route towards chromophore **82** was also begun, up to aldol product **90**. Again, more work needs to be carried out to increase the percentage yield of the aldol condensation reaction and increase the diastereomeric excess. After this, the **90** can be carried forward to complete the synthesis of polymer **47**.

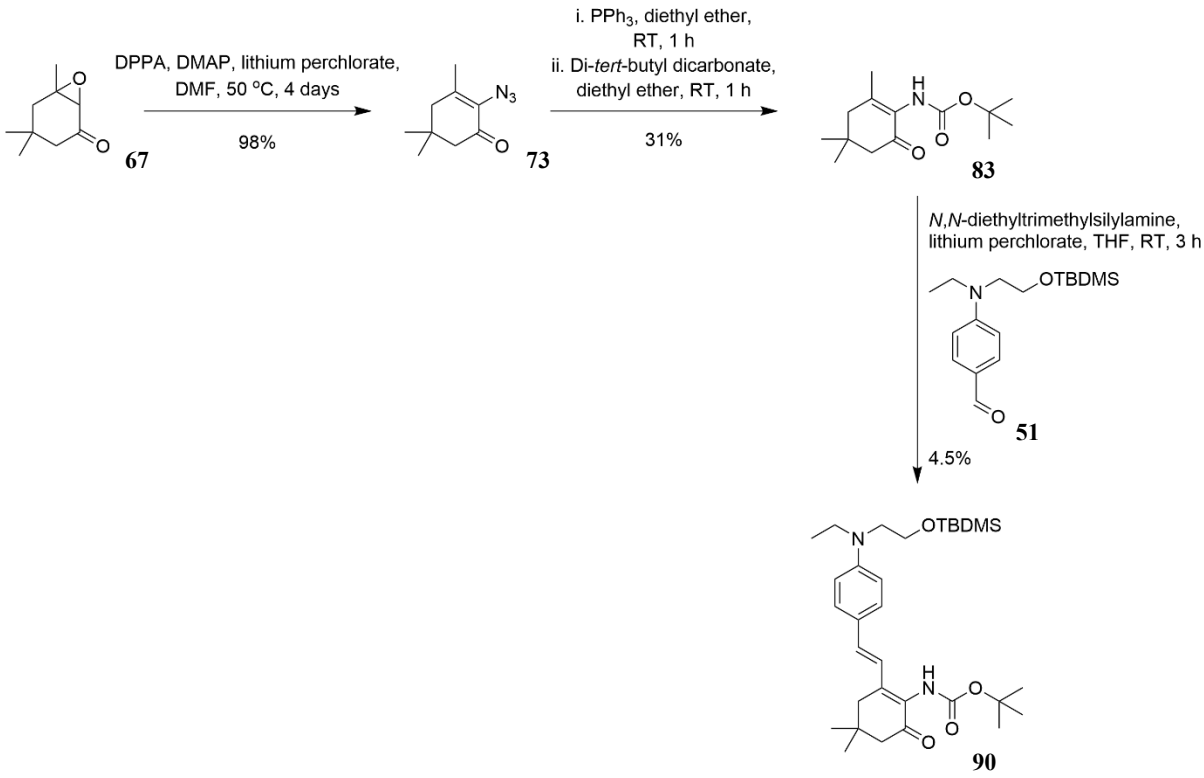

*Scheme 11: Reaction scheme for the partial synthesis of polymer **47** including yields.*

Chromophore **94** has been synthesised, with an overall yield of 0.2% with respect to the 4-fluorobenzaldehyde **50**. It is expected that the yield would increase both if the acetyl chloride **96** was added dropwise to the stirring solution of 2-methyl pyrrole **126** and also if the Knoevenagel conditions developed for the syntheses of chromophores **96** and **104** were used.

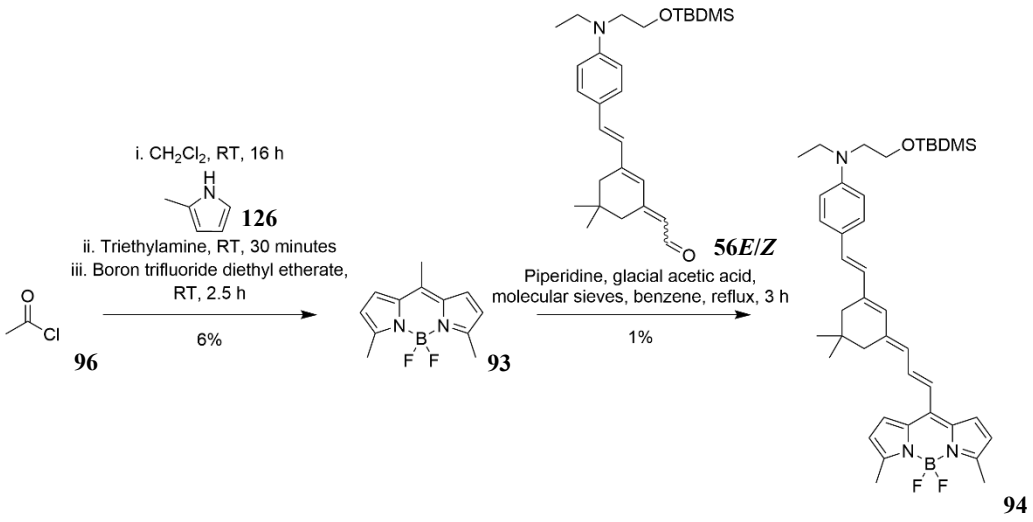

*Scheme 12: Reaction scheme for the partial synthesis of polymer **95** including yields.*

Chromophore **96** was synthesised with an overall yield of 1.7% with respect to the 4-fluorobenzaldehyde **50**.

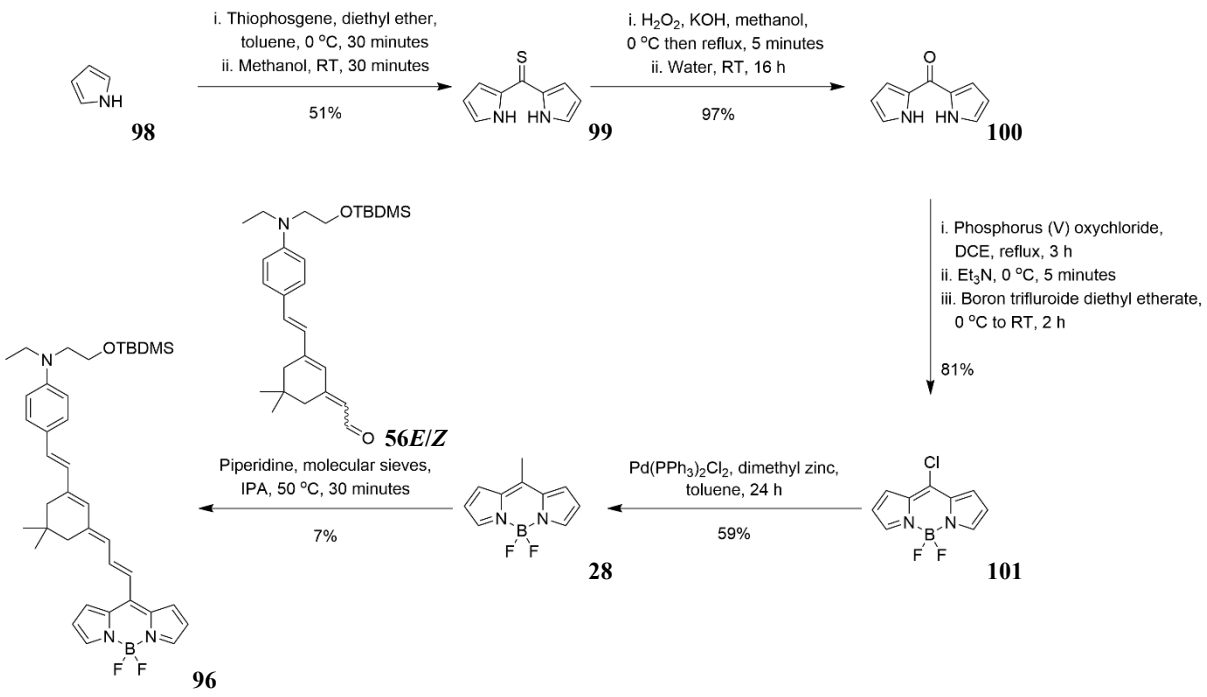

*Scheme 13: Reaction scheme for the partial synthesis of polymer **97** including yields.*

Chromophore **104** has been synthesised with an overall yield of 3.2% with respect to the 4-fluorobenzaldehyde **50**.

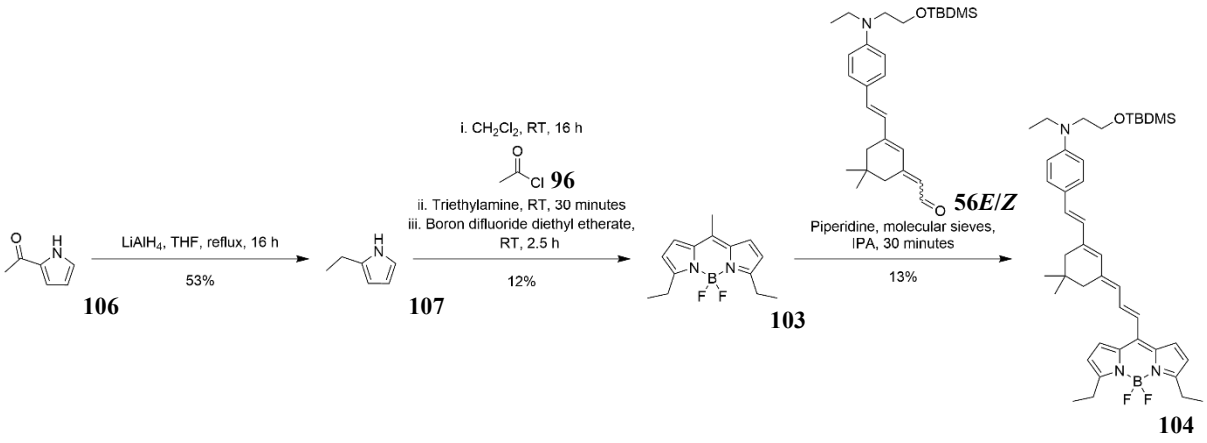

*Scheme 14: Reaction scheme for the partial synthesis of polymer **105** including yields.*

The next steps for this project are to take chromophores **49**, **94**, **96** and **104**, deprotect the alcohol using TBAF, connect to methacroloyl chloride and subsequently polymerise. It has been suggested that approximately 2 grams of each polymer are required for optoelectronic testing, so significantly scaled-up reactions will also need to occur.

Other reported Knoevenagel conditions can be tested on BODIPYs **109** and **110** with aldehyde **56*E*/*Z***. Alternatively, higher equivalents of piperidine or the addition of another base could encourage the deprotonation of the *p*-toluyl methyl group and the proceeding of

the reaction. Owing to the instability of the aldehyde **56*E*/*Z*** and chromophore **49** in acidic conditions seen in the deprotection step (Figure 33) and first Knoevenagel condensation (Figure 51), using acid would be discouraged.

BODIPYs **14**, **117** and **118** could be synthesised by a 3-step procedure featuring a Liebeskind−Srogl coupling, which has been reported for BODIPY **14**.[38] This route does not produce water in the final step, which will eliminate the double bond hydration.[38,87,95,96] Upon their synthesis, Knoevenagel conditions could be tested on all three.

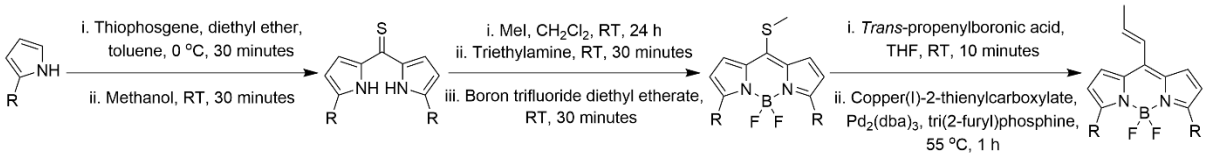

R = H = **98**
R = Me = **126**
R = Et = **107**

R = H = **99**
R = Me = **128**
R = Et = **129**

R = H = **130**
R = Me = **131**
R = Et = **132**

R = H = **117**
R = Me = **14**
R = Et = **118**

*Scheme 15: Proposed synthesis of BODIPYs **14**, **117** and **118**.*[38,87,95,96]

This synthetic route could also be used to synthesise BODIPY **108**, by replacing the *trans*-propenylboronic acid with *p*-methylphenylboronic acid. Similarly, BODIPYs with additional substitutions around the ring could be synthesised with the modified one-pot procedure. Again, Knoevenagel conditions could then be tested.

Looking further into the future, further novel structures can be synthesised by changing the electron-donating, withdrawing and bridge regions of the polymer. At first, other alkynes could be used for the click chemistry azide-alkyne cycloaddition from the synthesis of chromophore **79**, containing hydrogen bonding groups to increase the polarisability of the polymer. Then, other isophorone-based π-bridges from Figure 34 could be synthesised. These options will increase the rigidity of the polymer with side chains and also ideally increase the electro-optic coefficient.

As mentioned in Section 1.2.3, there is little variety currently reported in the donating region so this area could also be investigated; new donating groups such as pyrrole or an ether could be substituted in the place of the *para*-amine to see what effect this may have upon the properties of the polymer. Alternatively, the withdrawing region from chromophore **49** could be altered by changing the phenyl/trifluoromethyl groups such as in Figure 7.

Experimental Details

3.1 General details

Solvents were obtained from Sigma-Aldrich, Acros-Organics or Fisher Scientific. Reagents were purchased from Alpha Aesar, Fluorochem, Sigma-Aldrich or Acros-Organics and used as received, except for malononitrile **66** which was first distilled.

Analytical TLC were taken on aluminium-backed silica plates and compounds were visualised by fluorescence. Column chromatography was performed with Sigma-Aldrich 40-63 μm silica gel.

Nuclear magnetic resonance (NMR) spectra were recorded in $CDCl_3$ on a Bruker AV400 spectrometer. Chemical shifts (δ) are reported in parts per million (ppm). Coupling constants (*J*) are reported in Hz. Splitting patterns are abbreviated to: singlet (s), doublet (d), triplet (t), quartet (q), multiplet (m), or the appropriate combination of these. NMR assignments of the molecules were assisted by 2D experiments (COSY, HSQC and HMBC).

LCMS samples were analysed using a Waters (Manchester, UK) Acquity TQD mass tandem quadrupole mass spectrometer. Samples were introduced to the mass spectrometer *via* an Acquity H-Class quaternary solvent manager (with TUV detector at 254 nm, sample and column manager). Ultrahigh-performance liquid chromatography was undertaken using Waters BEH C18 (or equivalent) column (50 mm × 2.1mm 1.7μm). Gradient elution from 20% acetonitrile (0.2% formic acid) to 100% acetonitrile (0.2% formic acid) was performed over five/ten minutes at a flow rate of 0.6 mL/min. Low-resolution positive/negative ion electrospray ionisation mass spectra were recorded.

High-resolution mass spectrometry samples were analysed using a MaXis (Bruker Daltonics, Bremen, Germany) time of flight (TOF) mass spectrometer. Samples were introduced to the mass spectrometer via a Dionex Ultimate 3000 autosampler and uHPLC pump. Ultrahigh-performance liquid chromatography was performed using a Waters, Acquity UPLC BEH C18 (50 mm × 2.1 mm 1.7um) column. Gradient elution from 5% acetonitrile (0.2% formic acid) to 100% acetonitrile (0.2% formic acid) was performed in five minutes at 0.6 mL/min. High-resolution positive/negative ion electrospray ionisation mass spectra were recorded.

Infrared spectra were recorded on a Thermo Scientific Nicolet is5. 16 scans of the 4000-600 cm^{-1} were taken per spectrum with a resolution of 4 cm^{-1}. Absorption maxima (ν_{max}) are reported in wavenumbers (cm^{-1}).

3.2 4-(Ethyl(2-hydroxyethyl)amino)benzaldehyde **51**

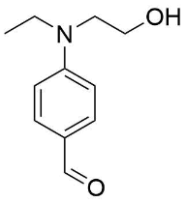

4-Fluorobenzaldehyde **50** (17.28 mL, 20.00 g, 0.16 mol, 1.0 eq.), 2-(ethylamino)ethanol **62** (47.12 mL, 43.08 g, 0.48 mol, 3.0 eq.), Aliquat-336 (0.64 mL, 0.56 g, 0.72 mmol, 4.5 $_{x10}^{-3}$ eq.) and K_2CO_3 (33.16 g, 0.24 mol, 1.5 eq.) were dissolved in DMSO (100 mL), heated to 95 °C and stirred for 4 days. The reaction mixture was allowed to cool to RT and then poured into an ice/water mixture. The aqueous/organic layers were separated then the aqueous layer was extracted with CH_2Cl_2 (2 × 200 mL). The combined organic layers were dried over $MgSO_4$ and concentrated in *vacuo*. The oil was re-dissolved in diethyl ether (100 mL) and $HCl_{(aq.)}$ (1 mol dm^{-3}, 300 mL) and stirred for 15 minutes. The aqueous and organic layers were separated. The aqueous layer was neutralised with Na_2CO_3 and then extracted with CH_2Cl_2 (3 × 100 mL). The CH_2Cl_2 layers were dried over $MgSO_4$ and concentrated in *vacuo*. The product was purified with column chromatography (0–40% ethyl acetate in CH_2Cl_2) giving 4-(ethyl(2-hydroxyethyl)amino)benzaldehyde **51** (18.06 g, 93 mmol, 58%) as a yellow oil. The analytical data matches that reported in the literature.[71]

R_f (40% ethyl acetate in CH_2Cl_2) 0.50; **^{1}H NMR** (400 MHz, $CDCl_3$) δ 9.71 (s, 1H, C*H*O), 7.73–7.68 (m, 2H, Ar(C*H*)-*m*-N), 6.78–6.72 (m, 2H, Ar(C*H*)-*o*-N), 3.86 (q, *J* = 6.0, 2H, CH_2-OH), 3.58 (t, *J* = 6.0, 2H, N-CH_2-CH_2), 3.53 (q, *J* = 7.0, 2H, N-CH_2-CH_3), 1.22 (t, *J* = 7.0, 3H, CH_3); **^{13}C NMR** (100 MHz, $CDCl_3$) δ 190.33 (*C*O), 152.86 (Ar(*C*)-*i*-N), 132.40 (Ar(*C*H)-*m*-N), 125.33 (Ar(*C*)-*p*-N), 111.18 (Ar(*C*H)-*o*-N), 60.25 (*C*H_2-OH), 52.32 (N-*C*H_2-CH_2), 45.90 (N-*C*H_2-CH_3), 12.05 (N-CH_2-*C*H_3); **MS** (ESI^+) m/z 194 $[M+H]^+$; **FTIR** (ν_{max}) 3393 (O-H stretching), 2972 (C-H stretching), 2820 and 2742 (C-H stretching, aldehyde, doublet), 1655 (C=O stretching) cm^{-1}.

3.3 (*E*)-3-(4-(Ethyl(2-hydroxyethyl)amino)styryl)-5,5-dimethylcyclohex-2-en-1-one **53**

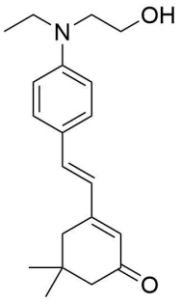

Isophorone **52** (0.47 mL, 0.43 g, 3.10 mmol, 1.2 eq.) was added to a vial and stirred vigorously. Powdered potassium hydroxide (0.17 g, 3.10 mmol, 1.2 eq.) was added and stirred for 10 minutes until a colour change to purple was observed. 4-(Ethyl(2-hydroxyethyl)amino)benzaldehyde **51** (0.50 g, 2.58 mmol, 1.0 eq.) was added then the reaction mixture was heated to 60 °C and stirred for 16 hours, overnight. The reaction mixture was cooled to RT then dissolved in CH_2Cl_2 (5 mL) and glacial acetic acid (0.17 mL, 3.10 mmol, 1.2 eq.) in water (5 mL), and stirred for 30 minutes. The aqueous and organic layers were separated before the organic layer was washed with water (5 mL) and then brine (5 mL). The crude solution was

dried over $MgSO_4$ then treated with activated charcoal (0.1 g) and stirred for 1 hour. The mixture was filtered through a plug of Celite® then the solvent was removed in *vacuo*. The viscous orange oil was re-dissolved in diethyl ether (2 mL) and ethyl acetate (1 mL) and stirred for 2 hours at 0 °C. The solid crude product was filtered and any excess solvent was removed in *vacuo* yielding (*E*)-3-(4-(ethyl(2-hydroxyethyl)amino)styryl)-5,5-dimethylcyclohex-2-en-1-one **53** (0.765 g, 2.44 mmol, 94%) as an orange-red oil. Recrystallisation from ethyl acetate gave orange crystals. The analytical data matches that reported in the literature.[72]

R_f (40% ethyl acetate in hexane) 0.20; **mp** 114–125 °C; **^{1}H NMR** (400 MHz, $CDCl_3$) δ 7.32 (d, *J* = 9.0, 2H, Ar(C*H*)-*o*-*N*), 6.94–6.84 (m, 1H, Ar-CH-C*H*), 6.72–6.60 (m, 3H, Ar(C*H*)-*m*-N and Ar-C*H*), 5.92 (s, 1H, CO-C*H*), 3.77 (t, *J* = 6.0, 2H, CH_2-OH), 3.48 (t, *J* = 6.0, 2H, N-CH_2-CH_2), 3.43 (q, *J* = 7.0, 2H, N-CH_2-CH_3), 2.40 (s, 2H, C(CH_3)$_2$-CH_2), 2.22 (s, 2H, CO-CH_2), 1.15 (t, *J* = 7.0, 3H, N-CH_2-CH_3), 1.05 (s, 6H, C(CH_3)$_2$); **^{13}C NMR** (100 MHz, $CDCl_3$) δ 200.56 (*C*O), 156.63 (Ar(*C*)-*i*-N), 148.97 (CO-CH-*C*), 135.88 (Ar-CH-*C*H), 129.02 (Ar(*C*H)-*m*-N), 124.62 (CO-*C*H), 124.30 (Ar-*C*H), 123.61 (Ar(*C*)-*p*-N), 111.91 (Ar(*C*H)-o-N), 59.81 (*C*H_2-OH), 52.28 (N-*C*H_2-CH_2), 51.28 (CO-*C*H_2), 45.44 (N-*C*H_2-CH_3), 39.02 (C(CH_3)$_2$-*C*H_2), 33.23 (*C*(CH_3)$_2$), 28.48 (C(*C*H_3)$_2$), 12.04 (N-CH_2-*C*H_3); **MS** (ESI$^+$) m/z 314 $[M+H]^+$; **FTIR** (ν_{max}) 3321 (O-H stretching), 2953 (C-H stretching), 2877 (C-H stretching), 1633 (C=O stretching), 1590 (C=C stretching) cm^{-1}.

3.4 (*E*)-3-(4-((2-((*Tert*-butyldimethylsilyl)oxy)ethyl)(ethyl)amino)styryl)-5,5-dimethylcyclohex-2-en-1-one **54**

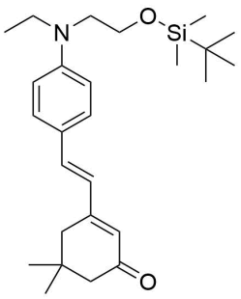

(*E*)-3-(4-(Ethyl(2-hydroxyethyl)amino)styryl)-5,5-dimethylcyclohex-2-en-1-one (1.650 g, 5.26 mmol, 1.0 eq.) **53**, imidazole (0.86 g, 0.013 mol, 2.4 eq.) and *tert*-butyldimethylsilylchloride (1.98 g, 0.013 mol, 2.4 eq.) were dissolved in DMF (10 mL) and stirred at RT for 16 hours, overnight. Water (5 mL) was added to quench the reaction then the product was extracted with ethyl acetate (3 × 10 mL). The combined organics were dried over $MgSO_4$ then the solvent was removed in *vacuo*. The product was purified by column chromatography (0-10% ethyl acetate in hexane) yielding (*E*)-3-(4-((2-((*tert*-butyldimethylsilyl)oxy)ethyl)(ethyl)amino)styryl)-5,5-dimethylcyclohex-2-en-1-one **54** (1.752 g, 4.10 mmol, 78%) as an orange oil. The analytical data matches that reported in the literature.[73]

R_f (20% ethyl acetate in hexane) 0.30; **^{1}H NMR** (400 MHz, $CDCl_3$) δ 7.35 (d, J = 9.0, 2H, Ar(C*H*)-*m*-N), 6.95–6.8 (m, 1H, Ar-CH-C*H*), 6.72–6.67 (m, 1H, Ar-C*H*), 6.64 (d, J =9.0, 2H, Ar(C*H*)-*o*-N), 5.99 (s, 1H, CO-C*H*), 3.76 (t, J = 6.5, 2H, CH_2-O-Si), 3.50–3.36 (m, 4H, N-CH_2-CH_2 and N-CH_2-CH_3), 2.45 (s, 2H, C$(CH_3)_2$-CH_2), 2.27 (s, 2H, CO-CH_2), 1.17 (t, J = 7.0, 3H, N-CH_2-CH_3), 1.08 (s, 6H, C$(CH_3)_2$), 0.88 (s, 9H, Si-C(C$H_3)_3$), 0.03 (s, 6H, Si(C$H_3)_2$); **^{13}C NMR** (100 MHz, $CDCl_3$) δ 200.16 (*C*O), 156.13 (Ar(*C*)-*i*-N), 148.80 (CO-CH-*C*), 135.73 (CO-CH-*C*H), 129.05 (Ar(*C*H)-*m*-N), 124.94 (CO-*C*H), 124.40 (Ar-*C*H), 123.48 (Ar(*C*)-*p*-N), 111.65 (Ar(*C*H)-*o*-N), 60.67 (*C*H_2-O-Si), 52.49 (N-*C*H_2-CH_2), 51.51 (CO-*C*H_2), 45.64 (N-*C*H_2-CH_3), 39.20 (C$(CH_3)_2$-*C*H_2), 33.36 (*C*$(CH_3)_2$), 28.63 (C(*C*$H_3)_2$), 25.98 (Si-C(*C*$H_3)_3$), 18.35 (Si-*C*$(CH_3)_3$), 12.26 (N-CH_2-*C*H_3), −5.29 (Si(*C*$H_3)_2$); **MS** (ESI^+) m/z 428 $[M+H]^+$; **FTIR** (ν_{max}) 2930 (C-H stretching), 2860 (C-H stretching), 1652 (C=O stretching), 1594 (C=C stretching) cm^{-1}.

3.5 (*E*)-2-(3-((*E*)-4-((2-((*Tert*-butyldimethylsilyl)oxy)ethyl)(ethyl)amino)styryl)-5,5-dimethylcyclohex-2-en-1-ylidene)acetonitrile **55*E/Z***

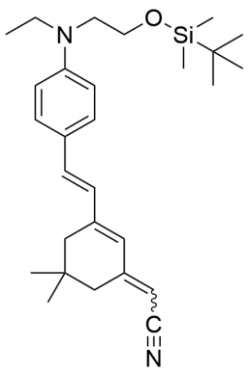

Sodium hydride (60% in mineral oil, 1.00 g, 0.025 mol, 3.0 eq.) was put under an inert atmosphere of argon gas and then dissolved in anhydrous THF (40 mL). The mixture was cooled to 0 °C and stirred while diethyl cyanomethylphosphonate **64** (1.819 mL, 0.41 g, 0.016 mol, 2.0 eq.) was added dropwise. The mixture was allowed to stir for 30 minutes until the solution became clear. (*E*)-3-(4-((2-((*tert*-butyldimethylsilyl)oxy)ethyl)(ethyl)amino)styryl)-5,5-dimethylcyclohex-2-en-1-one **54** (3.5 g, 8.34 mmol, 1.0 eq.) was dissolved in anhydrous THF (5 mL) and added to the reaction mixture via syringe, the solution was heated to reflux and allowed to stir for 3 hours. The reaction was quenched with ammonium chloride (saturated solution, 50 mL) then the product was extracted with ethyl acetate (3 × 30 mL). The combined organic layers were dried over $MgSO_4$ then the solvent was removed in *vacuo*. The product was purified by column chromatography (0-20% ethyl acetate in hexane) yielding an inseparable mix of isomers: (*E*)-2-(3-((*E*)-4-((2-((*tert*-butyldimethylsilyl)oxy)ethyl)(ethyl)amino)styryl)-5,5-dimethylcyclohex-2-en-1-ylidene)acetonitrile **55*E*** and (*Z*)-2-(3-((*E*)-4-((2-((*tert*-butyldimethylsilyl)oxy)ethyl)(ethyl)amino)styryl)-5,5-dimethylcyclohex-2-en-1-ylidene)acetonitrile **55*Z*** (E:Z, 54:46) (2.65 g of **55*E*/*Z***, 3.18 mmol (*E*), 38% (*E*)) as a dark orange oil.

R_f (20% ethyl acetate in hexane) 0.50; **^{1}H NMR** (400 MHz, $CDCl_3$) δ 7.35–7.30 (m, 2H, Ar(C*H*)-*m*-N), 6.76–6.70 (m, 1H, Ar-CH-C*H*), 6.71 (s, 0.5H, NC-CH-C-C*H* (*Z*)), 6.68 (m, 3H, Ar(C*H*)-*o*-N and Ar-C*H*), 6.21 (s, 0.5H, NC-CH-C-C*H* (*E*)), 5.06 (s, 0.54H, NC-C*H* (*E*)), 4.89 (s, 0.46H, NC-C*H*(*Z*)), 3.80–3.70 (m, 2H, CH_2-O-Si), 3.50–3.32(m, 4H, N-CH_2-CH_2 and N-CH_2-CH_3), 2.46 (d, *J* = 1.5, 1H, NC-CH-C-CH_2(*E*)), 2.30 (s, 2H, C(CH_3)$_2$-CH_2), 2.22 (d, *J* = 1.5, 1H, NC-CH-C-CH_2(*Z*)), 1.18 (td, *J* = 7.0 and 2.5, 3H, N-CH_2-CH_3), 1.03 (s, 3H, C(CH_3)$_2$(*E*)), 1.00 (s, 3H, C(CH_3)$_2$(*Z*)), 0.89 (d, *J* = 1.5, 9H, Si-C(CH_3)$_3$), 0.06–0.02 (m, 6H, Si(CH_3)$_2$); **^{13}C NMR** (100 MHz, $CDCl_3$) δ 158.42 (NC-CH-*C* (*E*)), 158.05 (NC-CH-*C* (*Z*)), 148.19 (Ar(*C*)-*i*-N), 145.97 (Ar-CH-CH-*C* (*Z*)), 145.54 (Ar-CH-CH-*C* (*E*)), 132.51 (Ar-CH-*C*H (*Z*)), 132.33 (NC-CH-C-*C*H (*Z*)), 128.45 (Ar(*C*H)-*m*-N (*E* or *Z*)), 128.39 (Ar(*C*H)-*m*-N (*E* or *Z*)), 125.37 (Ar-CH-*C*H (*E*)), 125.11 (Ar-*C*H (*E*)), 124.72 (NC-CH-C-*C*H (*E*)), 124.06 (Ar(*C*)-*p*-N (E or Z)), 124.04 (Ar(C)-*p*-N (E or Z)), 122.58 (Ar-*C*H (*Z*)), 118.73 (*C*N (*E*)), 117.94 (*C*N (*Z*)), 111.63 (Ar(*C*H)-*o*-N), 91.73 (NC-*C*H (*E*)), 90.26 (NC-*C*H (*Z*)), 60.68 (*C*H_2-O-Si), 52.44 (N-*C*H_2-CH_2), 45.54 (N-*C*H_2-CH_3), 44.74 (NC-CH-C-*C*H_2(*Z*)), 42.14 (NC-CH-C-*C*H_2(*E*)), 38.96 (C(CH_3)$_2$-*C*H_2(*Z*)), 38.91 (C(CH_3)$_2$-*C*H_2(*E*)), 31.21 (*C*(CH_3)$_2$(*Z*)), 31.04 (*C*(CH_3)$_2$(*E*)), 28.20 (C(*C*H_3)$_2$(*E*)), 28.15 (C(*C*H_3)$_2$(*Z*)), 25.95 (Si-C(*C*H_3)$_3$), 18.29 (Si-*C*(CH_3)$_3$), 12.26 (N-CH_2-*C*H_3), −5.32 (Si(*C*H_3)$_2$); **MS** (ESI^+) m/z 451 $[M+H]^+$; **FTIR** (ν_{max}) 2929 (C-H stretching), 2859 (C-H stretching), 2201 (C≡N stretching) cm^{-1}.

3.6 (*E*)-2-(3-((*E*)-4-((2-((*Tert*-butyldimethylsilyl)oxy)ethyl)(ethyl)amino)styryl)-5,5-dimethylcyclohex-2-en-1-ylidene)acetaldehyde **56*E/Z***

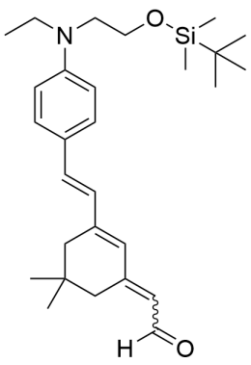

Under an inert atmosphere of argon gas, (*E/Z*)-2-(3-((*E*)-4-((2-((*tert*-butyldimethylsilyl)oxy)ethyl)(ethyl)amino)styryl)-5,5-dimethylcyclohex-2-en-1-ylidene)acetonitrile **55*E/Z*** (2.65 g, 5.88 mmol, 1.0 eq.) was dissolved in anhydrous toluene and cooled to −78 °C. DIBAL (1M in Hexane, 17.6 mL, 0.0176 mol, 3.0 eq.) was added dropwise and stirred for 2 hours. Wet silica gel (1.5 g) in diethyl ether (5 mL) and water (5 mL) was added and the solution was stirred at 0 °C for a further hour. The reaction mixture was concentrated in *vacuo* and then purified by column chromatography (0-20% EtOAc in Hexane) to afford an inseparable mix of isomers: (*E*)-2-(3-((*E*)-4-((2-((*tert*-butyldimethylsilyl)oxy)ethyl)(ethyl)amino)styryl)-5,5-dimethylcyclohex-2-en-1-ylidene)acetaldehyde **56*E*** and (*Z*)-2-(3-((*E*)-4-((2-((*tert*-butyldimethylsilyl)oxy)ethyl)(ethyl)amino)styryl)-5,5-dimethylcyclohex-2-en-1-ylidene)acetaldehyde **56*Z*** (1.287 g, 2.83 mmol, 48%) as a dark red oil.

R_f (20% ethyl acetate in hexane) 0.40; **^{1}H NMR** (400 MHz, $CDCl_3$) δ 10.21 (d, *J* = 8.0, 0.3H, C*H*O (*Z*)), 10.04 (d, *J* = 8.5, 0.7H, C*H*O (*E*)), 7.37–7.30 (m, 2H, Ar(C*H*)-*m*-N), 7.18 (s, 0.3H, CHO-CH-C-C*H* (*Z*)), 6.78–6.71 (m, 2H, Ar-C*H* and Ar-CH-C*H*), 6.70–6.60 (m, 2H, Ar(C*H*)-*o*-N), 6.26 (s, 0.7H, OHC-CH-C-C*H* (*E*)), 5.91 (d, *J* = 8.5, 0.7H, CHO-C*H* (*E*)), 5.70 (d, *J* = 8.5, 0.3H, CHO-C*H* (*Z*)), 3.77 (t, *J* = 6.5, 2H, CH_2-O-Si), 3.50–3.40 (m, 4H, N-CH_2-CH_2 and N-CH_2-CH_3), 2.67 (d, *J* = 1.5, 1.2H, CHO-CH-C-CH_2 (*E*)), 2.35 (s, 1.2H, C(CH_3)$_2$-CH_2 (*E*)), 2.34 (s, 0.6H, C(CH_3)$_2$-CH_2 (*Z*)), 2.28 (d, *J* = 1.5, 0.6H, CHO-CH-C-CH_2 (*Z*)), 1.17 (t, *J* = 7.0, 3H, N-CH_2-CH_3), 1.06 (s, 4.2H, C(CH_3)$_2$ (*E*)), 1.03 (s, 1.8H, C(CH_3)$_2$ (*Z*)), 0.89 (s, 9H, Si-C(CH_3)$_3$), 0.05–0.03 (m, 6H, Si(CH_3)$_2$); **^{13}C NMR** (100 MHz, $CDCl_3$) δ 190.71 (*C*HO (*E*)), 189.77 (*C*HO (*Z*)), 157.22 (CHO-CH-*C* (*E*)), 156.85 (CHO-CH-*C* (*Z*)), 148.38 (Ar(C)-*i*-N), 146.90 (Ar-CH-CH-*C* (*E*)), 146.76 (Ar-CH-CH-*C* (*Z*)), 132.66 (Ar-CH-*C*H (*Z*)), 132.54 (Ar-CH-*C*H (*E*)), 128.58 (Ar(*C*H)-*m*-N), 127.88 (CHO-CH-C-*C*H (*E*)), 126.21 (CHO-*C*H (*E*)), 125.68 (Ar-*C*H), 124.22 (Ar(*C*)-*p*-N), 124.18 (CHO-*C*H (*Z*)), 120.60 (CHO-CH-C-*C*H (*Z*)), 111.76 (Ar(*C*H)-*o*-N), 60.75 (*C*H_2-O-Si), 52.57 (N-*C*H_2-CH_2), 46.45 (CHO-CH-C-*C*H_2 (*Z*)), 45.68 (N-*C*H_2-CH_3), 39.64 (C(CH_3)$_2$-*C*H_2 (*Z*)), 39.34 (C(CH_3)$_2$-*C*H_2 (*E*)), 39.06 (CHO-CH-C-*C*H_2 (*E*)), 31.32 (*C*(CH_3)$_2$(*Z*)), 31.22 (*C*(CH_3)$_2$(*E*)), 28.53 (C(*C*H_3)$_2$(*E*)), 28.39 (C(*C*H_3)$_2$(*Z*)), 26.03 (Si-C(*C*H_3)$_3$), 18.41 (Si-*C*(CH_3)$_3$), 12.33 (N-CH_2-*C*H_3), −5.24 (Si(*C*H_3)$_2$); **MS** (ESI^+) m/z 454 $[M+H]^+$; **FTIR** (ν_{max}) 2952 (C-H stretching), 2927 (C-H stretching, aldehyde), 2856 (C-H stretching), 1652 (C=O stretching), 1602 (C=C stretching) cm^{-1}.

3.7 2-(4-((1*E*,3*E*)-3-(3-((*E*)-4-((2-((*Tert*-butyldimethylsilyl)oxy)ethyl)(ethyl)amino)styryl)-5,5-dimethylcyclohex-2-en-1-ylidene)prop-1-en-1-yl)-3-cyano-5-phenyl-5-(trifluoromethyl)furan-2(5H)-ylidene)malononitrile **49**

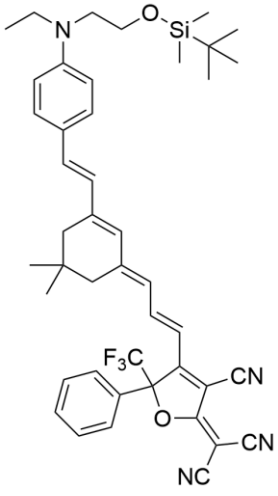

(*E*/*Z*)-2-(3-((*E*)-4-((2-((*Tert*-butyldimethylsilyl)oxy)ethyl)(ethyl)amino)styryl)-5,5-dimethylcyclohex-2-en-1-ylidene)acetaldehyde **56E/Z** (0.357 g, 0.78 mmol, 1.0 eq.) and 2-dicyanomethylene-3-cyano-4-methyl-5-phenyl-5-trifluoromethyl-2,5-dihydrofuran **48** (0.323 g, 1.02 mmol, 1.3 eq.) were dissolved in ethanol (3 mL), heated to 60 °C and stirred for 1 hour. The ethanol was removed in *vacuo* and the crude reaction mixture was redissolved in $CHCl_3$. The $CHCl_3$ was washed with water (10 mL) then brine (10 mL), dried over $MgSO_4$ then the solvent was removed in *vacuo*. The product was purified with column chromatography (20% ethyl

acetate in hexane) giving 2-(4-((1*E*,3*E*)-3-(3-((*E*)-4-((2-((*tert*-butyldimethylsilyl)oxy)ethyl)(ethyl)amino)styryl)-5,5-dimethylcyclohex-2-en-1-ylidene)prop-1-en-1-yl)-3-cyano-5-phenyl-5-(trifluoromethyl)furan-2(5H)-ylidene)malononitrile **49** (0.15 g, 0.20 mmol, 50%) as a dark green solid. The analytical data matches that reported in the literature.[30]

R_f (20% ethyl acetate in hexane) 0.40; **mp** compound decomposed upon heating; **^{1}H NMR** (400 MHz, $CDCl_3$) δ 8.60–8.40 (m, 0.2H, Ph-C-C-CH-C*H*-CH), 8.12–7.88 (m, 0.8H, Ph-C-C-CH-C*H*-CH), 7.54–7.43 (m, 5H, Ar(C*H*)-*o*-C-CF_3, Ar(C*H*)-*m*-C-CF_3 and Ar(C*H*)-*p*-C-CF_3), 7.34 (d, *J* = 9.0, Ar(C*H*)-*m*-N), 6.90 (d, 1H, *J* = 16.0, N-Ar-C*H*), 6.74 (d, 1H, *J* = 16.0, N-Ar-CH-C*H*), 6.63 (d, 2H, *J* = 9.0, Ar(C*H*)-*o*-N), 6.34 (s, 1H, N-Ar-CH-CH-C-C*H*), 6.32–6.21 (m, 1.6H, Ph-C-C-C*H*-CH-CH and Ph-C-C-CH-CH-C*H*), 6.17 (d, 0.2H, *J* = 14.5, Ph-C-C-CH-CH-C*H*), 6.05 (d, 0.2H, *J* = 12.5, Ph-C-C-C*H*-CH-CH), 3.75 (t, 2H, *J* = 6.0, CH_2-O-Si), 3.51–3.39 (m, 4H, N-CH_2-CH_2 and N-CH_2-CH_3), 2.37 (s, 2H, C(CH_3)$_2$-CH_2-C-CH-CH-Ar), 2.33–2.15 (m, 2H, C(CH_3)$_2$-CH_2-C-CH-CH-CH), 1.16 (t, 3H, *J* = 7.0, N-CH_2-CH_3), 0.98 (s, 3H, C(CH_3)$_2$) 0.93 (s, 3H, C(CH_3)$_2$), 0.85 (s, 9H, Si-C(CH_3)$_3$), 0.00 (s, 6H, Si(CH_3)$_2$); **^{13}C NMR** (100 MHz, $CDCl_3$) δ 176.03 (O-*C*=C$(CN)_2$), 161.96, 159.29, 152.70 (N-Ar-CH-CH-*C*), 149.50 (Ar(*C*)-*i*-N), 146.67 (Ph-C-C-CH-*C*H-CH), 145.44, 136.78 (N-Ar-*C*H), 131.30 (Ar(*C*H)-*p*-C-CF_3), 130.48 (Ar(*C*)-*i*-C-CF_3), 130.00 (N-Ar-CH-CH-C-*C*H), 129.81 (Ar(*C*H)-*o*-C-CF_3), 129.68 (Ar(*C*H)-*m*-N), 128.74 (Ph-C-C-*C*H-CH-CH), 126.86 (Ar(*C*H)-*m*-C-CF_3), 125.59 (N-Ar-CH-*C*H), 124.03 (Ar(*C*)-*p*-N), 120.87, 115.46 (Ph-C-C-CH-CH-*C*H), 112.14, 111.97 (Ar(*C*H)-*o*-N), 111. 79, 111.27, 60.75 (*C*H_2-O-Si), 52.57 (N-*C*H_2-CH_2), 45.84 (N-*C*H_2-CH_3), 39.97 (C(CH_3)$_2$-*C*H_2-C-CH-CH-CH), 39.72 (C(CH_3)$_2$-*C*H_2-C-CH-CH-Ar), 32.09, 31.75 (*C*(CH_3)$_2$), 29.83, 28.70 (C(*C*H_3)$_2$), 28.22 (C(*C*H_3)$_2$), 26.01 (Si-C(*C*H_3)$_3$), 18.40 (Si-*C*(CH_3)$_3$), 12.35 (N-CH_2-*C*H_3), −5.25 (Si(*C*H_3)$_2$); **^{19}F NMR** (376 MHz, $CDCl_3$) δ −72.85 (-C*F*$_3$); **MS** (ESI^+) m/z 751 $[M+H]^+$; **HRMS** (ESI^+) calcd. for $C_{44}H_{50}N_4F_3O_2Si$ $[M+H]^+$ 751.3650, found 751.3665; **FTIR** (ν_{max}) 2925 (C-H stretching), 2853 (C-H stretching), 2360 (C≡N stretching), 2227 (C≡N stretching) cm^{-1}.

3.8 2-(4-((1*E*,3*E*)-3-(3-((*E*)-4-(Ethyl(2-hydroxyethyl)amino)styryl)-5,5-dimethylcyclohex-2-en-1-ylidene)prop-1-en-1-yl)-3-cyano-5-phenyl-5-(trifluoromethyl)furan-2(5H)-ylidene)malononitrile **60**

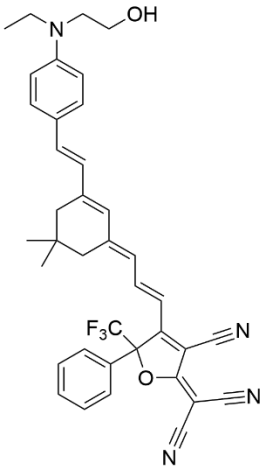

2-(4-((1*E*,3*E*)-3-(3-((*E*)-4-((2-((*Tert*-butyldimethylsilyl)oxy)ethyl)(ethyl)amino)styryl)-5,5-dimethylcyclohex-2-en-1-ylidene)prop-1-en-1-yl)-3-cyano-5-phenyl-5-(trifluoromethyl)furan-2(5H)-ylidene)malononitrile **49** (0.150 g, 0.20 mmol, 1.0 eq.) was dissolved in THF (5 mL) to which $HCl_{(aq.)}$ (2 mol dm^{-3}, 5 mL) was added and the solution stirred for 30 minutes. The reaction mixture was neutralised with Na_2CO_3 (saturated solution, 10 mL) then the product was extracted with $CHCl_3$ (3 × 20 mL). The organic layers were dried over $MgSO_4$ then the solvent was removed in *vacuo*. The product was purified with column chromatography (20% ethyl acetate in CH_2Cl_2) giving 2-(4-((1*E*,3*E*)-3-(3-((*E*)-4-(ethyl(2-hydroxyethyl)amino)styryl)-5,5-dimethylcyclohex-2-en-1-ylidene)prop-1-en-1-yl)-3-cyano-5-phenyl-5-(trifluoromethyl)furan-2(5H)-ylidene)malononitrile **60** (17 mg, 0.026 mmol, 11%) as a dark green solid.

R_f (20% ethyl acetate in CH_2Cl_2) 0.65; **mp** compound decomposed upon heating; **^{1}H NMR** (400 MHz, $CDCl_3$) δ 8.60–8.45 (m, 0.2H, Ph-C-C-CH-C*H*-CH), 8.09–7.92 (m, 0.8H, Ph-C-C-CH-C*H*-CH), 7.56–7.46 (m, 5H, Ar(C*H*)-*o*-C-CF_3, Ar(C*H*)-*m*-C-CF_3 and Ar(C*H*)-*p*-C-CF_3), 7.42–7.34 (m, 2H, Ar(C*H*)-*m*-N), 6.91 (d, 1H, *J* = 16.0, N-Ar-C*H*), 6.77 (d, 1H, *J* = 16.0, N-Ar-CH-C*H*), 6.75–6.69 (m, 2H, Ar(C*H*)-*o*-N), 6.36 (s, 1H, N-Ar-CH-CH-C-C*H*), 6.35–6.27 (m, 1.6H, Ph-C-C-C*H*-CH-CH and Ph-C-C-CH-CH-C*H*), 6.21 (d, 0.2H, *J* = 15.5, Ph-C-C-CH-CH-C*H*), 6.09 (d, 0.2H, *J* = 12.0, Ph-C-C-C*H*-CH-CH), 3.84 (t, 2H, *J* = 5.5, CH_2-OH), 3.54 (t, 2H, *J* = 6.0, N-CH_2-CH_2), 3.49 (q, 2H, *J* = 7.0, N-CH_2-CH_3), 2.40 (s, 2H, C(CH_3)$_2$-CH_2-C-CH-CH-Ar), 2.34–2.18 (m, 2H, C(CH_3)$_2$-CH_2-C-CH-CH-CH), 1.20 (t, 3H, *J* = 7.0, N-CH_2-CH_3), 1.01 (s, 3H, C(CH_3)$_2$), 0.95 (s, 3H, C(CH_3)$_2$); **^{13}C NMR** (100 MHz, $CDCl_3$) δ 175.96 (O-*C*=C(CN)$_2$), 162.14, 159.01, 152.17 (N-Ar-CH-CH-*C*), 149.55 (Ar(*C*)-*i*-N), 146.67 (Ph-C-C-CH-*C*H-CH), 136.23 (N-Ar-*C*H), 131.35 (Ar(*C*H)-*p*-C-CF_3), 130.39, 130.16 (N-Ar-CH-CH-C-*C*H), 129.88, 129.70 (Ar(*C*H)-*o*-C-CF_3 or Ar(*C*H)-*m*-N), 129.69 (Ar(*C*H)-*o*-C-CF_3 or Ar(*C*H)-*m*-N), 128.79 (Ph-C-C-*C*H-CH-CH or Ph-C-C-CH-CH-*C*H), 126.88 (Ar(*C*H)-*m*-C-CF_3), 126.03 (N-Ar-CH-*C*H), 124.64 (Ar(*C*)-*p*-N), 115.66 (Ph-C-C-*C*H-CH-CH or Ph-C-C-CH-CH-*C*H), 112.41 (Ar(*C*H)-*o*-N), 112.02, 111.68, 111.16, 60.45

(*C*H$_2$-OH), 52.43 (N-*C*H$_2$-CH$_2$), 45.80 (N-*C*H$_2$-CH$_3$), 39.97 (C(CH$_3$)$_2$-*C*H$_2$-C-CH-CH-CH), 39.70 (C(CH$_3$)$_2$-*C*H$_2$-C-CH-CH-Ar), 31.73, 29.84 (*C*(CH$_3$)$_2$), 28.71 (C(*C*H$_3$)$_2$), 28.23 (C(*C*H$_3$)$_2$), 12.20 (CH$_2$-*C*H$_3$); **^{19}F NMR** (376 MHz, CDCl$_3$) δ −72.80 (C*F*$_3$); **MS** (ESI$^+$) m/z 637 [M+H]$^+$; **HRMS** (ESI$^+$) calcd. for $C_{38}H_{36}N_4F_3O_2$ [M+H]$^+$ 637.2785, found 637.2790; **FTIR** (ν_{max}) 3447 (O-H stretching), 2926 (C-H stretching), 2360 (C≡N stretching), 2210 (C≡N stretching) cm^{-1}.

3.9 4,4,4-Trifluoro-3-hydroxy-3-phenyl-2-ethoxy-but-1-ene **58**

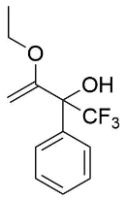

Ethyl vinyl ether **57** (0.82 mL, 0.62 g, 8.61 mmol, 3.0 eq.), was dissolved in THF (5 mL) and cooled to −78 °C. A solution of *tert*-butyl lithium in pentane (1.7 mol dm^{-3}, 3.38 mL, 5.74 mmol, 2.0 eq.) was added dropwise and stirred for 15 minutes. The reaction mixture was allowed to warm gradually to 0 °C then stirred for an additional 30 minutes at this temperature. The solution was re-cooled to −78 °C before a solution of 4,4,4-trifluoroacetophenone **65** (0.42 mL, 0.50 g, 2.87 mmol, 1.0 eq.) in THF (0.5 mL) was added in one portion. The reaction was stirred at −78 °C for 30 minutes, allowed to warm gradually to 0 °C then stirred for an additional hour at this temperature. The reaction was quenched with NH$_4$Cl (saturated solution, 5 mL) and stirred for 5 minutes. The aqueous and organic layers were separated then the aqueous layer was extracted with diethyl ether (3 × 10 mL). The combined organic layers were dried over MgSO$_4$ and concentrated in *vacuo* yielding a yellow oil. The crude 4,4,4-trifluoro-3-hydroxy-3-phenyl-2-ethoxy-but-1-ene **58** was deemed pure enough by ^{1}H NMR to use in the subsequent reaction without further purification. For characterisation, purification can be carried out using column chromatography (0-10% ethyl acetate in hexane) to afford 4,4,4-trifluoro-3-hydroxy-3-phenyl-2-ethoxy-but-1-ene **58** (0.45 g, 1.86 mmol, 65%) as a colourless oil.

R$_f$ (5% ethyl acetate in hexane) 0.20; **^{1}H NMR** (400 MHz, CDCl$_3$) δ 7.72–7.67 (m, 2H, Ar(C*H*)-*m*-R), 7.43–7.36 (m, 3H, Ar(C*H*)-*p*-R and Ar(C*H*)-*o*-R), 4.47 (d, *J* = 3.5, 1H, C=C*H*$_2$(*H* - Z - OCH$_2$CH$_3$)), 4.39 (d, *J* = 3.5, 1H, C=C*H*$_2$(*H* - E - OCH$_2$CH$_3$), 3.91–3.78 (m, 2H, O-C*H*$_2$CH$_3$), 3.71 (s, 1H, O*H*), 1.32 (t, *J* = 7.0, O-CH$_2$-C*H*$_3$); **^{13}C NMR** (100 MHz, CDCl$_3$) δ 157.70 (*C*=CH$_2$), 136.71 (Ar(*C*)-*i*-R), 128.87(Ar(*C*H)-*m*-R), 128.18 (Ar(*C*H)-*o*-R), 127.05 (Ar(*C*H)-*p*-R), 125.96 (C-*C*F$_3$), 123.12 (*C*-CF$_3$), 86.77 (C=*C*H$_2$), 64.19 (O-*C*H$_2$-CH$_3$), 14.18 (CH$_3$); **^{19}F NMR** (376 MHz, CDCl$_3$) δ −75.13 (C*F*$_3$); **MS** (ESI$^+$) m/z 247 [M+H]$^+$; **HRMS** (ESI$^+$) calcd. for $C_{12}H_{14}F_3O_2$ [M+H]$^+$ 247.0904, found 247.0942; **FTIR** (ν_{max}) 3437 (O-H stretching), 2982 (C-H stretching) cm^{-1}.

3.10 4,4,4-Trifluoro-3-hydroxy-3-phenylbutan-2-one **59**

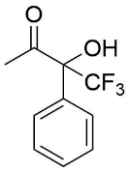

The crude 4,4,4-trifluoro-3-hydroxy-3-phenyl-2-ethoxy-but-1-ene **58** was mixed with methanol (2.5 mL) to which $HCl_{(aq.)}$ (1 mol dm^{-3}, 5 mL) was added dropwise at RT. The reaction was stirred for 2 hours while cooled in a water bath. The reaction was neutralised with $NaHCO_3$ before the methanol was removed in *vacuo* and the aqueous solution extracted with CH_2Cl_2 (3 × 15 mL). The product was purified with column chromatography (0–10% ethyl acetate in hexane) giving 4,4,4-trifluoro-3-hydroxy-3-phenylbutan-2-one **59** (0.310 g, 1.42 mmol, 63%, over two steps) as a pale-yellow oil. The analytical data matches that reported in the literature.[75]

R_f (10% ethyl acetate in hexane) 0.20; **^{1}H NMR** (400 MHz, $CDCl_3$) δ 7.61-7.55 (m, 2H, Ar(C*H*)-*m*-R, 7.47-7.39 (m, 3H, Ar(C*H*)-*o*-R and Ar(C*H*)-*p*-R), 4.96 (s, 1H, -O*H*), 2.33-2.31 (m, 3H, -CH_3); **^{13}C NMR** (100 MHz, $CDCl_3$) δ 201.59 (*C*O), 133.46 (Ar(*C*)-*i*-R), 129.67 (Ar(*C*)-*m*-R), 129.18 (Ar(*C*H)-*o*-R), 126.64 (*C*F_3), 125.06 (Ar(*C*)-*p*-R), 122.22 (*C*-CF_3), 25.30 (*C*H_3); **^{19}F NMR** (376 MHz, $CDCl_3$) δ −72.69 (C*F*$_3$); **MS** (ESI^+) m/z 241 $[M+Na]^+$; **FTIR** (ν_{max}) 3432 (O-H stretching), 1722 (C=O stretching) cm^{-1}.

3.11 2-Dicyanomethylene-3-cyano-4-methyl-5-phenyl-5-trifluoromethyl-2,5-dihydrofuran **48**

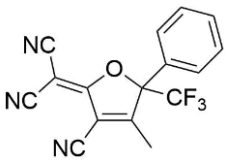

4,4,4-Trifluoro-3-hydroxy-3-phenylbutan-2-one **59** (3.04 g, 0.015 mol, 1.0 eq.), malononitrile **66** (1.93 g, 0.029 mol, 2.1 eq.) were dissolved in anhydrous ethanol (20 mL) to which sodium ethoxide (21% weight in ethanol, 0.26 mL, 0.05 eq.) was added. The solution was heated to reflux and stirred for 4 hours. The solvent was removed in *vacuo* then the mixture was re-dissolved in CH_2Cl_2 (2 mL) and washed with brine (2 mL) and then water (2 mL). The organic layer was dried over $MgSO_4$ and then concentrated in *vacuo*. The product was purified by flash column chromatography (20% EtOAc in CH_2Cl_2, then 10% MeOH in CH_2Cl_2) then recrystallised from cold ethanol to afford 2-dicyanomethylene-3-cyano-4-methyl-5-phenyl-5-trifluoromethyl-2,5-dihydrofuran **48** (3.2210 g, 0.010 mol, 73%) as a pale green powder. The analytical data matches that reported in the literature.[82]

R_f (30% ethyl acetate in CH_2Cl_2) 0.10; **mp** 129–135 °C; **^{1}H NMR** (400 MHz, $CDCl_3$) δ 7.62–7.53 (m, 3H, *o*-Ar(C*H*) and *p*-Ar(C*H*)), 7.46–7.41 (m, 2H, *m*-Ar(C*H*)), 2.48 (s, 3H, CH_3); **^{13}C NMR** (100 MHz, $CDCl_3$) δ 174.03 (O-*C*=C$(CN)_2$), 171.90 (*C*-CH_3) 131.93 (*p*-Ar(*C*H)), 130.21 (*o*-Ar(*C*H)), 127.48 (*i*-Ar(*C*)), 125.67 (*m*-Ar(*C*H)), 123.08, 120.22, 117.36, 109.42,

108.95, 108.00, 63.17 (*C*-CF_3), 15.45 (*C*H_3); **^{19}F NMR** (376 MHz, $CDCl_3$) δ −72.67 (C*F*$_3$); **MS** (ESI$^+$) m/z 333 $[M+NH_4]^+$; **FTIR** (ν_{max}) 2235 (C≡N stretching) cm^{-1}.

3.12 2-Azido-3,5,5-trimethylcyclohex-2-en-1-one **73**

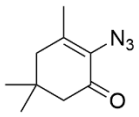

Isophorone oxide **67** (0.20 mL, 0.2 g, 1.3 mmol, 1.0 eq.) was dissolved in DMF (15 mL) and then mixed with DPPA (0.34 mL, 0.429 g, 1.56 mmol, 1.2 eq.), DMAP (0.19 g, 1.56 mmol, 1.2 eq.) and lithium perchlorate (0.014 g, 0.13 mmol, 0.10 eq.) then heated to 50 °C. The mixture was stirred for 4 days. The resulting solution was cooled to RT, diluted with EtOAc (30 mL), washed with $HCl_{(aq.)}$ (0.5 mol dm^{-3}, 30 mL) then water (30 mL) before being dried over $MgSO_4$, filtered and then concentrated in *vacuo*. The product was purified by column chromatography (10–20% ethyl acetate in hexane) to afford 2-azido-3,5,5-trimethylcyclohex-2-en-1-one **73** (0.175 g, 0.98 mmol, 75%) as a pale yellow oil. The analytical data matches that reported in the literature.[81]

R_f (20% ethyl acetate in hexane) 0.70; **^{1}H NMR** (400 MHz, $CDCl_3$) δ 2.35 (s, 2H, CO-CH_2), 2.27 (s, 2H, C$(CH_3)_2$-CH_2), 1.89 (t, *J* = 1.0, 3H, CH_3), 1.05 (s, 6H, C(CH_3)$_2$); **^{13}C NMR** (100 MHz, $CDCl_3$) δ 193.94 (*C*O), 143.55 (*C*-CH_3), 130.09 (*C*-N_3), 51.38 (CO-*C*H_2), 46.07 (C$(CH_3)_2$-*C*H_2), 33.13 (*C*$(CH_3)_2$), 28.27 (C(*C*H_3)$_2$), 20.10 (*C*H_3); **MS** (ESI$^+$) m/z 152 $[M-N_2+H]^+$; **HRMS** (ESI$^+$) calcd. for $C_9H_{13}N_3ONa$ $[M+Na]^+$ 202.0951, found 202.0950; **FTIR** (ν_{max}) 2959 (C-H stretching), 2871 (C-H stretching), 2114 (-N_3 stretching), 1674 (C=O stretching), 1624 (C=C stretching) cm^{-1}.

3.13 3,5,5-Trimethyl-2-(4-phenyl-1*H*-1,2,3-triazol-1-yl)cyclohex-2-en-1-one **78**

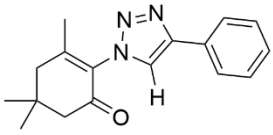

2-Azido-3,5,5-trimethylcyclohex-2-en-1-one **73** (2.20 g, 0.012 mol, 1.0 eq.), phenylacetylene **77** (1.35 mL, 1.25 g, 0.012 mol, 1.0 eq.), copper (II) sulphate solution (0.3M in H_2O, 4.1 mL, 0.10 eq.) and sodium-*L*-ascorbate solution (1M in H_2O, 12.3 mL, 1.0 eq.) were dissolved in H_2O (25 mL) and ^{t}BuOH (25 mL). The reaction was heated to 100 °C and stirred for 16 hours, overnight. The reaction was cooled to RT before $CHCl_3$ (50 mL) was added and the mixture was stirred for 15 minutes. The aqueous and organic layers were separated. The organic layer was washed with brine (20 mL), dried over $MgSO_4$ and concentrated in *vacuo*. The crude 43,5,5-trimethyl-2-(4-phenyl-1H-1,2,3-triazol-1-yl)cyclohex-2-en-1-one **78** was deemed pure enough by ^{1}H NMR to use in the subsequent reaction without further purification. If desired, purification can be carried out using column chromatography (0–10% ethyl acetate in

CH_2Cl_2) to afford 3,5,5-trimethyl-2-(4-phenyl-1H-1,2,3-triazol-1-yl)cyclohex-2-en-1-one **78** (2.927 g, 0.010 mol, 84%) as a pale yellow powder.

R_f (10% ethyl acetate in CH_2Cl_2) 0.60; **mp** 178–182 °C; **^{1}H NMR** (400 MHz, $CDCl_3$) δ 7.90–7.84 (m, 2H, *m*-Ar(C*H*)), 7.80 (s, 1H, C*H*-N), 7.46–7.40 (m, 2H, *o*-Ar(C*H*)), 7.36–7.30 (m, 1H, *p*-Ar(C*H*)), 2.56 (s, 2H, $C(CH_3)_2$-CH_2), 2.51 (s, 2H, CO-CH_2), 1.94 (s, 3H, CH_3), 1.18 (s, 6H, $C(CH_3)_2$); **^{13}C NMR** (100 MHz, $CDCl_3$) δ 192.01 (*C*O), 157.86 (N-*C*=C-CH_3), 147.19 (*C*-Ph), 131.59 (*C*-CH_3), 130.48 (*i*-Ar(*C*)), 128.98 (*o*-Ar(*C*H)), 128.34 (*p*-Ar(*C*H)), 125.99 (*m*-Ar(*C*H)), 122.36 (*C*H-N), 51.00 (CO-*C*H_2), 46.59 ($C(CH_3)_2$-*C*H_2), 33.15 (*C*$(CH_3)_2$), 28.38 ($C(CH_3)_2$), 21.08 (*C*H_3); **MS** (ESI^+) m/z 282 $[M+H]^+$; **HRMS** (ESI^+) calcd. for $C_{17}H_{19}N_3ONa$ $[M+Na]^+$ 304.1420, found 304.1420; **FTIR** (ν_{max}) 3089 (C-H stretching), 2956 (C-H stretching), 1682 (C=O stretching), 1644 (C=C stretching) cm^{-1}.

3.14 (*E*)-3-(4-(Ethyl(2-hydroxyethyl)amino)styryl)-5,5-dimethyl-2-(4-phenyl-1H-1,2,3-triazol-1-yl)cyclohex-2-en-1-one **80**

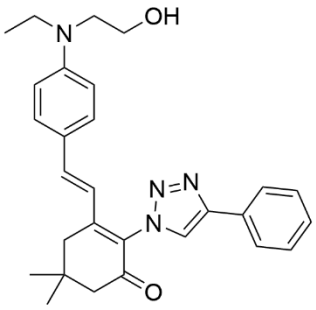

3,5,5-Trimethyl-2-(4-phenyl-1H-1,2,3-triazol-1-yl)cyclohex-2-en-1-one **78** (0.035 g, 0.12 mmol, 1.2 eq.) was dissolved in diethyl ether (1 mL) to which sodium ethoxide (21% wt. In EtOH, 0.072 mL, 2.2 eq.) was added and stirred at RT for 30 minutes. $LiClO_4$ (0.011 g, 0.10 mmol, 1.0 eq.) and 4-(Ethyl(2-hydroxyethyl)amino) benzaldehyde **51** (0.020 g, 0.10 mmol, 1.0 eq.) were added and the reaction left to stir at RT for 16 hours, overnight. Water (1 mL) and $CHCl_3$ (1 mL) were added and the mixture was stirred for 15 minutes before the aqueous and organic layers were separated. The organic layer was washed with brine (1 mL), dried over $MgSO_4$ and concentrated in *vacuo*. The product was purified by column chromatography (40% ethyl acetate in hexane) to afford (*E*)-3-(4-(ethyl(2-hydroxyethyl)amino)styryl)-5,5-dimethyl-2-(4-phenyl-1H-1,2,3-triazol-1-yl)cyclohex-2-en-1-one **80** (25% conversion by crude ^{1}H NMR) as a red/orange powder.

R_f (40% ethyl acetate in Hexane) 0.20; **mp** compound decomposed at 290 °C; **^{1}H NMR** (400 MHz, $CDCl_3$) δ 7.95–7.90 (m, 2H, Ar(C*H*)-*o*-(C_2N_3H)), 7.87 (s, 1H, C_2N_3H(C*H*)), 7.48–7.42 (m, 2H, Ar(C*H*)-*m*-(C_2N_3H)), 7.37–7.32 (m, 1H, (Ar(C*H*)-*p*-(C_2N_3H)), 7.24 (d, *J* = 9.0, 2H, Ar(C*H*)-*m*-N), 7.13 (d, *J* = 16.0, 1H, N-Ar-C*H*), 6.62 (d, *J* = 9.0, 2H, Ar(C*H*)-*o*-N), 6.48 (d, *J* = 16.0, 1H, N-Ar-CH-C*H*), 3.79 (t, *J* = 6.0, 2H, N-CH_2-CH_2), 3.49 (t, *J* = 6.0, 2H, CH_2-OH), 3.43 (q, *J* = 7.0, 2H, N-CH_2-CH_3), 2.83 (s, 2H, $C(CH_3)_2$-CH_2), 2.56 (s, 2H, CO-CH_2), 1.24 (s,

6H, C(CH_3)$_2$), 1.15 (t, J = 7.0, 3H, N-CH_2-CH_3); **^{13}C NMR** (100 MHz, $CDCl_3$) δ 192.20 (*C*O), 152.01 (N-Ar-CH-CH-*C*), 147.19 (Ar(*C*)-*i*-N), 140.65 (N-Ar-*C*H), 130.82 (N-Ar-*C*H), 130.20 (Ar(*C*H)-*m*-N), 128.96 (Ar(*C*H)-*m*-(C_2N_3H)), 128.19 (Ar(*C*H)-*p*-(C_2N_3H)), 128.09 (Ar(*C*)-*p*-N), 126.00 (Ar(*C*H)-*o*-(C_2N_3H)), 123.46 (C_2N_3H(*C*H)), 117.83 (N-Ar-CH-*C*H), 112.06 (Ar(*C*H)-*o*-N), 60.33 (N-*C*H_2-CH_2), 52.37 (*C*H_2-OH), 51.07 (CO-*C*H_2), 45.78 (N-*C*H_2-CH_3), 39.75 (C(CH_3)$_2$-*C*H_2), 32.83 (*C*(CH_3)$_2$), 28.67 (C(*C*H_3)$_2$), 12.09 (N-CH_2-*C*H_3); **MS** (ESI$^+$) m/z 457 [M+H]$^+$; **HRMS** (ESI$^+$) calcd. for $C_{28}H_{32}N_4O_2Na$ [M+Na]$^+$ 497.2417, found 479.2415; **FTIR** (ν_{max}) 3374 (O-H stretching), 2957 (C-H stretching), 2927 (C-H stretching), 1664 (C=O stretching), 1568 (C=C stretching) cm^{-1}.

3.15 *Tert*-butyl(2,4,4-trimethyl-6-oxocyclohex-1-en-1-yl)carbamate **83**

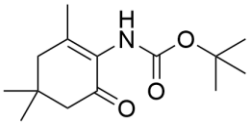

2-Azido-3,5,5-trimethylcyclohex-2-en-1-one **73** (1.30 g, 7.25 mmol, 1.0 eq.) was dissolved in diethyl ether (50 mL) and stirred under an inert atmosphere of argon gas at RT. Triphenylphosphine (2.09 g, 7.98 mmol, 1.1 eq.) in diethyl ether (10 mL) was added dropwise then the solution was stirred for 1 hour. The mixture was cooled to −46 °C before di-*tert*-butyl dicarbonate (1.83 mL, 1.74 g, 7.98 mmol, 1.1 eq.) in diethyl ether (20 mL) was added dropwise. The reaction mixture was stirred for a further hour at −46 °C. Na_2CO_3 (saturated solution, 40 mL) was added and the reaction was allowed to warm to RT. Na_2CO_3 (saturated solution, 200 mL) and diethyl ether (200 mL) were added and the layers were separated. The aqueous layer was washed with diethyl ether (200 mL × 2) then the combined organic layers were dried over $MgSO_4$ and concentrated in *vacuo*. The product was purified by column chromatography (5-10% ethyl acetate in hexane) to afford *tert*-butyl(2,4,4-trimethyl-6-oxocyclohex-1-en-1-yl)carbamate **83** (0.53 g, 2.27 mmol, 31%) as a pale yellow oil.

R$_f$ (10% ethyl acetate in hexane) 0.20; **^{1}H NMR** (400 MHz, $CDCl_3$) δ 2.35 (s, 2H, C(CH_3)$_2$-CH_2), 2.32 (s, 2H, CO-CH_2), 1.92 (s, 3H, CH_3), 1.45 (s, 9H, C(CH_3)$_3$ (Boc)), 1.05 (s, 6H, C(CH_3)$_2$); **^{13}C NMR** (100 MHz, $CDCl_3$) δ 195.27 (*C*O-CH_2), 193.38 (*C*O (Boc)), 145.89 (CH_3-*C*=C), 129.12 (CH_3-C=*C*), 80.20 (*C*(CH_3)$_3$ (Boc)), 50.66 (CO-*C*H_2), 46.35 (C(CH_3)$_2$-*C*H_2), 32.88 (*C*(CH_3)$_2$), 28.39 (C(*C*H_3)$_3$ (Boc)), 28.34 (C(*C*H_3)$_2$), 21.50 (*C*H_3-C=C); **MS** (ESI$^+$) m/z 276 [M+Na]$^+$; **HRMS** (ESI$^+$) calcd. for $C_{14}H_{23}NO_3Na$ [M+Na]$^+$ 276.1570, found 276.1571; **FTIR** (ν_{max}) 3321 (N-H stretching), 2959 (C-H stretching), 1718 (C=O stretching, carbamate) 1670 (C=O stretching, ketone), 1645 (C=C stretching) cm^{-1}.

3.16 4-((2-((*Tert*-butyldimethylsilyl)oxy)ethyl)(ethyl)amino)benzaldehyde **86**

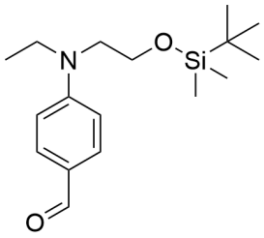

4-(Ethyl(2-hydroxyethyl)amino)benzaldehyde **51** (0.50 g, 2.58 mmol, 1.0 eq.), imidazole (0.42 g, 6.21 mmol, 2.4 eq.) and *tert*-butyldimethylsilyl chloride (0.97 g, 6.21 mmol, 2.4 eq.) were dissolved in DMF (2 mL) and stirred at RT for 16 hours, overnight. Water (5 mL) was added to quench the reaction then the product was extracted with ethyl acetate (3 × 10 mL). The combined organics were dried over $MgSO_4$ then the solvent was removed in *vacuo*. The product was purified by column chromatography (20% ethyl acetate in hexane) yielding 4-((2-((*tert*-butyldimethylsilyl)oxy)ethyl)(ethyl)amino)benzaldehyde **86** (0.75 g, 2.43 mmol, 94%) as pale yellow oil.

R$_f$ (20% ethyl acetate in hexane) 0.75; **^{1}H NMR** (400 MHz, $CDCl_3$) δ 9.71 (s, 1H, C*H*O), 7.73–7.67 (m, 2H, Ar(C*H*)-*m*-N), 6.74–6.68 (m, 2H, Ar(C*H*)-*o*-N), 3.80 (t, *J* = 6.0, 2H, CH_2-O-Si), 3.56–3.45 (m, 4H, N-CH_2-CH_2 and N-CH_2-CH_3), 1.21 (t, *J* = 7.0, 3H, N-CH_2-CH_3), 0.88 (s, 9H, Si-C(CH_3)$_3$), 0.03 (s, 6H, Si(CH_3)$_2$); **^{13}C NMR** (100 MHz, $CDCl_3$) δ 190.21 (*C*O), 152.76 (Ar(*C*)-*i*-N), 132.34 (Ar(*C*H)-*m*-N), 125.10 (Ar(*C*)-*p*-N), 110.98 (Ar(*C*H)-*o*-N), 60.60 (*C*H_2-O-Si), 52.53 (N-*C*H_2-CH_2), 45.96 (N-*C*H_2-CH_3), 26.00 (Si-C(*C*H_3)$_3$), 18.39 (Si-*C*(CH_3)$_3$), 12.16 (N-CH_2-*C*H_3), -5.28 (Si(*C*H_3)$_2$); **MS** (ESI$^+$) m/z 308 [M+H]$^+$; **HRMS** (ESI$^+$) calcd. for $C_{17}H_{30}NO_2Si$ [M+H]$^+$ 308.2040, found 308.2043; **FTIR** (ν_{max}) 2954 (C-H stretching), 2928 (C-H stretching), 2856 (C-H stretching), 1667 (C=O stretching) cm^{-1}.

3.17 *Tert*-butyl (E)-(2-(4-((2-((*tert*-butyldimethylsilyl)oxy)ethyl)(ethyl)amino)styryl)-4,4-dimethyl-6-oxocyclohex-1-en-1-yl)carbamate **90**

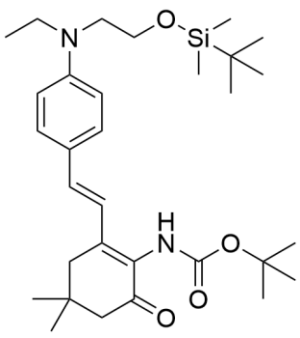

4-((2-((*Tert*-butyldimethylsilyl)oxy)ethyl)(ethyl)amino)benzaldehyde **86** (0.125 g, 0.41 mmol, 1.0 eq.), *N*,*N*-diethyltrimethylsilylamine (0.083 g, 0.57 mmol, 1.4 eq.) and lithium perchlorate (0.036 g, 0.35 mmol, 0.85 eq.) were dissolved in minimal THF and stirred under an inert atmosphere of nitrogen gas at RT. *Tert*-butyl(2,4,4-trimethyl-6-oxocyclohex-1-en-1-yl)carbamate **83** (0.103 g, 0.41 mmol, 1.0 eq.) was dissolved in minimal THF and added slowly to the reaction mixture. Approximately 2 mL of THF was used in total. The solution was stirred for 3 hours. $HCl_{(aq.)}$ (1 mol dm^{-3}, 1 mL) and the product was extracted with ethyl acetate (3 mL × 3). The combined organic layers were dried over $MgSO_4$ and then concentrated in *vacuo*. The product was purified by

column chromatography (15% ethyl acetate in hexane) yielding *tert*-butyl (E)-(2-(4-((2-((*tert*-butyldimethylsilyl)oxy)ethyl)(ethyl)amino)styryl)-4,4-dimethyl-6-oxocyclohex-1-en-1-yl)carbamate **90** (10 mg, 0.018 mmol, 4.5%) as a red powder.

R_f (20% ethyl acetate in hexane) 0.45; **mp** 140–152 °C; **^{1}H NMR** (400 MHz, $CDCl_3$) δ 7.38–7.33 (m, 2H, Ar(C*H*)-*m*-N), 7.02 (d, 1H, *J* = 16.0, N-Ar-C*H*), 6.89 (d, 1H, *J* = 16.0, N-Ar-CH-C*H*), 6.66–6.61 (m, 2H, Ar(C*H*)-*o*-N), 3.76 (t, 2H, *J* = 6.5, N-CH_2-CH_2), 3.50–3.40 (m, 4H, N-CH_2-CH_2 and N-CH_2-CH_3), 2.60 (s, 2H, C$(CH_3)_2$-CH_2), 2.38 (s, 2H, CO-CH_2), 1.47 (s, 9H, C(CH_3)$_3$ (Boc)), 1.17 (t, 3H, *J* = 7.0, N-CH_2-CH_3), 1.12 (s, 6H, C(CH_3)$_2$), 0.89 (s, 9H, Si-C(CH_3)$_3$), 0.03 (s, 6H, Si(CH_3)$_2$); **^{13}C NMR** (100 MHz, $CDCl_3$) δ 195.20 (*C*O-CH_2), 154.22 (*C*O (Boc)), 148.80 (Ar(C)-*i*-N), 145.03 (N-Ar-CH-CH-*C*), 135.74 (N-Ar-CH-*C*H), 129.18 (Ar(*C*H)-*m*-N), 127.42 (N-Ar-CH-CH-C-*C*), 124.27 (Ar(*C*)-*p*-N), 121.13 (N-Ar-*C*H), 111.66 (Ar(*C*H)-*o*-N), 80.32 (*C*$(CH_3)_3$ (Boc)), 60.75 (N-*C*H_2-CH_2), 52.52 (N-CH_2-*C*H_2), 50.76 (CO-*C*H_2), 45.66 (N-*C*H_2-CH_3), 39.51 (C$(CH_3)_2$-*C*H_2), 32.58 (*C*$(CH_3)_2$), 28.61 (C(*C*H_3)$_2$), 28.34 (C(*C*H_3)$_3$ (Boc)), 26.03 (Si-C(*C*H_3)$_3$), 18.42 (Si-*C*$(CH_3)_3$), 12.34 (N-CH_2-*C*H_3), -5.24 (Si(*C*H_3)$_2$); **MS** (ESI^+) m/z 543 $[M+H]^+$; **HRMS** (ESI^+) calcd. for $C_{31}H_{51}N_2O_4Si$ $[M+H]^+$ 543.3613, found 543.3621; **FTIR** (ν_{max}) 2928 (C-H stretching), 1724 (C=O stretching, carbamate), 1648 (C=O stretching, ketone), 1596 (C=C stretching) cm^{-1}.

3.18 (*E*)-3-(4-Fluorostyryl)-5,5-dimethylcyclohex-2-en-1-one **87**

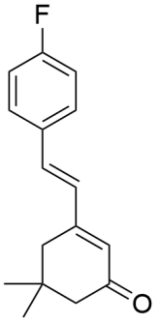

4-Fluorobenzaldehyde **50** (0.2 g, 0.17 mL, 1.61 mmol, 1.0 eq.) and isophorone **52** (0.26 g, 0.29 mL, 1.93 mmol, 1.2 eq.) were dissolved in THF (10 mL) to which sodium ethoxide (21% weight in ethanol, 1.32 mL, 3.54 mmol, 2.2 eq.) and lithium perchlorate (0.17 g, 1.61 mmol, 1 eq.) were added. The reaction mixture was stirred for 16 hours, overnight at RT. $HCl_{(aq.)}$ (1 mol dm^{-3}, 10 mL) was added and the mixture stirred for a further 10 minutes before the product was extracted with ethyl acetate (20 mL). The organic layer was washed with brine (10 mL), dried over $MgSO_4$ and concentrated in *vacuo*. Column chromatography (10–20% ethyl acetate in hexane) yielded (*E*)-3-(4-fluorostyryl)-5,5-dimethylcyclohex-2-en-1-one **87** (0.202 g, 0.82 mmol, 51%) as an orange solid.

R_f (20% ethyl acetate in hexane) 0.60; **mp** 77–81 °C; **^{1}H NMR** (400 MHz, $CDCl_3$) δ 7.50–7.43 (m, 2H, Ar(C*H*)-*m*-F), 7.09–7.02 (m, 2H, Ar(C*H*)-*o*-F), 6.95 (d, 1H, *J* = 16.0, Ar-C*H*), 6.82 (d, 1H, *J* = 16.0, Ar-CH-C*H*), 6.06 (s, 1H, Ar-CH-CH-C-C*H*), 2.46 (s, 2H, C$(CH_3)_2$-CH_2), 2.30 (s, 2H, CO-CH_2), 1.10 (s, 6H, C(CH_3)$_2$); **^{13}C NMR** (100 MHz, $CDCl_3$) δ 200.27

(C=O), 164.48 (Ar(*C*)-*i*-F or Ar(*C*)-*p*-F), 162.00 (Ar(*C*)-*i*-F or Ar(*C*)-*p*-F), 154.61 (Ar-CH-CH-*C*), 133.77 (Ar-*C*H), 133.76 (Ar-*C*H), 132.38, 132.34, 129.50 (Ar-CH-*C*H), 129.48 (Ar-CH-*C*H), 129.07 (Ar(*C*H)-*m*-F), 128.99 (Ar(*C*H)-*m*-F), 127.29 (Ar-CH-CH-C-*C*H), 127.28 (Ar-CH-CH-C-*C*H), 116.18 (Ar(*C*H)-*o*-F), 115.96 (Ar(*C*H)-*o*-F), 51.53 (CO-*C*H$_2$), 39.17 (C(CH$_3$)$_2$-*C*H$_2$), 33.46 (*C*(CH$_3$)$_2$), 28.61 (C(*C*H$_3$)$_2$); **^{19}F NMR** (376 MHz, CDCl$_3$) δ −111.73 (Ar-*F*); **MS** (ESI$^+$) m/z 245 [M+H]$^+$; **HRMS** (ESI$^+$) calcd. for C$_{16}$H$_{18}$FO [M+H]$^+$ 245.1336, found 245.1338; **FTIR** (ν_{max}) 2959 (C-H stretching), 1653 (C=O stretching), 1618 (C=C stretching) cm^{-1}.

3.19 Di(1*H*-pyrrol-2-yl)methanethione **99**

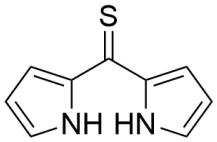

Thiophosgene **102** (4.28 g, 2.85 mL, 0.037 mol, 1.0 eq.) was dissolved in anhydrous toluene (80 mL) and cooled to 0 °C. Pyrrole **98** (5.00 g, 5.17 mL, 0.074 mol, 2.0 eq.) in anhydrous diethyl ether (90 mL) was added dropwise. The reaction mixture was stirred for 10 minutes before being warmed to RT. Methanol (10 mL) was added and the mixture was stirred for a further 30 minutes before the solvents were reduced in *vacuo*.[87] Column chromatography (0–30% ethyl acetate in hexane) yielded di(1*H*-pyrrol-2-yl)methanethione **99** (3.375 g, 0.019 mol, 51%) as red/purple crystals. The analytical data matches that reported in the literature.[87]

R$_f$ (20% ethyl acetate in hexane) 0.60; **mp** 95–99 °C; **^{1}H NMR** (400 MHz, CDCl$_3$) δ 9.77 (s, 2H, N*H*), 7.23–7.19 (m, 2H, C*H*-C-CS), 7.07– 7.03 (m, 2H, C*H*-NH), 6.43–6.39 (m, 2H, CH-C*H*-CH); **^{13}C NMR** (100 MHz, CDCl$_3$) δ 193.41 (*C*=S), 138.50 (*C*-CS), 127.76 (*C*H-C-CS), 114.90 (*C*H-NH), 112.64 (CH-*C*H-CH); **MS** (ESI$^+$) m/z 177 [M+H]$^+$; **FTIR** (ν_{max}) 3393 (N-H stretching), 3345 (N-H stretching), 3120 (C-H stretching) cm^{-1}.

3.20 Di(1*H*-pyrrol-2-yl)methanone **100**

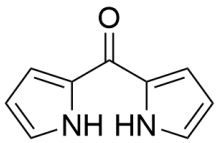

Di(1*H*-pyrrol-2-yl)methanethione **99** (3.20 g, 0.018 mol, 1.0 eq.) and potassium hydroxide (4.07 g, 0.073 mol, 4.0 eq.) were suspended in methanol (100 mL) and cooled to 0 °C. Hydrogen peroxide (30% in water, 13.2 mL, 0.129 mol, 7.1 eq.) was added dropwise and the reaction was stirred for 10 minutes before being warmed to RT. Water (200 mL) was added and the reaction was stirred for 16 hours, overnight. The product was extracted into diethyl ether (3 × 50 mL). The combined organics were dried over Na$_2$SO$_4$ and then concentrated in *vacuo*. The crude di(1*H*-pyrrol-2-yl)methanone **100** was deemed pure enough by ^{1}H NMR to use in the subsequent reaction without further purification. If desired, purification can be carried out using column

chromatography (30–40% ethyl acetate in hexane) to afford di(1*H*-pyrrol-2-yl)methanone **100** (2.81 g, 0.017 mol, 97%) as a pale yellow solid. The analytical data matches that reported in the literature.[89]

R*f* (40% ethyl acetate in hexane) 0.55; **mp** 156–158 °C; **^{1}H NMR** (400 MHz, $CDCl_3$) δ 10.04 (s, 2H, N*H*), 7.19–7.16 (m, 2H, C*H*-C-CO), 7.11–7.06 (m, 2H, C*H*-NH), 6.37–6.33 (m, 2H, CH-C*H*-CH); **^{13}C NMR** (100 MHz, $CDCl_3$) δ 173.12 (*C*=O), 130.68 (*C*-CO), 124.23 (*C*H-NH), 116.23 (*C*H-C-CO), 111.10 (CH-*C*H-CH); **MS** (ESI^+) m/z 161 $[M+H]^+$; **FTIR** (ν_{max}) 3361 (N-H stretching), 2923 (C-H stretching) cm^{-1}.

3.21 10-Chloro-5,5-difluoro-5*H*-4λ^4,5λ^4-dipyrrolo[1,2-*c*:2',1'-*f*][1,3,2]diazaborinine **101**

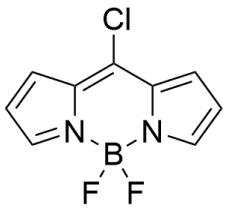

Di(1*H*-pyrrol-2-yl)methanone **101** (2.60 g, 0.016 mol, 1.0 eq.) was dissolved in DCE (80 mL) under an inert atmosphere of nitrogen gas. Phosphorous (V) oxychloride (4.97 g, 3.02 mL, 0.032 mol, 2.0 eq.) was added dropwise then the reaction was heated to reflux for 3 hours. The reaction mixture was cooled to 0 °C before triethylamine (19.34 g, 26.65 mL, 0.191 mol, 11.8 eq.) was added dropwise and the solution was stirred for 10 minutes. Boron trifluoride diethyl etherate (30.47 g, 26.50 mL, 0.216 mol, 13.3 eq.) was added dropwise then the reaction was stirred for a further 2 hours at RT. The reaction solvent was removed in *vacuo* then diethyl ether (300 mL) and water (300 mL) were added. The phases were separated, and then the aqueous phase was extracted with diethyl ether (100 mL × 2). The combined organics were dried over $MgSO_4$ and then concentrated in *vacuo*. Column chromatography (30–50% CH_2Cl_2 in hexane) yielded 10-chloro-5,5-difluoro-5*H*-4λ^4,5λ^4-dipyrrolo[1,2-*c*:2',1'-*f*][1,3,2]diazaborinine **101** (2.02 g, 8.93 mmol, 54%) as a red solid. The analytical data matches that reported in the literature.[89]

R*f* (50% CH_2Cl_2 in hexane) 0.40; **mp** 134–136 °C; **^{1}H NMR** (400 MHz, $CDCl_3$) δ 7.84–7.79 (m, 2H, C*H*-C-C-Cl), 7.34 (d, 2H, *J* = 4.0, *C*H-N-BF_2), 6.53–6.49 (m, 2H, CH-C*H*-CH); **^{13}C NMR** (100 MHz, $CDCl_3$) δ 145.18 (*C*H-C-C-Cl), 141.30 (CH-C-*C*-Cl), 134.14 (CH-*C*-C-Cl), 129.44 (*C*H-N-BF_2), 119.22 (CH-*C*H-CH); **^{19}F NMR** (376 MHz, $CDCl_3$) δ −145.76 (B*F*$_2$); **MS** (ESI^+) m/z 207 $[M-F]^+$; **FTIR** (ν_{max}) 2922 (C-H stretching) cm^{-1}.

3.22 10-(Methyl)-5,5-difluoro-5*H*-4λ^4,5λ^4-dipyrrolo[1,2-*c*:2',1'-*f*][1,3,2]diazaborinine **28**

10-Chloro-5,5-difluoro-5*H*-4λ^4,5λ^4-dipyrrolo[1,2-*c*:2',1'-*f*][1,3,2]diazaborinine **101** (2.00 g, 8.83 mmol, 1.0 eq.) and bis(triphenylphosphine) palladium(II) dichloride (0.62 g, 0.88 mmol, 0.10 eq.) were dissolved in anhydrous toluene (25 mL) under an inert atmosphere of nitrogen gas and cooled to 0 °C with stirring. $ZnMe_2$ (2M in toluene, 0.026 mol, 13.0 mL, 3.0 eq.) was added dropwise then the reaction was stirred at RT for 2 hours. The reaction was filtered through a plug of Celite® then the solvent was removed in *vacuo*. Column chromatography (50% CH_2Cl_2 in hexane) yielded 10-(Methyl)-5,5-difluoro-5*H*-4λ^4,5λ^4-dipyrrolo[1,2-*c*:2',1'-*f*][1,3,2]diazaborinine **28** (1.08 g, 5.23 mmol, 59%) as an orange solid. The analytical data matches that reported in the literature.[97]

R$_f$ (50% CH_2Cl_2 in hexane) 0.30; **mp** 155–157 °C; **^{1}H NMR** (400 MHz, $CDCl_3$) δ 7.87–7.82 (m, 2H, C*H*-C-C-CH_3), 7.30 (d, 2H, *J* = 4.0, C*H*-N-BF_2), 6.56–6.51 (m, 2H, CH-C*H*-CH), 2.63 (s, 3H, C*H*$_3$); **^{13}C NMR** (100 MHz, $CDCl_3$) δ 146.02 (*C*-CH_3), 143.54 (*C*H-C-C-CH_3), 135.68 (*C*-C-CH_3), 128.17 (*C*H-N-BF_2), 118.10 (CH-*C*H-CH), 16.27 (*C*H$_3$); **^{19}F NMR** (376 MHz, $CDCl_3$) δ −146.12 (B*F*$_2$); **MS** (ESI$^+$) m/z 187 $[M-F]^+$; **FTIR** (ν_{max}) 3110 (C-H stretching) cm^{-1}.

3.23 10-(Methyl)-5,5-difluoro-3,7-dimethyl-5*H*-4λ^4,5λ^4-dipyrrolo[1,2-*c*:2',1'-*f*][1,3,2]diazaborinine **93**

2-Methyl pyrrole **126** (1.00 g, 0.012 mol, 2.0 eq.) was dissolved in anhydrous CH_2Cl_2 (200 mL) under an inert atmosphere of nitrogen gas with light protection with stirring at RT. Acetyl chloride **96** (0.53 mL, 0.48 g, 6.2 mmol, 1.0 eq.) was added dropwise and the solution was stirred for 16 hours, overnight. Triethylamine (2.15 mL, 1.60 g, 0.015 ol, 2.5 eq.) was added and the solution stirred for 30 minutes. Boron trifluoride diethyl etherate (1.90 mL, 2.18 g, 0.015 mol, 2.5 eq.) was added dropwise then the reaction mixture was stirred for a further 2.5 hours. The reaction mixture was filtered through a plug of silica gel, and washed with CH_2Cl_2 (100 mL). The resulting filtrate was concentrated in *vacuo.* The product was purified by column chromatography (20–30% CH_2Cl_2 in hexane) to afford 10-(Methyl)-5,5-difluoro-3,7-dimethyl-5*H*-4λ^4,5λ^4-dipyrrolo[1,2-*c*:2',1'-*f*][1,3,2]diazaborinine **93** (80 mg, 0.34 mmol, 6%) as an orange-pink solid. The analytical data matches that reported in the literature.[98]

R$_f$ (20% CH_2Cl_2 in hexane) 0.75; **mp** 134–140 °C; **^{1}H NMR** (400 MHz, $CDCl_3$) δ 7.10 (d, *J* = 4.0, 2H, C*H*-C-C-CH_3), 6.26 (d, *J* = 4.0, 2H, C*H*-C-CH_3), 2.60 (s, 6H, CH_3-C-N-BF_2), 2.48 (s, 3H, CH_3-C-C-CH); **^{13}C NMR** (100 MHz, $CDCl_3$) δ 156.82, 140.28, 135.15, 127.06 (*C*H-C-C-CH_3), 118.85 (*C*H-C-CH_3), 15.37 (*C*H_3-C-C-CH), 14.90 (*C*H_3-C-CH); **^{19}F NMR** (376 MHz, $CDCl_3$) δ −148.59 (B*F*$_2$); **MS** (ESI$^+$) m/z 235 $[M+H]^+$; **FTIR** (ν_{max}) 2920 (C-H stretching) cm^{-1}.

3.24 10-(*p*-Toluyl)-5,5-difluoro-3,7-dimethyl-5*H*-4λ^4,5λ^4-dipyrrolo[1,2-*c*:2',1'-*f*][1,3,2]diazaborinine **109**

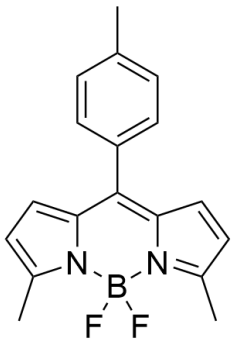

Under an inert atmosphere of nitrogen gas, 2-methyl pyrrole **126** (2.52 mL, 2.43 g, 0.030 mol, 2.0 eq.) was dissolved in anhydrous CH_2Cl_2 (150 mL) and cooled to 0 °C. *P*-toluyl chloride (1.94 mL, 2.27 g, 0.015 mol, 1.0 eq.) was added dropwise. The reaction was stirred for 30 minutes at 0 °C, warmed to RT then stirred for an additional 30 minutes. The reaction was re-cooled to 0°C before triethylamine (5.23 mL, 3.79 g, 0.038 mol, 2.5 eq.) was added slowly and allowed to stir for 10 minutes. Boron trifluoride diethyl etherate (1.15 mL, 5.32 g, 0.038 mol, 2.5 eq.) was then added dropwise and the solution was stirred at RT for 16 hours, overnight. The reaction was quenched with CH_2Cl_2 (200 mL) and water (200 mL). The layers were separated, and the organic layer was washed with water (200 mL × 3) then dried over $MgSO_4$ and concentrated in *vacuo*. The crude product was purified by column chromatography (10–40% CH_2Cl_2 in hexane) to afford 10-(*p*-toluyl)-5,5-difluoro-3,7-dimethyl-5*H*-4λ^4,5λ^4-dipyrrolo[1,2-*c*:2',1'-*f*][1,3,2]diazaborinine **109** (0.466 g, 1.50 mmol, 10%) as an orange/green solid. The analytical data matches that reported in the literature.[93]

R$_f$ (50% CH_2Cl_2 in hexane) 0.45; **mp** 193–198 °C; **^{1}H NMR** (400 MHz, $CDCl_3$) δ 7.39 (d, 2H, *J* = 8.0, Ar(C*H*)-*m*-CH_3), 7.28 (d, 2H, *J* = 8.0, Ar(C*H*)-*o*-CH_3), 6.73 (d, 2H, *J* = 4.0, CH-C*H*-C-C-Ar), 6.26 (d, 2H, *J* = 4.0, C*H*-C(CH_3)-N-BF_2), 2.65 (s, 6H, CH_3-C-N-BF_2), 2.45 (s, 3H, CH_3-Ar); **^{13}C NMR** (100 MHz, $CDCl_3$) δ 157.40 (CH_3-*C*-N-BF_2), 143.03 (CH-CH-C-*C*-Ar), 140.42 (Ar(*C*)-*i*-CH_3), 134.68 (CH-CH-*C*-C-Ar), 131.43 (Ar(*C*)-*p*-CH_3), 130.56 (Ar(*C*H)-*m*-CH_3), 130.52 (CH-*C*H-C-C-Ar), 129.04 (Ar(*C*H)-*o*-CH_3), 119.35 (*C*H-C(CH_3)-N-BF_2), 21.54 (*C*H_3-Ar), 15.03 (*C*H_3-C-N-BF_2); **^{19}F NMR** (376 MHz, $CDCl_3$) δ −147.87 (B*F*$_2$); **MS** (ESI$^+$) m/z 311 $[M+H]^+$; **FTIR** (ν_{max}) 2922 (C-H stretching) cm^{-1}.

3.25 2-Ethyl pyrrole **107**

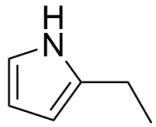

Lithium aluminium hydride (6.98 g, 0.183 mol, 2.0 eq.) was suspended in anhydrous THF (100 mL) under nitrogen gas and cooled to 0 °C. 2-Acetyl pyrrole **106** (10.00 g, 0.092 mol, 1.0 eq.) was dissolved in anhydrous THF (100 mL) which was added dropwise to the stirring aluminium hydride suspension. The resulting solution was heated to reflux and stirred for 16 hours, overnight. The reaction was quenched with sodium sulphate (saturated solution, 100 mL). The crude reaction mixture was filtered through a plug of Celite® and washed with CH_2Cl_2 then the solvent was removed in *vacuo*. Column chromatography (0–10% ethyl acetate in hexane) yielded 2-ethyl pyrrole **107** (4.66 g, 0.049 mol, 53% yield) as a yellow oil. The analytical data matches that reported in the literature.[91]

R_f (10% ethyl acetate in hexane) 0.55; **^{1}H NMR** (400 MHz, $CDCl_3$) δ 6.71–6.67 (m, 1H, C*H*-NH), 6.18–6.14 (m, 1H, CH-C*H*-CH), 5.98–5.93 (m, 1H, C*H*-C), 2.66 (q, 2H, *J* = 7.5, C*H*$_2$-CH_3), 1.28 (t, 3H, *J* = 7.5, CH_2-C*H*$_3$); **^{13}C NMR** (100 MHz, $CDCl_3$) δ 134.30 (*C*-CH_2-CH_3), 116.19 (C*H*-NH), 108.37 (CH-C*H*-CH), 104.30 (*C*H-C), 20.93 (*C*H_2-CH_3), 13.72 (CH_2-*C*H_3); **MS** (ESI^+) m/z 96 $[M+H]^+$; **FTIR** (ν_{max}) 3376 (N-H stretching), 2967 (C-H stretching) cm^{-1}.

3.26 10-(Methyl)-5,5-difluoro-3,7-diethyl-5*H*-4λ^4,5λ^4-dipyrrolo[1,2-*c*:2',1'-*f*][1,3,2]diazaborinine **103**

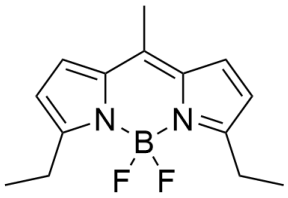

Under an inert atmosphere of nitrogen gas, ethyl pyrrole **107** (3.00 g, 0.031 mol, 2.0 eq.) was dissolved in anhydrous CH_2Cl_2 (250 mL) and cooled to 0 °C. Acetyl chloride **96** (1.12 mL, 1.24 g, 0.016 mol, 1.0 eq.) was added dropwise. The reaction was stirred for 30 minutes at 0 °C, warmed to RT then stirred for an additional 30 minutes. The reaction was re-cooled to 0 °C before triethylamine (5.49 mL, 3.98 g, 0.039 mol, 2.5 eq.) was added slowly and allowed to stir for 10 minutes. Boron trifluoride diethyl etherate (4.86 mL, 5.59 g, 0.039 mol, 2.5 eq.) was then added dropwise and the solution was heated to reflux and stirred for 16 hours, overnight. The reaction was quenched with CH_2Cl_2 (200 mL) and water (200 mL). The layers were separated, and the organic layer was washed with water (100 mL × 3) then dried over $MgSO_4$, filtered through a plug of silica and concentrated in *vacuo*. The crude product was purified by column chromatography (10–40% CH_2Cl_2 in hexane) to afford 10-(Methyl)-5,5-difluoro-3,7-diethyl-5*H*-4λ^4,5λ^4-dipyrrolo[1,2-*c*:2',1'-*f*][1,3,2]diazaborinine **103** (0.496 g, 1.89 mmol, 12%) as a red solid. The analytical data matches that reported in the literature.[89]

R_f (50% CH_2Cl_2 in hexane) 0.55; **mp** 119–122 °C; **^{1}H NMR** (400 MHz, $CDCl_3$) δ 7.14 (d, 2H, *J* = 4.0, CH-C*H*-C-C(CH_3)), 6.34 (d, 2H, *J* = 4.0, C*H*-C(CH_2CH_3)), 3.03 (q, 4H, *J* = 7.5, CH_2-CH_3), 2.49 (s, 3H, CH_3-C), 1.32 (t, 6H, *J* = 7.5, CH_2-CH_3); **^{13}C NMR** (100 MHz, $CDCl_3$) δ 162.79 (*C*-CH_2CH_3)), 140.61 (CH_3-*C*), 134.82 (CH-CH-*C*-C(CH_3)), 127.09 (CH-*C*H-C-C(CH_3)), 116.72 (*C*H-C(CH_2CH_3)), 22.04 (*C*H_2CH_3), 15.46 (*C*H_3-C), 12.95 (CH_2*C*H_3); **^{19}F NMR** (376 MHz, $CDCl_3$) δ −146.21 (B*F*$_2$); **MS** (ESI$^+$) m/z 263 $[M+H]^+$; **FTIR** (ν_{max}) 2972 (C-H stretching), 2877 (C-H stretching) cm^{-1}.

3.27 10-(*p*-Toluyl)-5,5-difluoro-3,7-diethyl-5*H*-4λ^4,5λ^4-dipyrrolo[1,2-*c*:2',1'-*f*][1,3,2]diazaborinine **110**

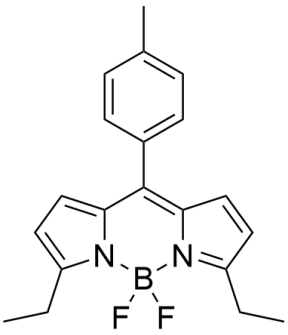

Under an inert atmosphere of nitrogen gas, 2-ethyl pyrrole **107** (2.85 g, 0.030 mol, 2.0 eq.) was dissolved in anhydrous CH_2Cl_2 (250 mL) and cooled to 0 °C. *p*-Toluyl chloride (1.95 mL, 2.27 g, 0.015 mol, 1.0 eq.) was added dropwise. The reaction was stirred for 30 minutes at 0 °C, warmed to RT then stirred for an additional 30 minutes. The reaction was re-cooled to 0 °C before triethylamine (5.23 mL, 3.78 g, 0.038 mol, 2.5 eq.) was added slowly and allowed to stir for 10 minutes. Boron trifluoride diethyl etherate (4.63 mL, 5.32 g, 0.038 mol, 2.5 eq.) was then added dropwise and the solution was heated to reflux and stirred for 16 hours, overnight. The reaction was quenched with water (200 mL). The layers were separated, and the organic layer was washed with water (50 mL × 3), filtered through a plug of silica and concentrated in *vacuo*. The crude product was purified by column chromatography (0–20% CH_2Cl_2 in hexane) to afford 10-(*p*-toluyl)-5,5-difluoro-3,7-diethyl-5*H*-4λ^4,5λ^4-dipyrrolo[1,2-*c*:2',1'-*f*][1,3,2]diazaborinine **110** (0.508 g, 1.5 mmol, 10%) as an orange/green solid. The analytical data matches that reported in the literature.[94]

R_f (50% CH_2Cl_2 in hexane) 0.60; **mp** 128–130 °C; **^{1}H NMR** (400 MHz, $CDCl_3$) δ 7.42–7.37 (m, 2H, Ar(C*H*)-*m*-CH_3), 7.31–7.26 (m, 2H, Ar(C*H*)-*o*-CH_3), 6.76 (d, 2H, *J* = 4.0, CH-C*H*-C-C-Ar), 6.34 (d, 2H, *J* = 4.0, C*H*-C(CH_2CH_3)), 3.08 (q, 4H, *J* = 7.5, CH_2-CH_3), 2.45 (s, 3H, CH_3-Ar), 1.34 (t, 6H, *J* = 7.5, CH_2-CH_3); **^{13}C NMR** (100 MHz, $CDCl_3$) δ 163.40 (*C*-CH_2-CH_3), 143.36 (CH-CH-C-*C*-Ar), 140.35 (Ar(*C*)-*i*-CH_3), 134.40 (CH-CH-*C*-C-Ar), 131.56 (Ar(*C*)-*p*-CH_3), 130.56 (Ar(*C*H)-*m*-CH_3 and CH-C*H*-C-C-Ar), 129.03 (Ar(*C*H)-*o*-CH_3), 117.22 (*C*H-C(CH_2CH_3)), 22.16 (CH_2-CH_3), 21.55 (*C*H_3-Ar), 12.95 (CH_2-*C*H_3); **^{19}F NMR** (376 MHz, $CDCl_3$) δ −145.52 (B*F*$_2$); **MS** (ESI$^+$) m/z 339 $[M+H]^+$; **FTIR** (ν_{max}) 2931 (C-H stretching) cm^{-1}.

3.28 *N*-(2-((*Tert*-butyldimethylsilyl)oxy)ethyl)-4-((E)-2-((E)-3-((E)-3-(5,5-difluoro-5H-4λ^4,5λ^4-dipyrrolo[1,2-c:2',1'-f][1,3,2]diazaborinin-10-yl)allylidene)-5,5-dimethylcyclohex-1-en-1-yl)vinyl)-N-ethylaniline **96**

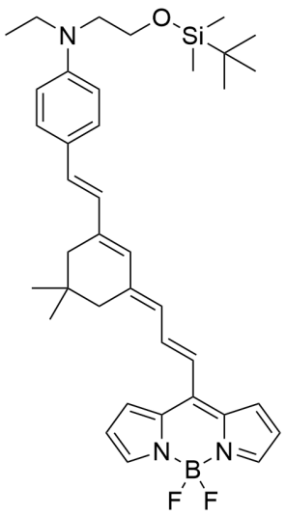

(*E*)-2-(3-((*E*)-4-((2-((*Tert*-butyldimethylsilyl)oxy)ethyl)(ethyl)amino)styryl)-5,5-dimethylcyclohex-2-en-1-ylidene)acetaldehyde **56*E*/*Z*** (50 mg, 0.11 mmol, 1.0 eq.) was dissolved in anhydrous IPA (10 mL) to which a small number of molecular sieves were added. 10-(Methyl)-5,5-difluoro-5*H*-4λ^4,5λ^4-dipyrrolo[1,2-*c*:2',1'-*f*][1,3,2]diazaborinine **28** (22 mg, 0.11 mmol, 1.0 eq.) and piperidine (11 mg, 0.013 mL, 0.13 mmol, 1.2 eq.) were added, the mixture was heated to 50 °C and stirred for 30 minutes. After allowing the reaction mixture to cool to RT, water (10 mL) and chloroform (10 mL) were added. The layers were separated, and the organic layer was washed with $MgSO_4$ before being concentrated in *vacuo*. Column chromatography (0–50% CH_2Cl_2 in hexane) yielded N-(2-((*tert*-butyldimethylsilyl)oxy)ethyl)-4-((E)-2-((E)-3-((E)-3-(5,5-difluoro-5H-4λ^4,5λ4-dipyrrolo[1,2-c:2',1'-f][1,3,2]diazaborinin-10-yl)allylidene)-5,5-dimethylcyclohex-1-en-1-yl)vinyl)-N-ethylaniline **96** (5 mg, 7.8 µmol, 7%) as a dark solid.

R$_f$ (50% CH_2Cl_2 in hexane) 0.17; **mp** compound decomposed upon heating; **^{1}H NMR** (400 MHz, $CDCl_3$) δ 7.94 (dd, 0.2H, *J* = 12.0 and 14.5, CH-C*H*-CH-BODIPY), 7.82–7.73 (m, 0.8H, CH-C*H*-CH-BODIPY), 7.63 (d, 1H, *J* = 15.5, N-Ar-CH-C*H*), 7.52 (d, 2H, *J* = 9.0, Ar(C*H*)-*m*-N), 7.36–7.27 (m, 3H, CH-C*H*-CH-N-BF_2 and N-Ar-C*H*-CH), 6.96 (d, 0.8H, *J* = 14.5, CH-CH-C*H*-BODIPY), 6.90 (d, 0.2H, *J* = 14.5, CH-CH-C*H*-BODIPY), 6.79–6.68 (m, 2H, N-Ar(C*H*)-*o*-N), 6.68–6.62 (m, 2H, CH-CH-C*H*-N-BF_2), 6.57–6.48 (m, 2H, C*H*-CH-CH-N-BF_2), 6.42 (d, 0.8H, *J* = 12.0, C*H*-CH-CH-BODIPY), 6.33 (s, 1H, N-Ar-CH-CH-C-C*H*), 6.18 (d, 0.2H, *J* = 12.0, C*H*-CH-CH-BODIPY), 3.83–3.74 (m, 2H, CH_2-O-Si), 3.56–3.40 (m, 4H, N-CH_2-CH_3 and N-CH_2-CH_2), 2.41 (s, 2H, C(CH_3)$_2$-CH_2-C-CH-CH-CH-BODIPY), 2.35 (s, 2H, C(CH_3)$_2$-CH_2-C-CH-CH-Ar), 1.23 (t, 3H, *J* = 7.0, N-CH_2-CH_3), 1.05 (s, 6H, C(CH_3)$_2$), 0.90 (s, 9H, Si-C(CH_3)$_3$), 0.05 (s, 6H, Si(CH_3)$_2$); **^{13}C NMR** (125 MHz, $CDCl_3$) δ 150.59 (Ar(*C*)-*i*-N), 149.51 (*C*-CH-CH-CH-BODIPY), 148.28, 147.44 (N-Ar-CH-*C*H), 145.28, 144.60 (N-Ar-CH-CH-*C*), 143.12 (CH-*C*H-CH-BODIPY), 133.61 (*C*-C-CH-CH-CH-N-BF_2), 131.62, 130.95 (Ar(*C*H)-*m*-N), 129.56 (N-Ar-CH-CH-C-*C*H), 128.55, 128.36 (*C*H-

CH-CH-BODIPY), 126.56 (N-Ar-*C*H-CH), 126.45, 126.35, 124.66 (C-*C*-CH-CH-CH-N-BF_2), 123.72 (Ar(*C*)-*p*-N), 123.53 (CH-CH-*C*H-BODIPY), 116.88 (*C*H-CH-CH-N-BF_2), 116.15 (CH-C*H*-CH-N-BF_2), 111.94 (Ar(*C*H)-*o*-N), 111.84 (CH-CH-*C*H-N-BF_2), 60.80, 60.73 (*C*H_2-O-Si), 52.64 (N-C*H*$_2$-CH_2), 45.98 (N-*C*H_2-CH_3), 45.72, 39.94 (C(CH_3)$_2$-*C*H_2-C-CH-CH-CH-BODIPY), 39.43 (C(CH_3)$_2$-*C*H_2-C-CH-CH-Ar), 32.08, 31.20, 29.85 (*C*(CH_3)$_2$), 28.71 (C(*C*H_3)$_2$), 26.06, 26.03 (Si-C(*C*H_3)$_3$), 14.27, 12.39, 12.32 (N-CH_2-*C*H_3), −5.20 (Si(*C*H_3)$_2$); **^{19}F NMR** (376 MHz, $CDCl_3$) δ −146.41 (B*F*$_2$); **MS** (ESI$^+$) m/z 642 $[M+H]^+$; **HRMS** (ESI$^+$) calcd. for $C_{38}H_{51}N_3BF_2OSi$ $[M+H]^+$ 642.3864, found 642.3854; **FTIR** (ν_{max}) 2923 (C-H stretching), 2852 (C-H stretching) cm^{-1}.

3.29 *N*-(2-((*Tert*-butyldimethylsilyl)oxy)ethyl)-4-((E)-2-((E)-3-((E)-3-(5,5-difluoro-3,7-dimethyl-5H-4λ^4,5λ^4-dipyrrolo[1,2-c:2',1'-f][1,3,2]diazaborinin-10-yl)allylidene)-5,5-dimethylcyclohex-1-en-1-yl)vinyl)-N-ethylaniline **94**

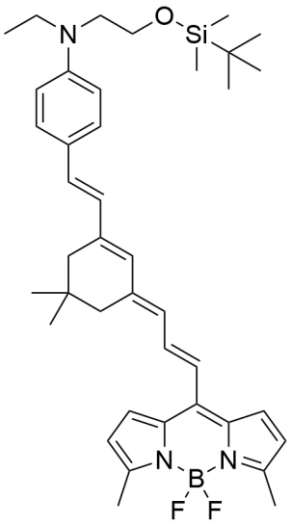

Under an inert atmosphere of nitrogen gas, fitted with a Dean-Stark apparatus, (*E*)-2-(3-((*E*)-4-((2-((*tert*-butyldimethylsilyl)oxy)ethyl)(ethyl)amino)styryl)-5,5-dimethylcyclohex-2-en-1-ylidene)acetaldehyde **56*E*/*Z*** (140 mg, 0.03 mmol, 1.0 eq.) was dissolved in anhydrous benzene (10 mL) containing a small number of molecular sieves. 10-(Methyl)-5,5-difluoro-3,7-dimethyl-5*H*-4λ^4,5λ^4-dipyrrolo[1,2-*c*:2',1'-*f*][1,3,2]diazaborinine **93** (70 mg, 0.03 mmol, 1.0 eq.) was added followed by piperidine (0.91 g, 1.07 mL, 10.8 mmol, 36.0 eq.) and glacial acetic acid (0.7 mL). The mixture was heated to reflux and stirred for 3 hours. The solvent was removed in *vacuo*. The crude mixture was resuspended in ethyl acetate (10 mL), washed with water (10 mL) then brine (10 mL) before being dried over $MgSO_4$ and concentrated in *vacuo*. Column chromatography (10%–20% ethyl acetate in hexane) yielded N-(2-((*tert*-butyldimethylsilyl)oxy)ethyl)-4-((E)-2-((E)-3-((E)-3-(5,5-difluoro-3,7-dimethyl-5H-4λ^4,5λ^4-dipyrrolo[1,2-c:2',1'-f][1,3,2]diazaborinin-10-yl)allylidene)-5,5-dimethylcyclohex-1-en-1-yl)vinyl)-N-ethylaniline (2 mg, 3.00 µmol, 1%) as a dark solid.

R$_f$ (20% ethyl acetate in hexane) 0.55; **mp** compound decomposed upon heating °C; **^{1}H NMR** (400 MHz, $CDCl_3$) δ 7.67 (dd, 0.2H, *J* = 12.0 and 15.0, CH-C*H*-CH-BODIPY), 7.50 (dd, 0.8H, *J* = 12.0 and 15.0, CH-C*H*-CH-BODIPY), 7.32 (d, 2H, *J* = 9.0, Ar(C*H*)-*m*-N), 7.15 (d, 0.4H, *J* = 4.0, C*H*-CH-C(CH_3)-N-BF_2), 7.12 (d, 1.6H, *J* = 4.0, C*H*-CH-C(CH_3)-N-BF_2),

6.82 (d, 1H, J = 15.0, CH-CH-C*H*-BODIPY), 6.79–6.55 (m, 2H, N-Ar-C*H*-CH and N-Ar-CH-C*H*), 6.65 (d, 2H, J = 9.0, Ar(C*H*)-*o*-N), 6.33 (d, 1H, J = 11.5, C*H*-CH-CH-BODIPY), 6.29 (s, 1H, N-Ar-CH-CH-C-C*H*), 6.27 (d, 2H, J = 4.5, CH-C*H*-C(CH_3)-N-BF_2), 3.77 (t, 2H, J = 6.5, CH_2-O-Si), 3.53–3.37 (m, 4H, N-CH_2-CH_2 and N-CH_2-CH_3), 2.62 (s, 6H, CH_3-BODIPY), 2.35 (s, 2H, C(CH_3)$_2$-CH_2-C-CH-CH-CH-BODIPY), 2.31 (s, 2H, C(CH_3)$_2$-CH_2-C-CH-CH-Ar), 1.17 (t, 3H, J = 7.0, N-CH_2-CH_3), 1.02 (s, 6H, C(CH_3)$_2$), 0.90 (s, 9H, Si-C(CH_3)$_3$), 0.04 (s, 6H, Si(CH_3)$_2$); **^{13}C NMR** (125 MHz, $CDCl_3$) δ 155.03 (*C*(CH_3)-N-BF_2), 148.00 (Ar(*C*)-*i*-N), 146.30 (*C*-CH-CH-CH-BODIPY), 142.40 (N-Ar-CH-CH-*C*), 140.01 (CH-*C*H-CH-BODIPY), 133.37 (CH-CH-CH-*C*-C-N-BF_2 or CH-CH-CH-C-*C*-N-BF_2), 130.30 (N-Ar-*C*H-CH or N-Ar-CH-*C*H), 129.51 (N-Ar-CH-CH-C-*C*H), 128.27 (Ar(*C*H)-*m*-N), 127.93 (*C*H-CH-CH-BODIPY), 126.61 (N-Ar-*C*H-CH or N-Ar-CH-*C*H), 126.32 (*C*H-CH-C(CH_3)-N-BF_2), 124.87 (Ar(*C*)-*p*-N), 123.45 (CH-CH-C*H*-BODIPY), 118.31 (CH-*C*H-C(CH_3)-N-BF_2), 111.82 (Ar(*C*H)-*o*-N), 60.81 (*C*H_2-O-Si), 52.61 (N-*C*H_2-CH_2), 45.69 (N-*C*H_2-CH_3), 39.75 (C(CH_3)$_2$-*C*H_2-C-CH-CH-CH-BODIPY), 39.33 (C(CH_3)$_2$-*C*H_2-C-CH-CH-Ar), 30.97, 29.85 (*C*(CH_3)$_2$), 28.73 (C(*C*H_3)$_2$), 28.53, 26.06 (Si-C(*C*H_3)$_3$), 14.98 (C(*C*H_3)-N-BF_2), 12.39 (N-CH_2-*C*H_3), −5.20 (Si(*C*H_3)$_2$); **^{19}F NMR** (376 MHz, $CDCl_3$) δ −147.95 (B*F*$_2$); **MS** (ESI^+) m/z 670 $[M+H]^+$; **HRMS** (ESI^+) calcd. for $C_{40}H_{55}N_3OBF_2Si$ $[M+H]^+$ 670.4177, found 670.4174; **FTIR** (ν_{max}) 2919 (C-H stretching), 2850 (C-H stretching) cm^{-1}.

3.30 *N*-(2-((*Tert*-butyldimethylsilyl)oxy)ethyl)-4-((E)-2-((E)-3-((E)-3-(5,5-difluoro-3,7-diethyl-5H-4λ^4,5λ^4-dipyrrolo[1,2-c:2',1'-f][1,3,2]diazaborinin-10-yl)allylidene)-5,5-dimethylcyclohex-1-en-1-yl)vinyl)-N-ethylaniline **104**

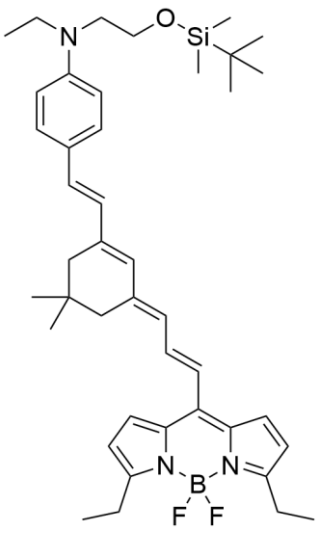

(*E*)-2-(3-((*E*)-4-((2-((*Tert*-butyldimethylsilyl)oxy)ethyl)(ethyl)amino)styryl)-5,5-dimethylcyclohex-2-en-1-ylidene)acetaldehyde **56*E*/*Z*** (50 mg, 0.11 mmol, 1.0 eq.) was dissolved in anhydrous IPA (10 mL) to which a small number of molecular sieves were added. 10-(Methyl)-5,5-difluoro-3,7-diethyl-5*H*-4λ^4,5λ^4-dipyrrolo[1,2-*c*:2',1'-*f*][1,3,2]diazaborinine **103** (29 mg, 0.11 mmol, 1.0 eq.) and piperidine (11 mg, 0.013 mL, 0.13 mmol, 1.2 eq.) were added, the mixture was heated to 50 °C and stirred for 30 minutes. After allowing the reaction mixture to cool to RT, water (10 mL) and chloroform (10 mL) were added. The layers were separated, and the organic layer was washed with $MgSO_4$ before being concentrated in *vacuo*. Column chromatography (0–50%

CH_2Cl_2 in hexane) yielded N-(2-((*tert*-butyldimethylsilyl)oxy)ethyl)-4-((E)-2-((E)-3-((E)-3-(5,5-difluoro-3,7-diethyl-5H-4λ^4,5λ^4-dipyrrolo[1,2-c:2',1'-f][1,3,2]diazaborinin-10-yl)allylidene)-5,5-dimethylcyclohex-1-en-1-yl)vinyl)-N-ethylaniline **104** (10 mg, 14 μmol, 13%) as a dark solid.

R_f (50% CH_2Cl_2 in hexane) 0.42; **mp** compound decomposed upon heating; **^{1}H NMR** (400 MHz, $CDCl_3$) δ 7.67 (dd, 0.2H, *J* = 12.0 and 15.0, CH-C*H*-CH), 7.50 (dd, 0.8H, *J* = 12.0 and 15.0, CH-C*H*-CH), 7.32 (d, 2H, *J* = 9.0, Ar(C*H*)-*m*-N), 7.19 (d, 0.5H, *J* = 4.0, C*H*-CH-C(CH_2CH_3)-N-BF_2), 7.16 (d, 1.5H, *J* = 4.0, C*H*-CH-C(CH_2CH_3)-N-BF_2), 6.84 (d, 1H, *J* = 14.5, CH-CH-C*H*-BODIPY), 6.74, (d, 1H, *J* = 15.5, N-Ar-CH-C*H*), 6.69–6.60 (m, 3H, N-Ar-C*H*-CH and Ar(C*H*)-*o*-N), 6.38–6.30 (m, 3H, CH-C*H*-C(CH_2CH_3)-N-BF_2 and C*H*-CH-CH-BODIPY), 6.28 (s, 1H, N-Ar-CH-CH-C-C*H*), 3.77 (t, 2H, *J* = 6.5, CH_2-O-Si), 3.50–3.39 (m, 4H, N-CH_2-CH_2 and N-CH_2-CH_3), 3.06 (q, , *J* = 7.5, CH_3-CH_2-BODIPY), 2.35 (s, 2H, C(CH_3)$_2$-CH_2-C-CH-CH-CH-BODIPY), 2.31 (s, 2H, C(CH_3)$_2$-CH_2-C-CH-CH-Ar), 1.34 (t, 6H, *J* = 7.5, CH_3-CH_2-BODIPY), 1.17 (t, 3H, *J* = 7.0, N-CH_2-CH_3), 1.03 (s, 6H, C(CH_3)$_2$), 0.90 (s, 9H, Si-C(CH_3)$_3$), 0.04 (s, 6H, Si(CH_3)$_2$); **^{13}C NMR** (125 MHz, $CDCl_3$) δ 161.14 (CH-CH-*C*(CH_2CH_3)-N-BF_2), 147.99 (Ar(*C*)-*i*-N), 146.21 (*C*-CH-CH-CH-BODIPY), 142.34 (N-Ar-CH-CH-*C*), 140.43 (CH-CH-CH-*C*-C-N-BF_2), 139.98 (CH-*C*H-CH-BODIPY), 133.08 (CH-CH-CH-C-*C*-N-BF_2), 130.26 (N-Ar-*C*H), 129.52 (N-Ar-CH-CH-C-*C*H), 128.27 (Ar(*C*H)-*m*-N), 127.94 (*C*H-CH-CH-BODIPY), 126.63 (N-Ar-CH-*C*H), 126.39 (*C*H-CH-C(CH_2CH_3)-N-BF_2), 124.89 (Ar(*C*)-*p*-N), 123.57 (CH-CH-*C*H-BODIPY), 116.16 (CH-*C*H-C(CH_2CH_3)-N-BF_2), 111.82 (Ar(*C*H)-*o*-N), 60.81 (*C*H_2-O-Si), 52.61 (N-*C*H_2-CH_2), 45.70 (N-*C*H_2-CH_3), 39.75 (C(CH_3)$_2$-*C*H_2-C-CH-CH-CH-BODIPY), 39.33 (C(CH_3)$_2$-*C*H_2-C-CH-CH-Ar), 29.14 (*C*(CH_3)$_2$), 28.73 (C(*C*H_3)$_2$), 26.07 (Si-C(*C*H_3)$_3$), 22.11 (BODIPY-*C*H_2-CH_3), 18.45 (Si-*C*(CH_3)$_3$), 13.06 (BODIPY-CH_2-*C*H_3), 12.40 (N-CH_2-*C*H_3), −5.20 (Si(*C*H_3)$_2$); **^{19}F NMR** (376 MHz, $CDCl_3$) δ −145.72 (B*F*$_2$); **MS** (ESI^+) m/z 697 $[M]^+$; **HRMS** (ESI^+) calcd. for $C_{42}H_{59}N_3BF_2OSi$ $[M+H]^+$ 698.4490, found 698.4487; **FTIR** (ν_{max}) 2924 (C-H stretching), 2854 (C-H stretching) cm^{-1}.

References

1 P. Weinberger, *Philos. Mag. Lett.*, 2008, **88**, 897–907.

2 G. Millot and P. Tchofo-Dinda, in *Encyclopedia of Modern Optics*, Elsevier, 2018, vol. 1–5, pp. 345–350.

3 N. Bloembergen, *IEEE J. Sel. Top. Quantum Electron.*, 2000, **6**, 876–880.

4 L. Novotny and B. Hecht, *Principles of Nano-Optics*, Cambridge University Press, Cambridge, 2nd edn., 2012.

5 C. Bosshard, in *Nonlinear Optical Effects and Materials*, Springer, Berlin, Heidelberg, 2000, pp. 7–161.

6 S. Bhadra, A. Ghatak and A. Ghatak, *Guided Wave Optics and Photonic Devices*, CRC Press, 1st edn., 2017.

7 L. Dalton, A. Harper, A. Ren, F. Wang, G. Todorova, J. Chen, C. Zhang and M. Lee, *Ind. Eng. Chem. Res.*, 1999, **38**, 8–33.

8 D. Inoue, T. Ichikawa, A. Kawasaki and T. Yamashita, *Micromachines*, 2019, **10**, 482.

9 M. Ahlheim, M. Barzoukas, P. V. Bedworth, M. Blanchard-Desce, A. Fort, Z.-Y. Hu, S. R. Marder, J. W. Perry, C. Runser, M. Staehelin and B. Zysset, *Science (80-.).*, 1996, **271**, 335–337.

10 A. Jen, J. Luo, T.-D. Kim, B. Chen, S.-H. Jang, J.-W. Kang, N. M. Tucker, S. Hau, Y. Tian, J.-W. Ka, M. Haller, Y. Liao, B. Robinson, L. Dalton and W. Herman, in *Linear and Nonlinear Optics of Organic Materials V*, ed. M. Eich, San Diego, 2005, vol. 5935, p. 593506.

11 A. V. Syuy and E. O. Kile, in *Asia-Pacific Conference on Fundamental Problems of Opto- and Microelectronics*, eds. Y. N. Kulchin, R. V. Romashko and A. V. Syuy, 2016, vol. 10176, p. 101761N.

12 S. Bauer, *J. Appl. Phys.*, 1996, **80**, 5531–5558.

13 H. Kawai, *Jpn. J. Appl. Phys.*, 1969, **8**, 975–976.

14 W. Wang, J. Wu, K. Chen, Q. Huang, J. Luo and K. Seng Chiang, *Opt. Lett.*, 2020, **45**, 2383.

15 R. Gerhard-Multhaupt, M. Wegener, W. Wirges, J. A. Giacometti, R. A. C. Altafim, L. F. Santos, R. M. Faria and M. Paajanen, in *Conference on Electrical Insulation and Dielectric Phenomena (CEIDP), Annual Report*, 2002, pp. 299–302.

16 M. Kato, M. Okunaka, N. Sugita, M. Kiguchi and Y. Taniguchi, *Bull. Chem. Soc. Jpn.*, 1997, **70**, 583–585.

17 W. Lin, Y. Cui, J. Gao, J. Yu, T. Liang and G. Qian, *J. Mater. Chem.*, 2012, **22**, 9202.

18 A. Shrivastava, in *Introduction to Plastics Engineering*, Elsevier, 2018, pp. 1–16.

19 N. A. Pikhtin, S. O. Slipchenko, Z. N. Sokolova and I. S. Tarasov, *Semiconductors*, 2004, **38**, 360–367.

20 A. J. Miller, A. E. Lita, B. Calkins, I. Vayshenker, S. M. Gruber and S. W. Nam, *Opt. Express*, 2011, **19**, 9102.

21 S. L. Chuang, *Physics of Photonic Devices*, Wiley, Illinois at Urbana-Champaign, 2nd edn., 2009.

22 K. H. Lee, C. S. Tan, Y. Wang, B. Wang, L. Zhang, W. A. Sasangka, S. C. Goh, S. Bao, K. E. Lee and E. A. Fitzgerald, *IEEE J. Electron Devices Soc.*, 2018, **6**, 571–578.

23 K. A. Reinhardt and W. Kern, *Handbook of Silicon Wafer Cleaning Technology*, 2018.

24 D. J. Peng, Y. S. Duh and C. M. Shu, *J. Loss Prev. Process Ind.*, 2006, **19**, 743–753.

25 S. K. Yesodha, C. K. Sadashiva Pillai and N. Tsutsumi, *Prog. Polym. Sci.*, 2004, **29**, 45–74.

26 F. Kajzar, K. S. Lee, A. K. Y. Jen, B. Kippelen, N. Peyghambarian, T. C. Lin, S. J. Chung, K. S. Kim, X. Wang, G. S. He and J. Swiatkiewicz, *Polymers for Photonics Applications II*, Springer Berlin Heidelberg, Berlin, Heidelberg, 2003, vol. 161.

27 J. Skindhøj, J. W. Perry and S. R. Marder, *Ind. Eng. Chem. Res.*, 1994, **38**, 8–33.

28 F. Liu, S. Mo, Z. Zhai, M. Peng, S. Wu, C. Li, C. Yu and J. Liu, *J. Mater. Chem. C*, 2020, **8**, 9226–9235.

29 W. Gao, J. Liu and I. V. Kityk, *Mini. Rev. Org. Chem.*, 2018, **16**, 228–235.

30 X.-H. Zhou, J. Davies, S. Huang, J. Luo, Z. Shi, B. Polishak, Y.-J. Cheng, T.-D. Kim, L. Johnson and A. Jen, *J. Mater. Chem.*, 2011, **21**, 4437.

31 M. He, T. M. Leslie and J. A. Sinicropi, *Chem. Mater.*, 2002, **14**, 2393–2400.

32 S.-S. Sun, C. Zhang, L. R. Dalton, S. M. Garner, A. Chen and W. H. Steier, *Chem. Mater.*, 1996, **8**, 2539–2541.

33 A. B. Marco, P. M. Burrezo, L. Mosteo, S. Franco, J. Garín, J. Orduna, B. E. Diosdado, B. Villacampa, J. T. López Navarrete, J. Casado and R. Andreu, *RSC Adv.*, 2015, **5**, 231–242.

34 Y. Liao, B. E. Eichinger, K. A. Firestone, M. Haller, J. Luo, W. Kaminsky, J. B. Benedict, P. J. Reid, A. K. Y. Jen, L. R. Dalton and B. H. Robinson, *J. Am. Chem. Soc.*, 2005, **127**, 2758–2766.

35 N. Martínez de Baroja, J. Garín, J. Orduna, R. Andreu, M. J. Blesa, B. Villacampa, R. Alicante and S. Franco, *J. Org. Chem.*, 2012, **77**, 4634–4644.

36 A. Treibs and F. -H Kreuzer, *Justus Liebigs Ann. Chem.*, 1968, **718**, 208–223.

37 N. Boens, V. Leen and W. Dehaen, *Chem. Soc. Rev.*, 2012, **41**, 1130–1172.

38 I. J. Arroyo, R. Hu, B. Z. Tang, F. I. López and E. Peña-Cabrera, *Tetrahedron*, 2011, **67**, 7244–7250.

39 Y. F. Wei, X. Wang, W. J. Shi, R. Chen, L. Zheng, Z. Z. Wang, K. Chen and L. Gao, *Eur. J. Med. Chem.*, 2021, **226**, 113828.

40 C. Ray, E. Avellanal-Zaballa, M. Muñoz-Úbeda, J. Colligan, F. Moreno, G. Muller, I. López-Montero, J. Bañuelos, B. L. Maroto and S. de la Moya, *Org. Chem. Front.*, 2023, **10**, 5834–5842.

41 H. Sakai, Y. Suzuki, M. Tsurui, Y. Kitagawa, T. Nakashima, T. Kawai, Y. Kondo, G. Matsuba, Y. Hasegawa and T. Hasobe, *J. Mater. Chem. C*, 2023, **11**, 2889–2896.

42 R. G. Clarke, J. Weatherston, R. A. Taj-Aldeen, P. G. Waddell, W. McFarlane, T. J. Penfold, J. Bogaerts, W. Herrebout, L. E. Mackenzie, R. Pal and M. J. Hall, *ChemPhotoChem*, 2023, **7**, e20220194.

43 S. Zhang, Y. Wang, F. Meng, C. Dai, Y. Cheng and C. Zhu, *Chem. Commun.*, 2015, **51**, 9014–9017.

44 A. Guerrero-Corella, J. Asenjo-Pascual, T. J. Pawar, S. Díaz-Tendero, A. Martín-Sómer, C. V. Gómez, J. L. Belmonte-Vázquez, D. E. Ramírez-Ornelas, E. Peña-

Cabrera, A. Fraile, D. C. Cruz and J. Alemán, *Chem. Sci.*, 2019, **10**, 4346–4351.

45 M. Meazza, C. M. Cruz, A. M. Ortuño, J. M. Cuerva, L. Crovetto and R. Rios, *Chem. Sci.*, 2021, **12**, 4503–4508.

46 J. H. Boyer, A. Haag, M.-L. Soong, K. Thangaraj and T. G. Pavlopoulos, *Appl. Opt.*, 1991, **30**, 3788_1.

47 M. Shah, K. Thangaraj, M. -L Soong, L. T. Wolford, J. H. Boyer, I. R. Politzer and T. G. Pavlopoulos, *Heteroat. Chem.*, 1990, **1**, 389–399.

48 X. F. Zhang, G. Q. Zhang and J. Zhu, *J. Fluoresc.*, 2019, **29**, 407–416.

49 G. Jones, S. Kumar, O. Klueva and D. Pacheco, *J. Phys. Chem. A*, 2003, **107**, 8429–8434.

50 B. R. Groves, S. M. Crawford, T. Lundrigan, C. F. Matta, S. Sowlati-Hashjin and A. Thompson, *Chem. Commun.*, 2013, **49**, 816–818.

51 T. Lundrigan and A. Thompson, *J. Org. Chem.*, 2013, **78**, 757–761.

52 Z. Wang, C. Cheng, Z. Kang, W. Miao, Q. Liu, H. Wang and E. Hao, *J. Org. Chem.*, 2019, **84**, 2732–2740.

53 Z. Wang, X. Guo, Z. Kang, Q. Wu, H. Li, C. Cheng, C. Yu, L. Jiao and E. Hao, *Org. Lett.*, 2023, **25**, 744–749.

54 G. Ulrich, C. Goze, S. Goeb, P. Retailleau and R. Ziessel, *New J. Chem.*, 2006, **30**, 982–986.

55 D. Listunov, S. Mazères, Y. Volovenko, E. Joly, Y. Génisson, V. Maraval and R. Chauvin, *Bioorganic Med. Chem. Lett.*, 2015, **25**, 4652–4656.

56 L. J. Patalag, S. Ahadi, O. Lashchuk, P. G. Jones, S. Ebbinghaus and D. B. Werz, *Angew. Chemie - Int. Ed.*, 2021, **60**, 8766–8771.

57 L. Zhao, H. Zhou, Q. Zhou, C. Peng, T. Cheng and G. Liu, *Sensors Actuators B Chem.*, 2020, **320**, 128383.

58 K. Korpis, F. Weber, S. Brune, B. Wünsch and P. J. Bednarski, *Bioorganic Med. Chem.*, 2014, **22**, 221–233.

59 S. Schaffer, R. Tandon, H. Zipse, W. Siess, A. Schmidt, J. Jamasbi, E. Karshovska, W.

Steglich and R. Lorenz, *Biochem. Pharmacol.*, 2013, **86**, 279–285.

60 C. Ray, L. Díaz-Casado, E. Avellanal-Zaballa, J. Bañuelos, L. Cerdán, I. García-Moreno, F. Moreno, B. L. Maroto, Í. López-Arbeloa and S. de la Moya, *Chem. - A Eur. J.*, 2017, **23**, 9383–9390.

61 C. Coutant, J. Fischer, P. Nun and V. Coeffard, *ChemistrySelect*, 2023, **8**, e202303316.

62 P. H. Marek-Urban, K. A. Urbanowicz, K. Wrochna, P. Pander, A. Blacha-Grzechnik, S. T. Hauer, H. R. V. Berens, K. Woźniak, T. J. J. Müller and K. Durka, *Chem. – A Eur. J.*, 2023, **29**, e20230068.

63 X. L. Li, N. Han, R. Z. Zhang, K. K. Niu, R. Z. Dong, H. Liu, S. Yu, Y. B. Wang and L. B. Xing, *ACS Appl. Mater. Interfaces*, 2023, **15**, 55803–55812.

64 J. Fischer, L. Mele, H. Serier-Brault, P. Nun and V. Coeffard, *European J. Org. Chem.*, 2019, **2019**, 6352–6358.

65 A. Da Lama, B. Bartolomei, C. Rosso, G. Filippini, M. M. Martínez, L. A. Sarandeses and M. Prato, *European J. Org. Chem.*, 2022, **2022**, e202200622.

66 L. Pantaine, V. Coeffard, X. Moreau and C. Greck, *European J. Org. Chem.*, 2015, **2015**, 2005–2011.

67 Y. Zhang, G. Li, J. Li, M. Wu, X. Liu and J. Liu, *J. Innov. Opt. Health Sci.*, 2022, **15**, e2240009.

68 Y. Tang, L. Xue, Q. Yu, D. Chen, Z. Cheng, W. Wang, J. Shao and X. Dong, *ACS Appl. Bio Mater.*, 2019, **2**, 5888–5897.

69 M. Li, Y. Gao, Y. Yuan, Y. Wu, Z. Song, B. Z. Tang, B. Liu and Q. C. Zheng, *ACS Nano*, 2017, **11**, 3922–3932.

70 L. Espinar-Barranco, M. Meazza, A. Linares-Perez, R. Rios, J. M. Paredes and L. Crovetto, *Sensors*, 2019, **19**, 4932.

71 J. Zhang, X. Zhang, X. Meng, L. Li, J. Yao, W. Liu and Y. Liu, *Synth. Met.*, 2013, **185**–**186**, 120–125.

72 M. C. Davis and A. J. Sathrum, *Synth. Commun.*, 2007, **37**, 921–926.

73 M. C. Davis, A. P. Chafin, R. A. Hollins, L. C. Baldwin, E. D. Erickson, P. Zarras and

E. C. Drury, *Synth. Commun.*, 2004, **34**, 3419–3429.

74 J. Luo, Y.-J. Cheng, T.-D. Kim, S. Hau, S.-H. Jang, Z. Shi, X.-H. Zhou and A. K. Y. Jen, *Org. Lett.*, 2006, **8**, 1387–1390.

75 S. Liu, M. A. Haller, J. Luo, S. H. Jang, H. Ma, L. R. Dalton and A. K. Y. Jen, *Adv. Mater.*, 2003, **15**, 375–380.

76 B. C. Ranu, L. Adak and S. Banerjee, *Can. J. Chem.*, 2007, **85**, 366–371.

77 B. C. Ranu and S. Banerjee, *J. Org. Chem.*, 2005, **70**, 4517–4519.

78 R. Zhu, L. Xing, X. Wang, C. Cheng, B. Liu and Y. Hu, *Synlett*, 2007, **2007**, 2267–2271.

79 B. Kasum, R. Prager and C. Tsopelas, *Aust. J. Chem.*, 1990, **43**, 355.

80 M. M. Mojtahedi, M. S. Abaee, M. M. Zahedi, M. R. Jalali, A. W. Mesbah, W. Massa, R. Yaghoubi and M. Forouzani, *Monatshefte fur Chemie*, 2008, **139**, 917–921.

81 M. Mizuno and T. Shioiri, *Tetrahedron Lett.*, 1999, **40**, 7105–7108.

82 W. Jin, P. V. Johnston, D. L. Elder, K. T. Manner, K. E. Garrett, W. Kaminsky, R. Xu, B. H. Robinson and L. R. Dalton, *J. Mater. Chem. C*, 2016, **4**, 3119–3124.

83 C. A. M. Afonso, *Tetrahedron Lett.*, 1995, **36**, 8857–8858.

84 G. Guanti, L. Banfi, E. Narisano and C. Scolastico, *Tetrahedron*, 1988, **44**, 3671–3684.

85 M. Macias-Contreras, K. L. Daykin, J. T. Simmons, J. R. Allen, Z. S. Hooper, M. W. Davidson and L. Zhu, *Org. Biomol. Chem.*, 2017, **15**, 9139–9148.

86 E. Palao, A. R. Agarrabeitia, J. Bañuelos-Prieto, T. A. Lopez, I. Lopez-Arbeloa, D. Armesto and M. J. Ortiz, *Org. Lett.*, 2013, **15**, 4454–4457.

87 D. Kim, K. Yamamoto and K. H. Ahn, *Tetrahedron*, 2012, **68**, 5279–5282.

88 E. Palao, G. Duran-Sampedro, S. De La Moya, M. Madrid, C. García-López, A. R. Agarrabeitia, B. Verbelen, W. Dehaen, N. Boens and M. J. Ortiz, *J. Org. Chem.*, 2016, **81**, 3700–3710.

89 T. Rigotti, J. Asenjo-Pascual, A. Martín-Somer, P. Milán Rois, M. Cordani, S. Díaz-

Tendero, Á. Somoza, A. Fraile and J. Alemán, *Adv. Synth. Catal.*, 2020, **362**, 1345–1355.

90 D. A. Conlon, A. Drahus-Paone, G.-J. Ho, B. Pipik, R. Helmy, J. M. McNamara, Y.-J. Shi, J. M. Williams, D. Macdonald, D. Deschênes, M. Gallant, A. Mastracchio, B. Roy and J. Scheigetz, *Org. Process Res. Dev.*, 2006, **10**, 36–45.

91 P. Kancharla, J. X. Kelly and K. A. Reynolds, *J. Med. Chem.*, 2015, **58**, 7286–7309.

92 N. Kaur, P. Kaur, G. Bhatia, K. Singh and J. Singh, *RSC Adv.*, 2016, **6**, 82810–82816.

93 Y. Chen, L. Wan, D. Zhang, Y. Bian and J. Jiang, *Photochem. Photobiol. Sci.*, 2011, **10**, 1030–1038.

94 G. Duran-Sampedro, E. Palao, A. R. Agarrabeitia, S. D. La Moya, N. Boens and M. J. Ortiz, *RSC Adv.*, 2014, **4**, 19210–19213.

95 E. Peña-Cabrera, A. Aguilar-Aguilar, M. González-Domínguez, E. Lager, R. Zamudio-Vázquez, J. Godoy-Vargas and F. Villanueva-García, *Org. Lett.*, 2007, **9**, 3985–3988.

96 T. V. Goud, A. Tutar and J. F. Biellmann, *Tetrahedron*, 2006, **62**, 5084–5091.

97 A. Da Lama, J. Pérez Sestelo, L. A. Sarandeses and M. M. Martínez, *Org. Biomol. Chem.*, 2022, **20**, 9132–9137.

98 F. Sozmen, S. Kolemen, H. O. Kumada, M. Ono, H. Saji and E. U. Akkaya, *RSC Adv.*, 2014, **4**, 51032–51037.

Appendices

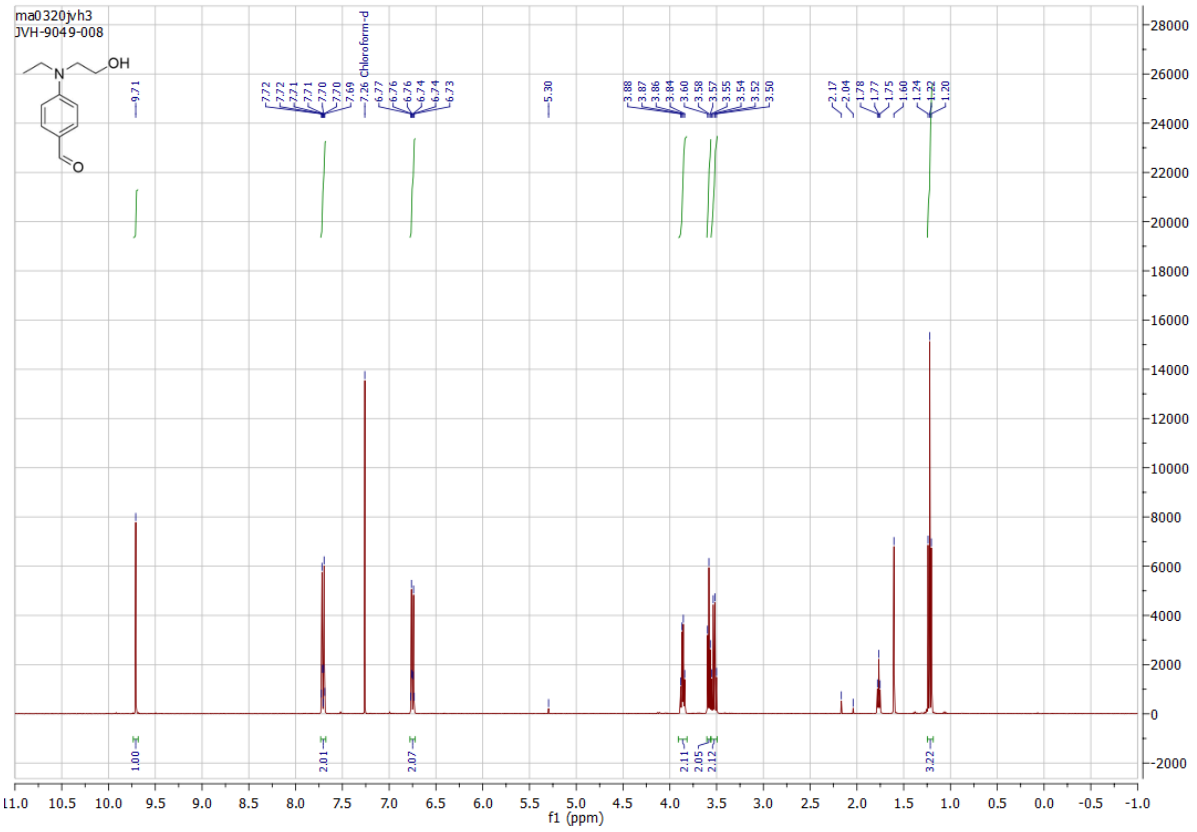

*Appendix 1: ^{1}H NMR spectrum of 4-(ethyl(2-hydroxyethyl)amino)benzaldehyde **51**.*

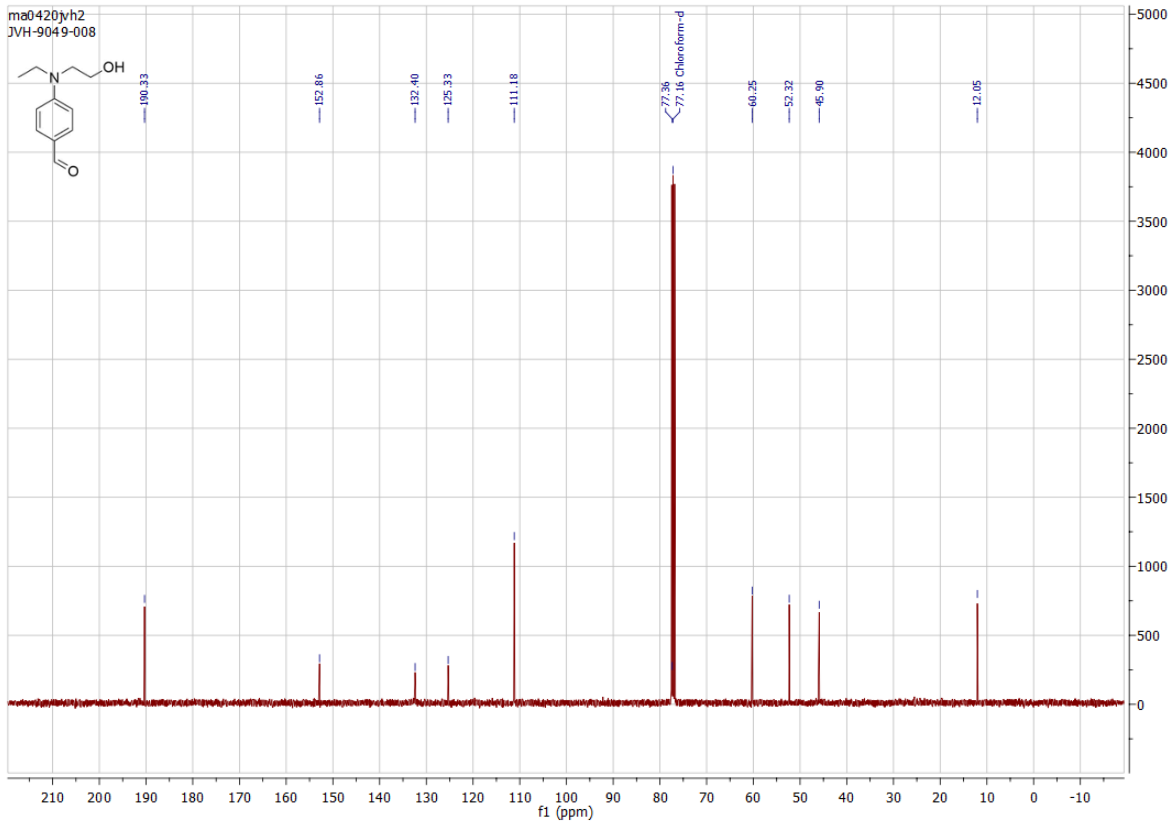

*Appendix 2: ^{13}C NMR spectrum of 4-(ethyl(2-hydroxyethyl)amino)benzaldehyde **51**.*

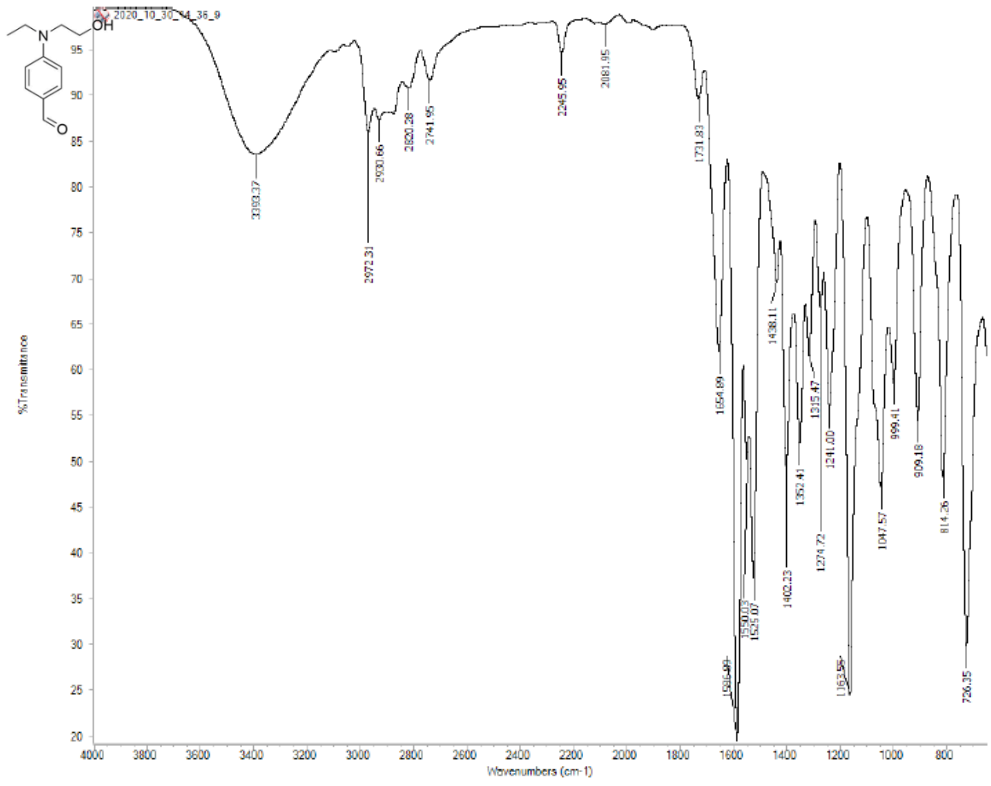

*Appendix 3: FTIR spectrum of 4-(ethyl(2-hydroxyethyl)amino)benzaldehyde **51**.*

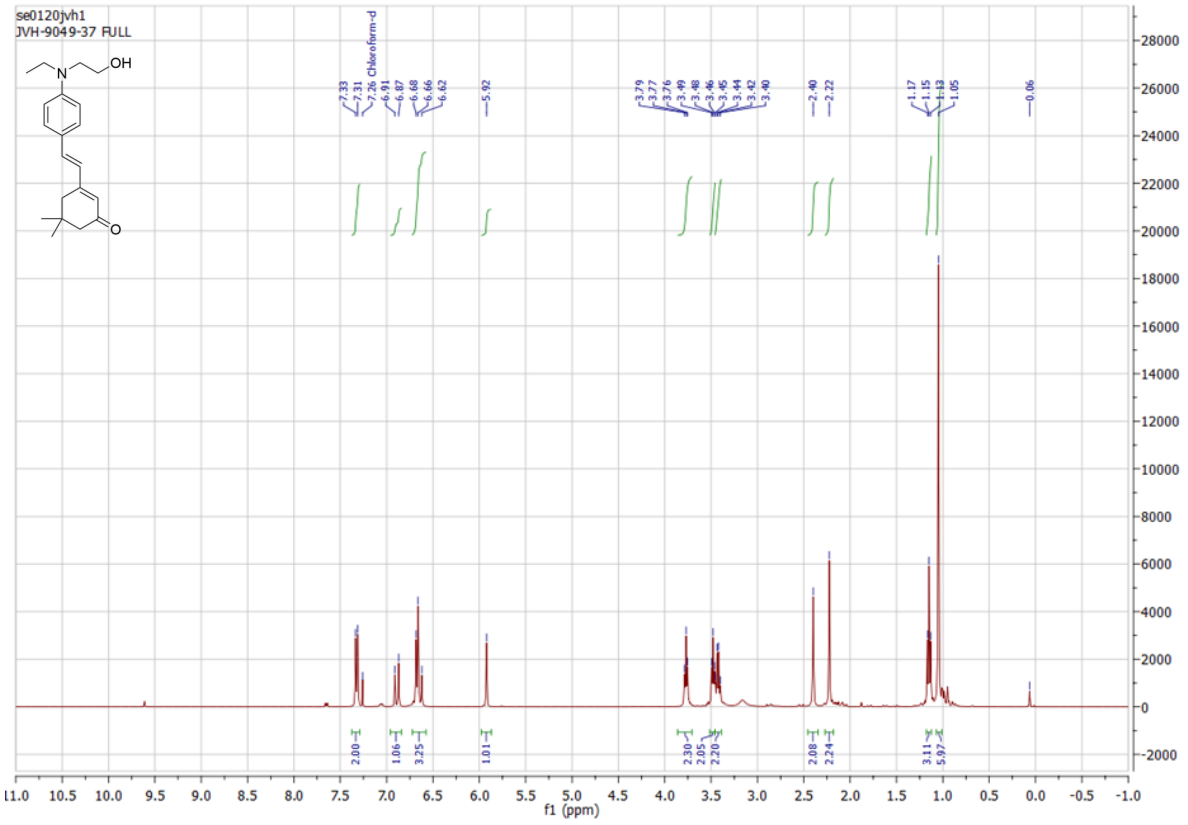

*Appendix 4: [1]H NMR spectrum of (E)-3-(4-(ethyl(2-hydroxyethyl)amino)styryl)-5,5-dimethylcyclohex-2-en-1-one **53**.*

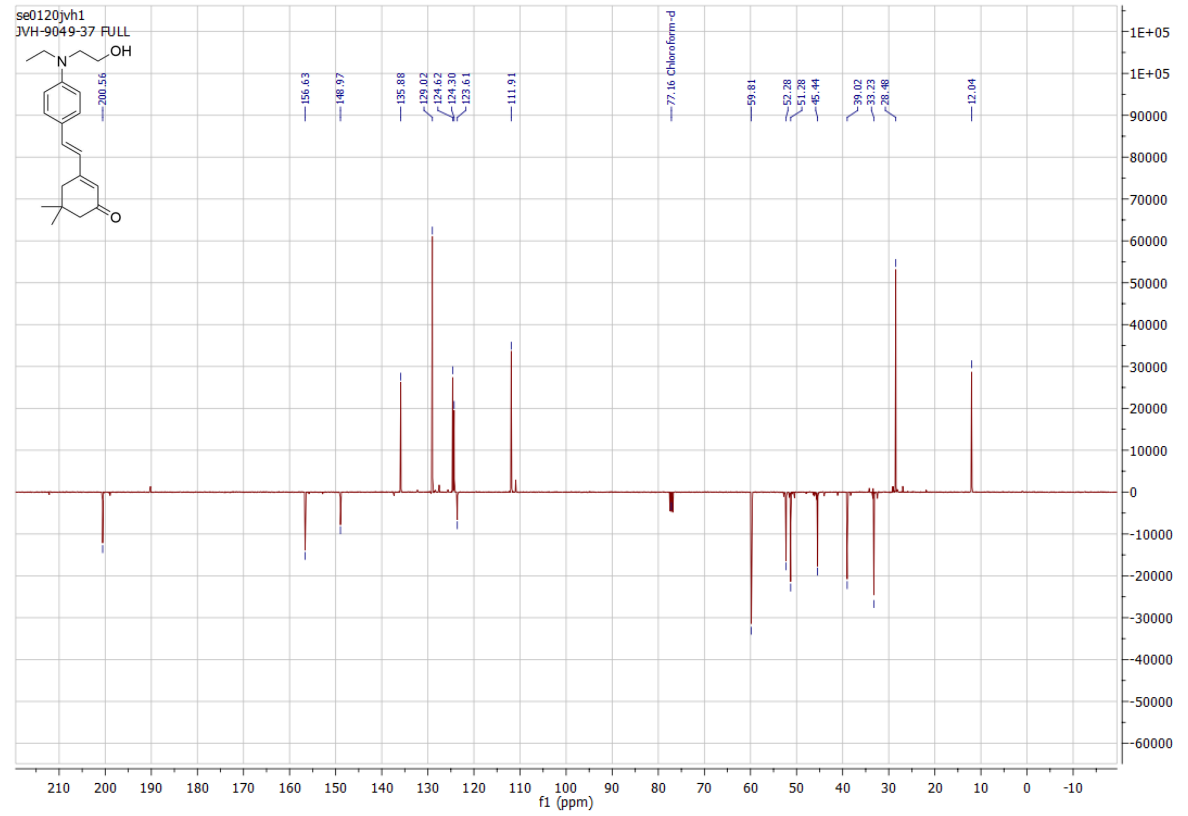

*Appendix 5: [13]C NMR spectrum of (E)-3-(4-(ethyl(2-hydroxyethyl)amino)styryl)-5,5-dimethylcyclohex-2-en-1-one **53**.*

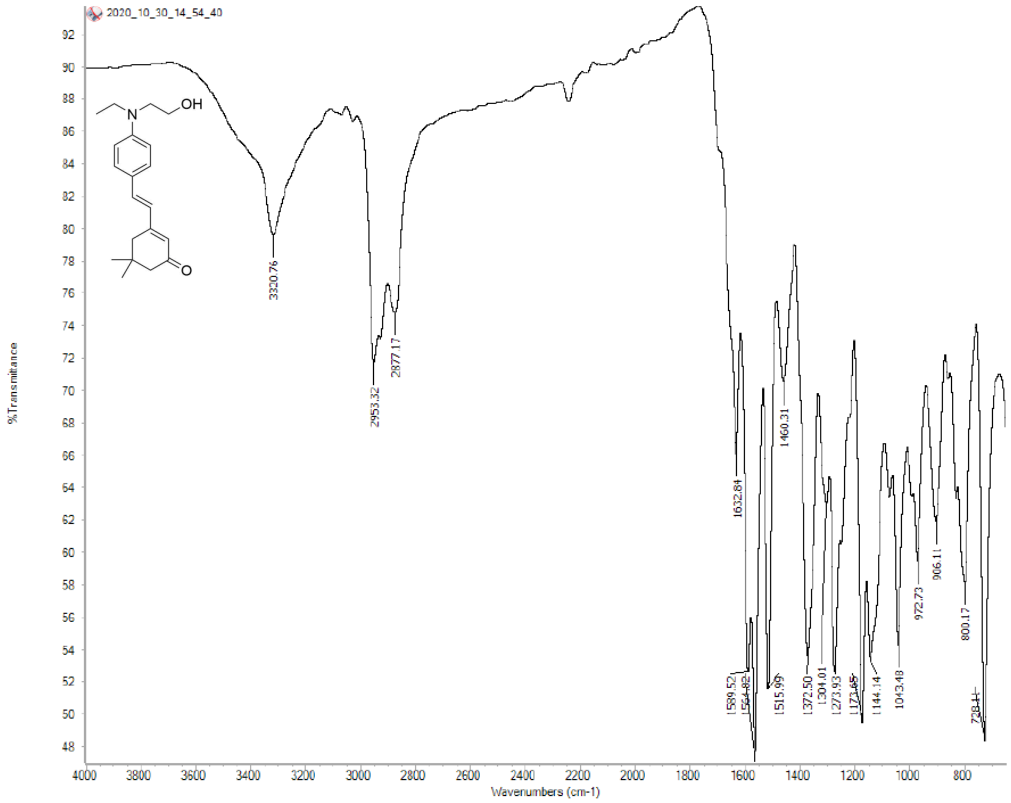

*Appendix 6: FTIR spectrum of (E)-3-(4-(ethyl(2-hydroxyethyl)amino)styryl)-5,5-dimethylcyclohex-2-en-1-one **53**.*

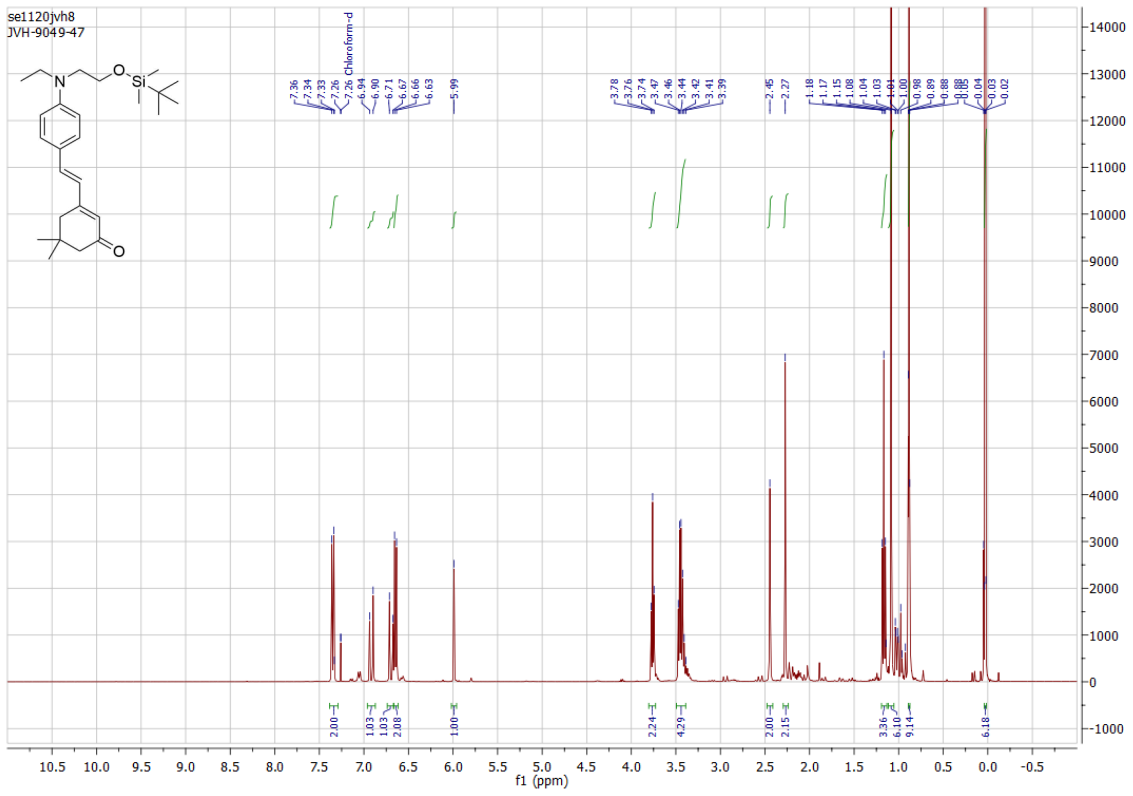

*Appendix 7: [1]H NMR spectrum of (E)-3-(4-((2-((tert-butyldimethylsilyl)oxy)ethyl)(ethyl)amino)styryl)-5,5-dimethylcyclohex-2-en-1-one **54**.*

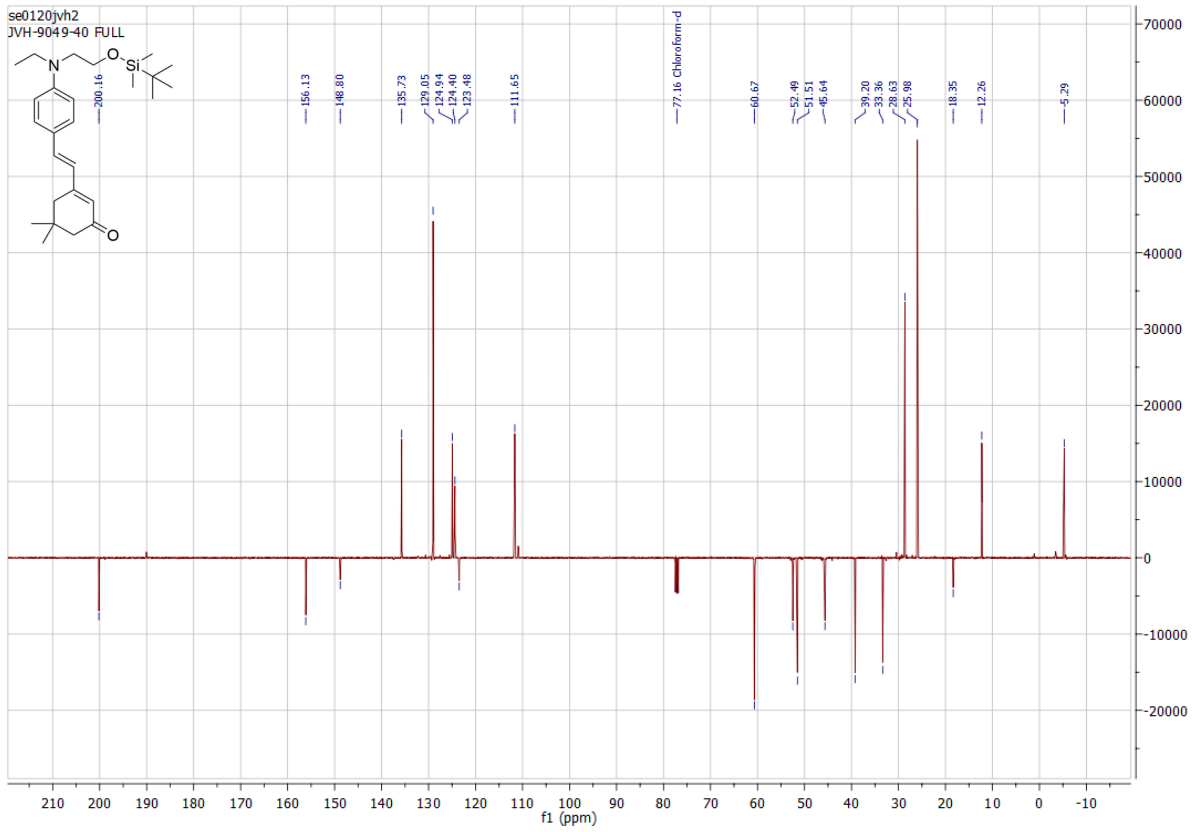

*Appendix 8: ^{13}C NMR spectrum of (E)-3-(4-((2-((tert-butyldimethylsilyl)oxy)ethyl)(ethyl)amino)styryl)-5,5-dimethylcyclohex-2-en-1-one **54**.*

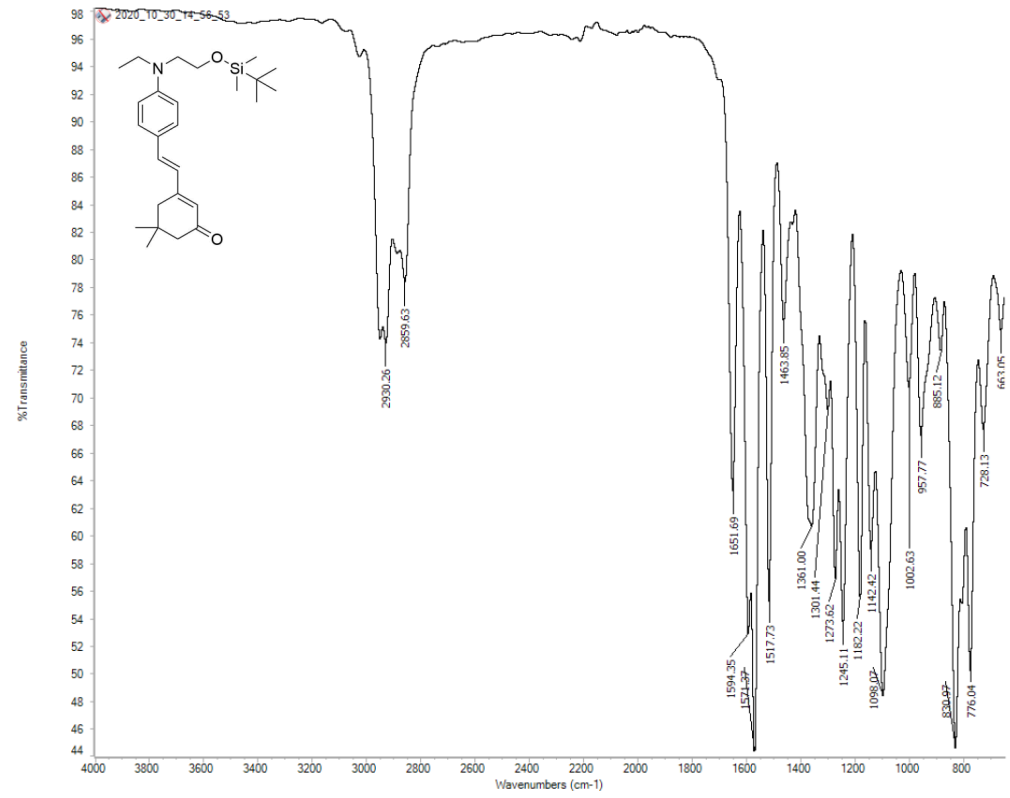

Appendix 9: FTIR spectrum of *(E)-3-(4-((2-((tert-butyldimethylsilyl)oxy)ethyl)(ethyl)amino)styryl)-5,5-dimethylcyclohex-2-en-1-one **54**.*

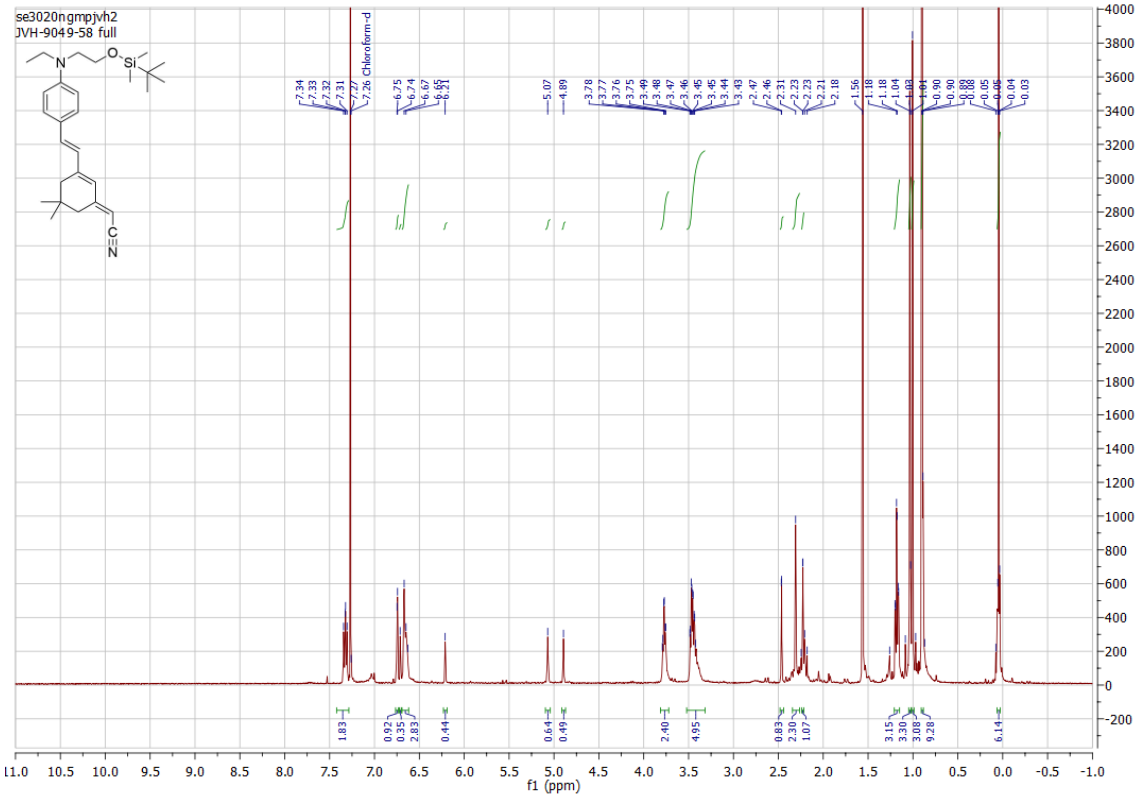

*Appendix 10: [1]H NMR spectrum of (E/Z)-2-(3-((E)-4-((2-((tert-butyldimethylsilyl)oxy)ethyl)(ethyl)amino)styryl)-5,5-dimethylcyclohex-2-en-1-ylidene)acetonitrile **55E/Z**.*

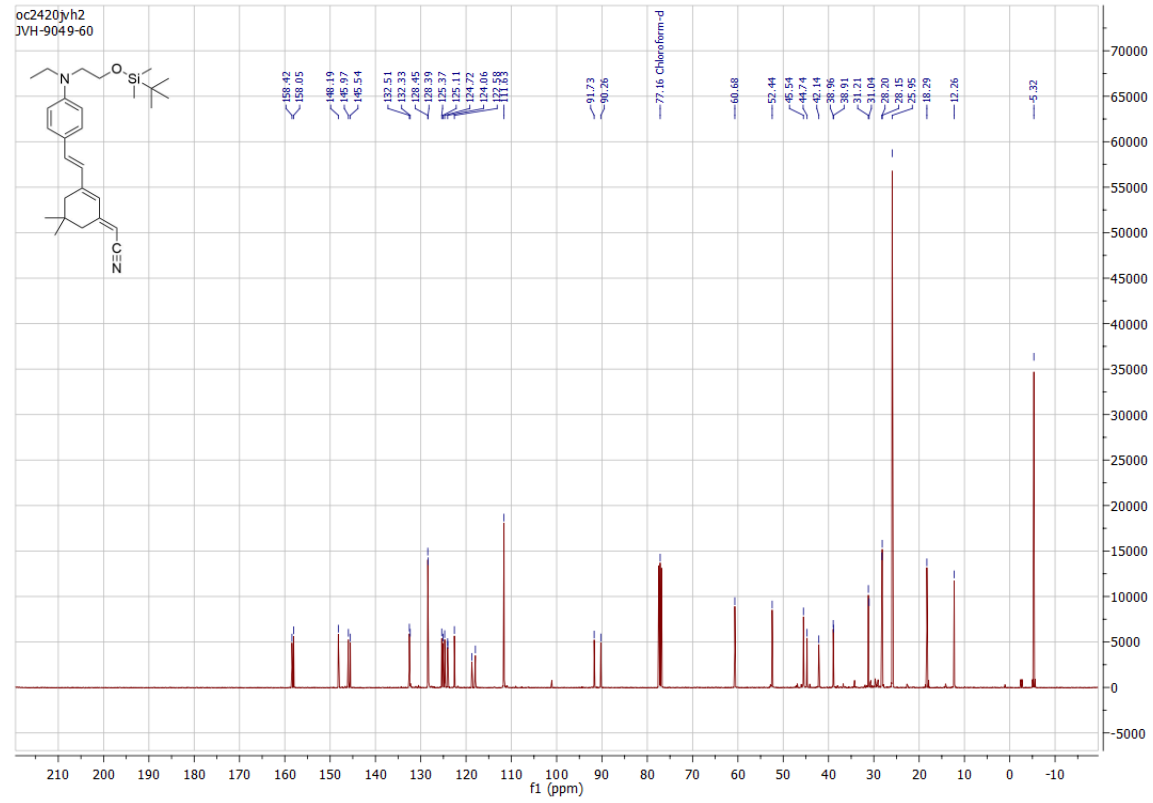

*Appendix 11: [13]C NMR spectrum of (E/Z)-2-(3-((E)-4-((2-((tert-butyldimethylsilyl)oxy)ethyl)(ethyl)amino)styryl)-5,5-dimethylcyclohex-2-en-1-ylidene)acetonitrile **55E/Z**.*

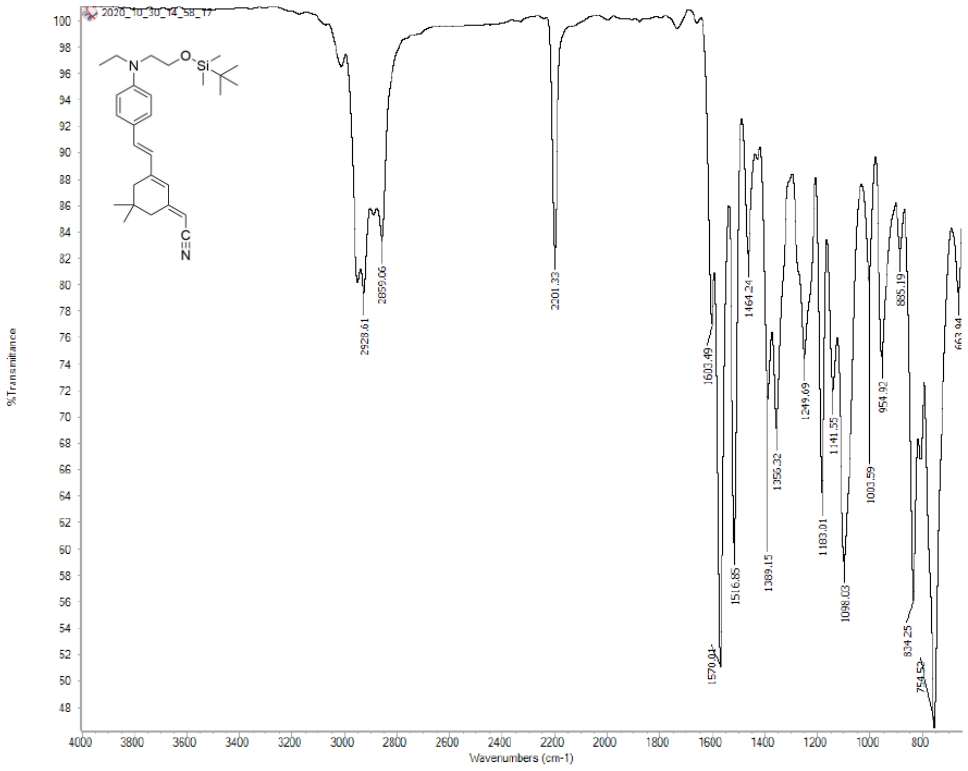

Appendix 12: FTIR spectrum of (E/Z)-2-(3-((E)-4-((2-((tert-butyldimethylsilyl)oxy)ethyl)(ethyl)amino)styryl)-5,5-dimethylcyclohex-2-en-1-ylidene)acetonitrile ***55E/Z****.*

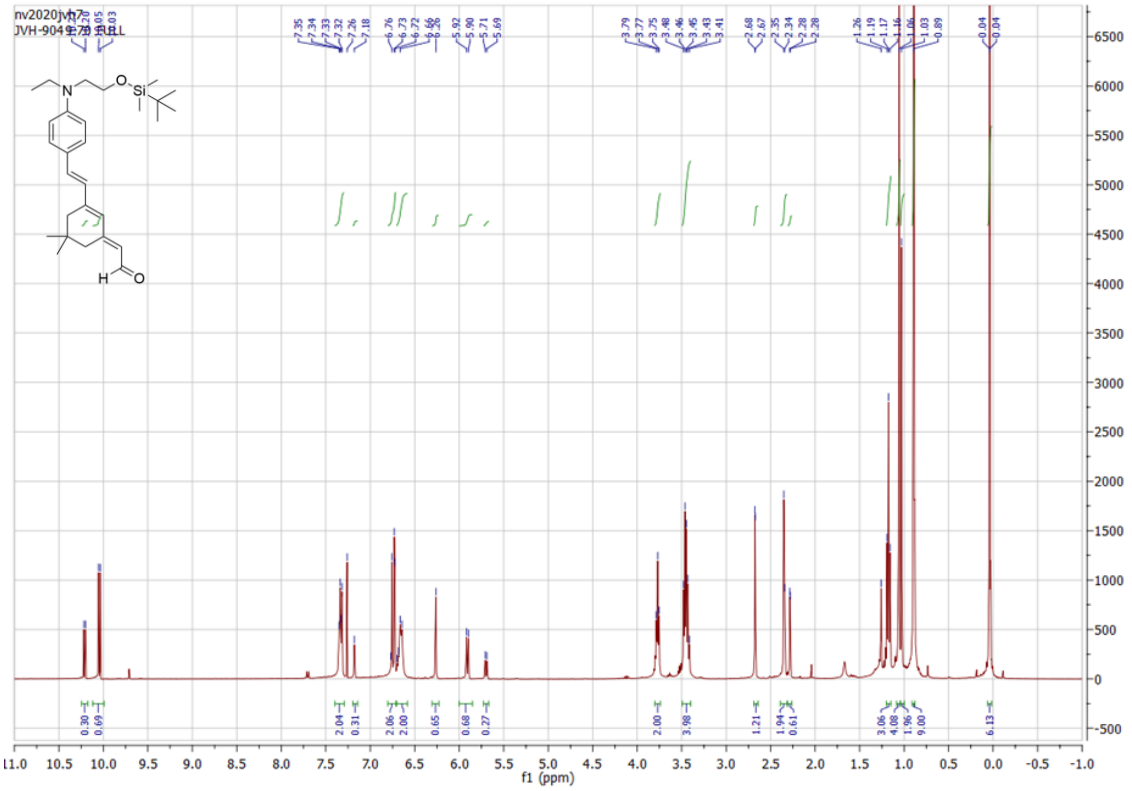

Appendix 13: ^{1}H NMR spectrum of *(E/Z)-2-(3-((E)-4-((2-((tert-butyldimethylsilyl)oxy)ethyl)(ethyl)amino)styryl)-5,5-dimethylcyclohex-2-en-1-ylidene)acetaldehyde* ***56E/Z****.*

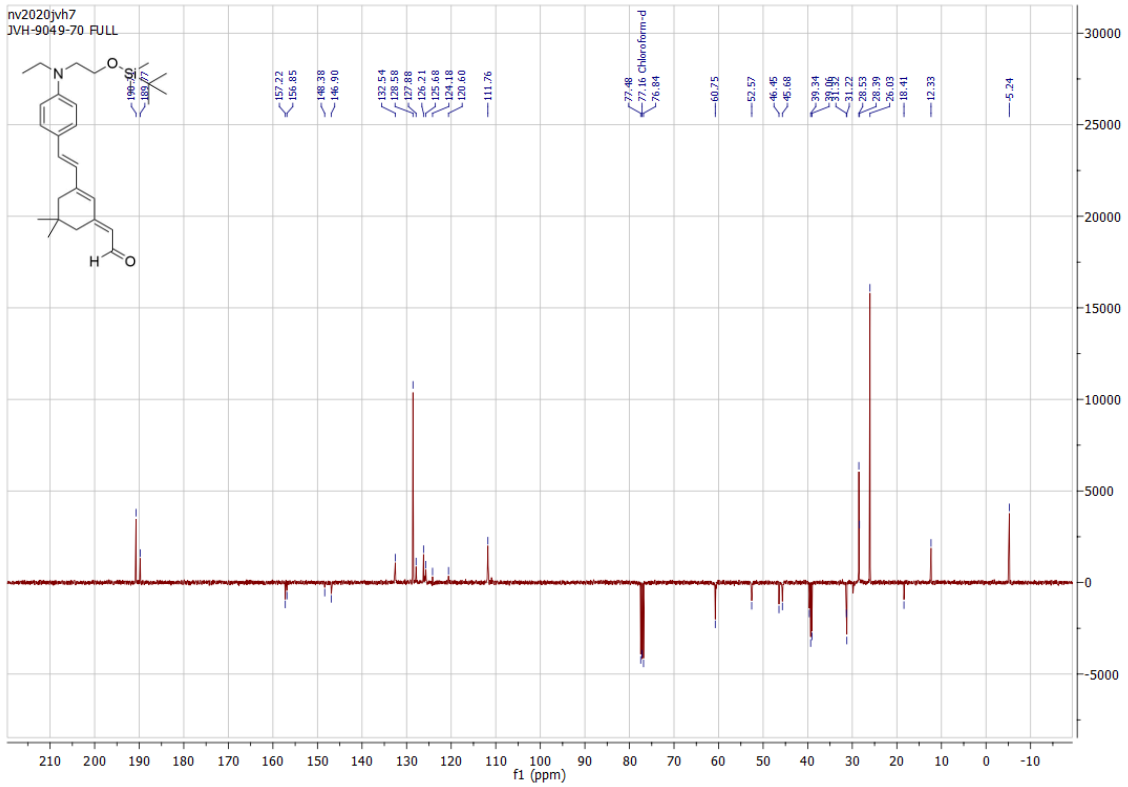

Appendix 14: ^{13}C NMR spectrum of (E/Z)-2-(3-((E)-4-((2-((tert-butyldimethylsilyl)oxy)ethyl)(ethyl)amino)styryl)-5,5-dimethylcyclohex-2-en-1-ylidene)acetaldehyde ***56E/Z****.*

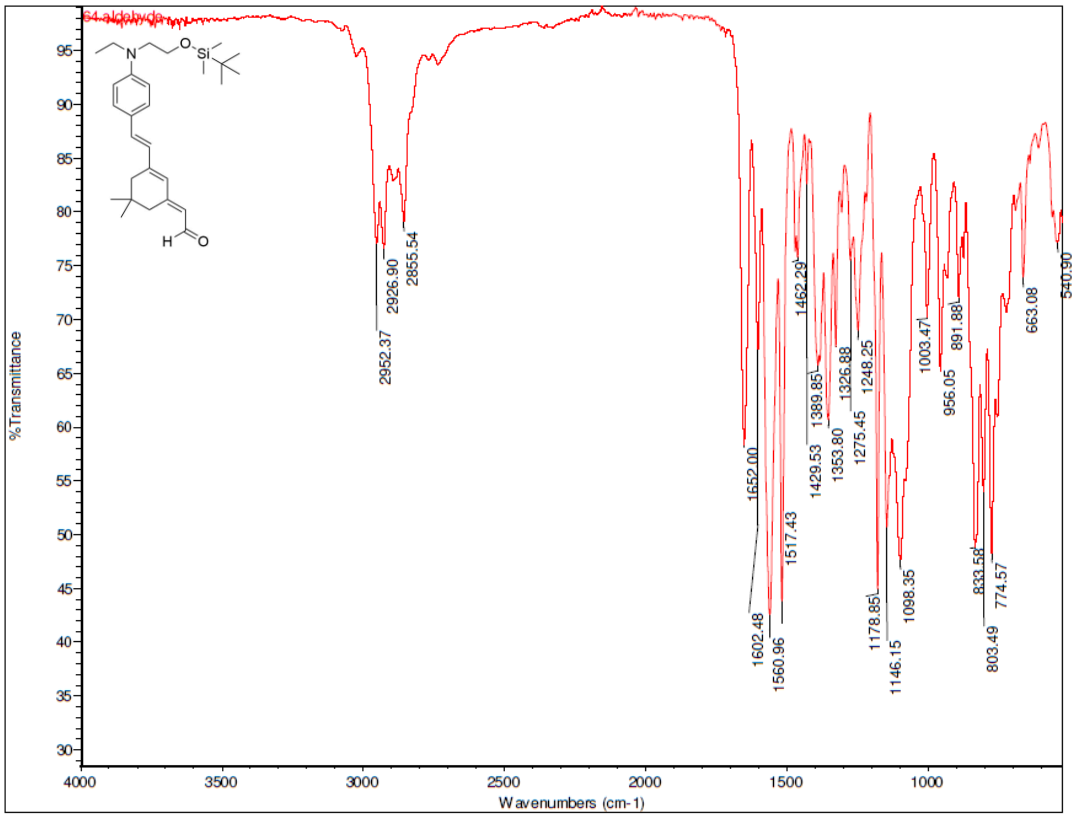

Appendix 15 FTIR spectrum of (E/Z)-2-(3-((E)-4-((2-((tert-butyldimethylsilyl)oxy)ethyl)(ethyl)amino)styryl)-5,5-dimethylcyclohex-2-en-1-ylidene)acetaldehyde ***56E/Z****.*

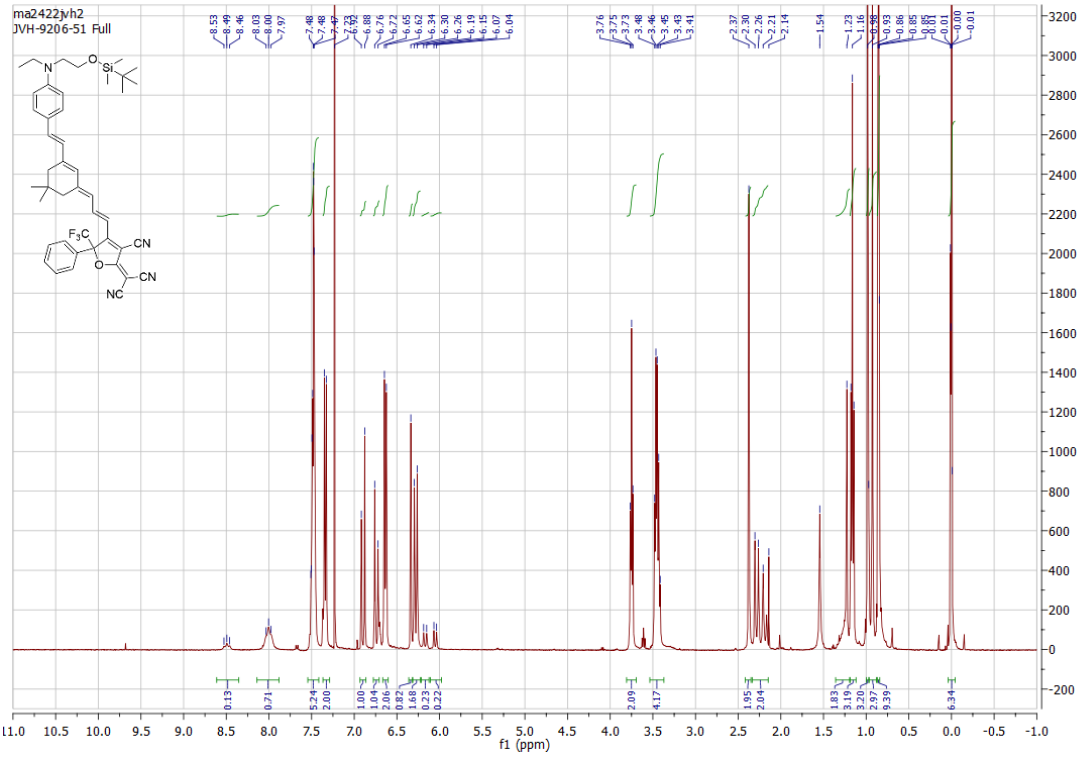

*Appendix 16: [1]H NMR spectrum of 2-(4-((1E,3E)-3-(3-((E)-4-((2-((tert-butyldimethylsilyl)oxy)ethyl)(ethyl)amino)styryl)-5,5-dimethylcyclohex-2-en-1-ylidene)prop-1-en-1-yl)-3-cyano-5-phenyl-5-(trifluoromethyl)furan-2(5H)-ylidene)malononitrile **49**.*

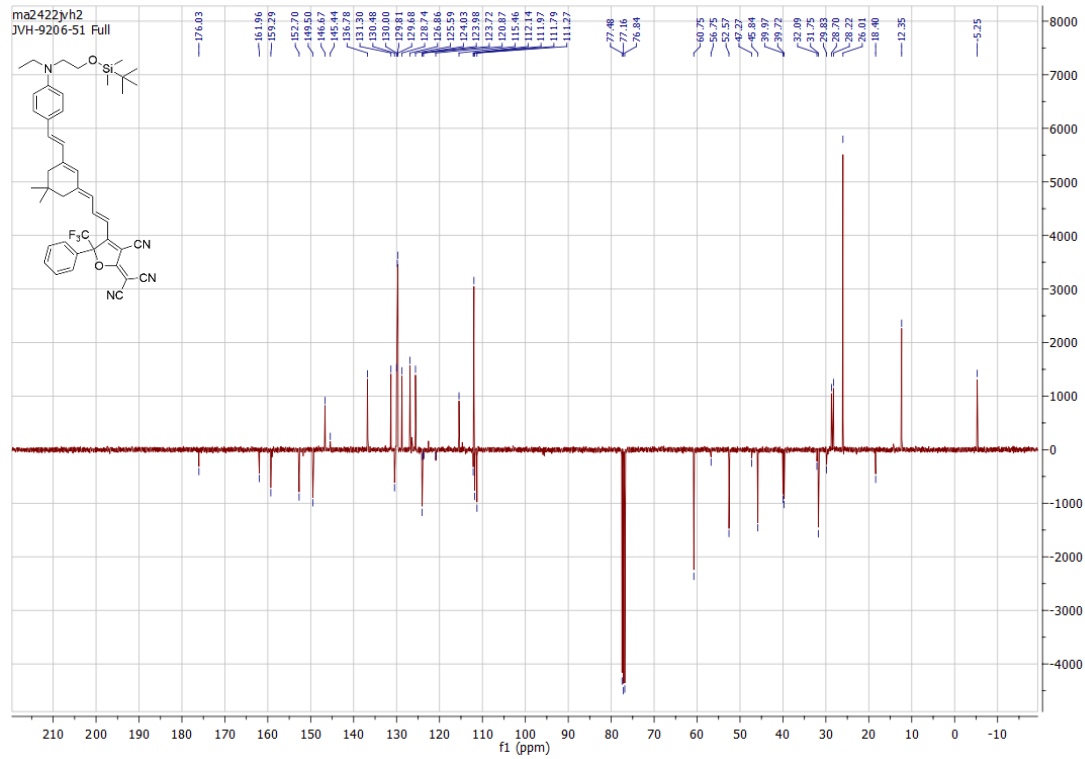

*Appendix 17: [13]C NMR spectrum of 2-(4-((1E,3E)-3-(3-((E)-4-((2-((tert-butyldimethylsilyl)oxy)ethyl)(ethyl)amino)styryl)-5,5-dimethylcyclohex-2-en-1-ylidene)prop-1-en-1-yl)-3-cyano-5-phenyl-5-(trifluoromethyl)furan-2(5H)-ylidene)malononitrile **49**.*

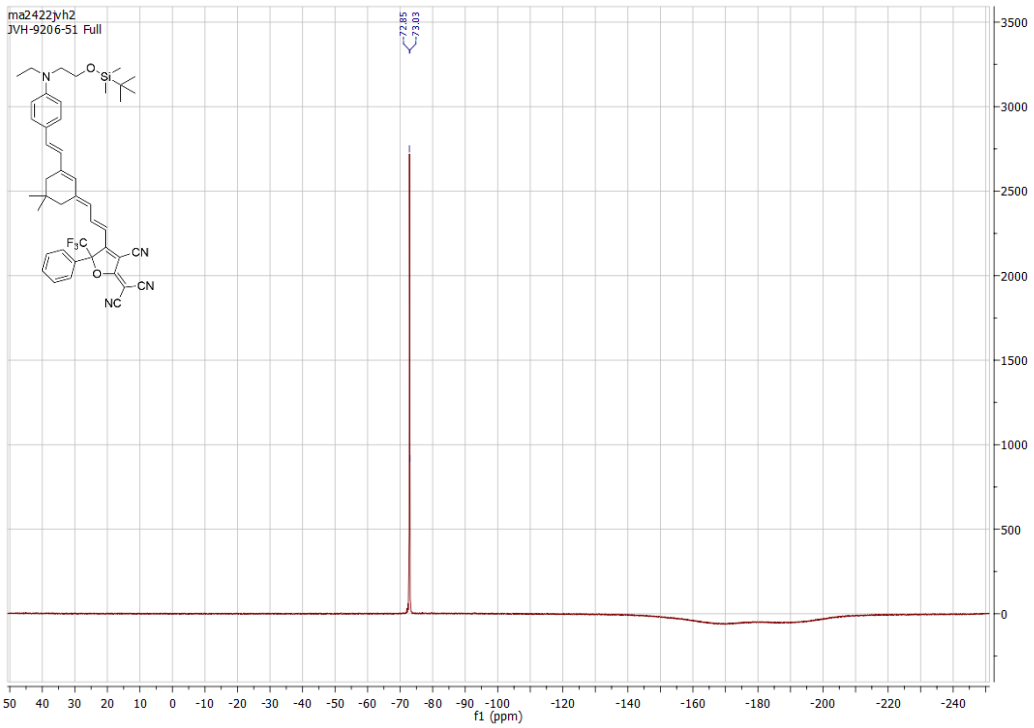

*Appendix 18: ^{19}F NMR spectrum of 2-(4-((1E,3E)-3-(3-((E)-4-((2-((tert-butyldimethylsilyl)oxy)ethyl)(ethyl)amino)styryl)-5,5-dimethylcyclohex-2-en-1-ylidene)prop-1-en-1-yl)-3-cyano-5-phenyl-5-(trifluoromethyl)furan-2(5H)-ylidene)malononitrile **49**.*

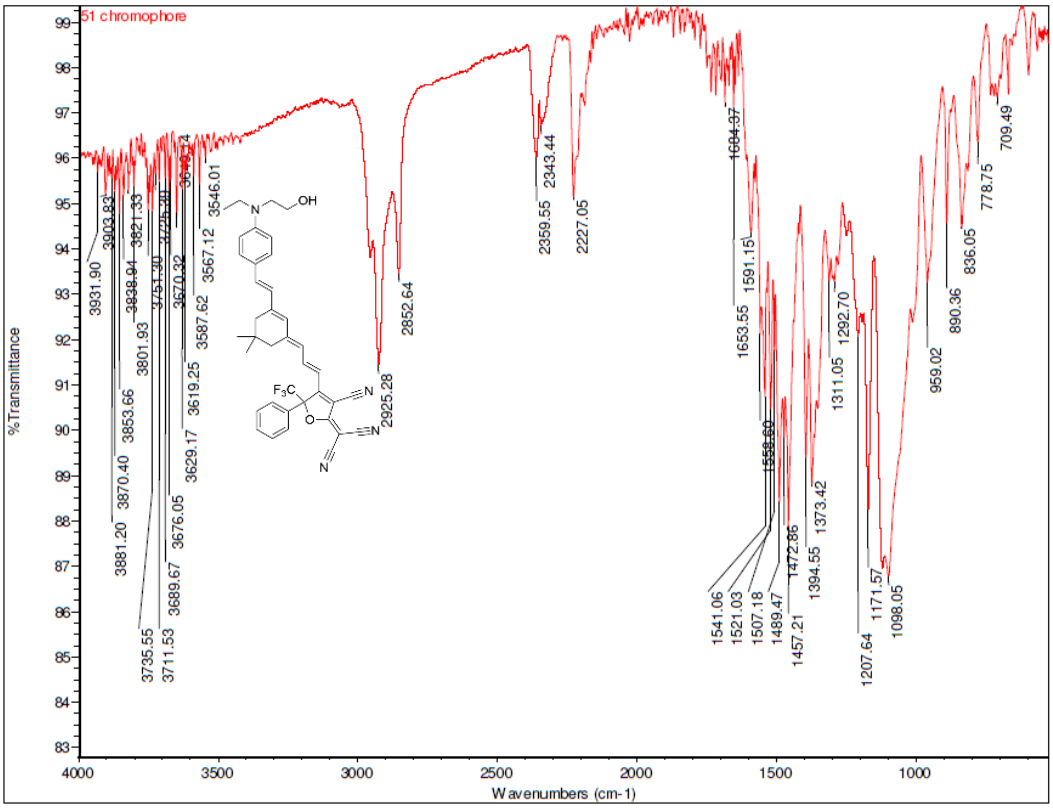

*Appendix 19: FTIR specrtum of 2-(4-((1E,3E)-3-(3-((E)-4-((2-((tert-butyldimethylsilyl)oxy)ethyl)(ethyl)amino)styryl)-5,5-dimethylcyclohex-2-en-1-ylidene)prop-1-en-1-yl)-3-cyano-5-phenyl-5-(trifluoromethyl)furan-2(5H)-ylidene)malononitrile **49**.*

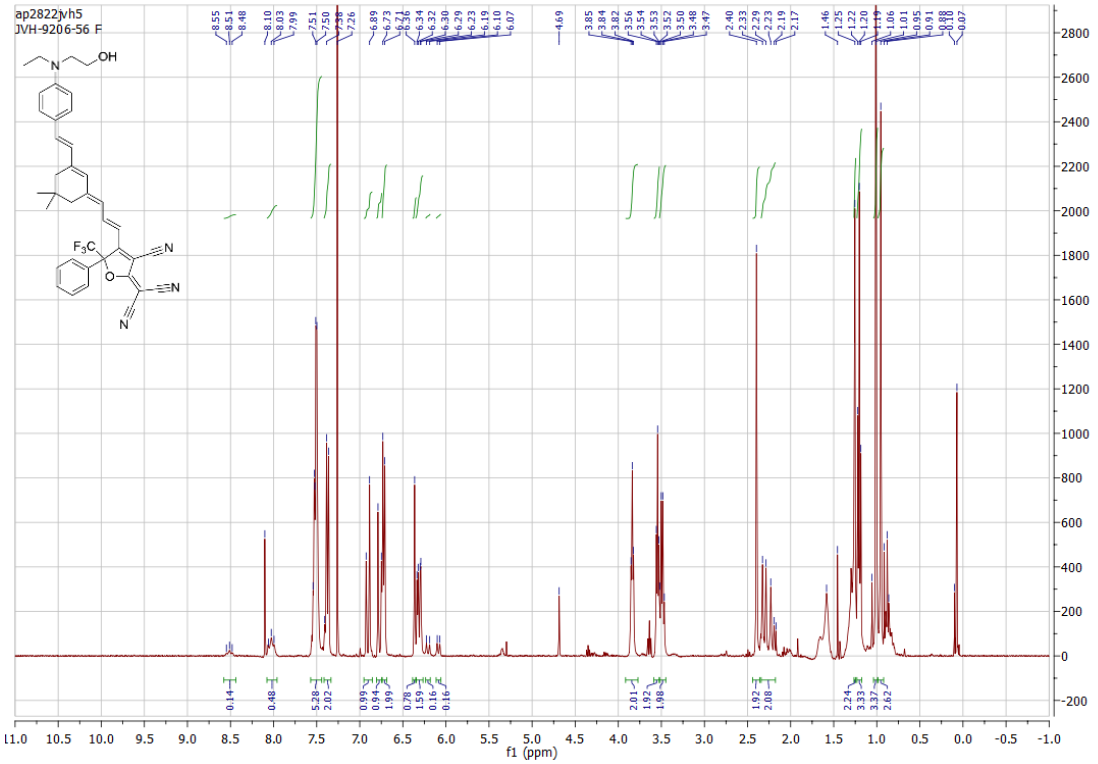

*Appendix 20: [1]H NMR spectrum of 2-(4-((1E,3E)-3-(3-((E)-4-(ethyl(2-hydroxyethyl)amino)styryl)-5,5-dimethylcyclohex-2-en-1-ylidene)prop-1-en-1-yl)-3-cyano-5-phenyl-5-(trifluoromethyl)furan-2(5H)-ylidene)malononitrile **60**.*

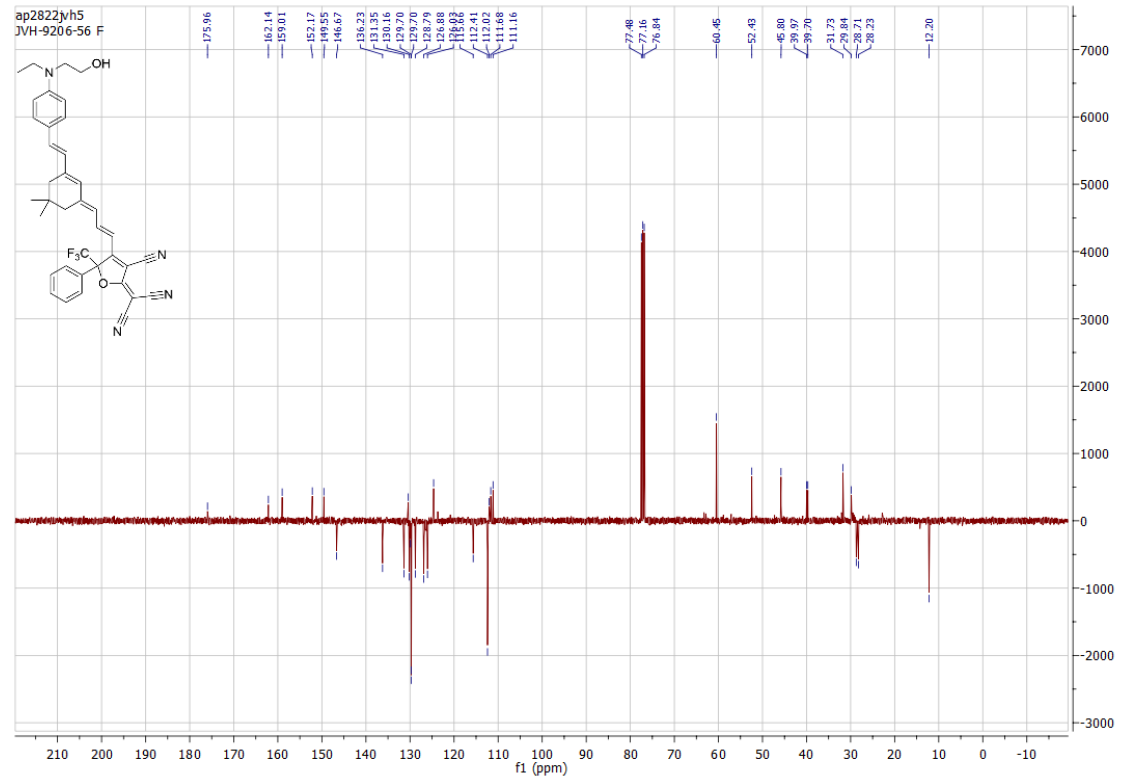

*Appendix 21: [13]C NMR spectrum of 2-(4-((1E,3E)-3-(3-((E)-4-(ethyl(2-hydroxyethyl)amino)styryl)-5,5-dimethylcyclohex-2-en-1-ylidene)prop-1-en-1-yl)-3-cyano-5-phenyl-5-(trifluoromethyl)furan-2(5H)-ylidene)malononitrile **60.***

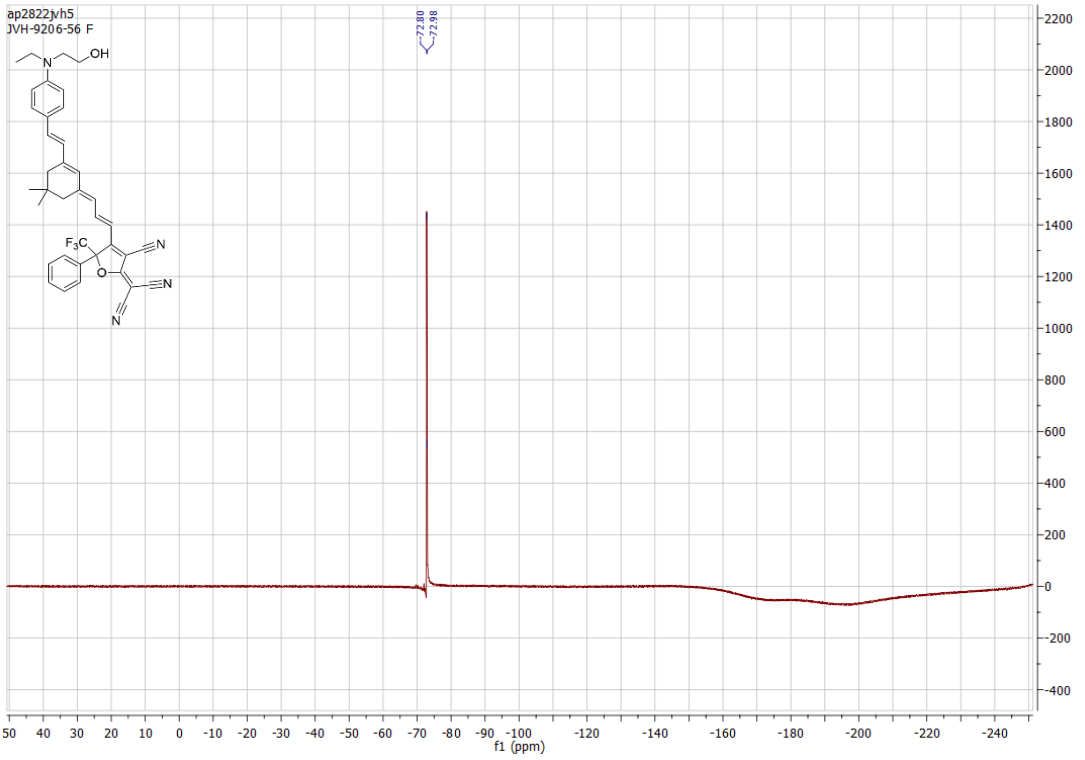

*Appendix 22: ^{19}F NMR spectrum of 2-(4-((1E,3E)-3-(3-((E)-4-(ethyl(2-hydroxyethyl)amino)styryl)-5,5-dimethylcyclohex-2-en-1-ylidene)prop-1-en-1-yl)-3-cyano-5-phenyl-5-(trifluoromethyl)furan-2(5H)-ylidene)malononitrile **60.***

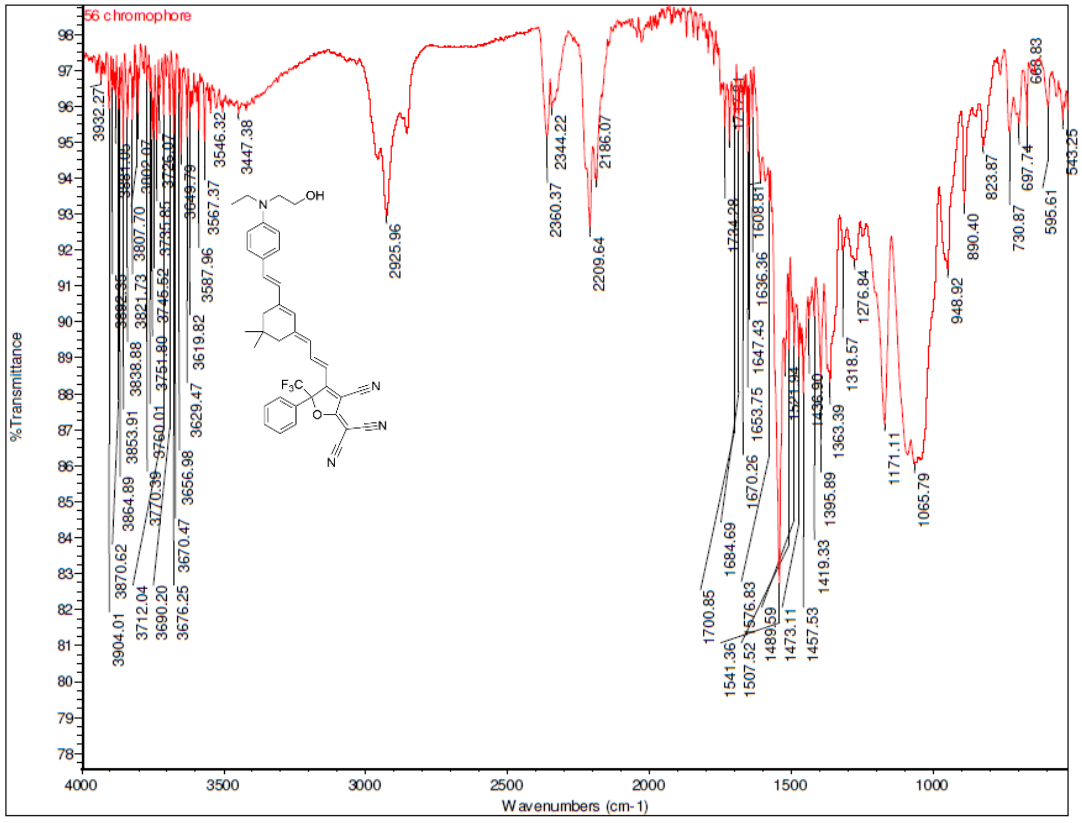

*Appendix 23: FTIR spectrum of 2-(4-((1E,3E)-3-(3-((E)-4-(ethyl(2-hydroxyethyl)amino)styryl)-5,5-dimethylcyclohex-2-en-1-ylidene)prop-1-en-1-yl)-3-cyano-5-phenyl-5-(trifluoromethyl)furan-2(5H)-ylidene)malononitrile **60.***

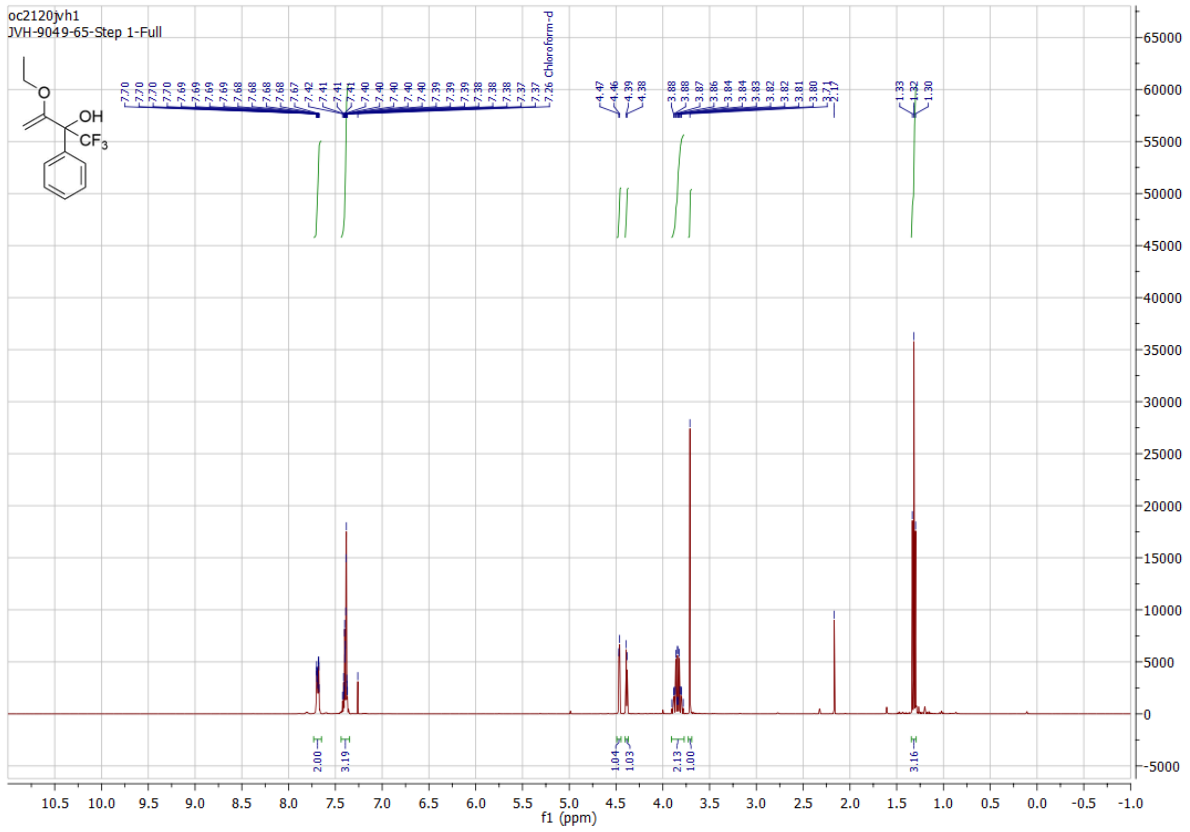

*Appendix 24: [1]H NMR spectrum of 4,4,4-trifluoro-3-hydroxy-3-phenyl-2-ethoxy-but-1-ene **58**.*

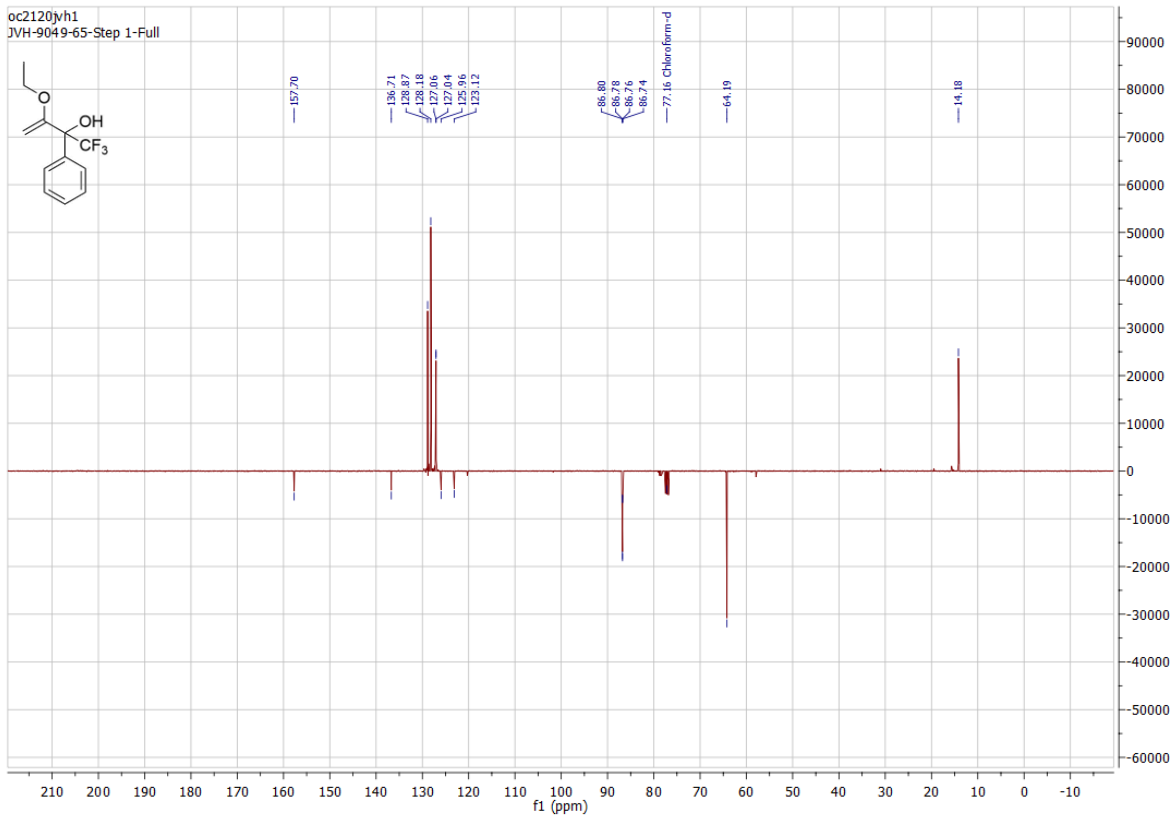

*Appendix 25: [13]C NMR spectrum of 4,4,4-trifluoro-3-hydroxy-3-phenyl-2-ethoxy-but-1-ene **58**.*

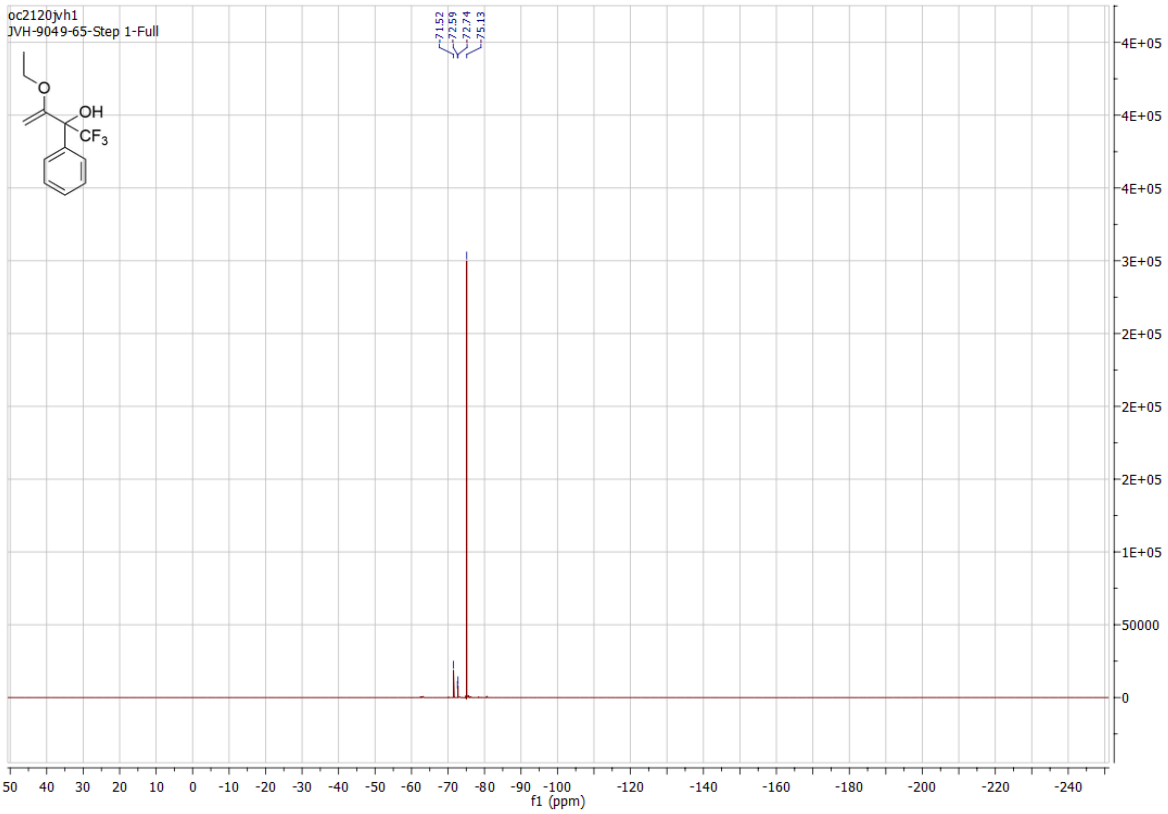

*Appendix 26: ^{19}F NMR spectrum of 4,4,4-trifluoro-3-hydroxy-3-phenyl-2-ethoxy-but-1-ene **58**.*

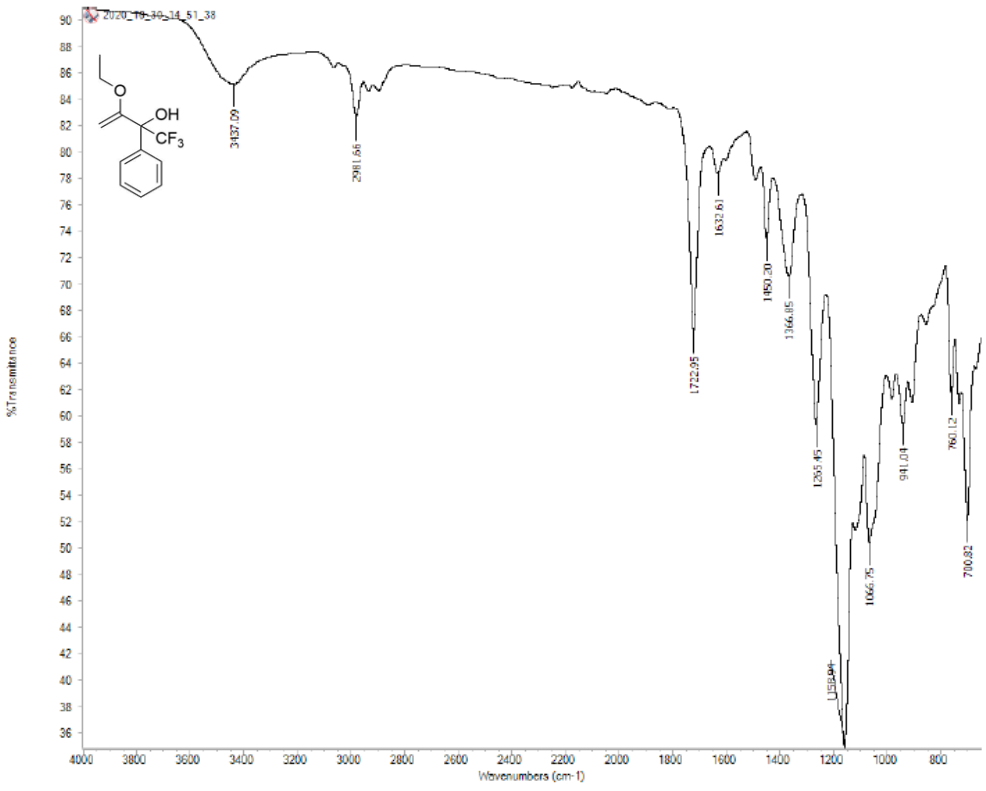

*Appendix 27: FTIR spectrum of 4,4,4-trifluoro-3-hydroxy-3-phenyl-2-ethoxy-but-1-ene **58**.*

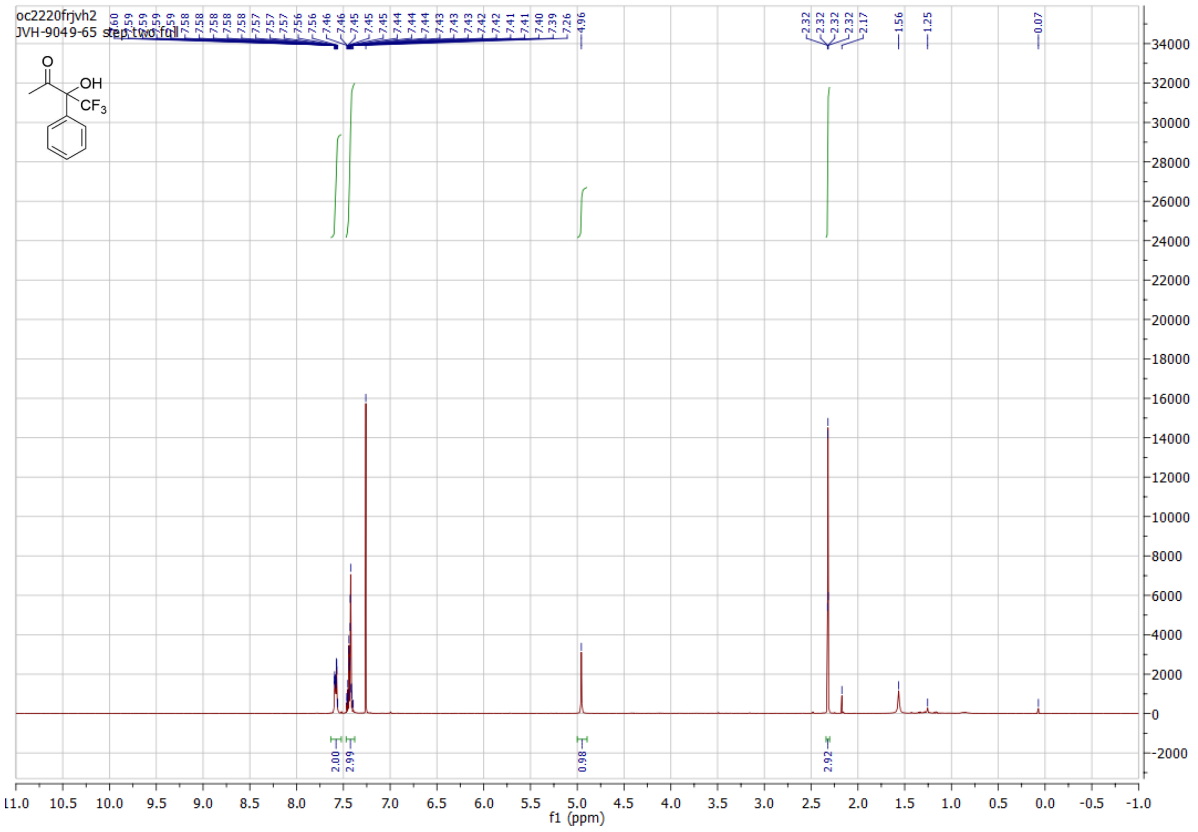

*Appendix 28: [1]H NMR spectrum of 4,4,4-trifluoro-3-hydroxy-3-phenylbutan-2-one **59**.*

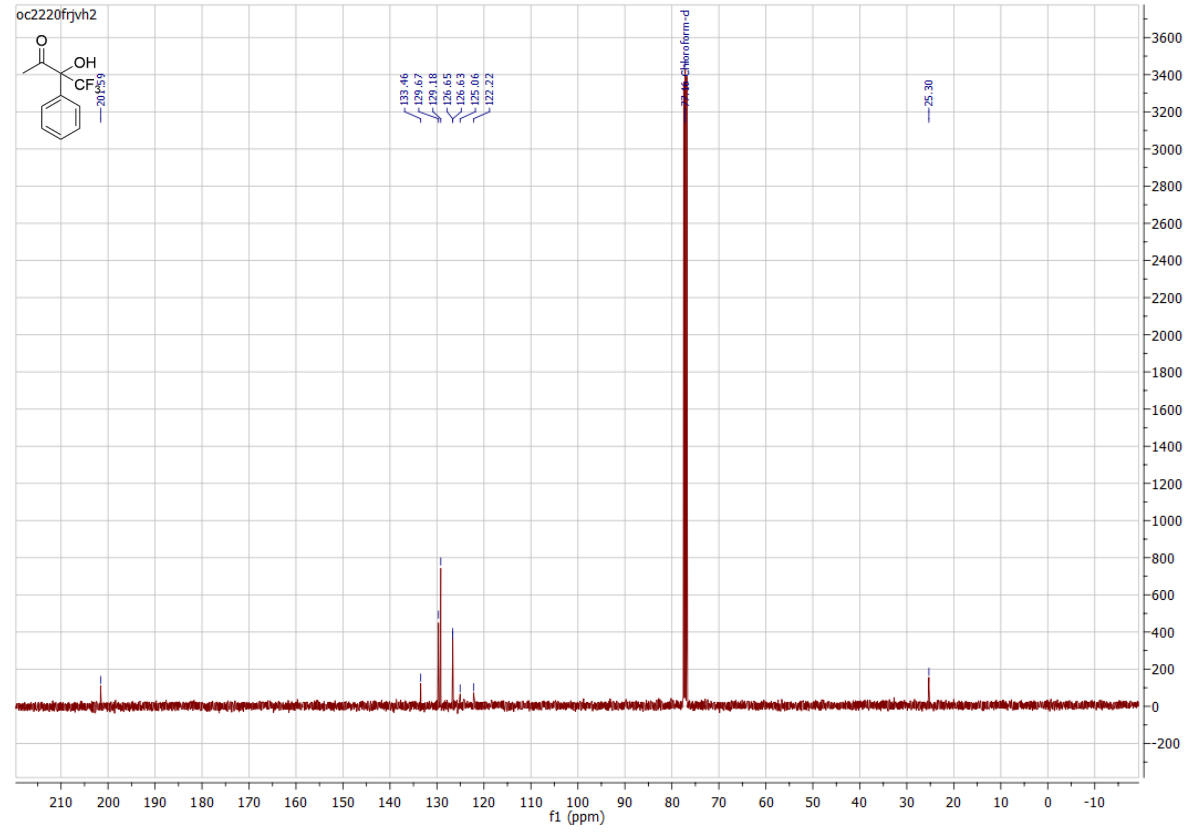

*Appendix 29: [13]C NMR spectrum of 4,4,4-trifluoro-3-hydroxy-3-phenylbutan-2-one **59**.*

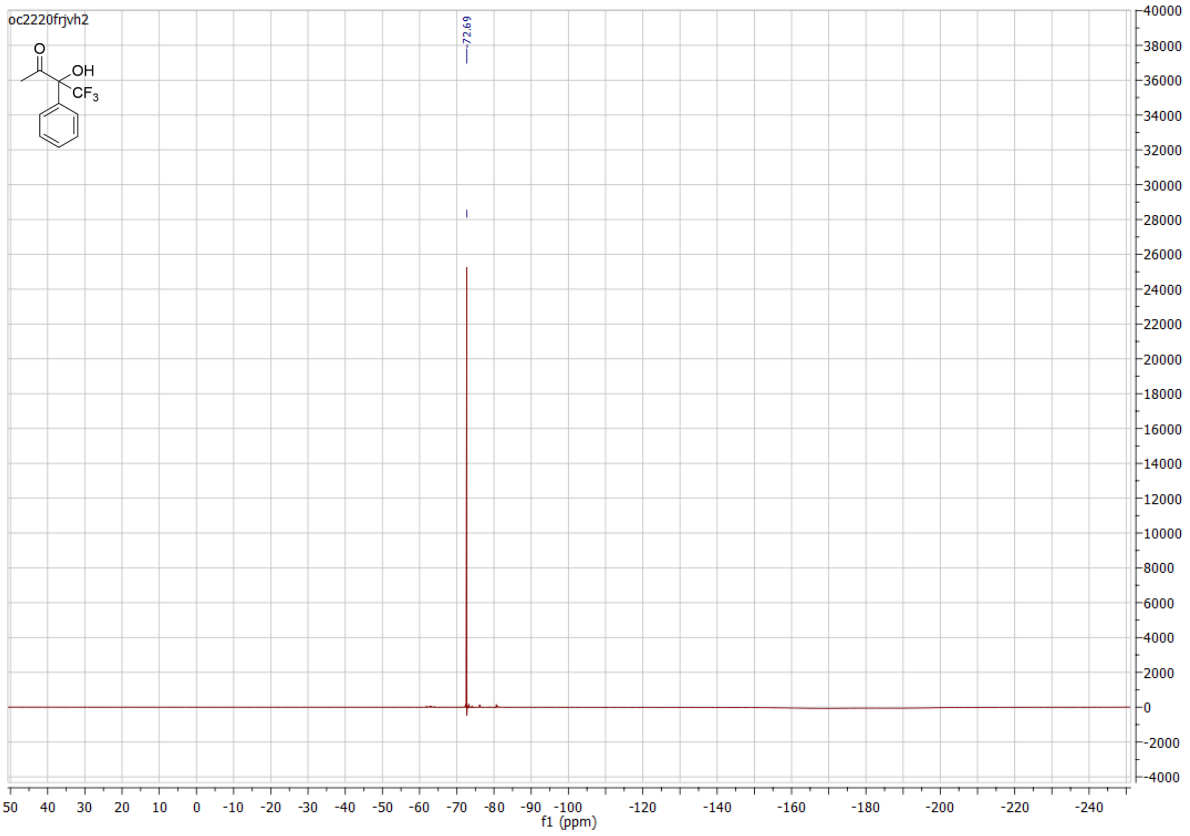

*Appendix 30: ^{19}F Spectrum of 4,4,4-trifluoro-3-hydroxy-3-phenylbutan-2-one **59**.*

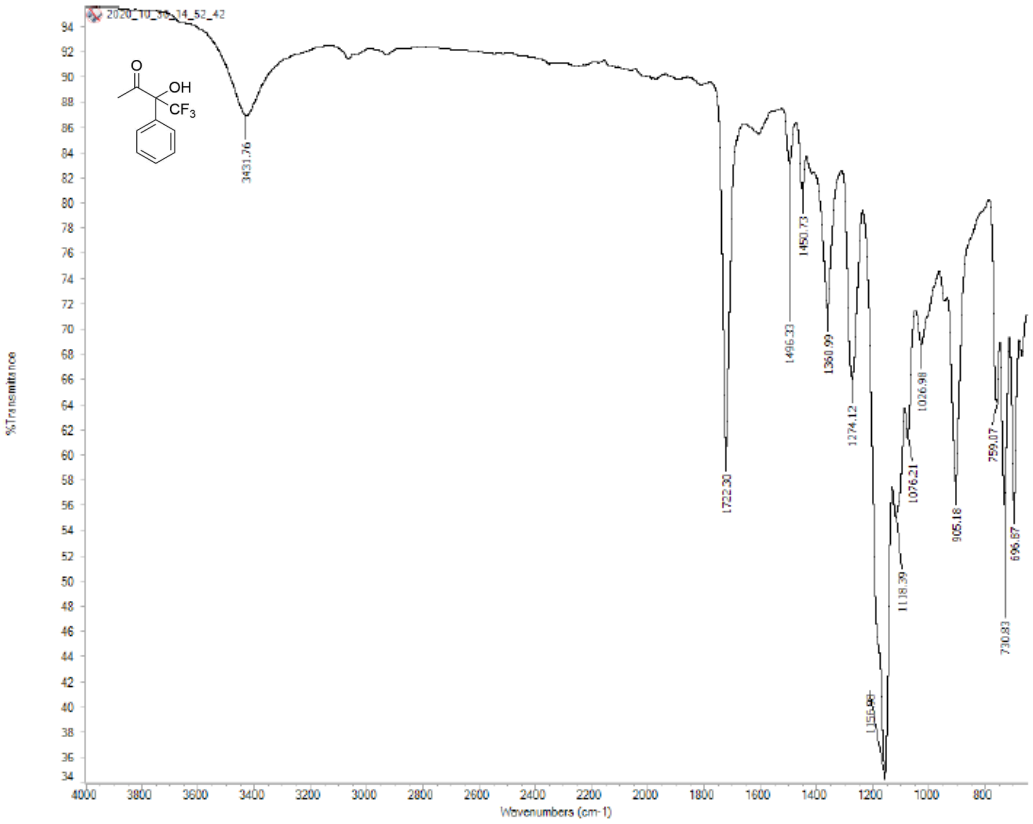

*Appendix 31: FTIR spectrum of 4,4,4-trifluoro-3-hydroxy-3-phenylbutan-2-one **59**.*

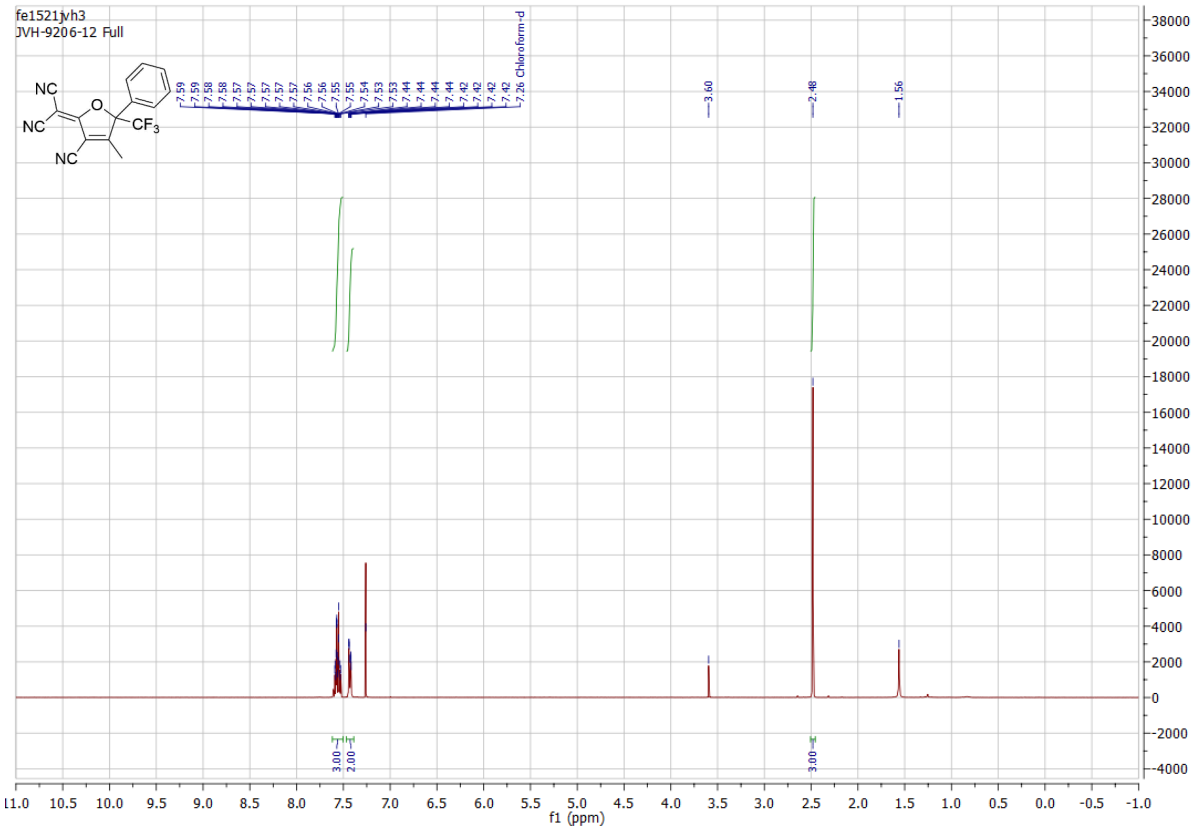

*Appendix 32: [1]H NMR spectrum of 2-Dicyanomethylene-3-cyano-4-methyl-5-phenyl-5-trifluoromethyl-2,5-dihydrofuran **48**.*

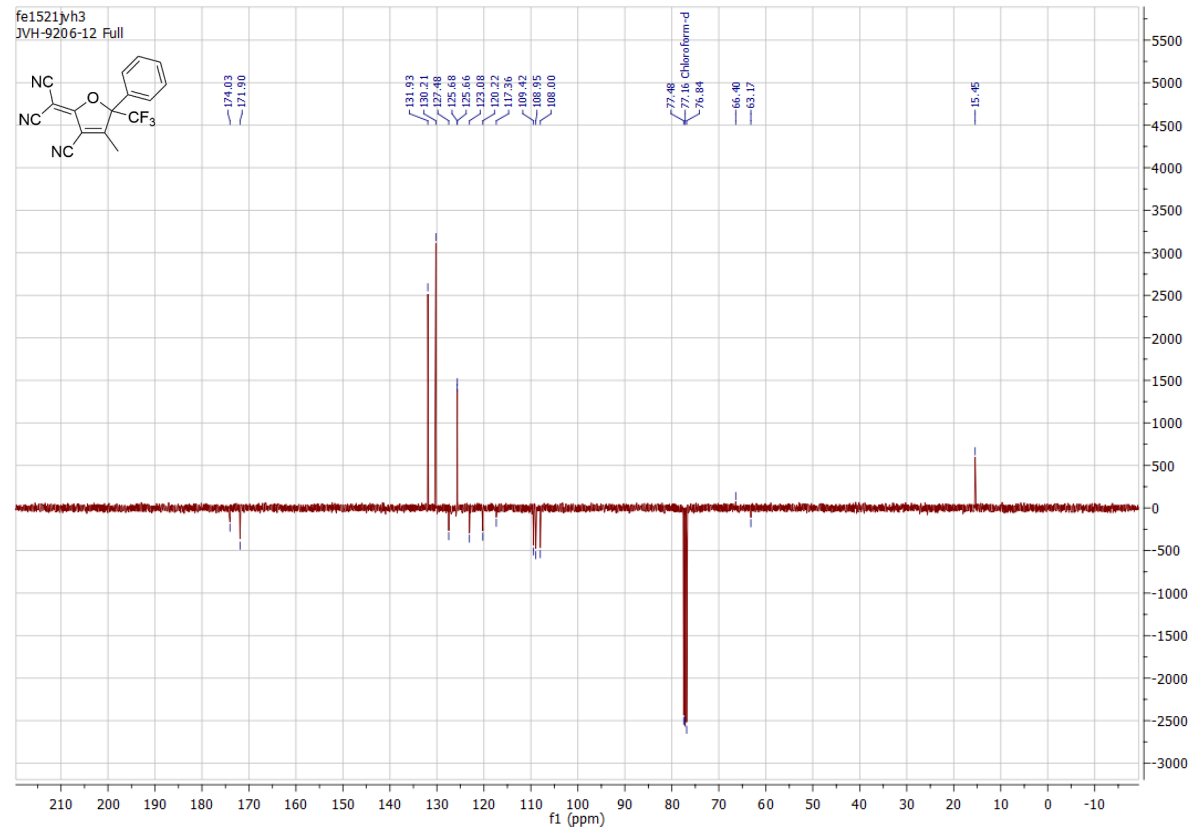

*Appendix 33: [13]C NMR spectrum of 2-Dicyanomethylene-3-cyano-4-methyl-5-phenyl-5-trifluoromethyl-2,5-dihydrofuran **48**.*

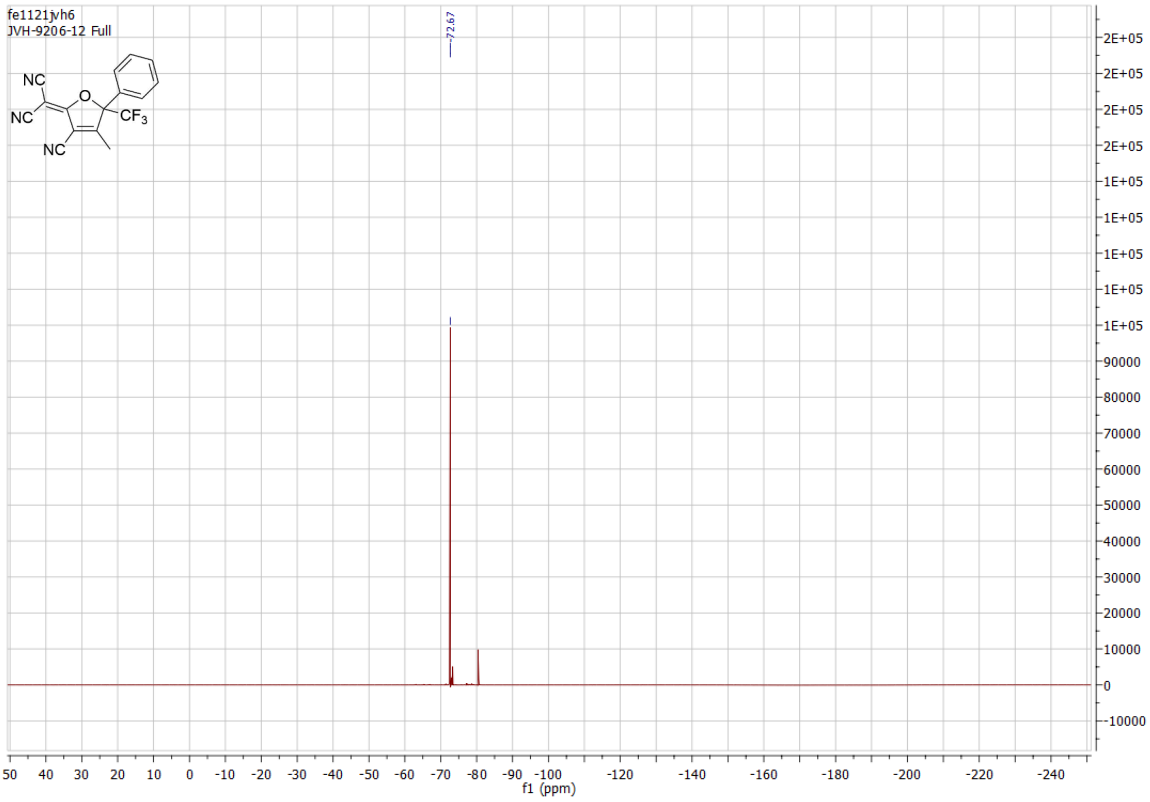

*Appendix 34: ^{19}F NMR spectrum of 2-Dicyanomethylene-3-cyano-4-methyl-5-phenyl-5-trifluoromethyl-2,5-dihydrofuran **48**.*

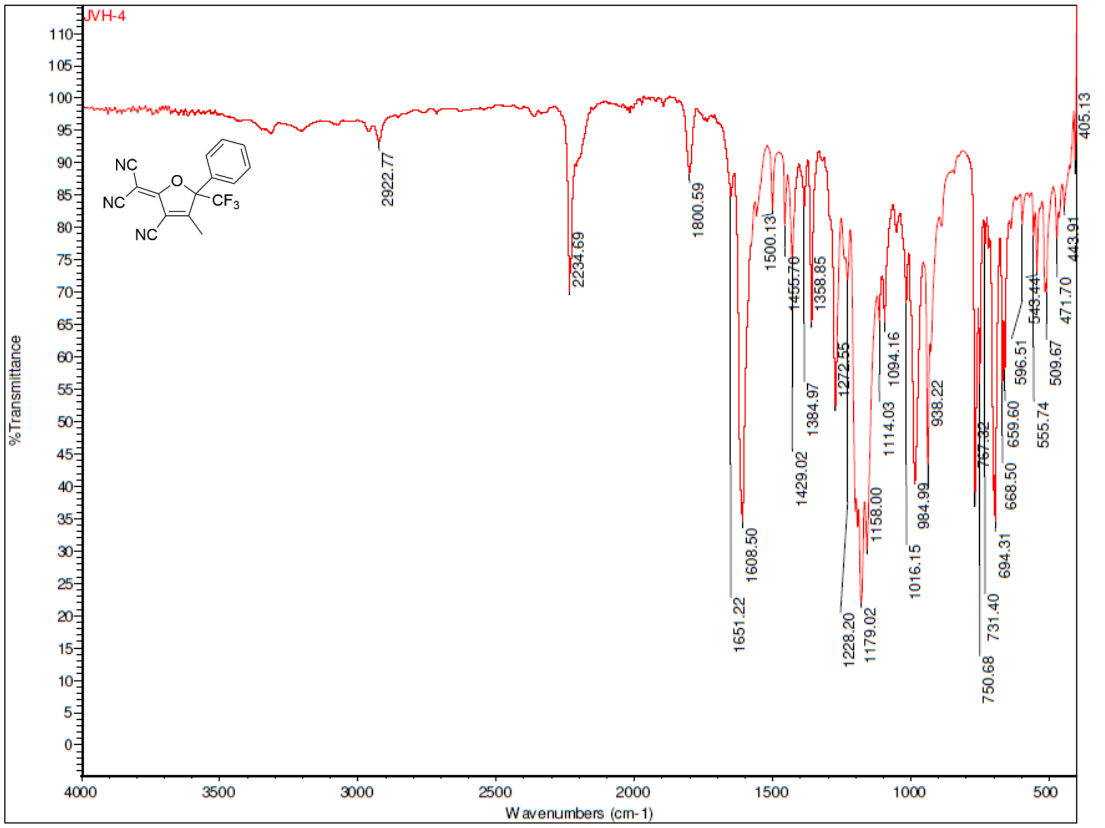

*Appendix 35: FTIR spectrum of 2-Dicyanomethylene-3-cyano-4-methyl-5-phenyl-5-trifluoromethyl-2,5-dihydrofuran **48**.*

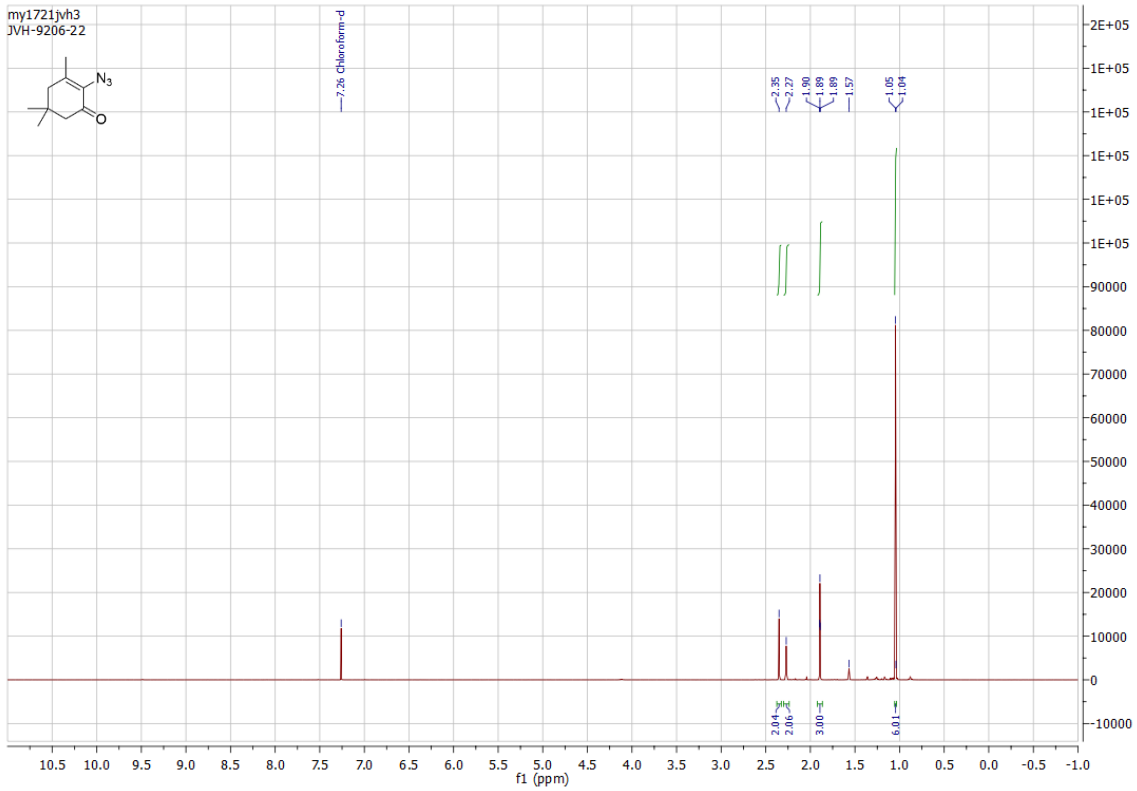

*Appendix 36: [1]H NMR spectrum of 2-Azido-3,5,5-trimethylcyclohex-2-en-1-one **73**.*

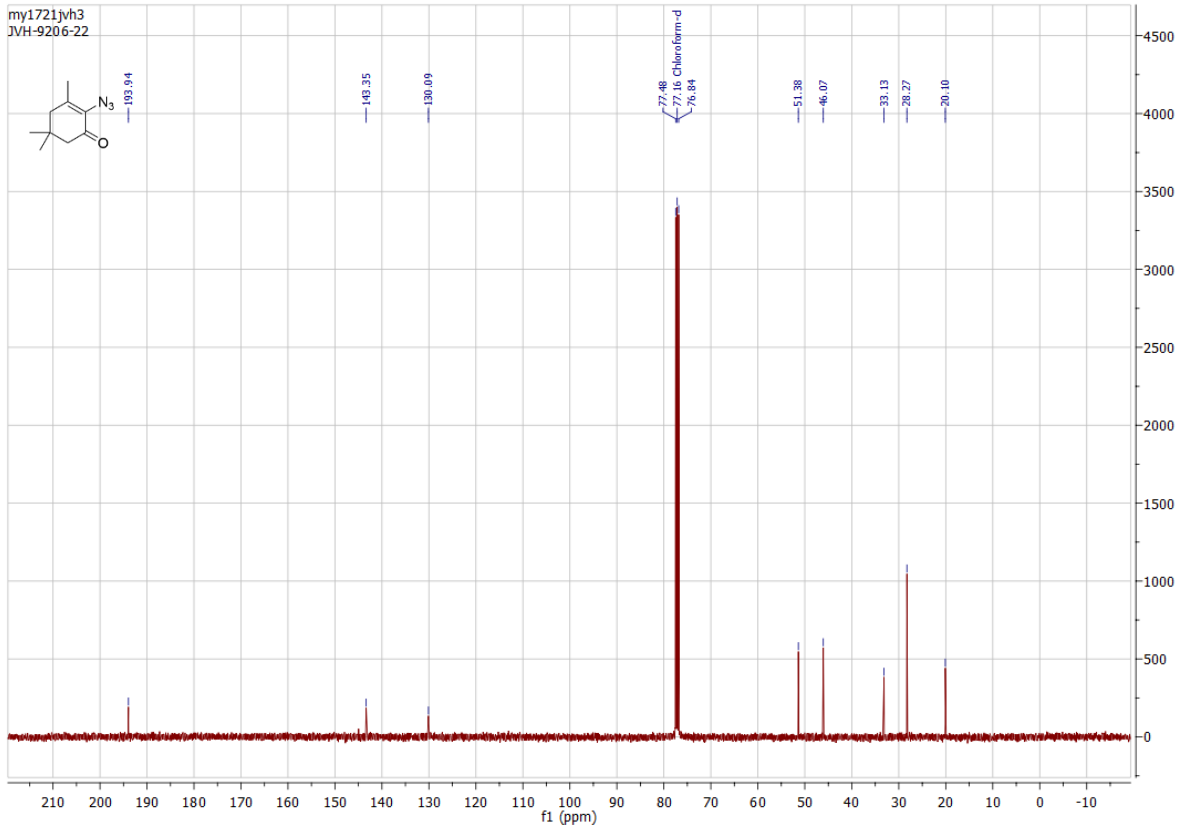

*Appendix 37: [13]C NMR spectrum of 2-Azido-3,5,5-trimethylcyclohex-2-en-1-one **73**.*

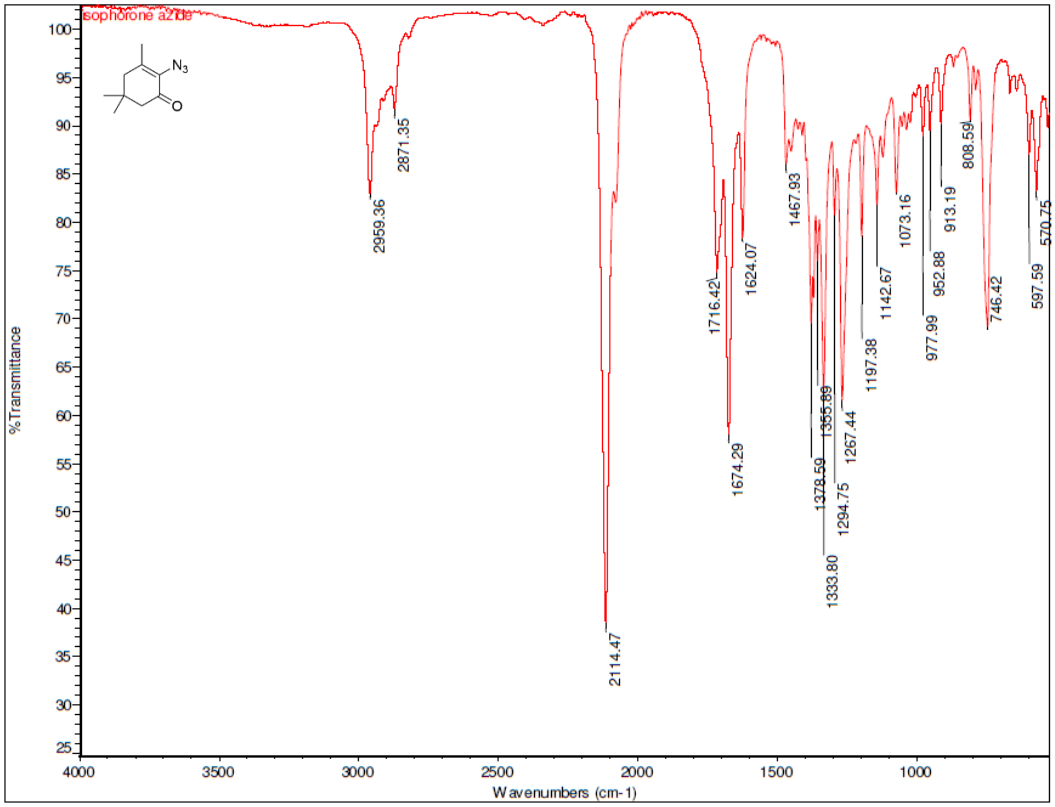

Appendix 38: FTIR spectrum of 2-Azido-3,5,5-trimethylcyclohex-2-en-1-one ***73****.*

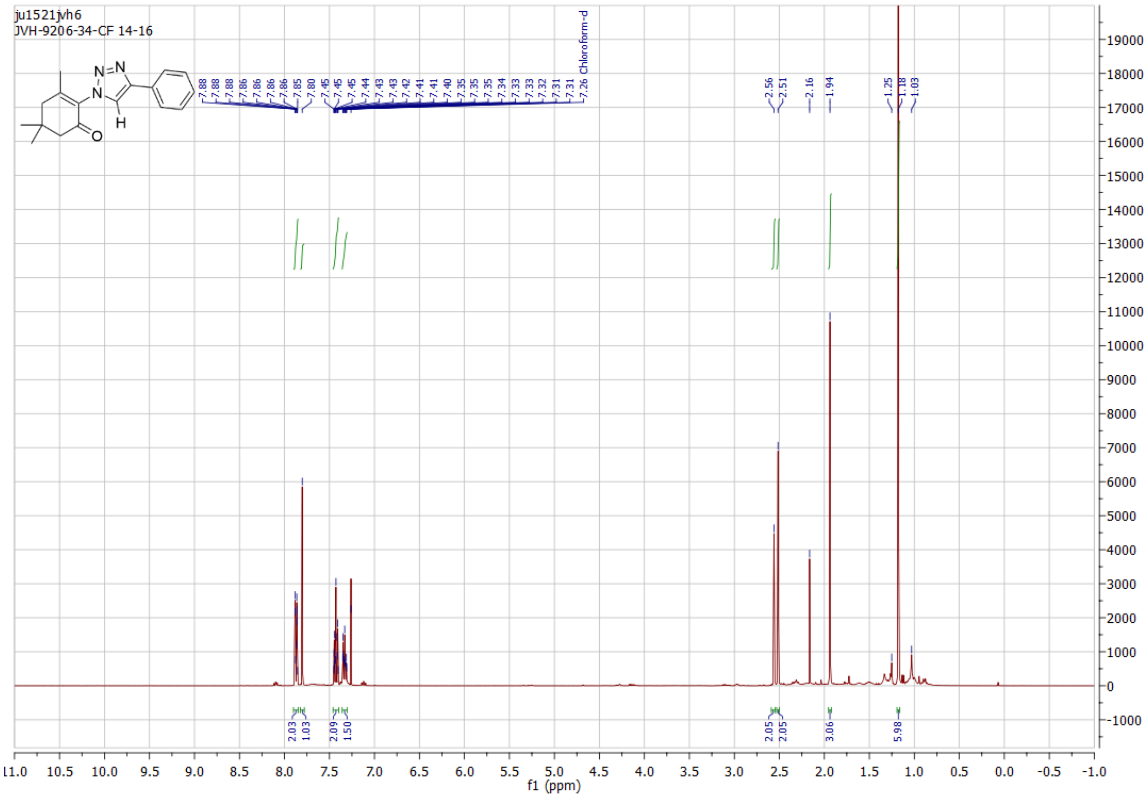

Appendix 39: [1]H NMR spectrum of 3,5,5-Trimethyl-2-(4-phenyl-1H-1,2,3-triazol-1-yl)cyclohex-2-en-1-one ***78****.*

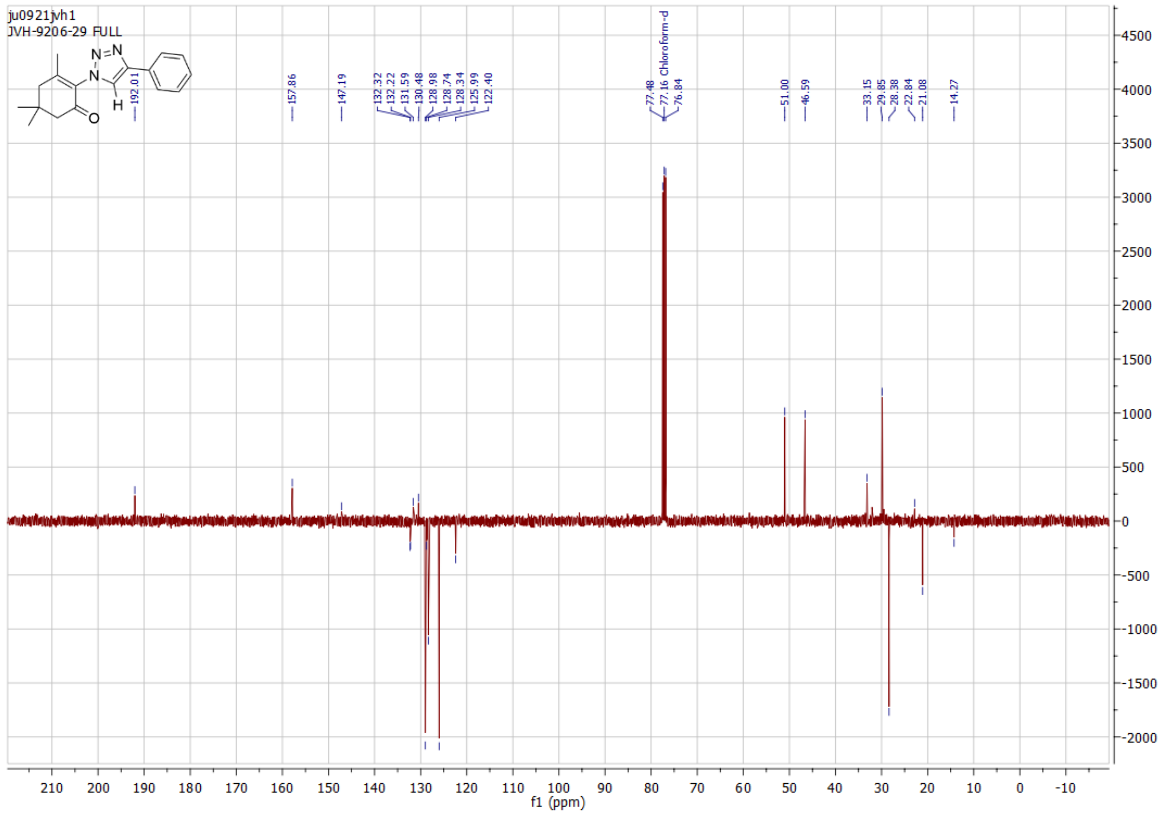

*Appendix 40: ^{13}C NMR spectrum of 3,5,5-Trimethyl-2-(4-phenyl-1H-1,2,3-triazol-1-yl)cyclohex-2-en-1-one **78**.*

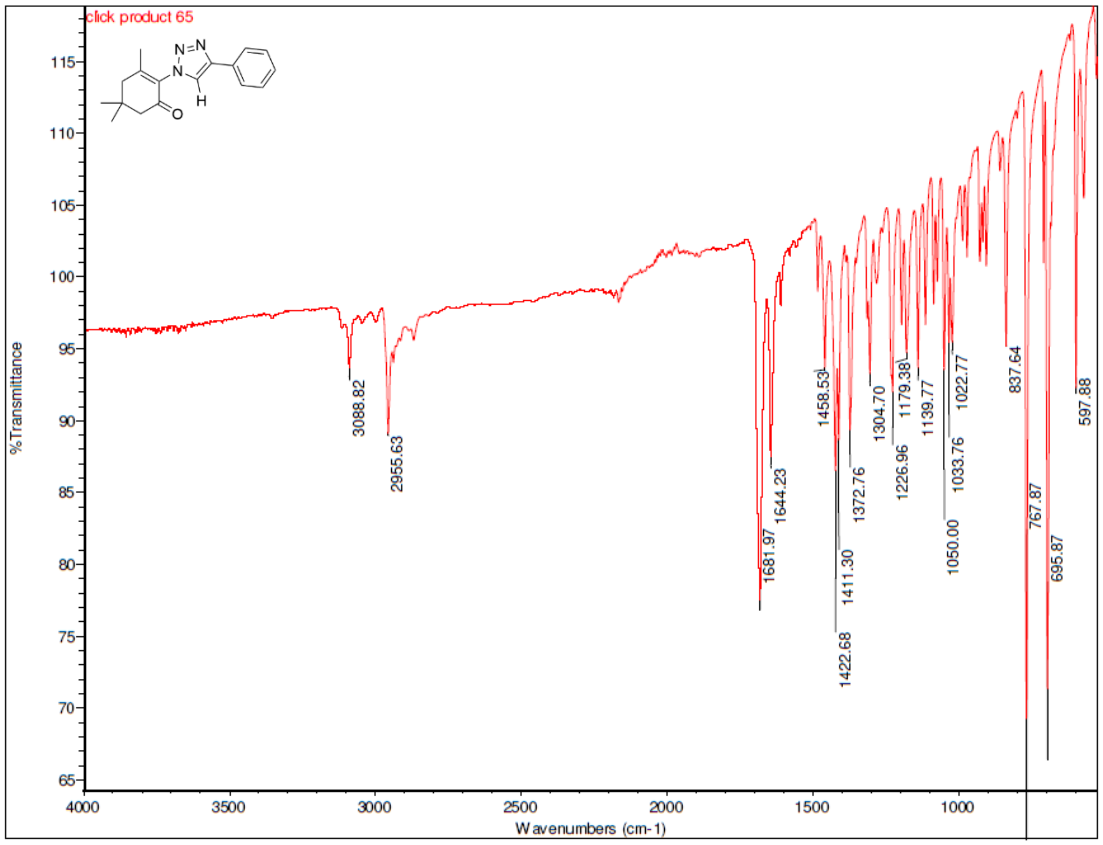

*Appendix 41: FTIR spectrum of 3,5,5-Trimethyl-2-(4-phenyl-1H-1,2,3-triazol-1-yl)cyclohex-2-en-1-one **78**.*

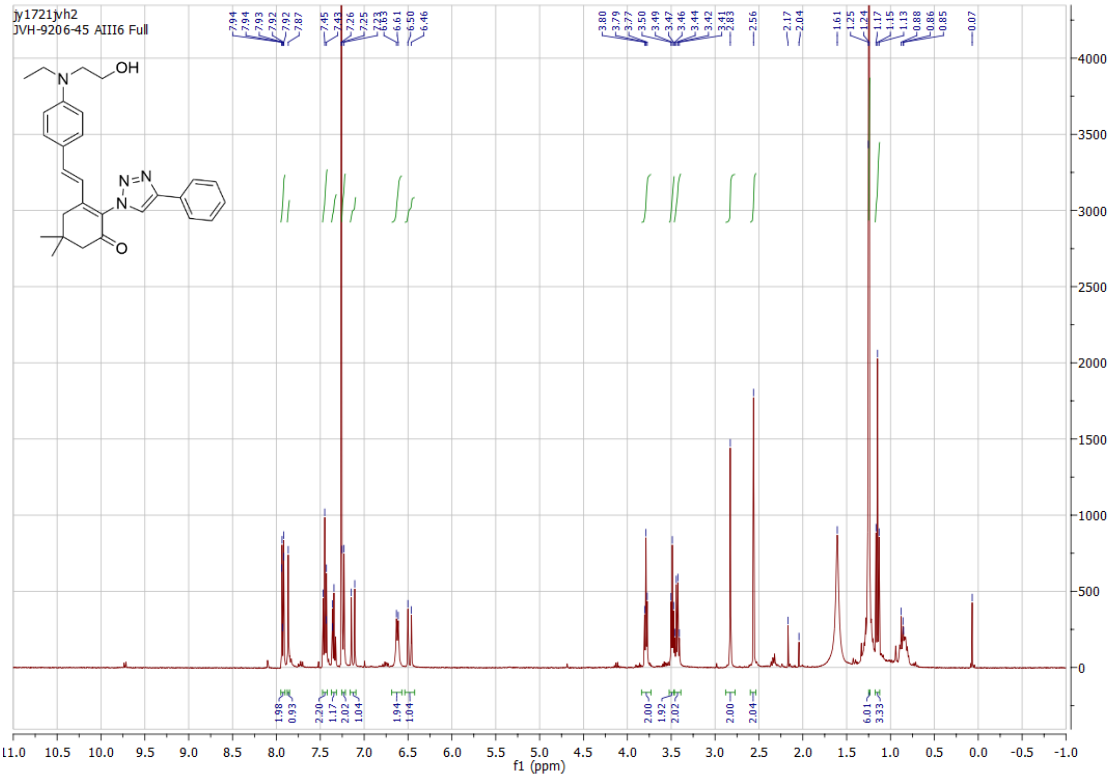

*Appendix 42: [1]H NMR spectrum of (E)-3-(4-(Ethyl(2-hydroxyethyl)amino)styryl)-5,5-dimethyl-2-(4-phenyl-1H-1,2,3-triazol-1-yl)cyclohex-2-en-1-one **80**.*

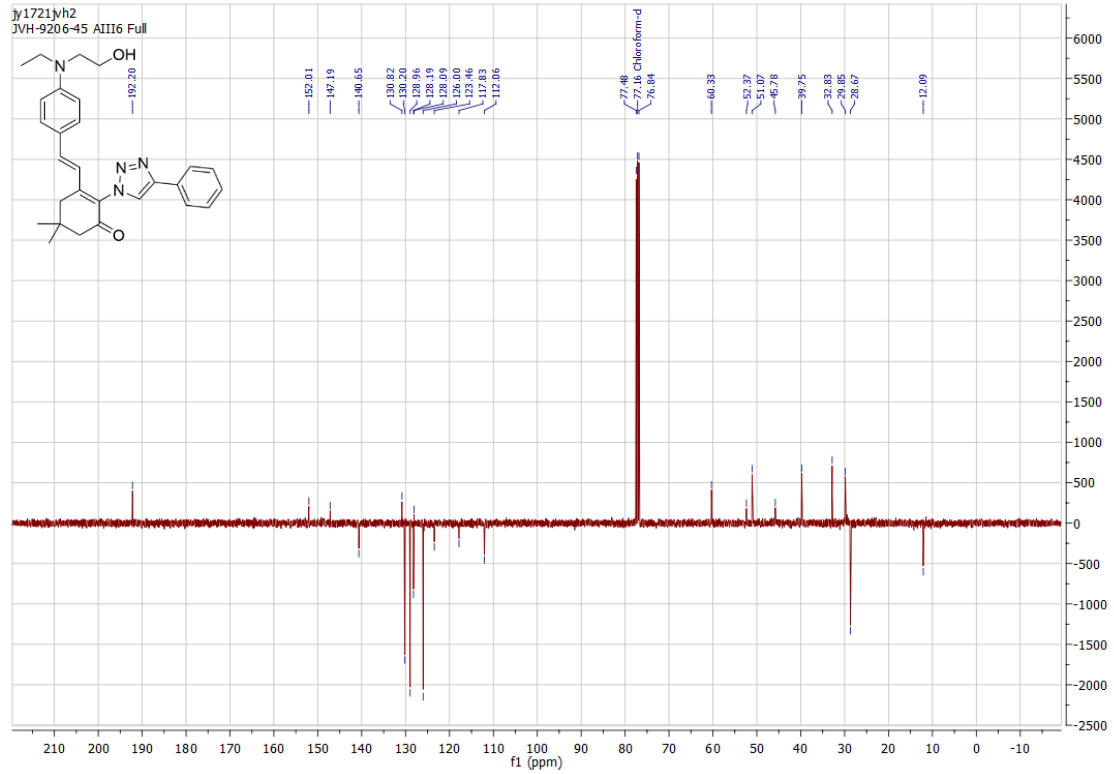

*Appendix 43: [13]C NMR spectrum of (E)-3-(4-(Ethyl(2-hydroxyethyl)amino)styryl)-5,5-dimethyl-2-(4-phenyl-1H-1,2,3-triazol-1-yl)cyclohex-2-en-1-one **80**.*

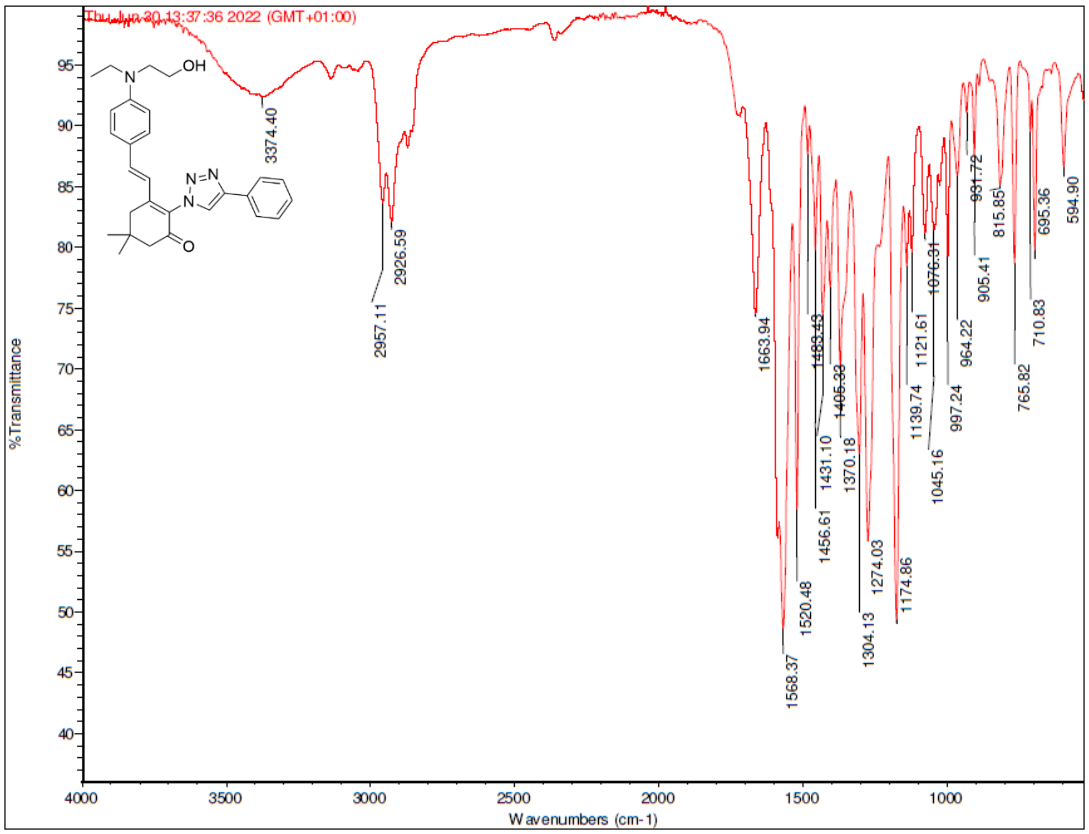

Appendix 44: FTIR spectrum of (E)-3-(4-(Ethyl(2-hydroxyethyl)amino)styryl)-5,5-dimethyl-2-(4-phenyl-1H-1,2,3-triazol-1-yl)cyclohex-2-en-1-one ***80****.*

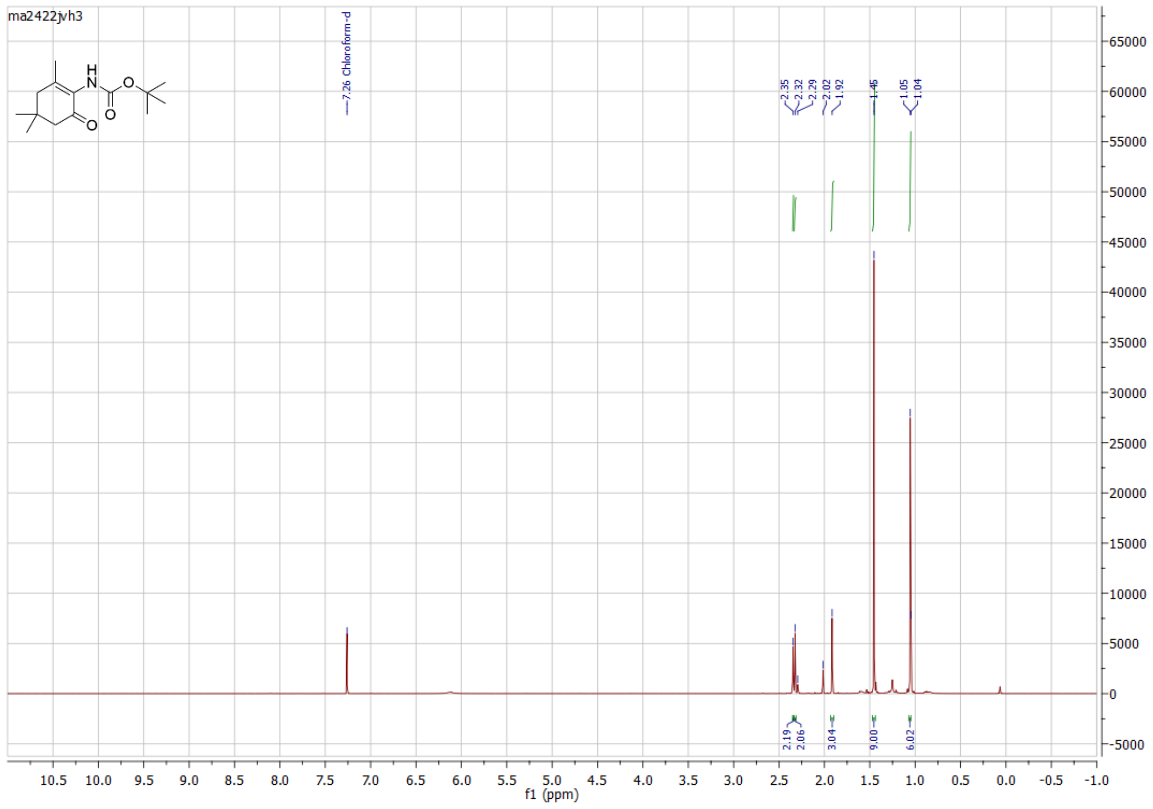

Appendix 45: [1]H NMR spectrum of tert-butyl(2,4,4-trimethyl-6-oxocyclohex-1-en-1-yl)carbamate ***83****.*

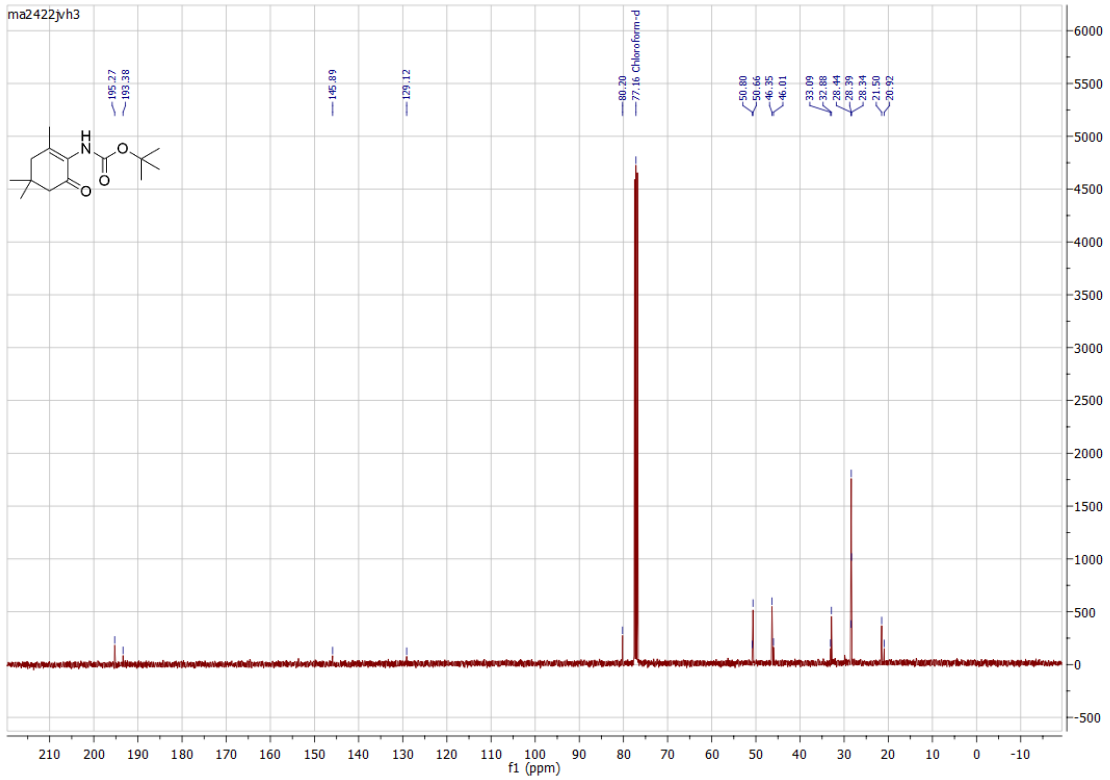

*Appendix 46: ^{13}C NMR spectrum of tert-butyl(2,4,4-trimethyl-6-oxocyclohex-1-en-1-yl)carbamate **83**.*

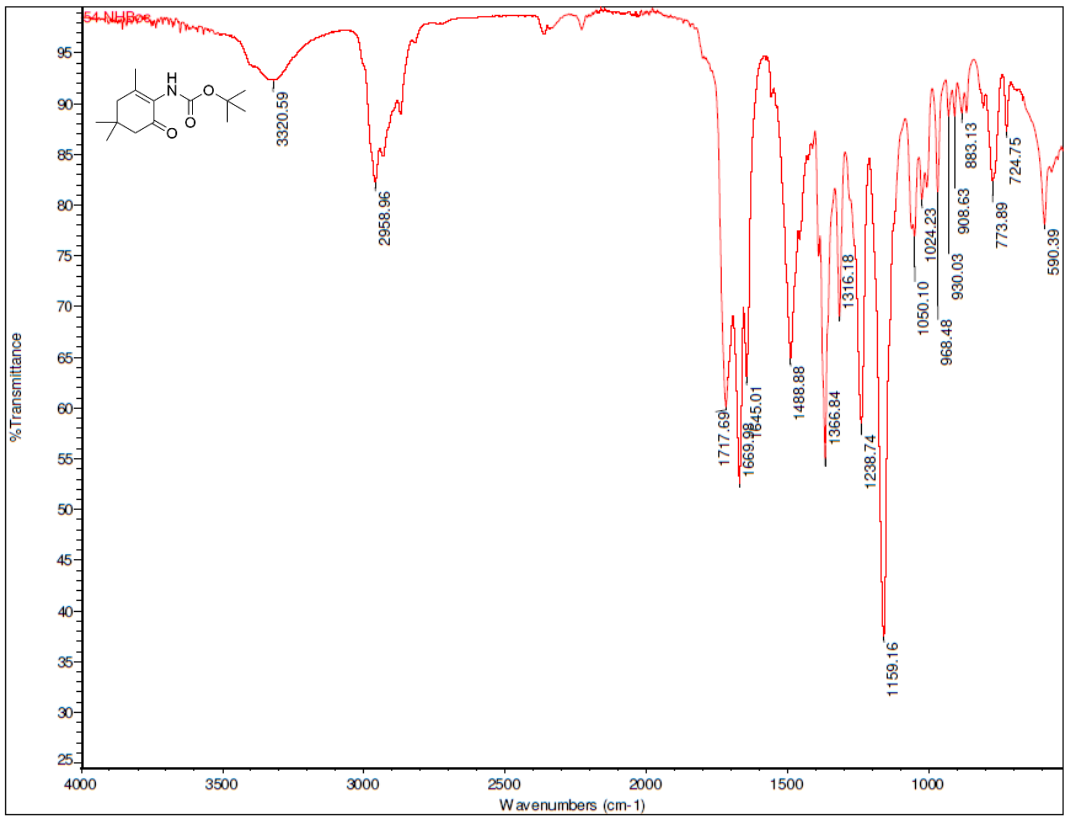

*Appendix 47: FTIR spectrum of tert-butyl(2,4,4-trimethyl-6-oxocyclohex-1-en-1-yl)carbamate **83**.*

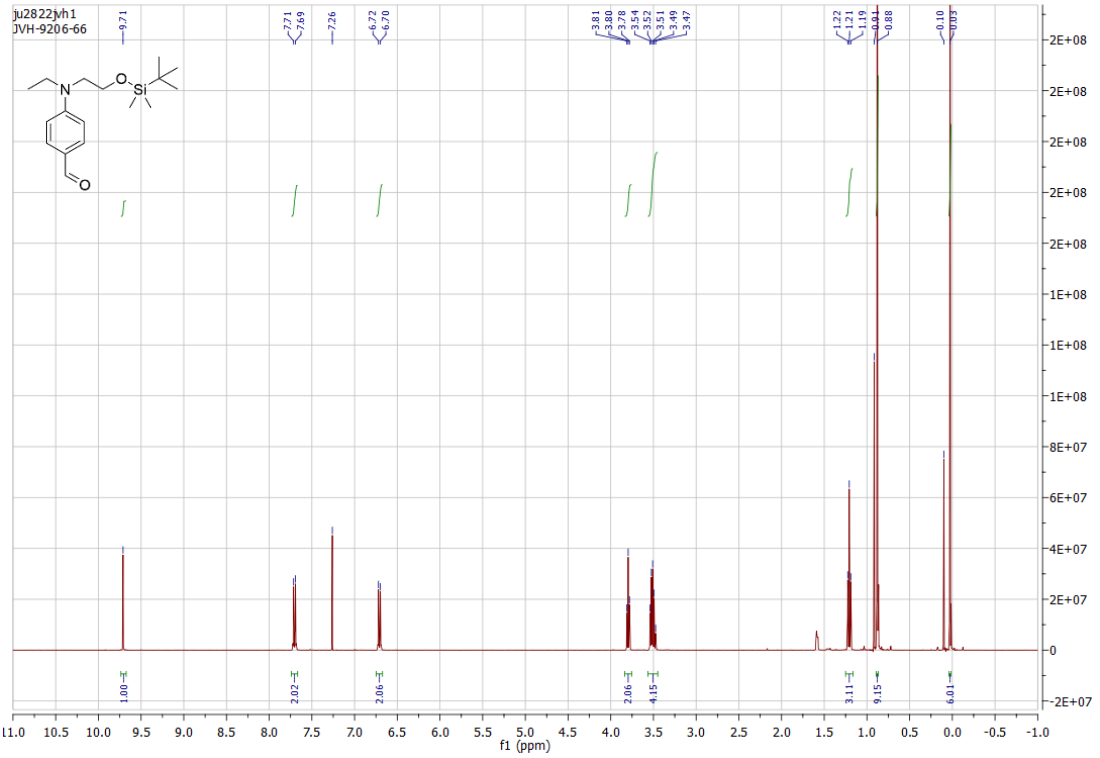

*Appendix 48: ^{1}H NMR spectrum of 4-((2-((tert-butyldimethylsilyl)oxy)ethyl)(ethyl)amino)benzaldehyde **86**.*

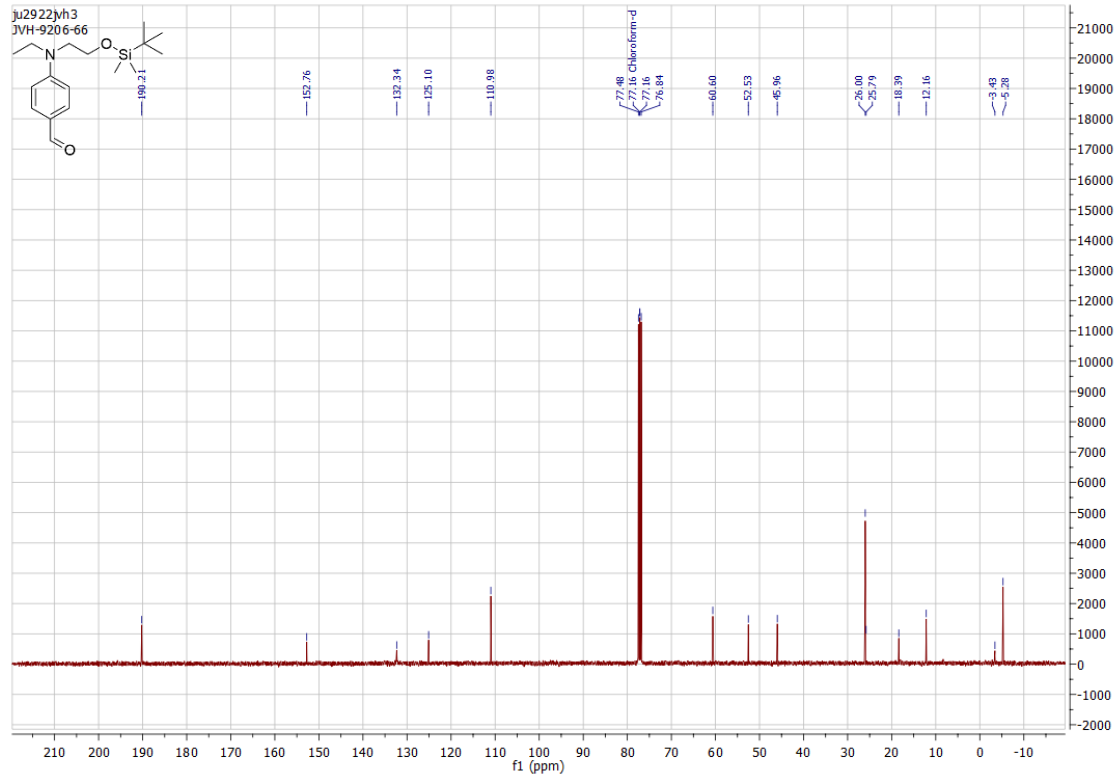

*Appendix 49: ^{13}C NMR spectrum of 4-((2-((tert-butyldimethylsilyl)oxy)ethyl)(ethyl)amino)benzaldehyde **86**.*

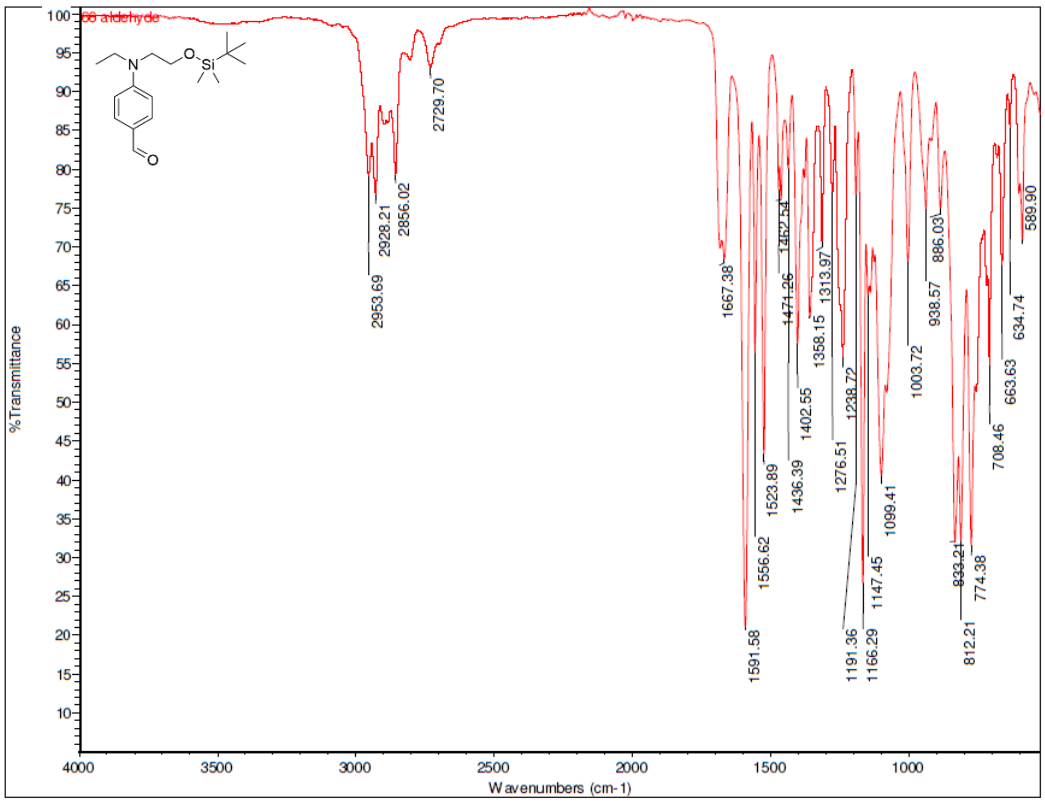

*Appendix 50: FTIR spectrum of 4-((2-((tert-butyldimethylsilyl)oxy)ethyl)(ethyl)amino)benzaldehyde **86**.*

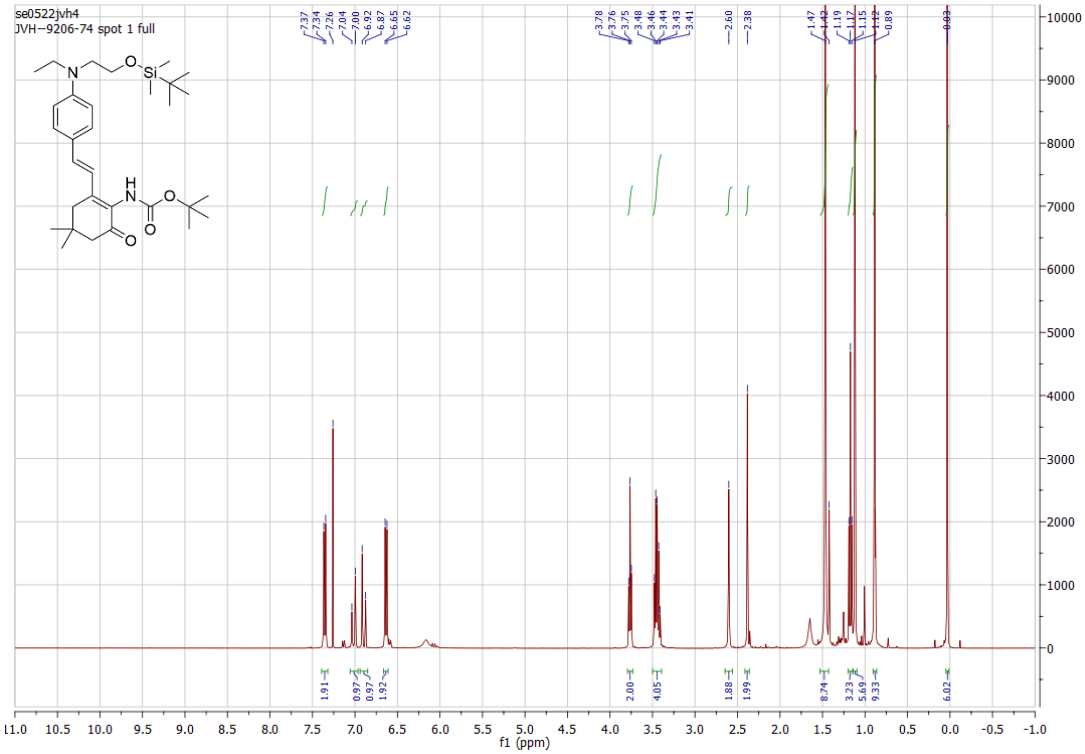

*Appendix 51: ^{1}H NMR spectrum of tert-butyl (E)-(2-(4-((2-((tert-butyldimethylsilyl)oxy)ethyl)(ethyl)amino)styryl)-4,4-dimethyl-6-oxocyclohex-1-en-1-yl)carbamate **90**.*

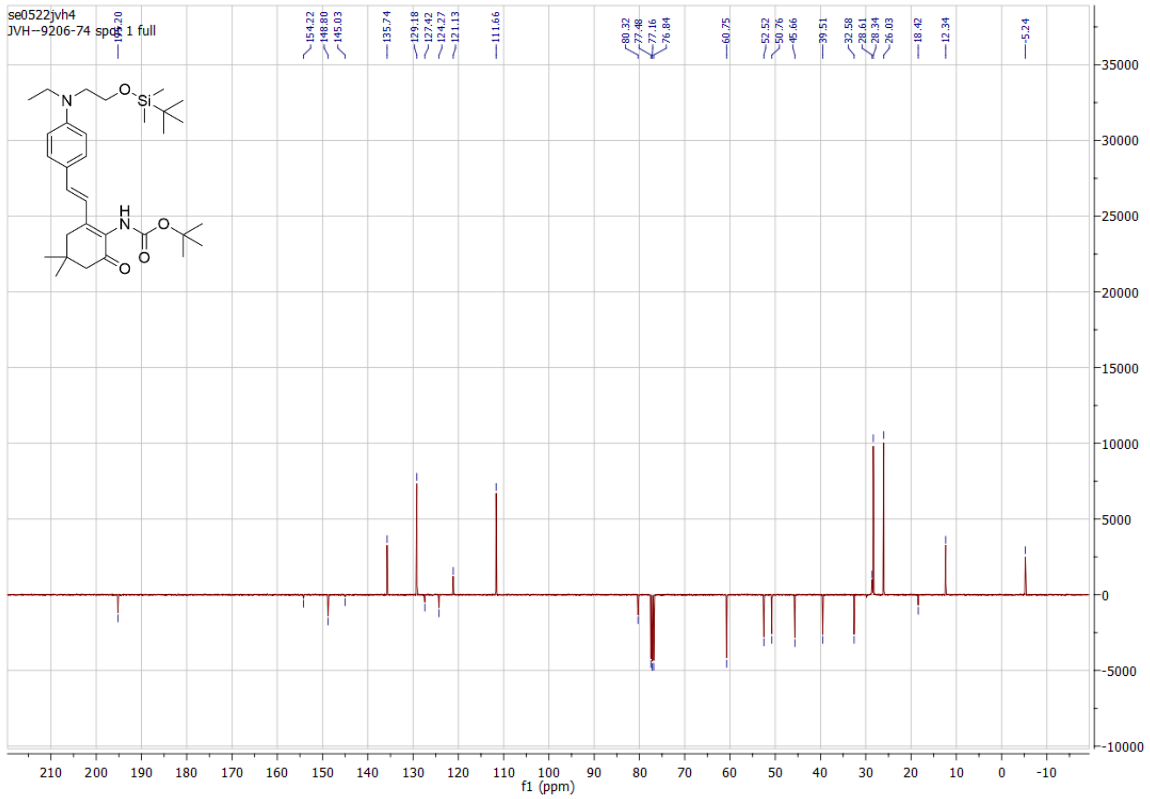

*Appendix 52: [1]H NMR spectrum of tert-butyl (E)-(2-(4-((2-((tert-butyldimethylsilyl)oxy)ethyl)(ethyl)amino)styryl)-4,4-dimethyl-6-oxocyclohex-1-en-1-yl)carbamate **90**.*

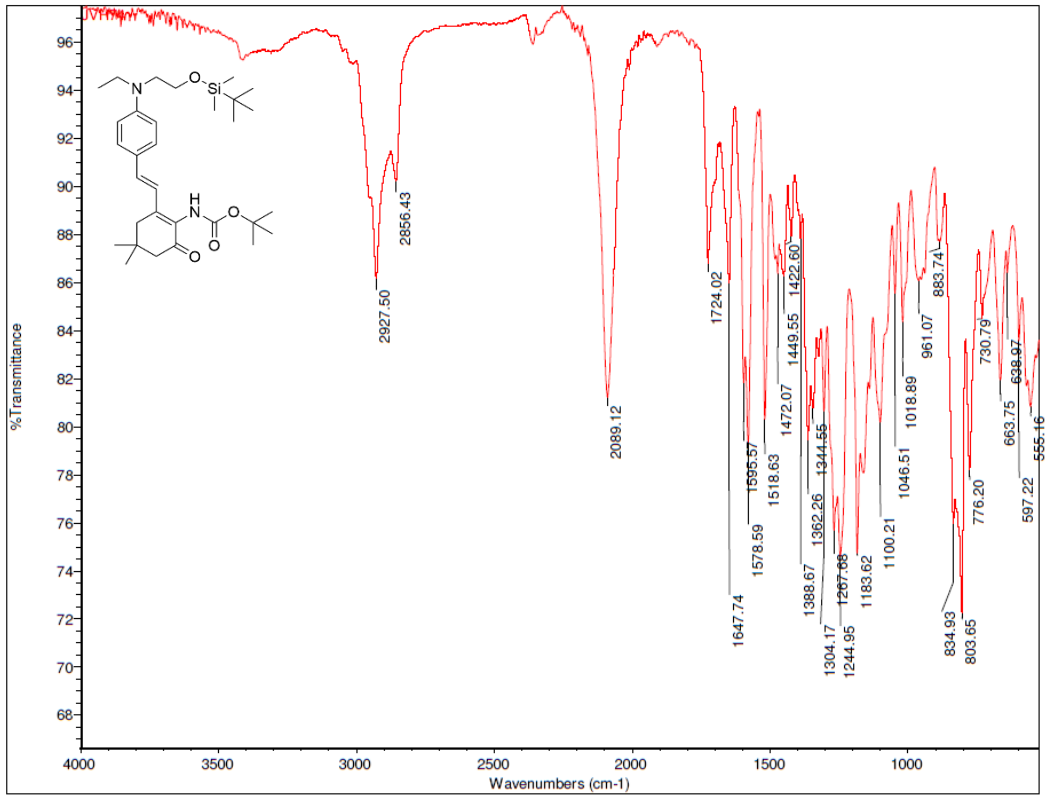

*Appendix 53: FTIR spectrum of tert-butyl (E)-(2-(4-((2-((tert-butyldimethylsilyl)oxy)ethyl)(ethyl)amino)styryl)-4,4-dimethyl-6-oxocyclohex-1-en-1-yl)carbamate **90**.*

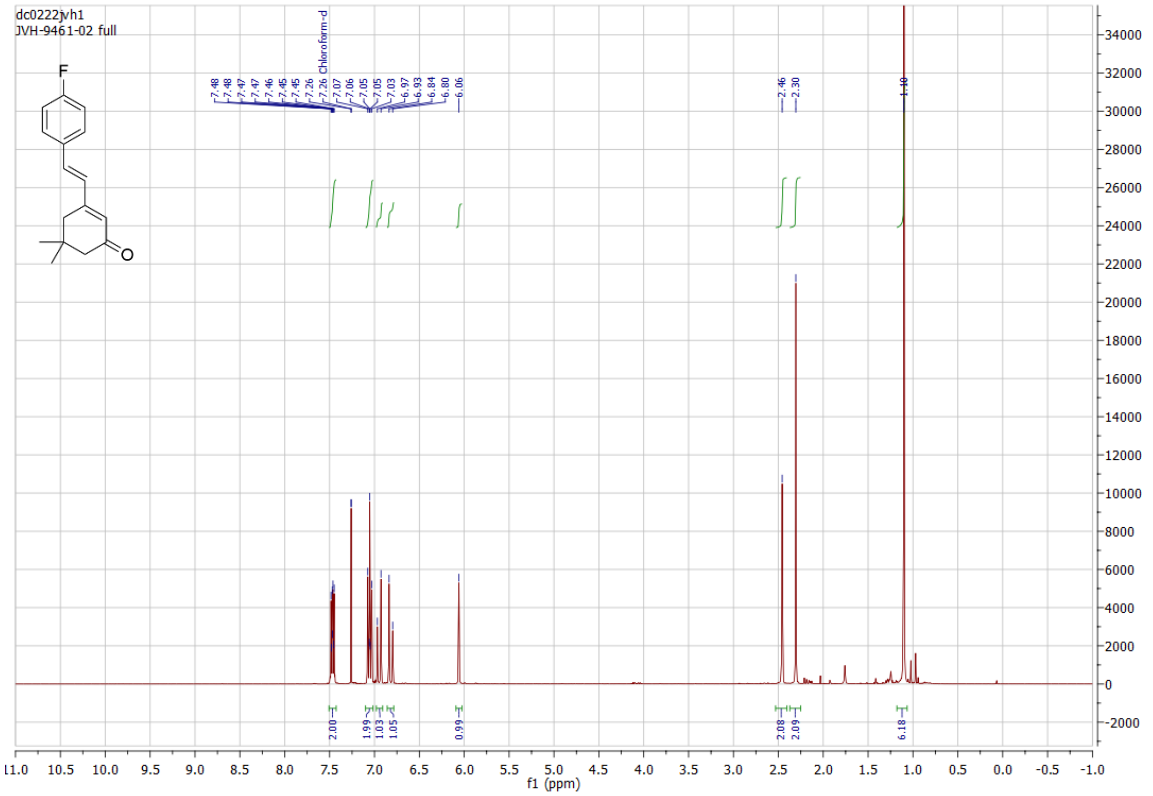

*Appendix 54: [1]H NMR spectrum of (E)-3-(4-fluorostyryl)-5,5-dimethylcyclohex-2-en-1-one **87**.*

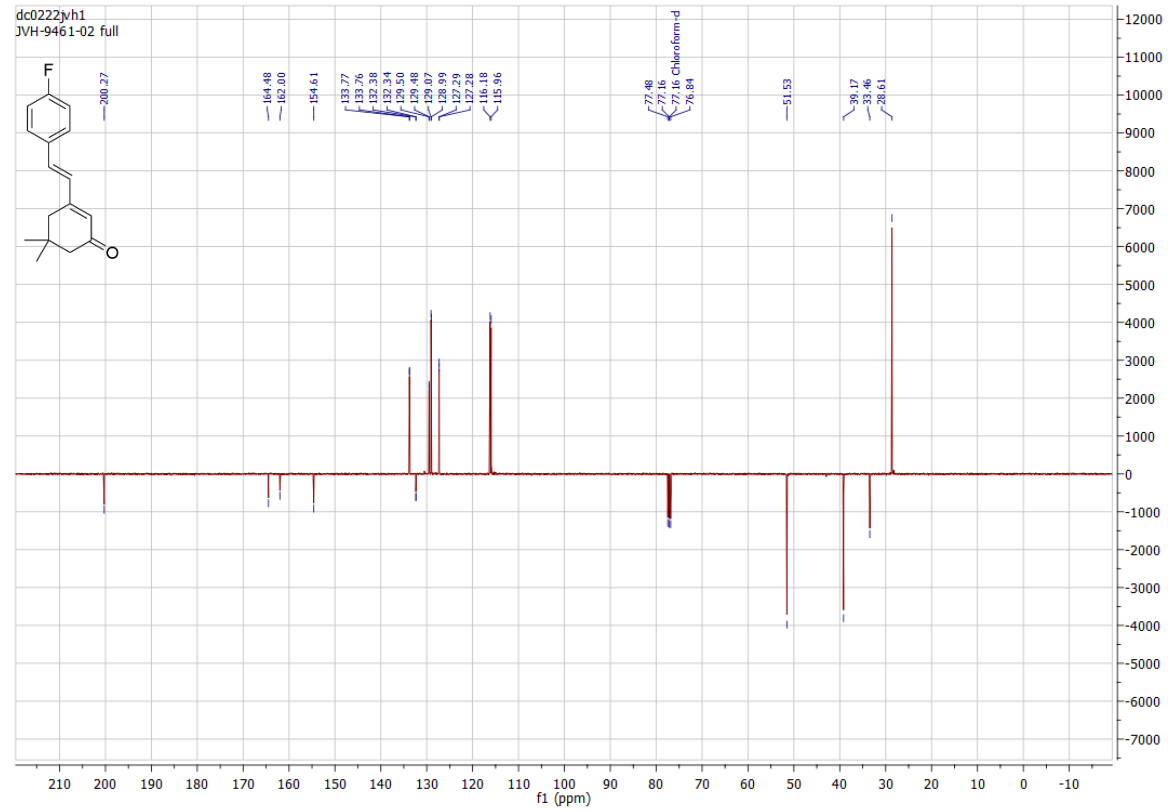

*Appendix 55: [13]C NMR spectrum of (E)-3-(4-fluorostyryl)-5,5-dimethylcyclohex-2-en-1-one **87**.*

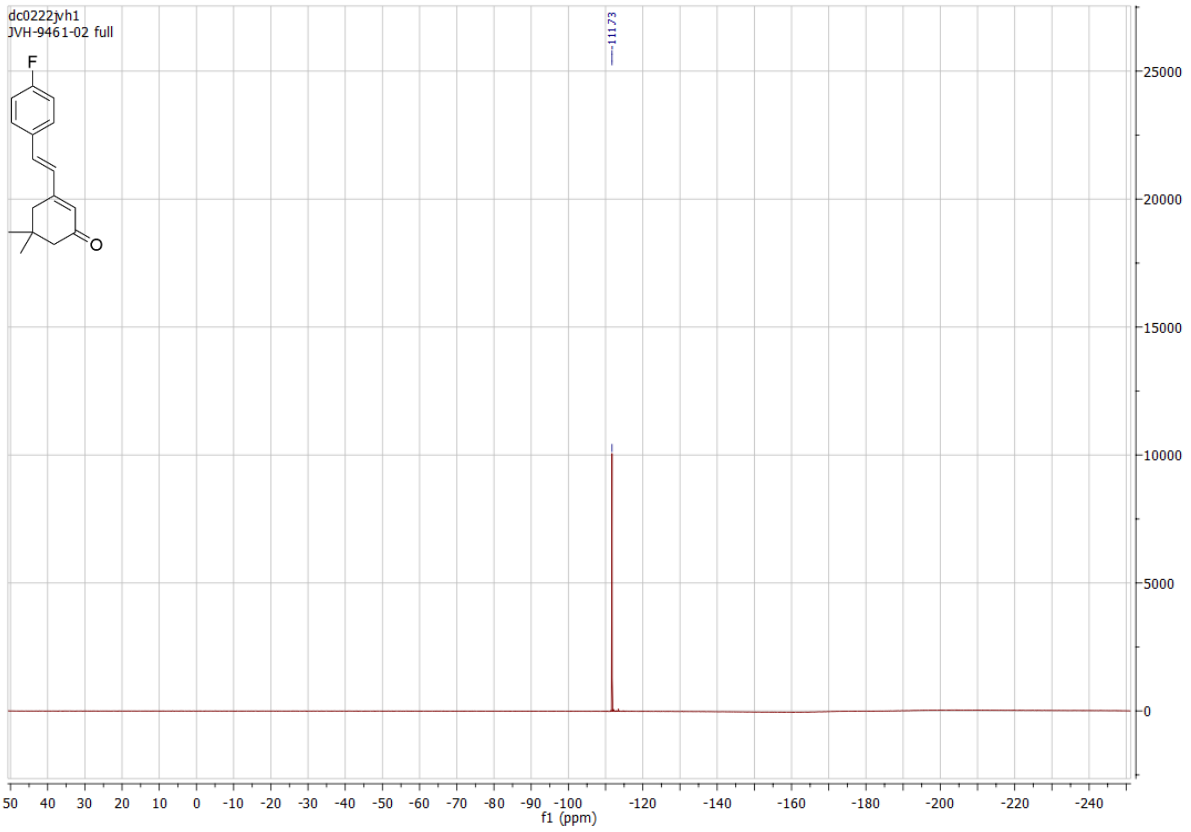

*Appendix 56: ^{19}F NMR spectrum of (E)-3-(4-fluorostyryl)-5,5-dimethylcyclohex-2-en-1-one **87**.*

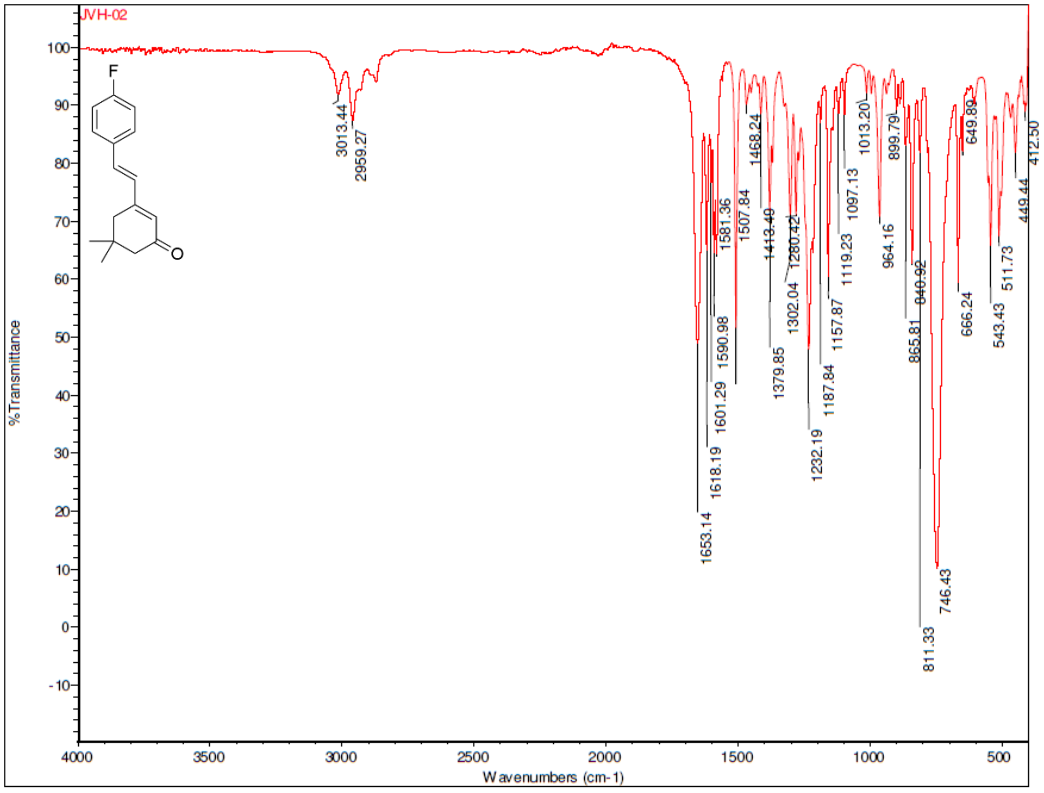

*Appendix 57: FTIR spectrum of (E)-3-(4-fluorostyryl)-5,5-dimethylcyclohex-2-en-1-one **87**.*

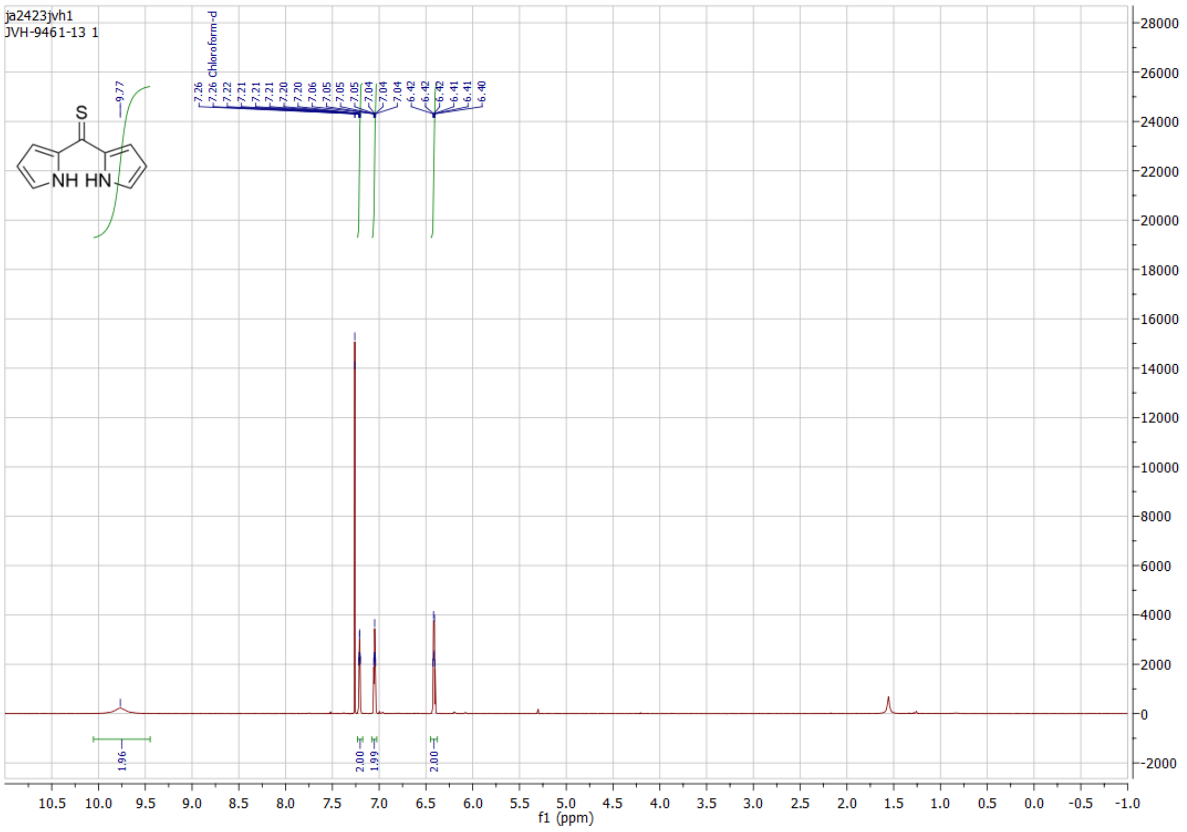

*Appendix 58: [1]H NMR spectrum of di(1H-pyrrol-2-yl)methanethione **99**.*

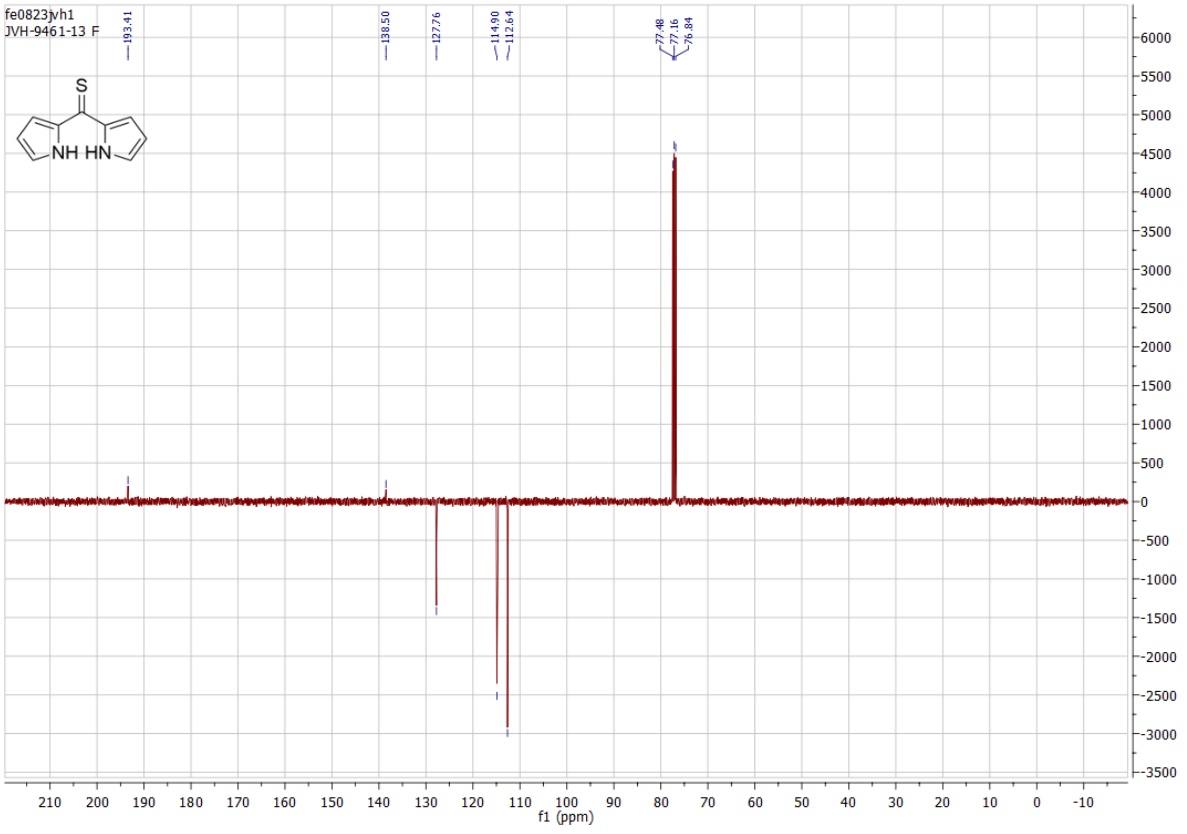

*Appendix 59: [13]C NMR spectrum of di(1H-pyrrol-2-yl)methanethione **99**.*

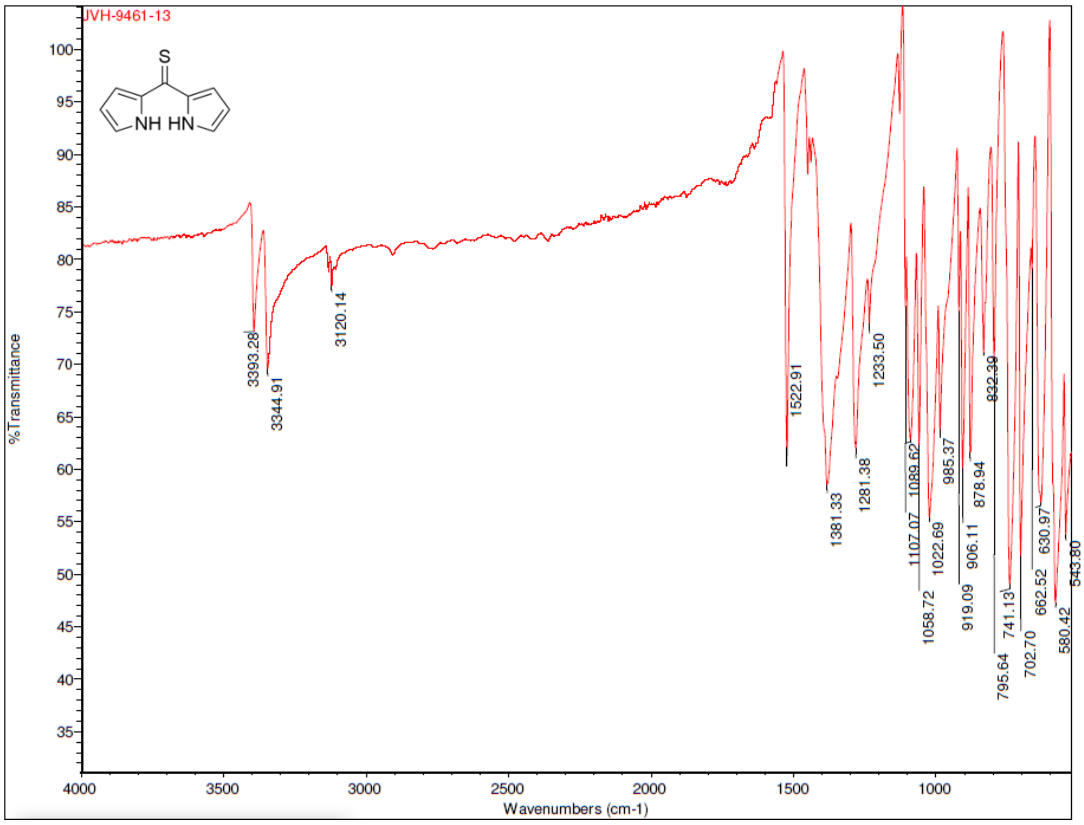

*Appendix 60: FTIR spectrum of di(1H-pyrrol-2-yl)methanethione **99**.*

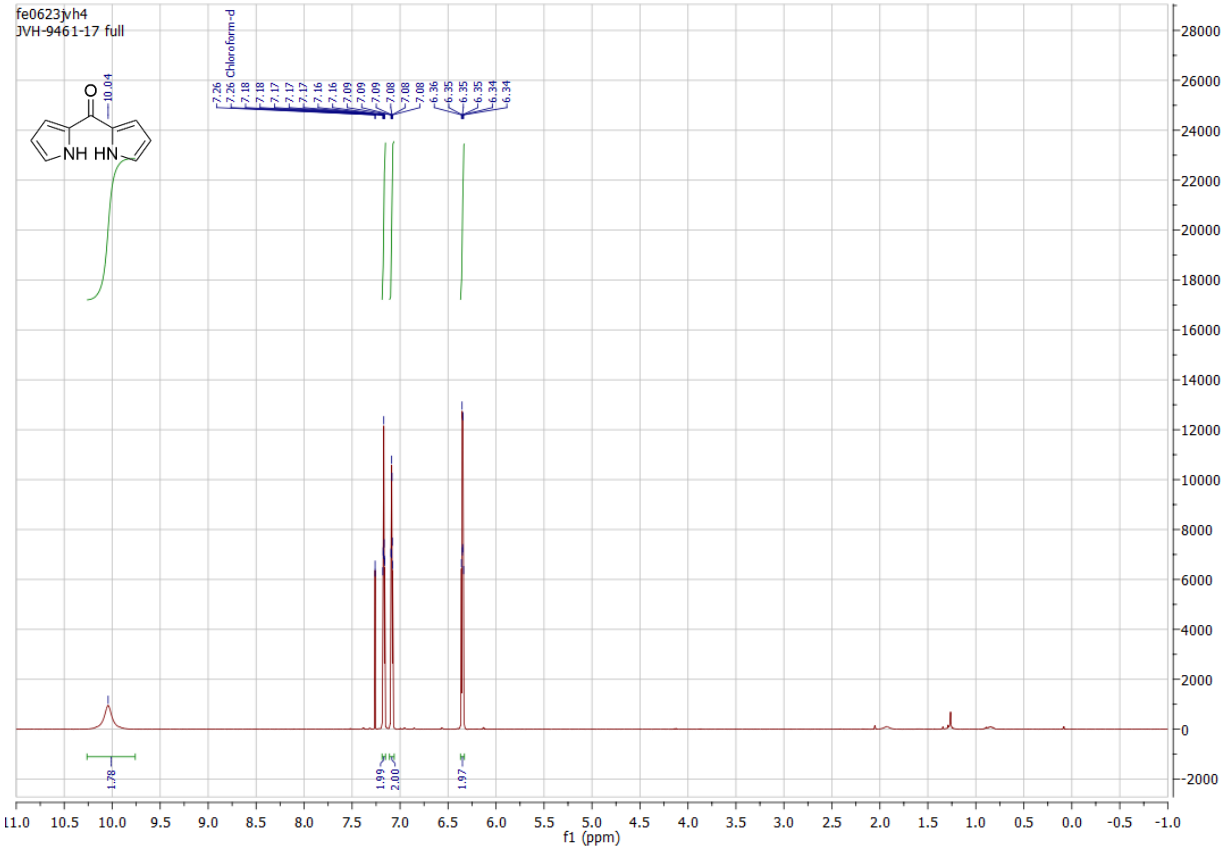

*Appendix 61: ^{1}H NMR spectrum of di(1H-pyrrol-2-yl)methanethione **99**.*

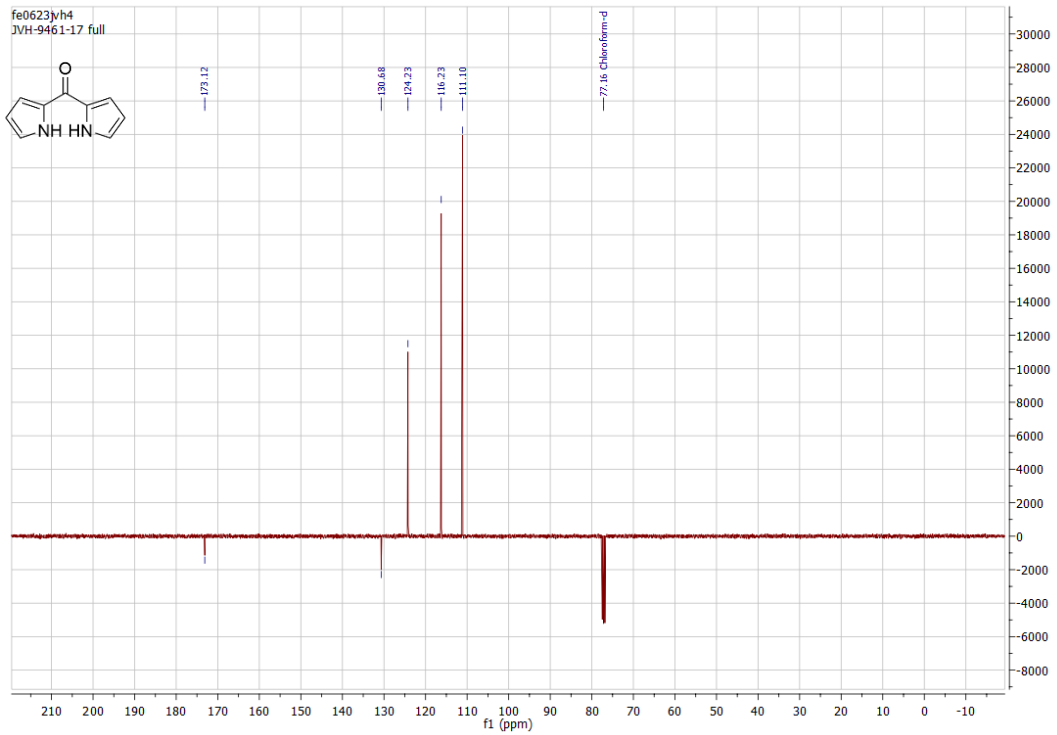

*Appendix 62: ^{13}C NMR spectrum of di(1H-pyrrol-2-yl)methanethione **100**.*

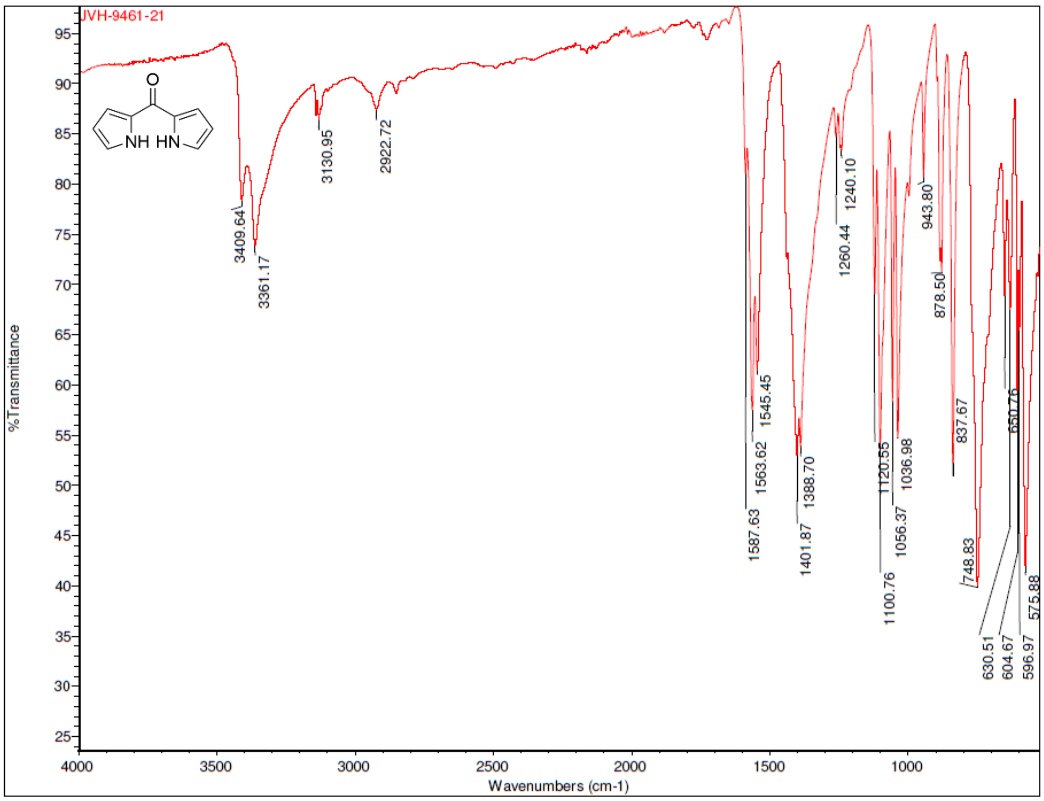

*Appendix 63: FTIR spectrum of di(1H-pyrrol-2-yl)methanethione **100**.*

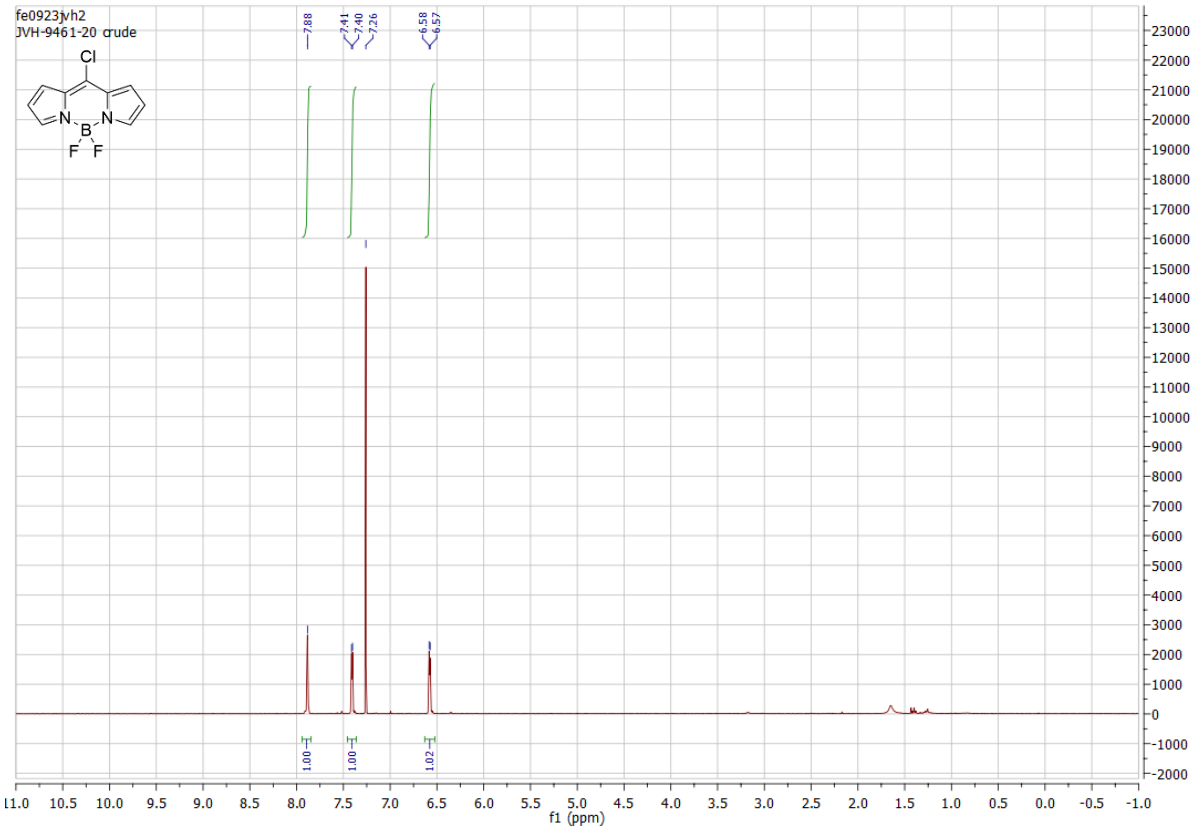

*Appendix 64: [1]H NMR spectrum of 10-chloro-5,5-difluoro-5H-4λ⁴,5λ⁴-dipyrrolo[1,2-c:2',1'-f][1,3,2]diazaborinine **101**.*

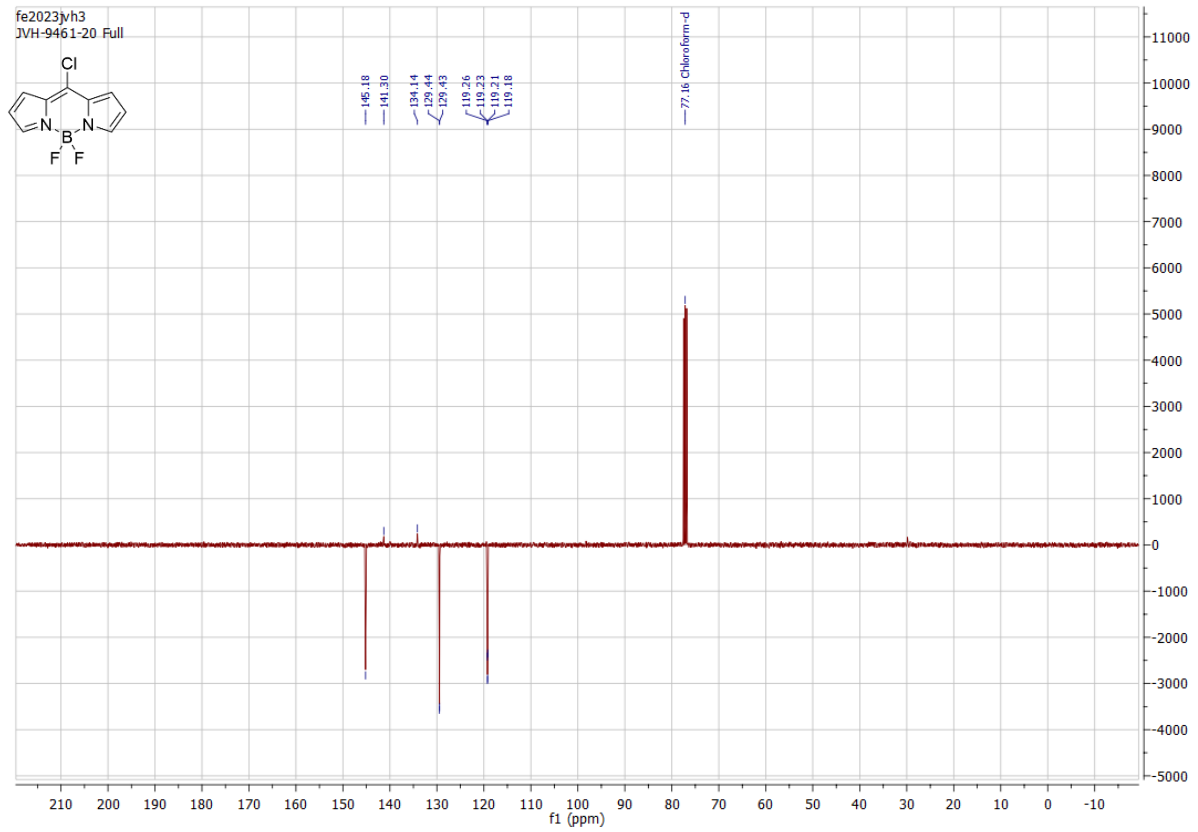

*Appendix 65: : [13]C NMR spectrum of 10-chloro-5,5-difluoro-5H-4λ⁴,5λ⁴-dipyrrolo[1,2-c:2',1'-f][1,3,2]diazaborinine **101**.*

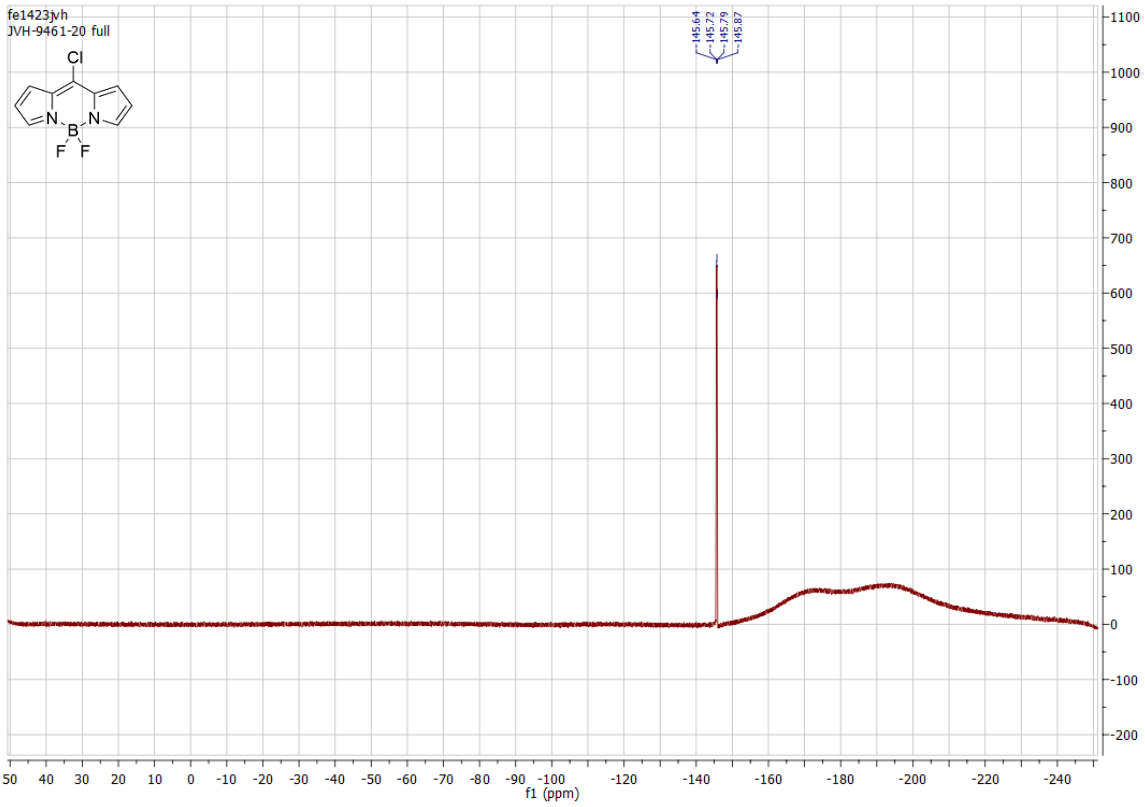

*Appendix 66: ^{19}F NMR spectrum of 10-chloro-5,5-difluoro-5H-4λ⁴,5λ⁴-dipyrrolo[1,2-c:2',1'-f][1,3,2]diazaborinine **101**.*

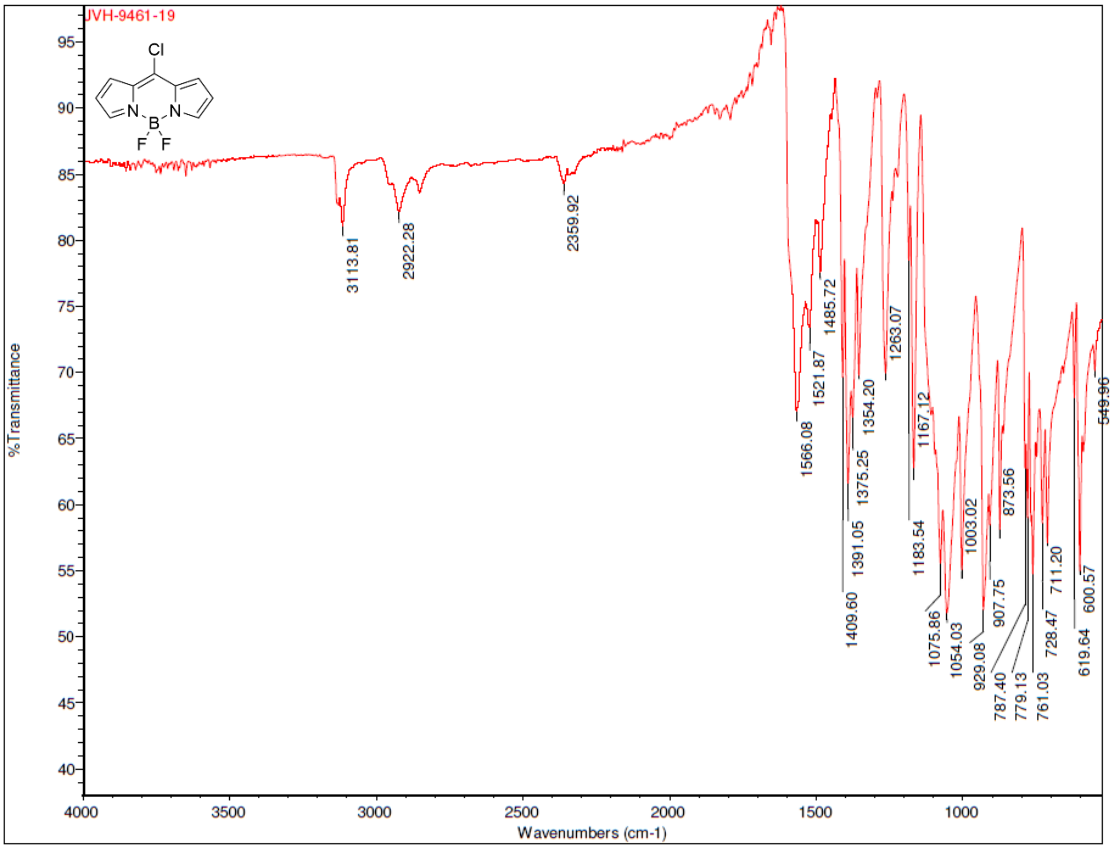

*Appendix 67: FTIR spectrum of 10-chloro-5,5-difluoro-5H-4λ⁴,5λ⁴-dipyrrolo[1,2-c:2',1'-f][1,3,2]diazaborinine **101**.*

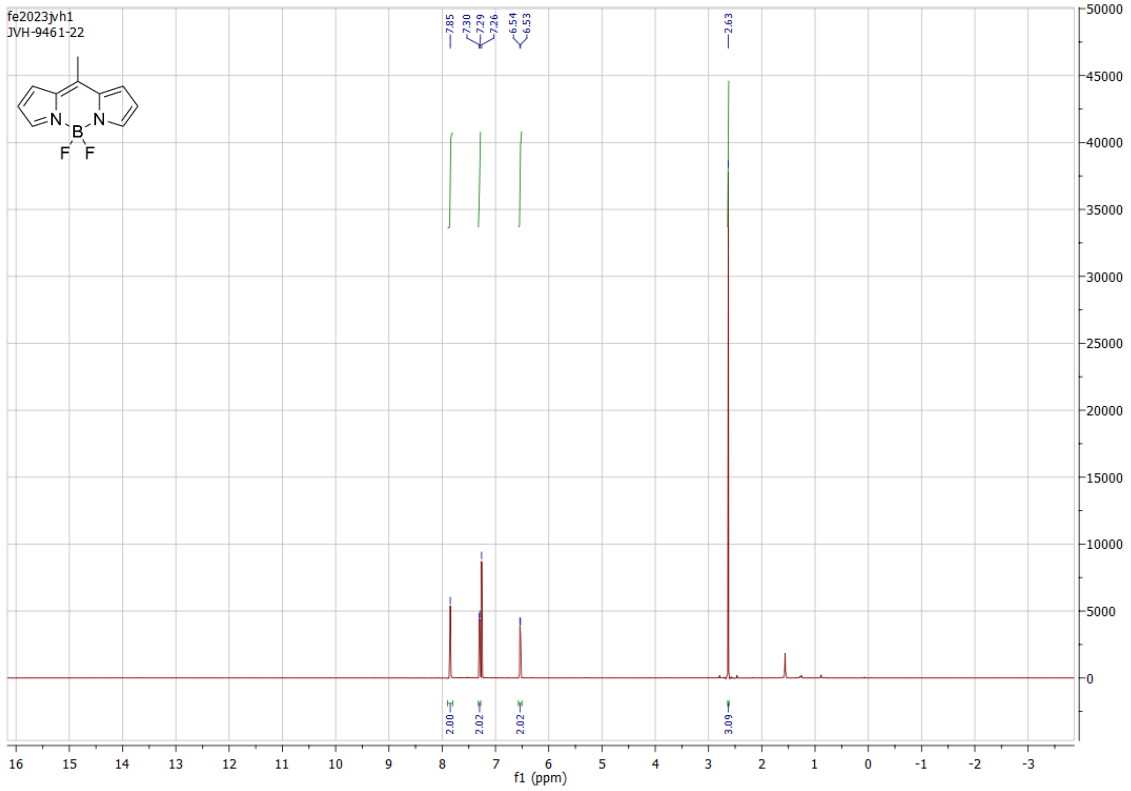

*Appendix 68: ^{1}H NMR spectrum of 10-(Methyl)-5,5-difluoro-5H-4λ⁴,5λ⁴-dipyrrolo[1,2-c:2',1'-f][1,3,2]diazaborinine **28**.*

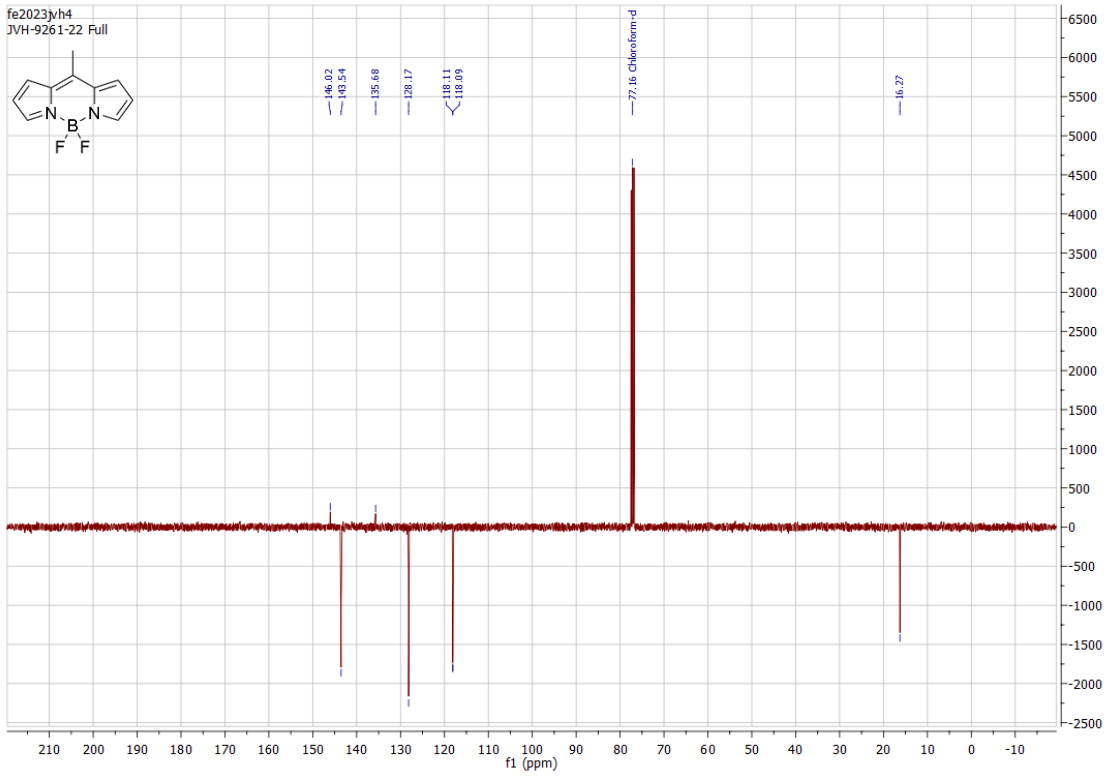

*Appendix 69: ^{13}C NMR spectrum of 10-(Methyl)-5,5-difluoro-5H-4λ⁴,5λ⁴-dipyrrolo[1,2-c:2',1'-f][1,3,2]diazaborinine **28**.*

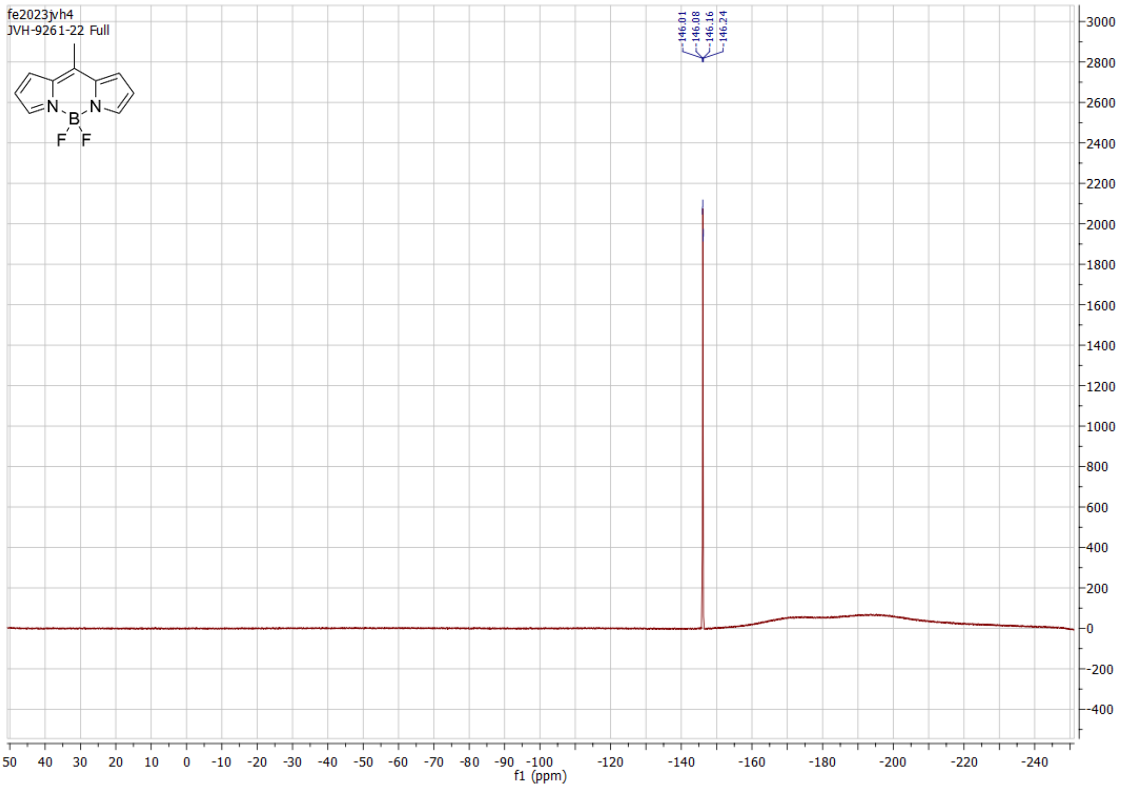

*Appendix 70: ^{19}F NMR spectrum of 10-(Methyl)-5,5-difluoro-5H-4λ⁴,5λ⁴-dipyrrolo[1,2-c:2',1'-f][1,3,2]diazaborinine **28**.*

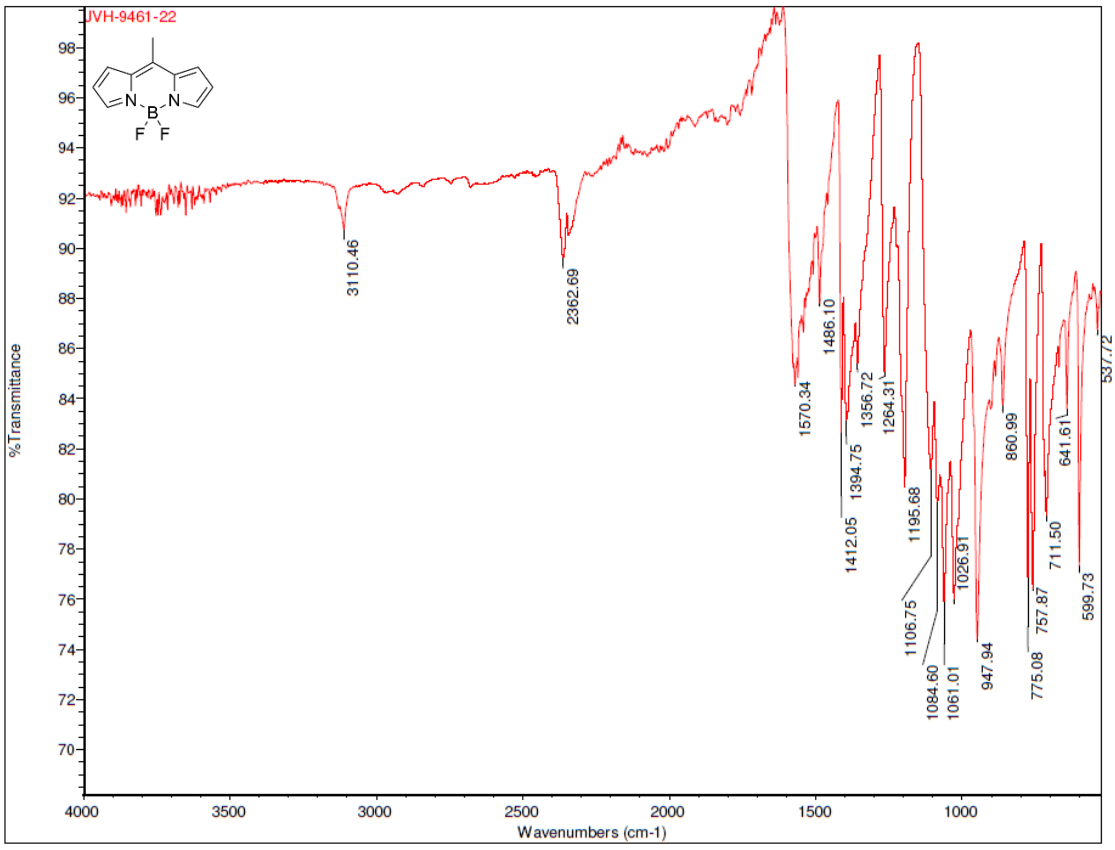

*Appendix 71: FTIR spectrum of 10-(Methyl)-5,5-difluoro-5H-4λ⁴,5λ⁴-dipyrrolo[1,2-c:2',1'-f][1,3,2]diazaborinine **28**.*

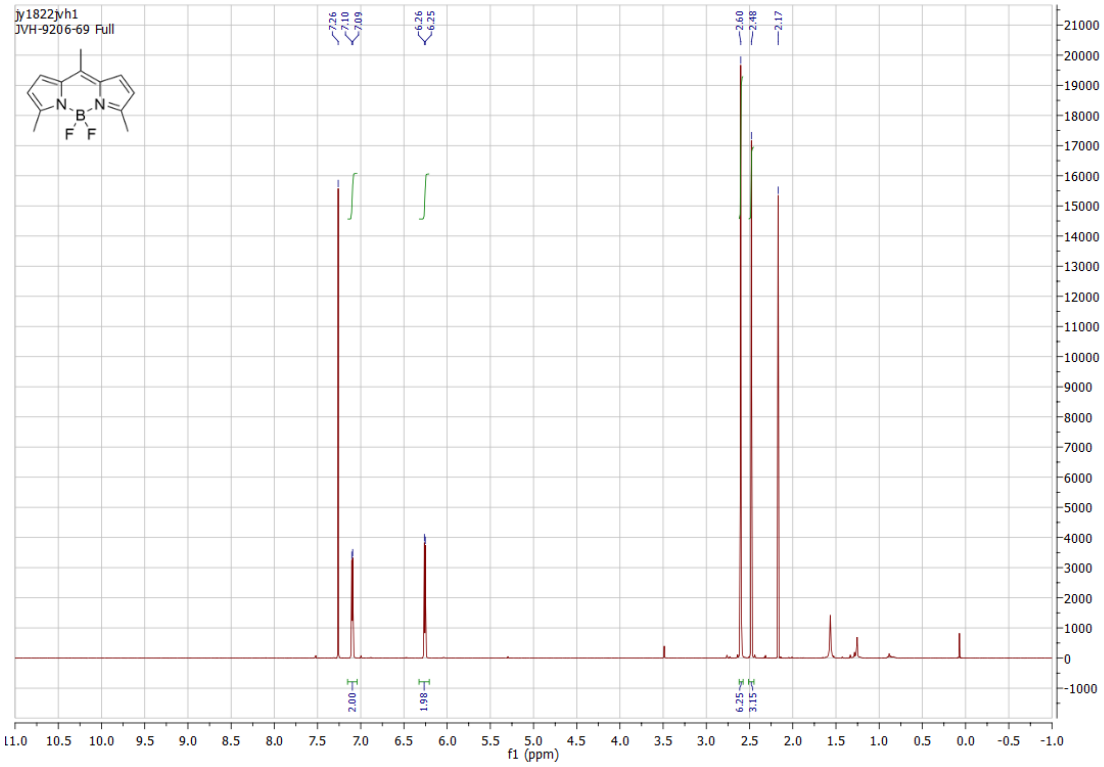

*Appendix 72: [1]H NMR spectrum of 10-(Methyl)-5,5-difluoro-3,7-dimethyl-5H-4λ⁴,5λ⁴-dipyrrolo[1,2-c:2',1'-f][1,3,2]diazaborinine **93**.*

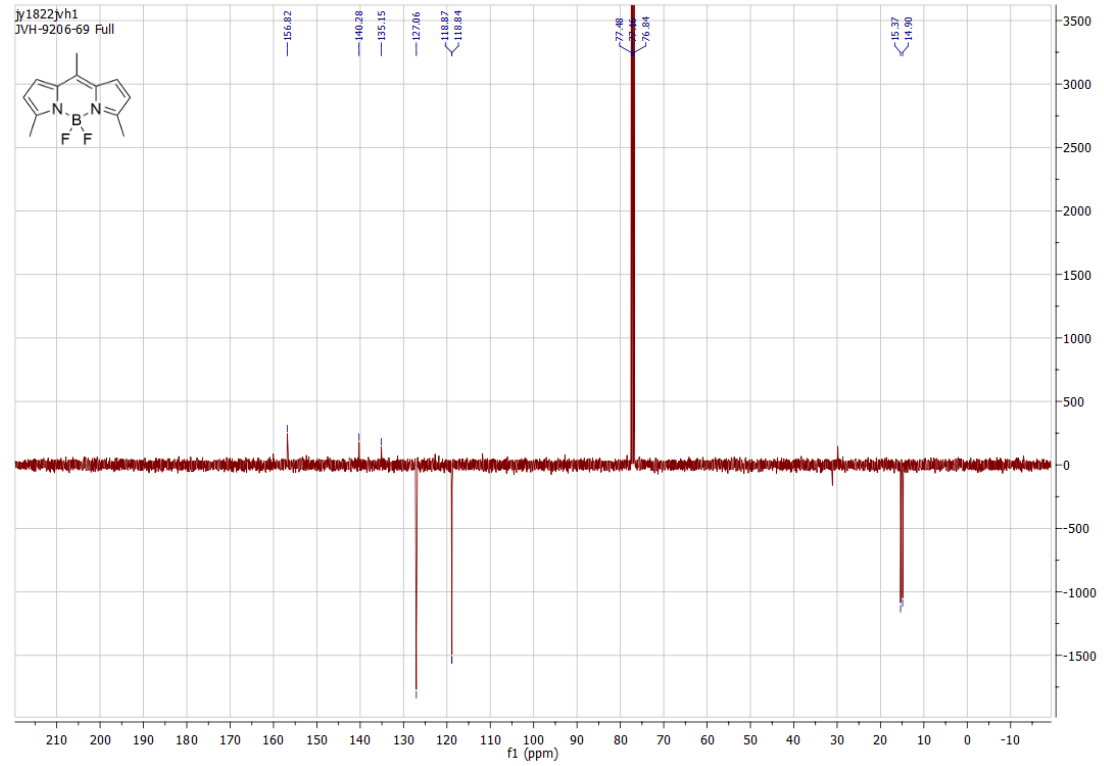

*Appendix 73: [13]C NMR spectrum of 10-(Methyl)-5,5-difluoro-3,7-dimethyl-5H-4λ⁴,5λ⁴-dipyrrolo[1,2-c:2',1'-f][1,3,2]diazaborinine **93**.*

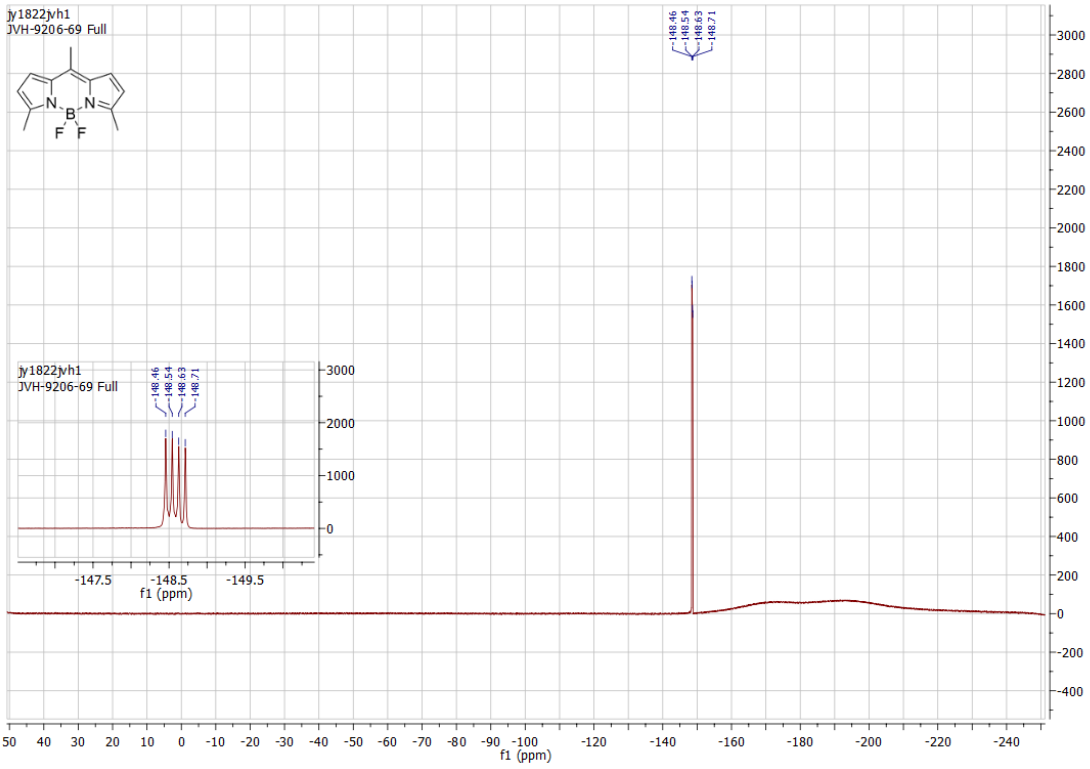

Appendix 74: ^{1}H NMR spectrum of 10-(Methyl)-5,5-difluoro-3,7-dimethyl-5H-4λ^{4},5λ^{4}-dipyrrolo[1,2-c:2',1'-f][1,3,2]diazaborinine ***93.***

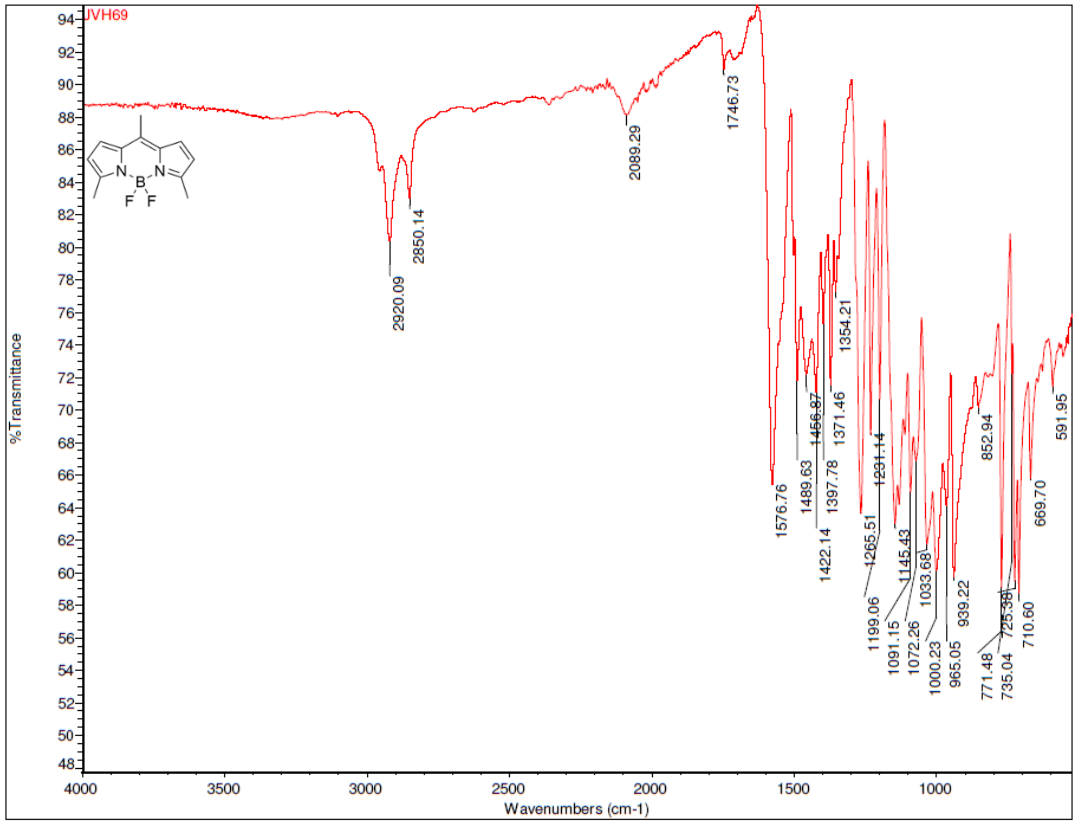

Appendix 75: FTIR spectrum of 10-(Methyl)-5,5-difluoro-3,7-dimethyl-5H-4λ^{4},5λ^{4}-dipyrrolo[1,2-c:2',1'-f][1,3,2]diazaborinine ***93.***

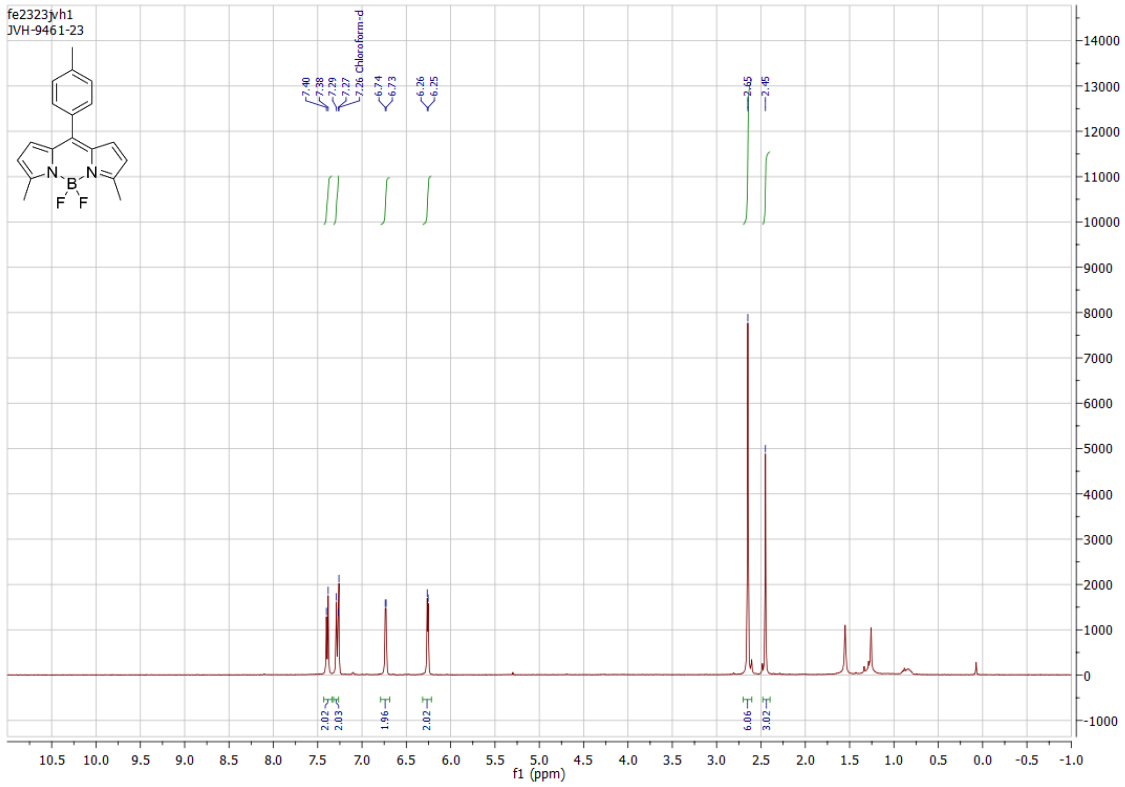

*Appendix 76: ^{1}H NMR spectrum of 10-(p-toluyl)-5,5-difluoro-3,7-dimethyl-5H-4λ^{4},5λ^{4}-dipyrrolo[1,2-c:2',1'-f][1,3,2]diazaborinine **109**.*

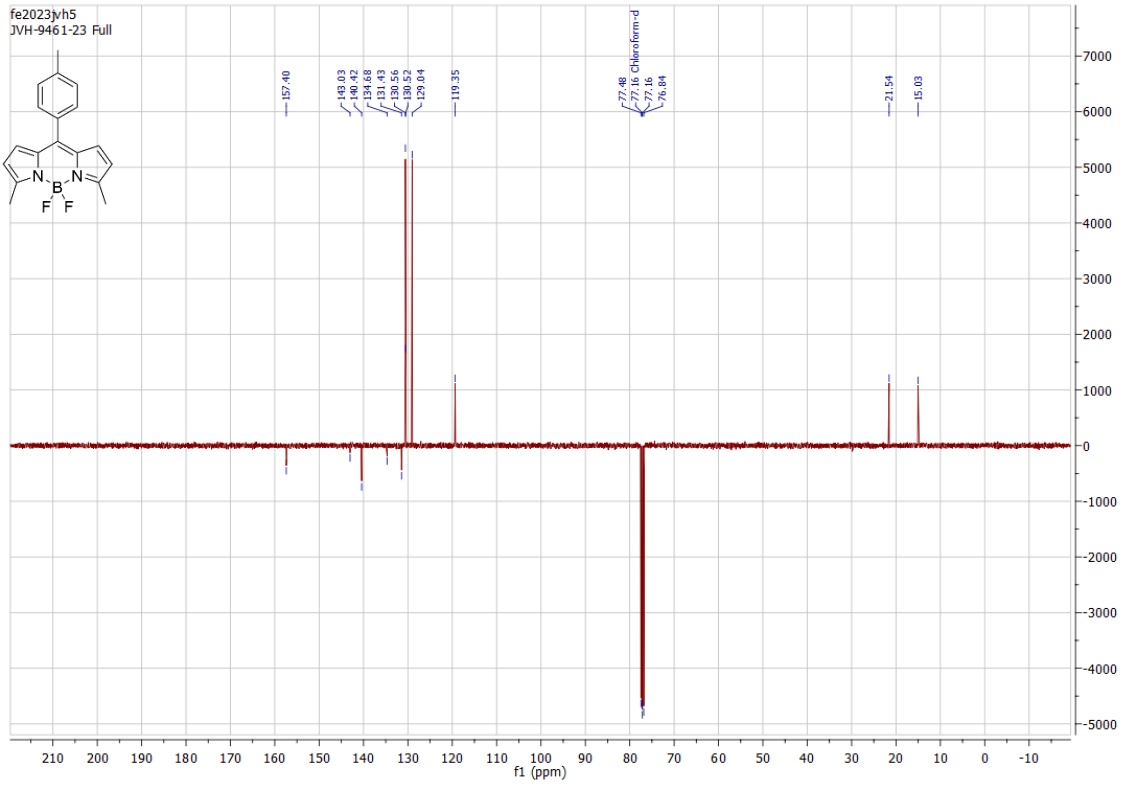

*Appendix 77: ^{13}C NMR spectrum of 10-(p-toluyl)-5,5-difluoro-3,7-dimethyl-5H-4λ^{4},5λ^{4}-dipyrrolo[1,2-c:2',1'-f][1,3,2]diazaborinine **109**.*

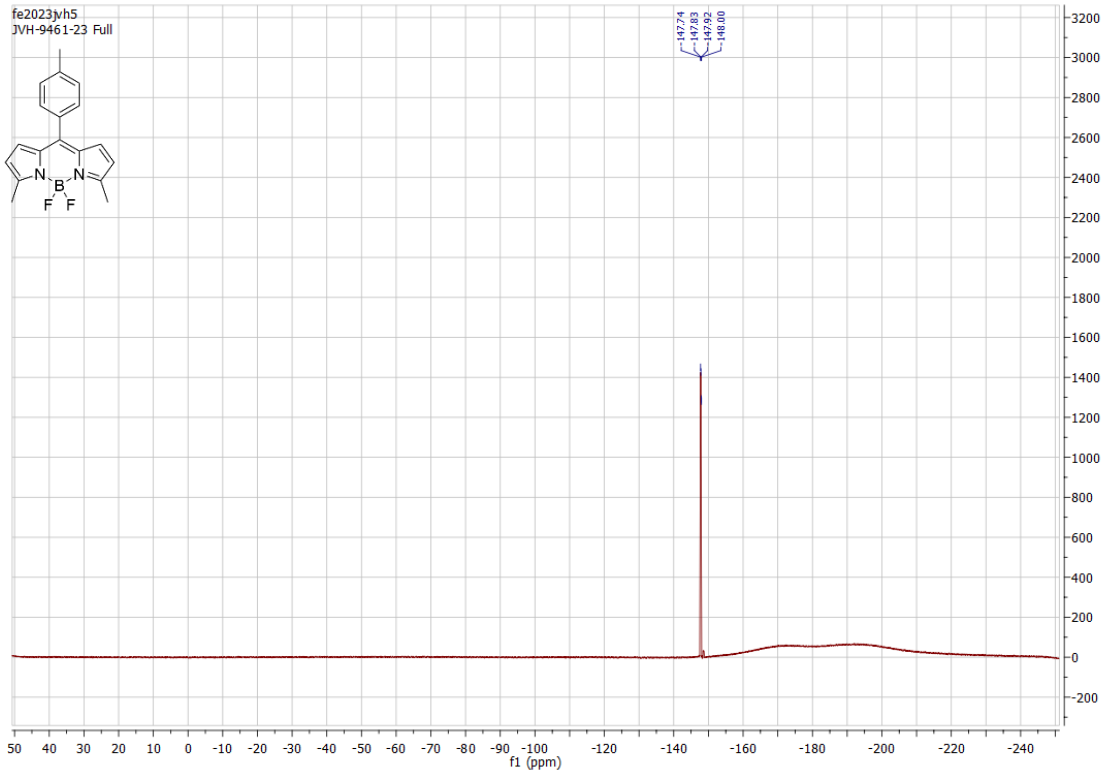

*Appendix 78: ^{19}F NMR spectrum of 10-(p-toluyl)-5,5-difluoro-3,7-dimethyl-5H-4λ⁴,5λ⁴-dipyrrolo[1,2-c:2',1'-f][1,3,2]diazaborinine **109**.*

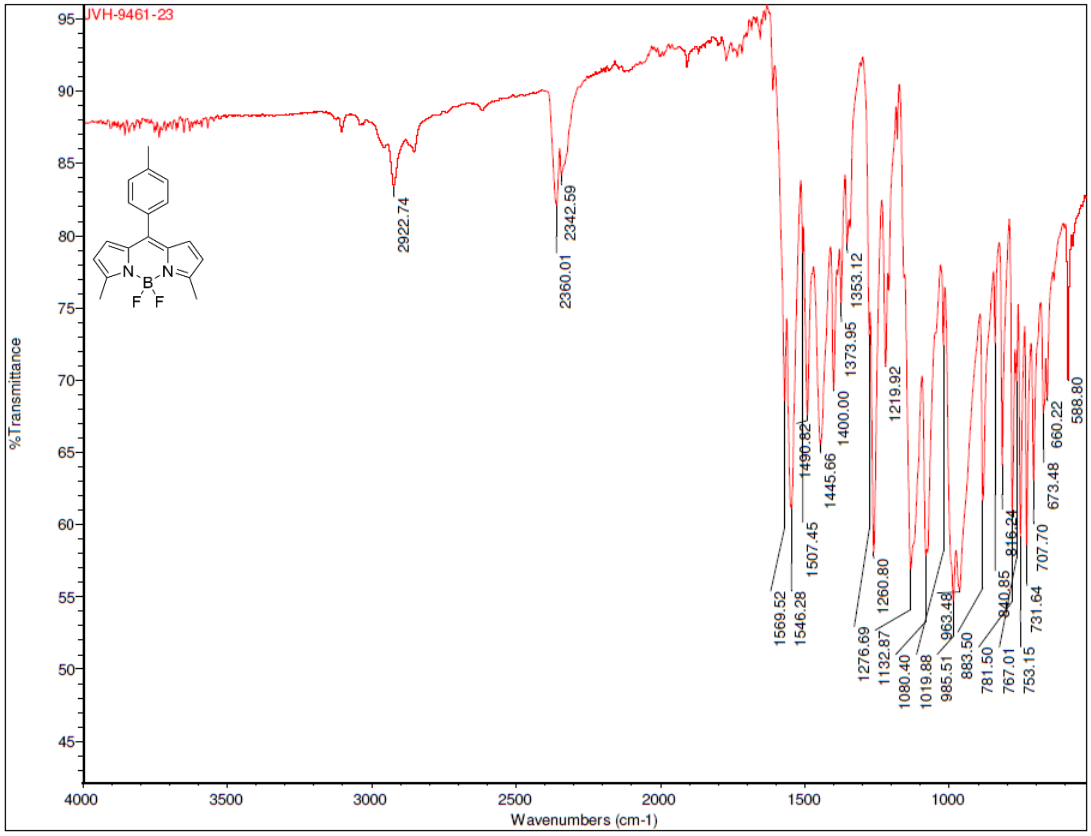

*Appendix 79: FTIR spectrum of 10-(p-toluyl)-5,5-difluoro-3,7-dimethyl-5H-4λ⁴,5λ⁴-dipyrrolo[1,2-c:2',1'-f][1,3,2]diazaborinine **109**.*

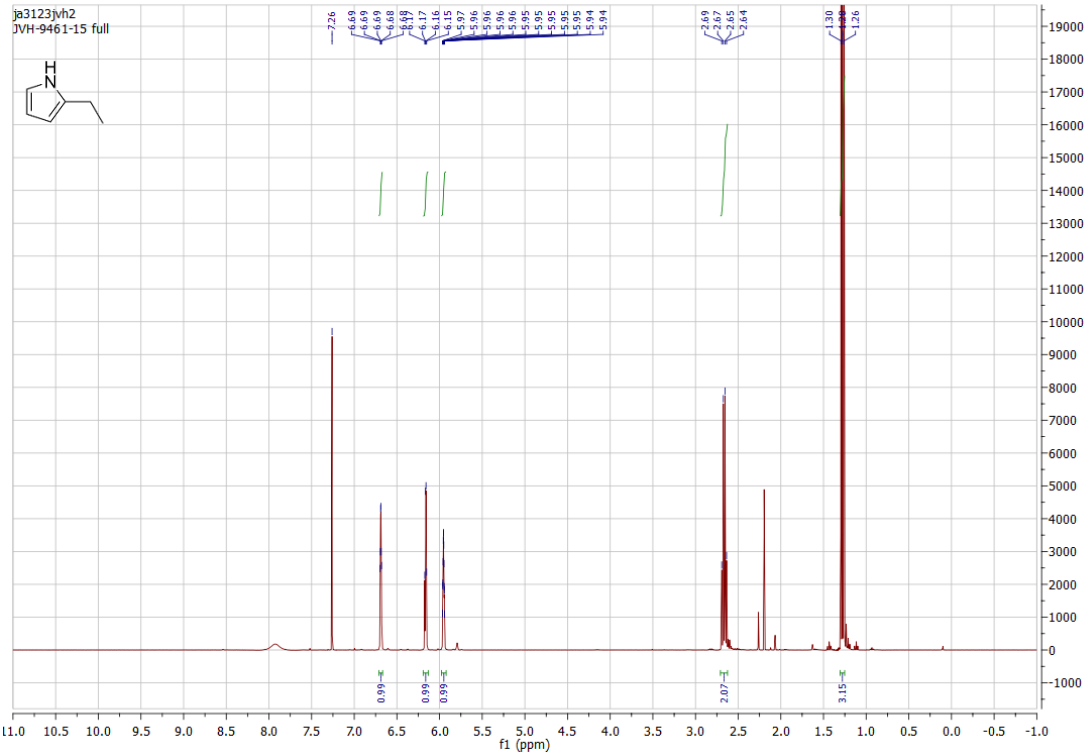

*Appendix 80: [1]H NMR spectrum of 2-ethyl pyrrole **107**.*

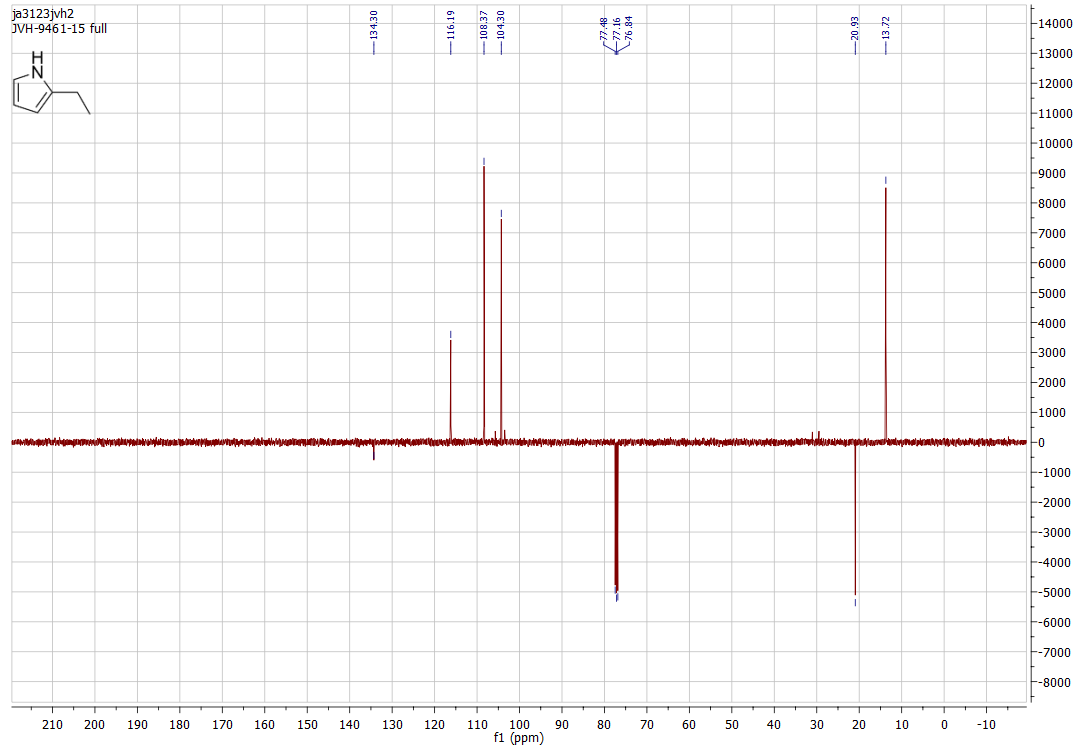

*Appendix 81: [13]C NMR spectrum of 2-ethyl pyrrole **107**.*

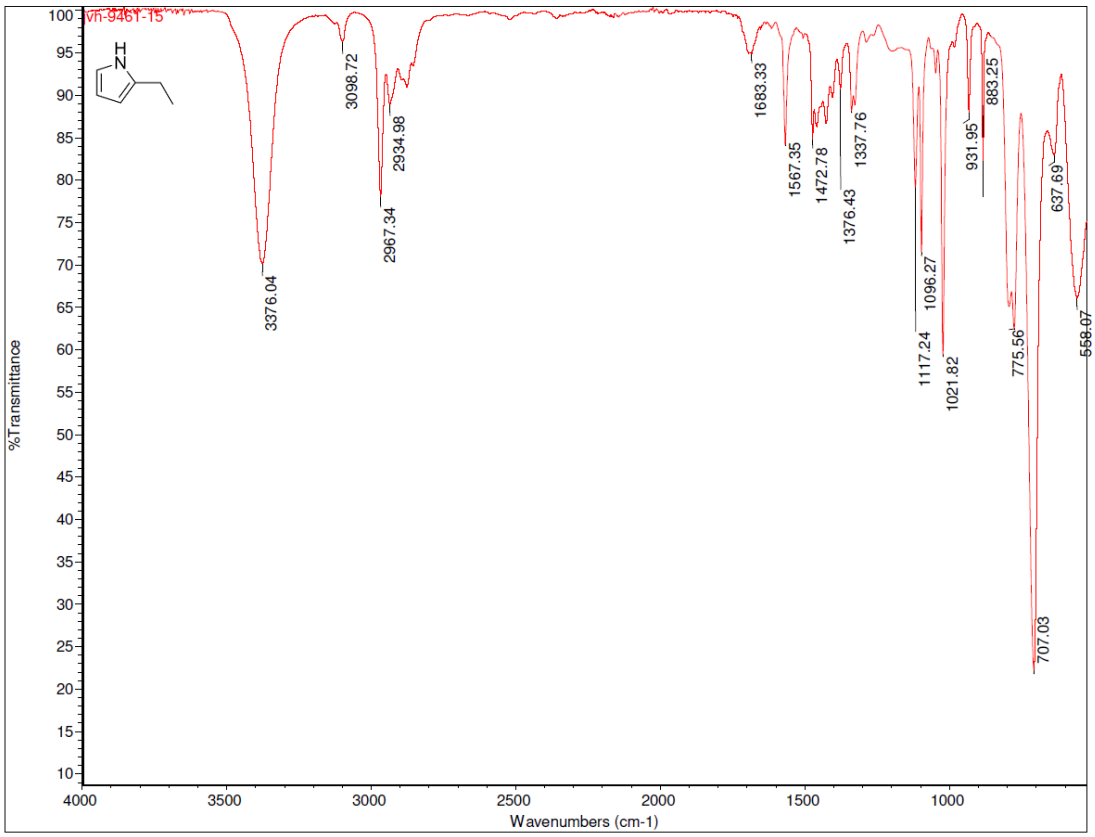

*Appendix 82: FTIR spectrum of 2-ethyl pyrrole **107**.*

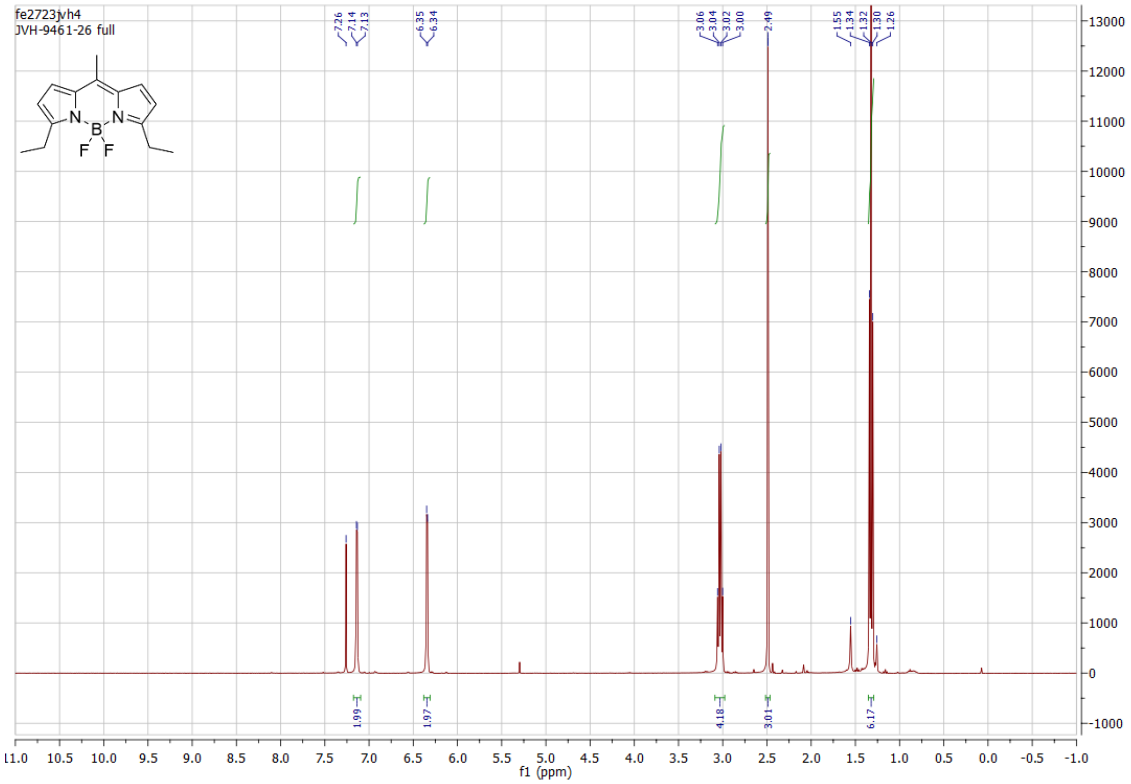

*Appendix 83: ^{1}H NMR spectrum of 10-(Methyl)-5,5-difluoro-3,7-diethyl-5H-4λ⁴,5λ⁴-dipyrrolo[1,2-c:2',1'-f][1,3,2]diazaborinine **103**.*

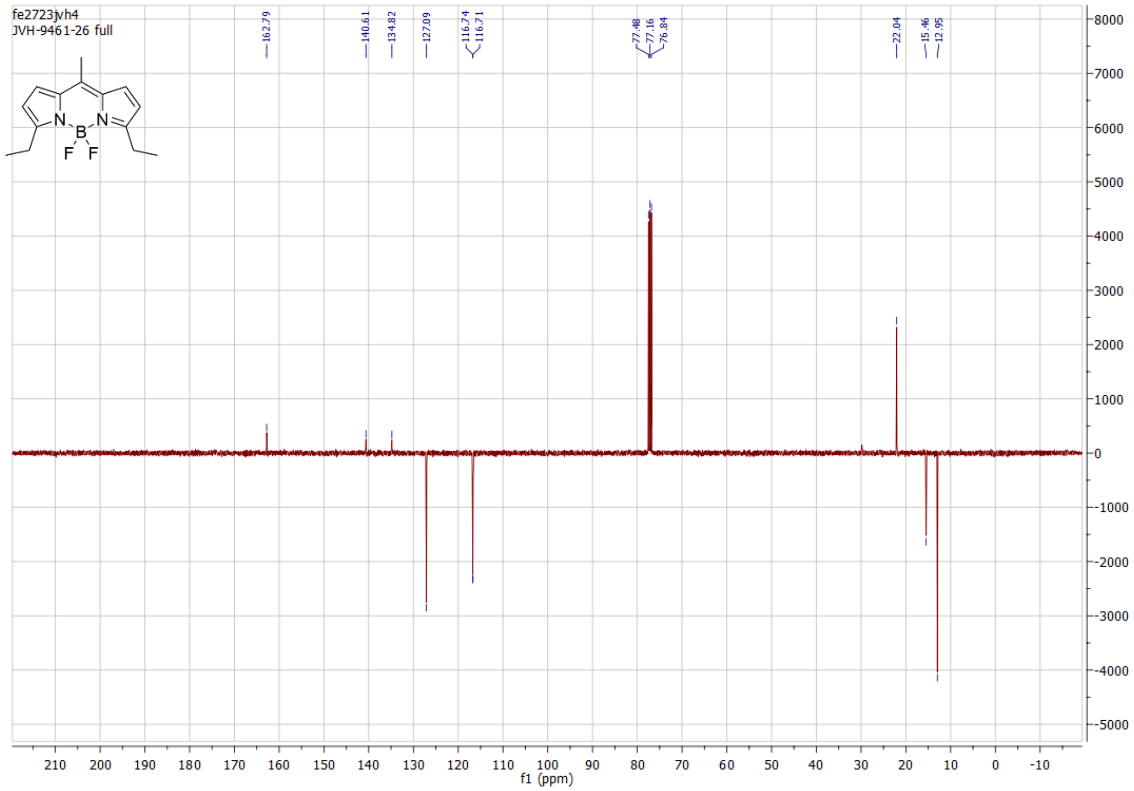

*Appendix 84: ^{13}C NMR spectrum of 10-(Methyl)-5,5-difluoro-3,7-diethyl-5H-4λ^4,5λ^4-dipyrrolo[1,2-c:2',1'-f][1,3,2]diazaborinine **103**.*

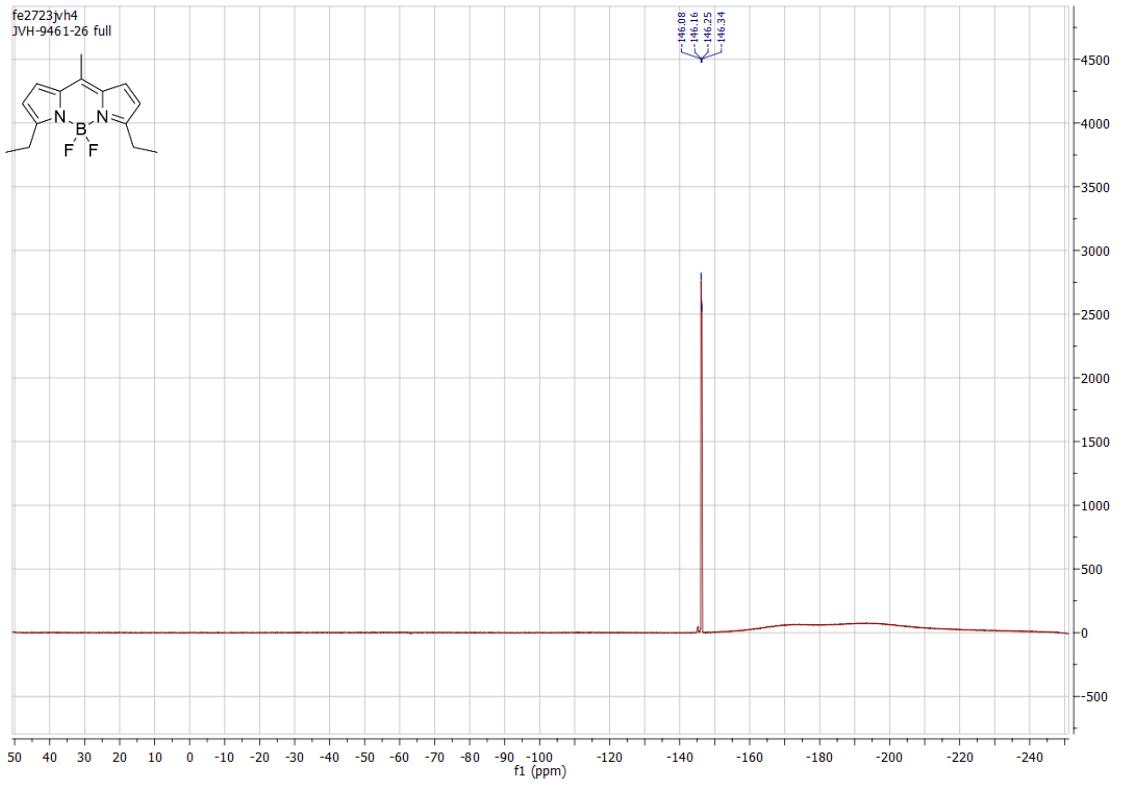

*Appendix 85: ^{19}F NMR spectrum of 10-(Methyl)-5,5-difluoro-3,7-diethyl-5H-4λ^4,5λ^4-dipyrrolo[1,2-c:2',1'-f][1,3,2]diazaborinine **103**.*

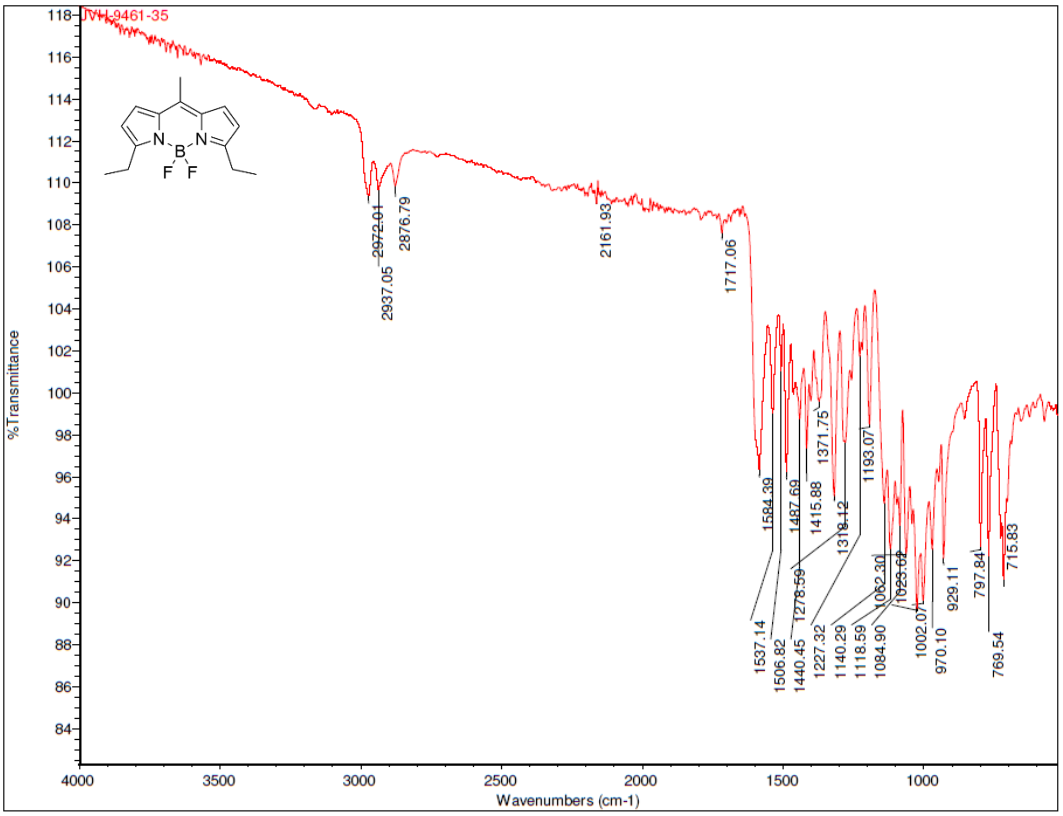

*Appendix 86: FTIR specrum of 10-(Methyl)-5,5-difluoro-3,7-diethyl-5H-4λ⁴,5λ⁴-dipyrrolo[1,2-c:2',1'-f][1,3,2]diazaborinine **103**.*

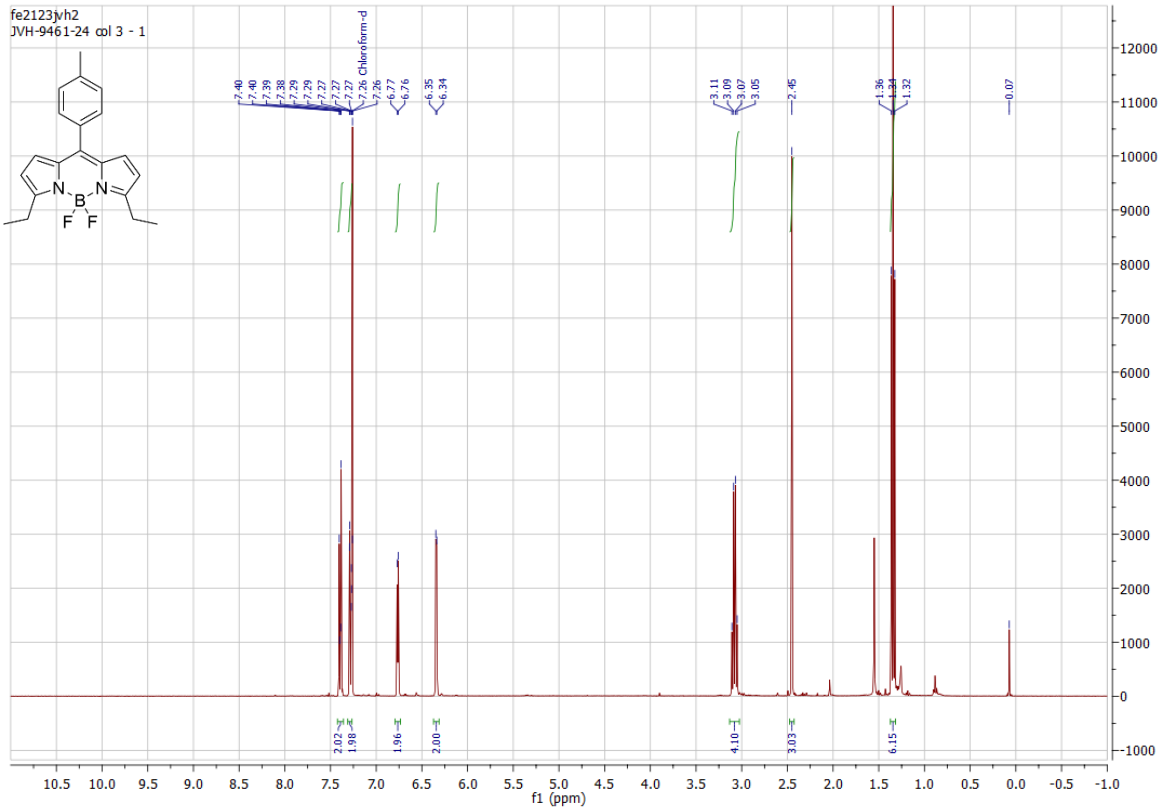

*Appendix 87: ^{1}H NMR spectrum of 10-(p-toluyl)-5,5-difluoro-3,7-diethyl-5H-4λ⁴,5λ⁴-dipyrrolo[1,2-c:2',1'-f][1,3,2]diazaborinine **110**.*

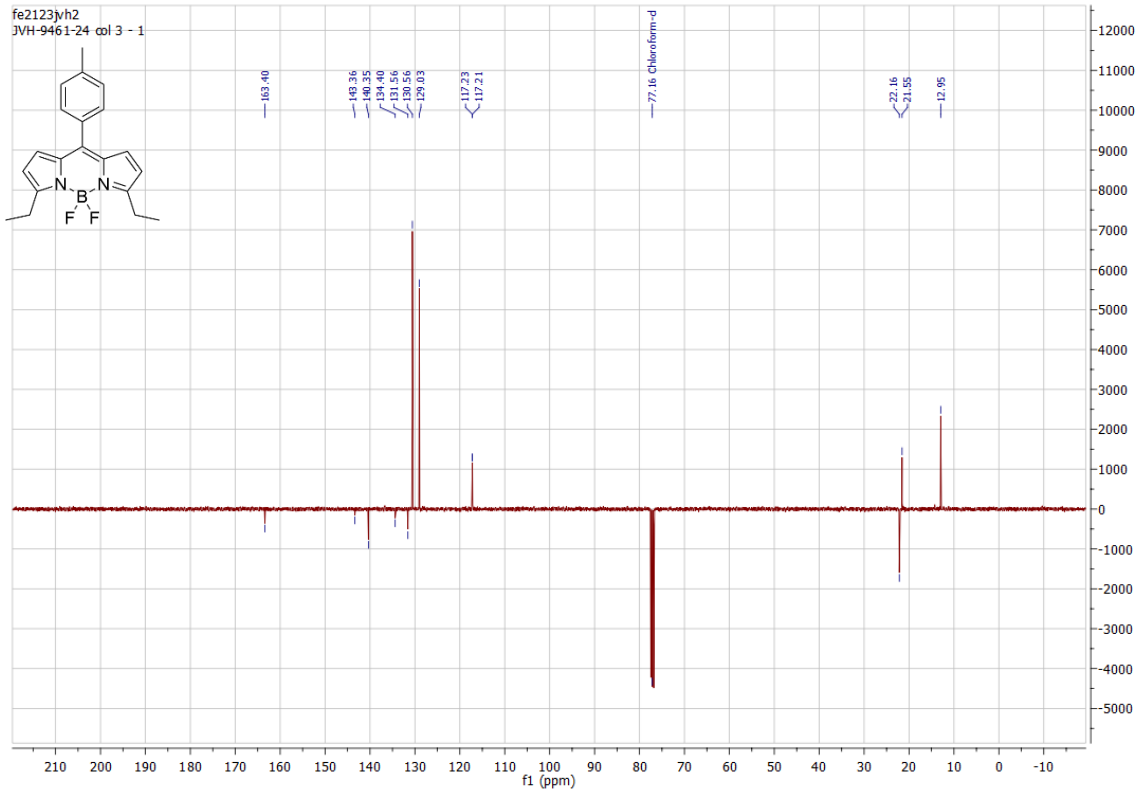

*Appendix 88: ^{13}C NMR spectrum of 10-(p-toluyl)-5,5-difluoro-3,7-diethyl-5H-4λ⁴,5λ⁴-dipyrrolo[1,2-c:2',1'-f][1,3,2]diazaborinine **110**.*

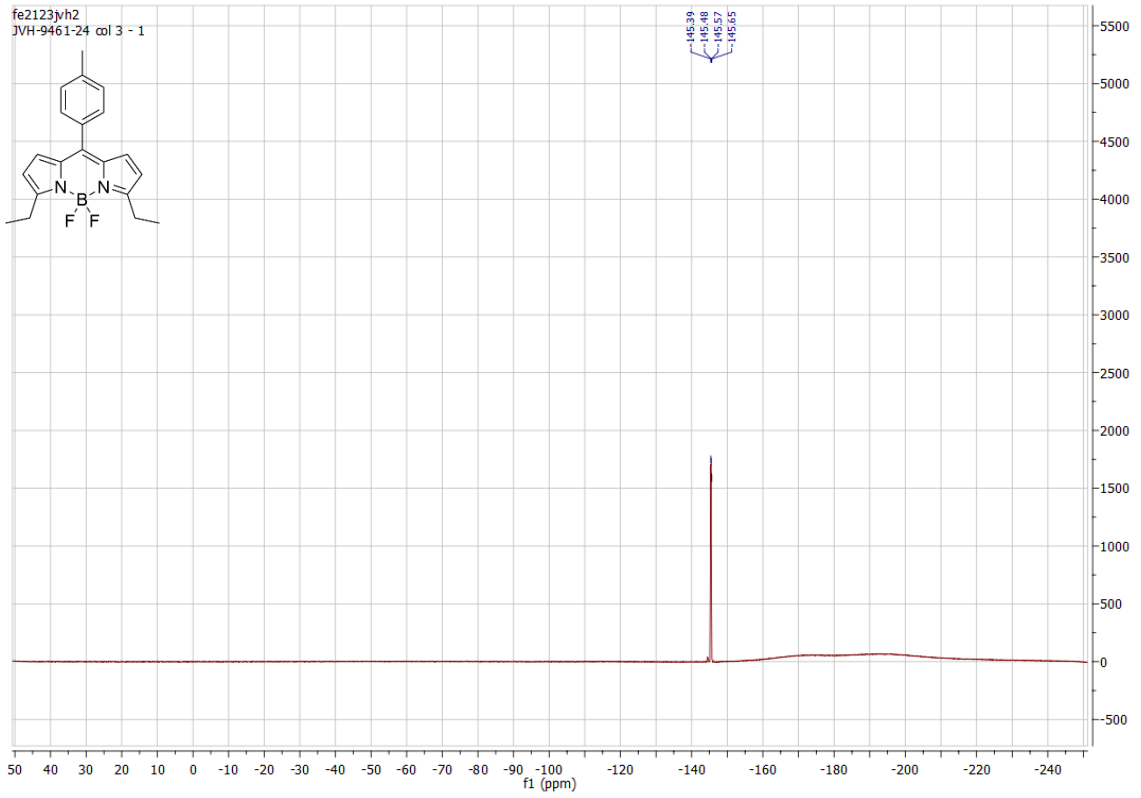

*Appendix 89: ^{19}F NMR spectrum of 10-(p-toluyl)-5,5-difluoro-3,7-diethyl-5H-4λ⁴,5λ⁴-dipyrrolo[1,2-c:2',1'-f][1,3,2]diazaborinine **110**.*

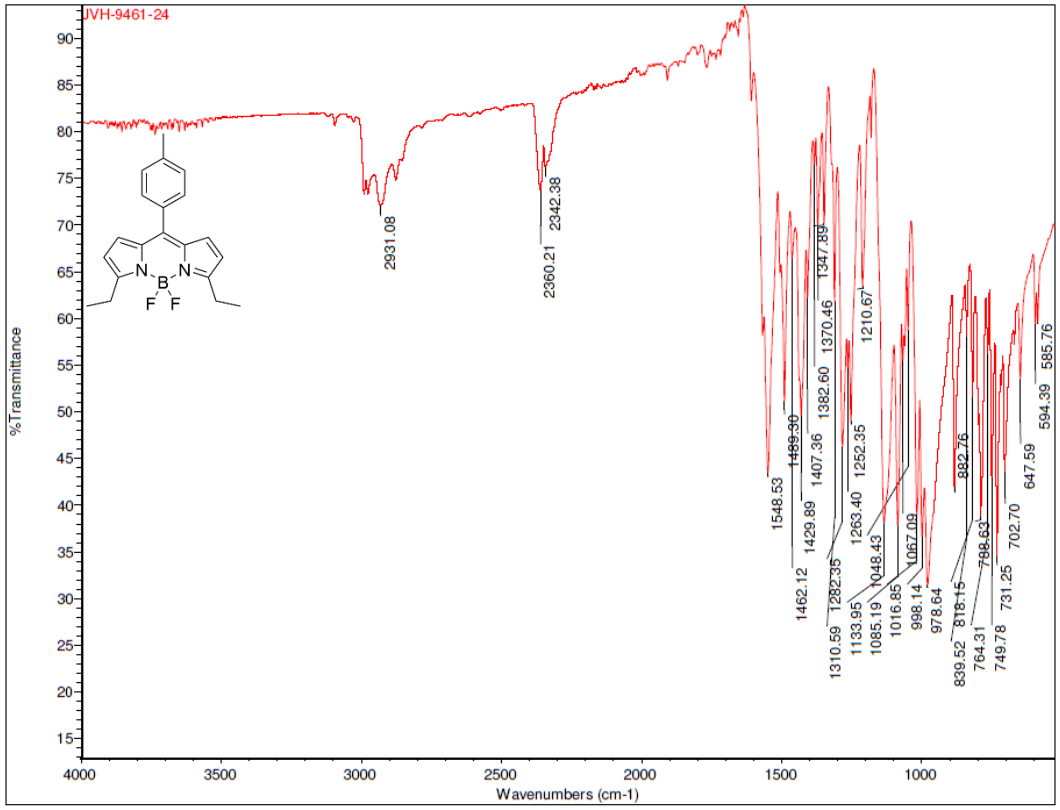

*Appendix 90: FTIR spectrum of 10-(p-toluyl)-5,5-difluoro-3,7-diethyl-5H-4λ⁴,5λ⁴-dipyrrolo[1,2-c:2',1'-f][1,3,2]diazaborinine **110**.*

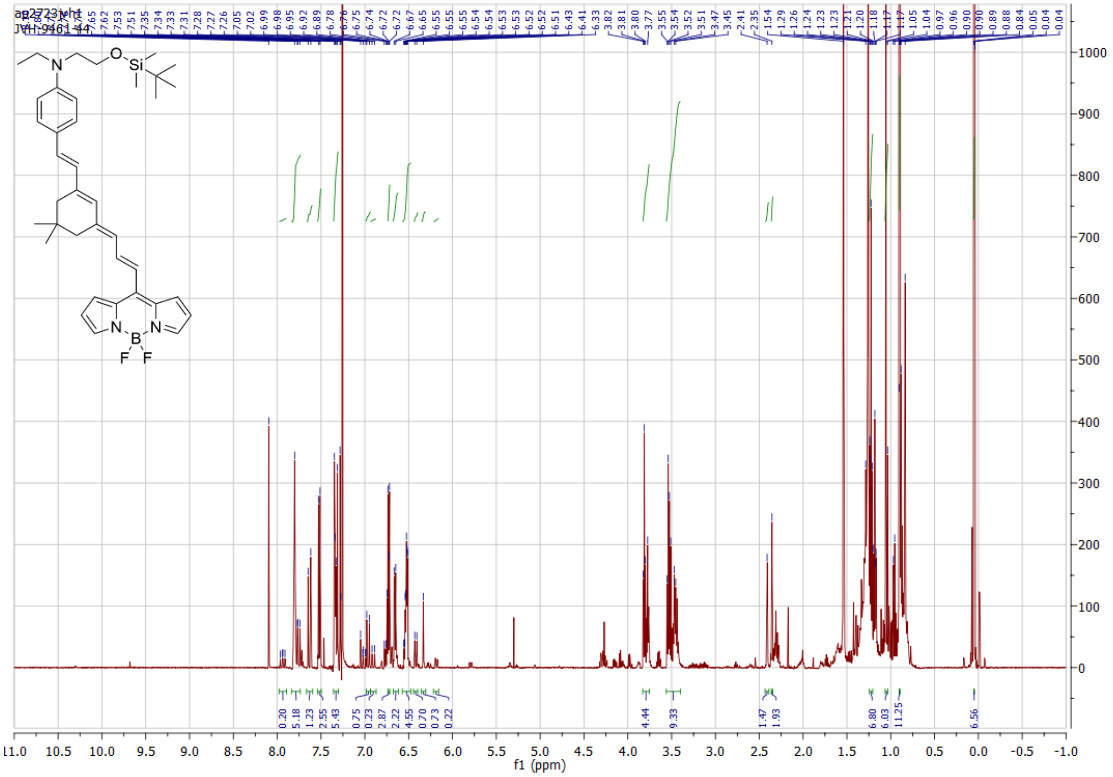

*Appendix 91: ^{1}H NMR spectrum of N-(2-((tert-butyldimethylsilyl)oxy)ethyl)-4-((E)-2-((E)-3-((E)-3-(5,5-difluoro-5H-4λ⁴,5λ⁴-dipyrrolo[1,2-c:2',1'-f][1,3,2]diazaborinin-10-yl)allylidene)-5,5-dimethylcyclohex-1-en-1-yl)vinyl)-N-ethylaniline **96**.*

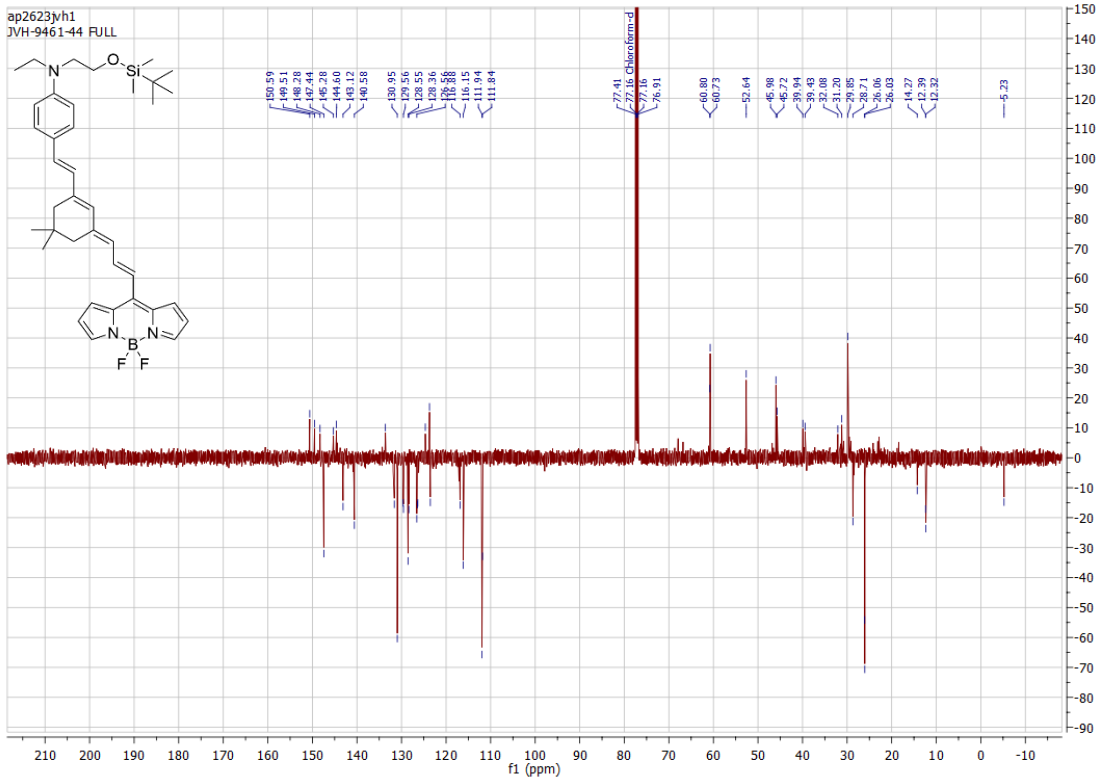

*Appendix 92: ^{13}C NMR spectrum of N-(2-((tert-butyldimethylsilyl)oxy)ethyl)-4-((E)-2-((E)-3-((E)-3-(5,5-difluoro-5H-4λ⁴,5λ⁴-dipyrrolo[1,2-c:2',1'-f][1,3,2]diazaborinin-10-yl)allylidene)-5,5-dimethylcyclohex-1-en-1-yl)vinyl)-N-ethylaniline **96**.*

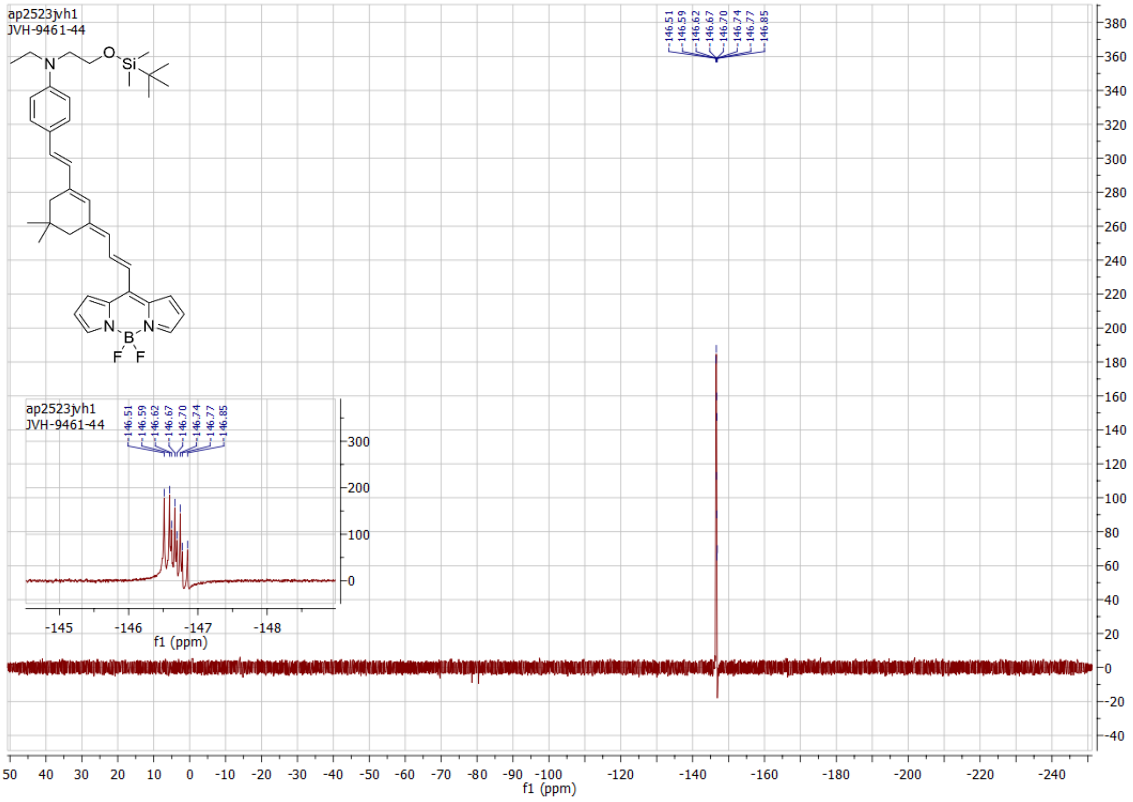

*Appendix 93: ^{19}F NMR spectrum of N-(2-((tert-butyldimethylsilyl)oxy)ethyl)-4-((E)-2-((E)-3-((E)-3-(5,5-difluoro-5H-4λ⁴,5λ⁴-dipyrrolo[1,2-c:2',1'-f][1,3,2]diazaborinin-10-yl)allylidene)-5,5-dimethylcyclohex-1-en-1-yl)vinyl)-N-ethylaniline **96**.*

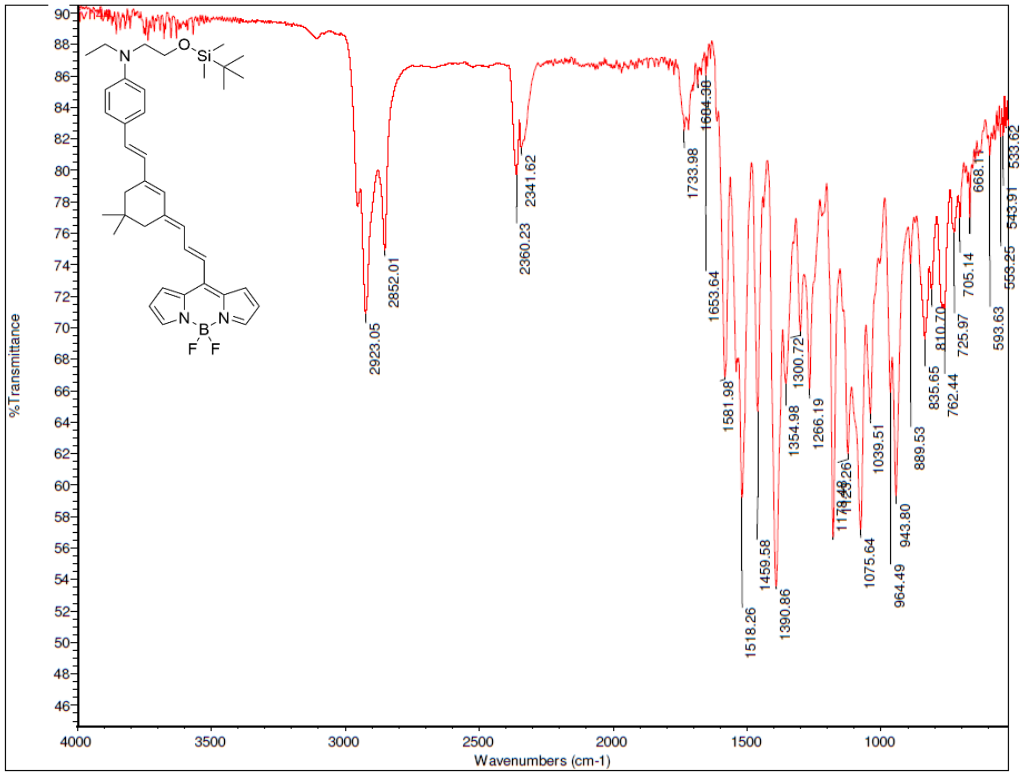

*Appendix 94: FTIR spectrum of N-(2-((tert-butyldimethylsilyl)oxy)ethyl)-4-((E)-2-((E)-3-((E)-3-(5,5-difluoro-5H-4λ^4,5λ^4-dipyrrolo[1,2-c:2',1'-f][1,3,2]diazaborinin-10-yl)allylidene)-5,5-dimethylcyclohex-1-en-1-yl)vinyl)-N-ethylaniline **96**.*

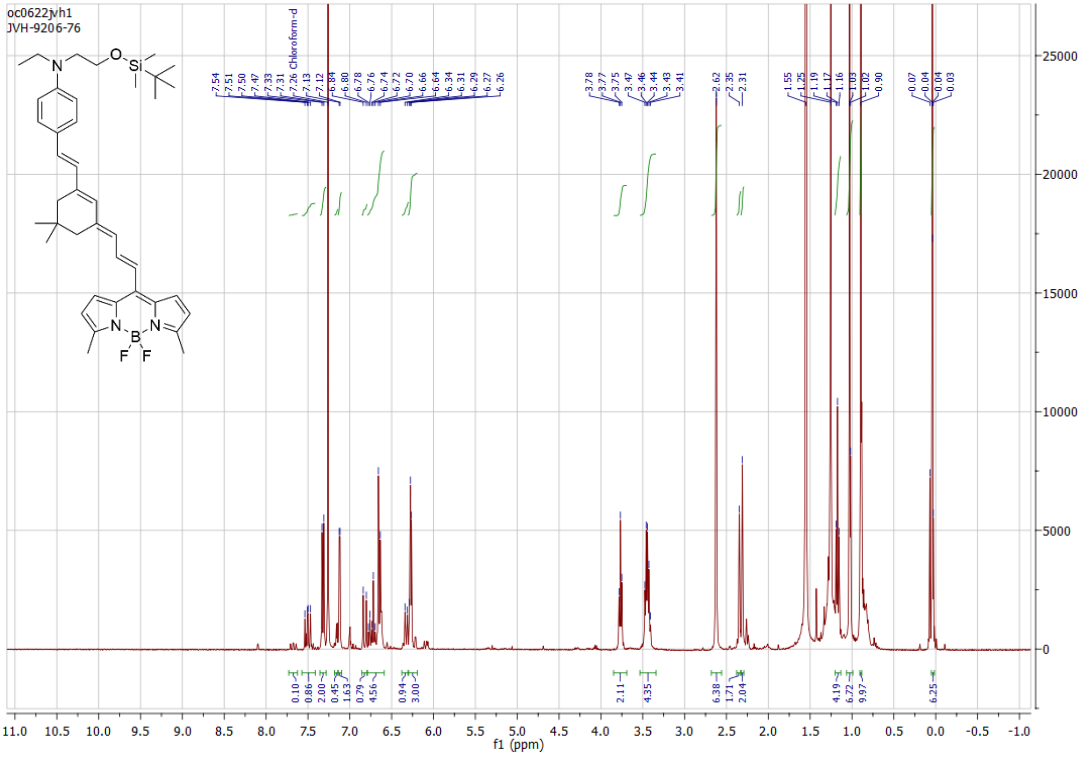

*Appendix 95: ^{1}H NMR spectrum of N-(2-((tert-butyldimethylsilyl)oxy)ethyl)-4-((E)-2-((E)-3-((E)-3-(5,5-difluoro-3,7-dimethyl-5H-4λ^4,5λ^4-dipyrrolo[1,2-c:2',1'-f][1,3,2]diazaborinin-10-yl)allylidene)-5,5-dimethylcyclohex-1-en-1-yl)vinyl)-N-ethylaniline **94**.*

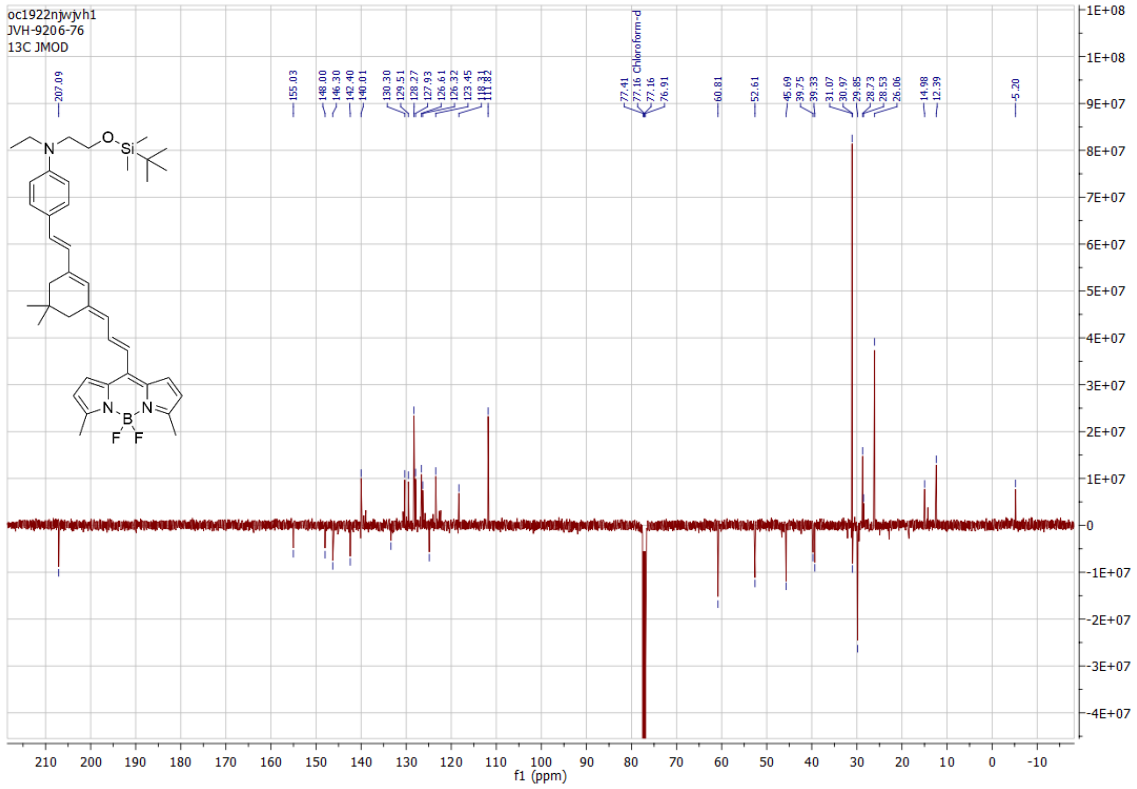

*Appendix 96: ^{13}C NMR spectrum of N-(2-((tert-butyldimethylsilyl)oxy)ethyl)-4-((E)-2-((E)-3-((E)-3-(5,5-difluoro-3,7-dimethyl-5H-4λ⁴,5λ⁴-dipyrrolo[1,2-c:2',1'-f][1,3,2]diazaborinin-10-yl)allylidene)-5,5-dimethylcyclohex-1-en-1-yl)vinyl)-N-ethylaniline **94**.*

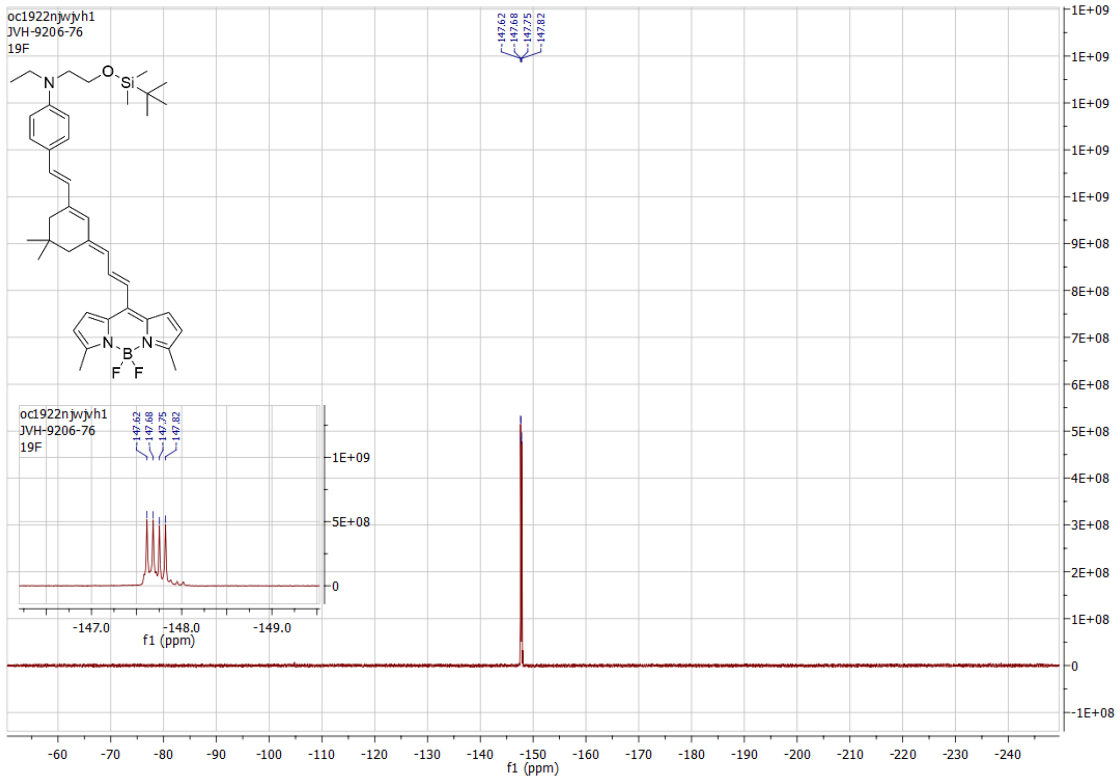

*Appendix 97: ^{19}F NMR spectrum of N-(2-((tert-butyldimethylsilyl)oxy)ethyl)-4-((E)-2-((E)-3-((E)-3-(5,5-difluoro-3,7-dimethyl-5H-4λ⁴,5λ⁴-dipyrrolo[1,2-c:2',1'-f][1,3,2]diazaborinin-10-yl)allylidene)-5,5-dimethylcyclohex-1-en-1-yl)vinyl)-N-ethylaniline **94**.*

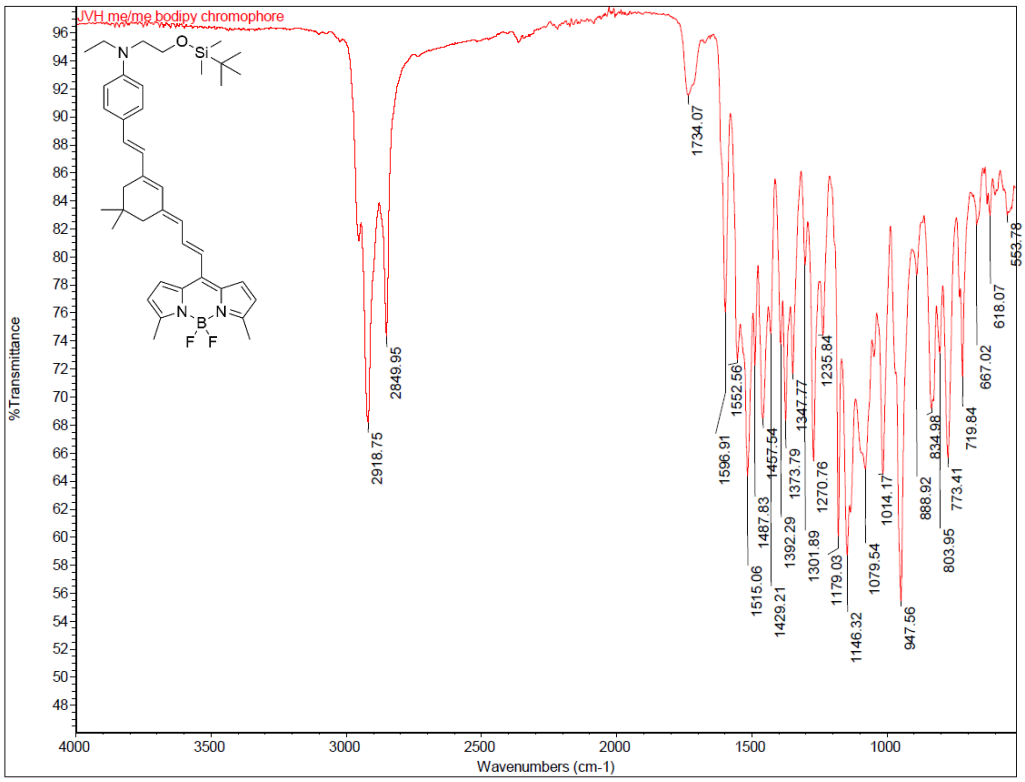

*Appendix 98: FTIR spectrum of N-(2-((tert-butyldimethylsilyl)oxy)ethyl)-4-((E)-2-((E)-3-((E)-3-(5,5-difluoro-3,7-dimethyl-5H-4λ⁴,5λ⁴-dipyrrolo[1,2-c:2',1'-f][1,3,2]diazaborinin-10-yl)allylidene)-5,5-dimethylcyclohex-1-en-1-yl)vinyl)-N-ethylaniline **94**.*

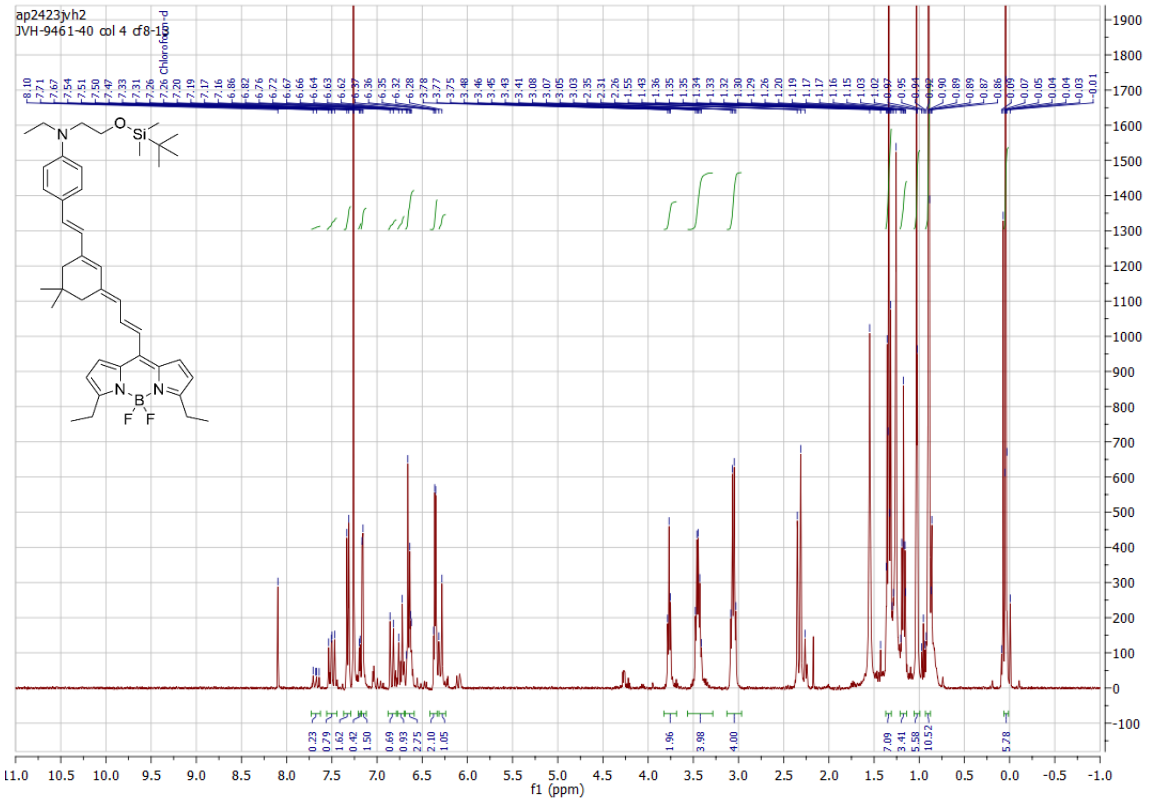

*Appendix 99: ^{1}H NMR spectrum of N-(2-((tert-butyldimethylsilyl)oxy)ethyl)-4-((E)-2-((E)-3-((E)-3-(5,5-difluoro-3,7-diethyl-5H-4λ⁴,5λ⁴-dipyrrolo[1,2-c:2',1'-f][1,3,2]diazaborinin-10-yl)allylidene)-5,5-dimethylcyclohex-1-en-1-yl)vinyl)-N-ethylaniline **104**.*

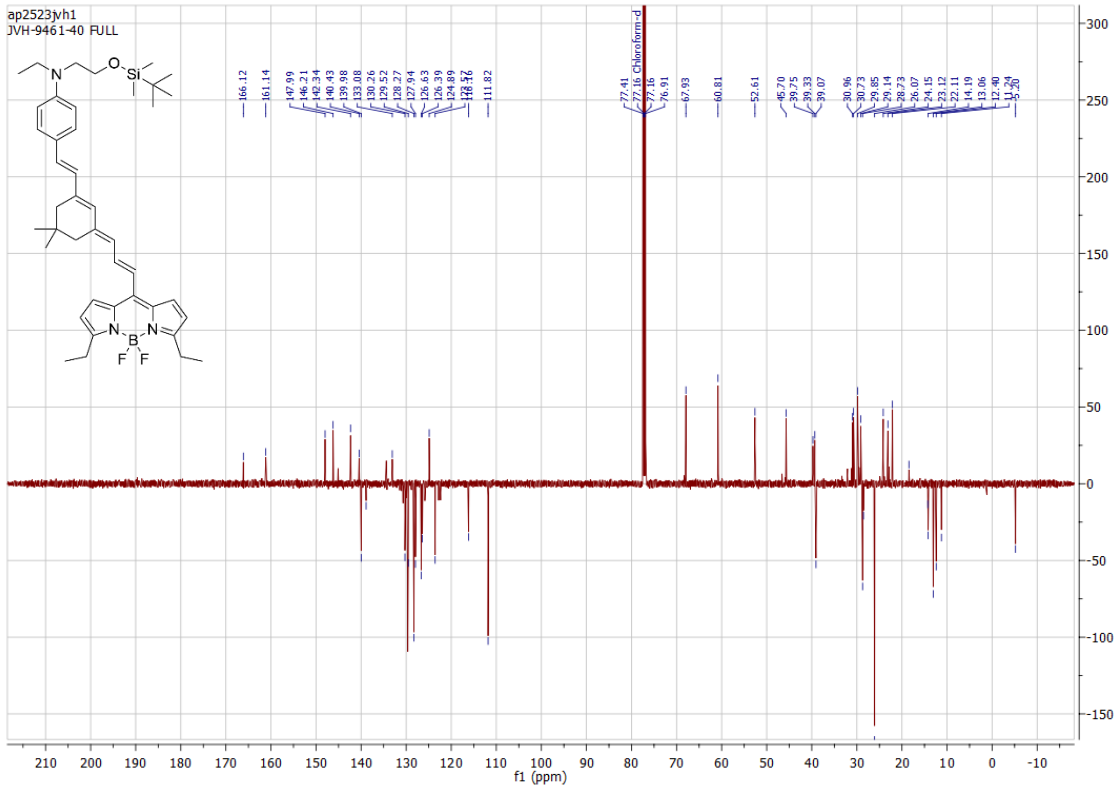

*Appendix 100: ^{13}C NMR spectrum of N-(2-((tert-butyldimethylsilyl)oxy)ethyl)-4-((E)-2-((E)-3-((E)-3-(5,5-difluoro-3,7-diethyl-5H-4λ⁴,5λ⁴-dipyrrolo[1,2-c:2',1'-f][1,3,2]diazaborinin-10-yl)allylidene)-5,5-dimethylcyclohex-1-en-1-yl)vinyl)-N-ethylaniline **104**.*

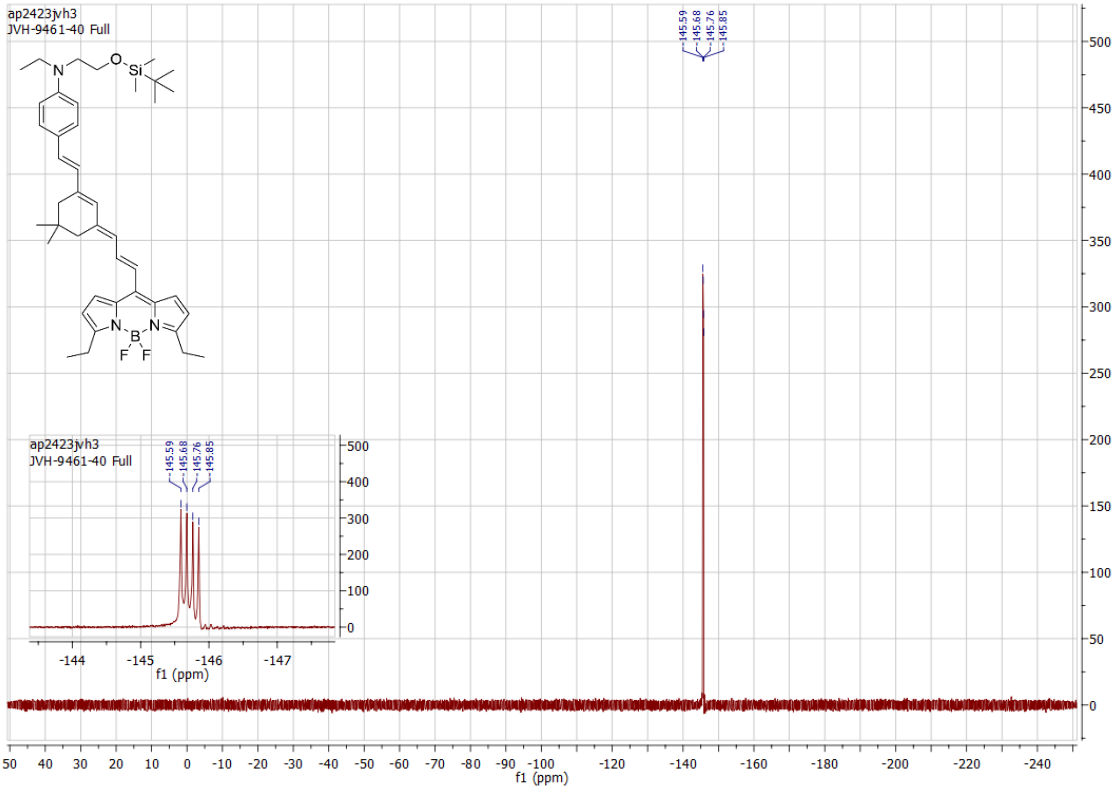

*Appendix 101: ^{19}F NMR spectrum of N-(2-((tert-butyldimethylsilyl)oxy)ethyl)-4-((E)-2-((E)-3-((E)-3-(5,5-difluoro-3,7-diethyl-5H-4λ⁴,5λ⁴-dipyrrolo[1,2-c:2',1'-f][1,3,2]diazaborinin-10-yl)allylidene)-5,5-dimethylcyclohex-1-en-1-yl)vinyl)-N-ethylaniline **104**.*

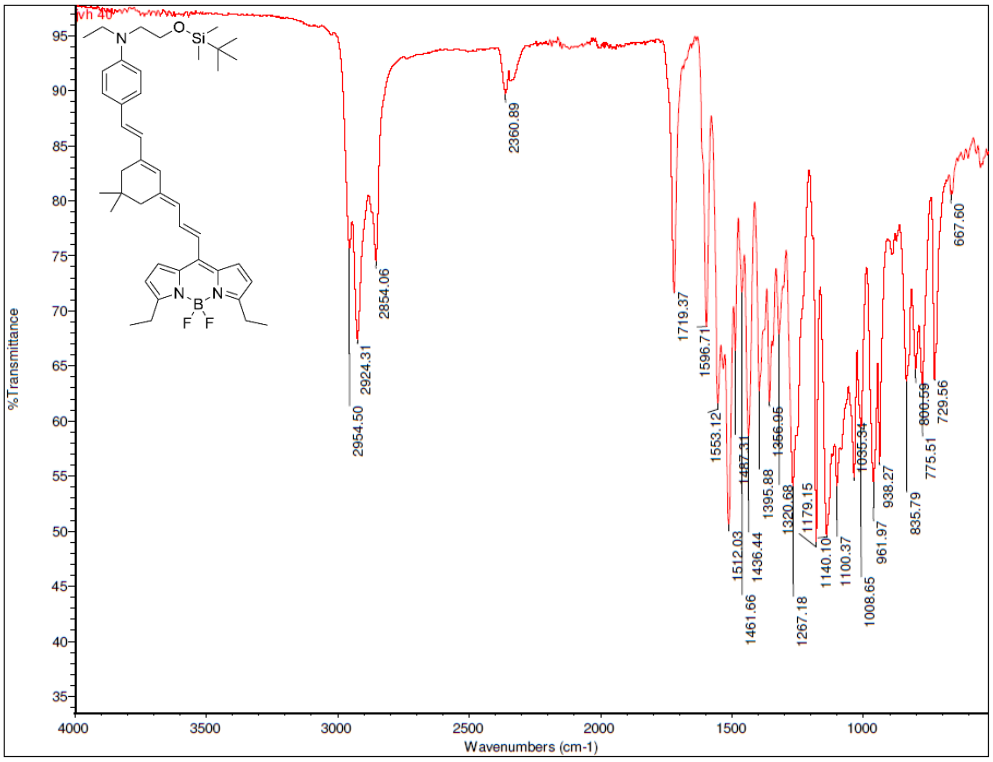

*Appendix 102: FTIR spectrum of N-(2-((tert-butyldimethylsilyl)oxy)ethyl)-4-((E)-2-((E)-3-((E)-3-(5,5-difluoro-3,7-diethyl-5H-4λ⁴,5λ⁴-dipyrrolo[1,2-c:2',1'-f][1,3,2]diazaborinin-10-yl)allylidene)-5,5-dimethylcyclohex-1-en-1-yl)vinyl)-N-ethylaniline **104**.*

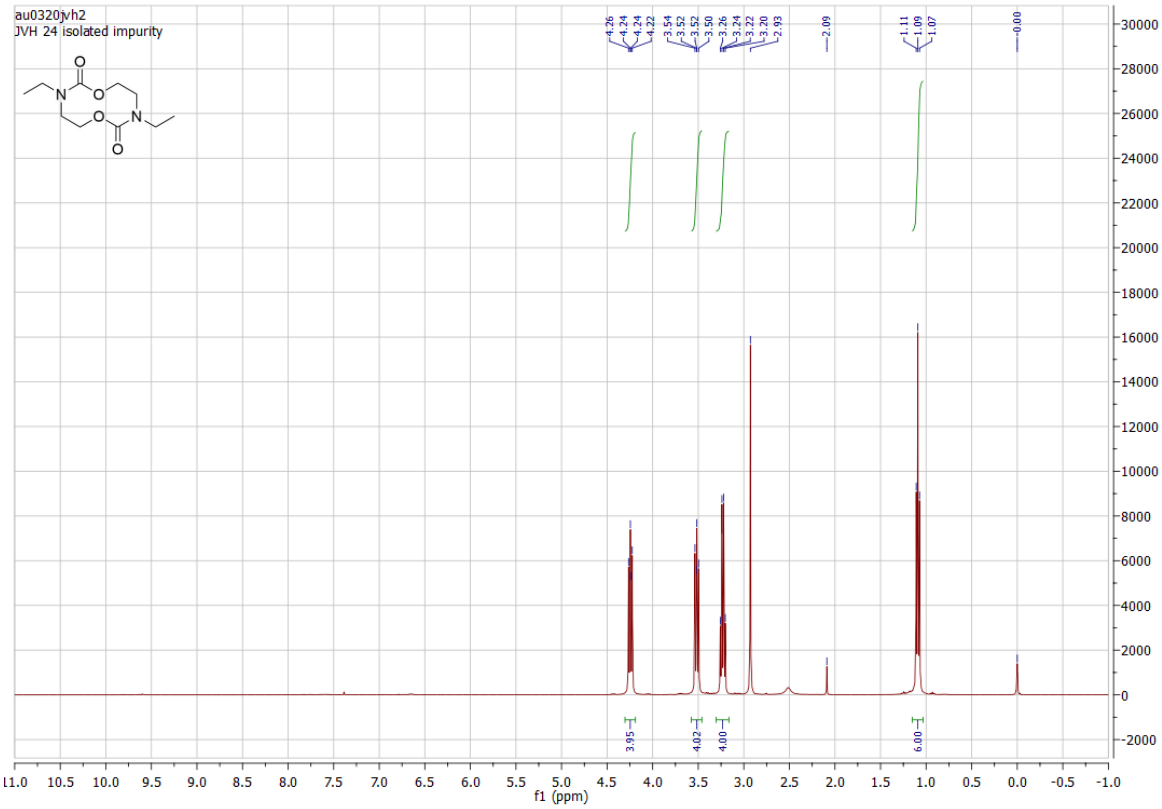

*Appendix 103: ^{1}H NMR spectrum of 3,8-diethyl-1,6,3,8-dioxadiazecane-2,7-dione **63**.*

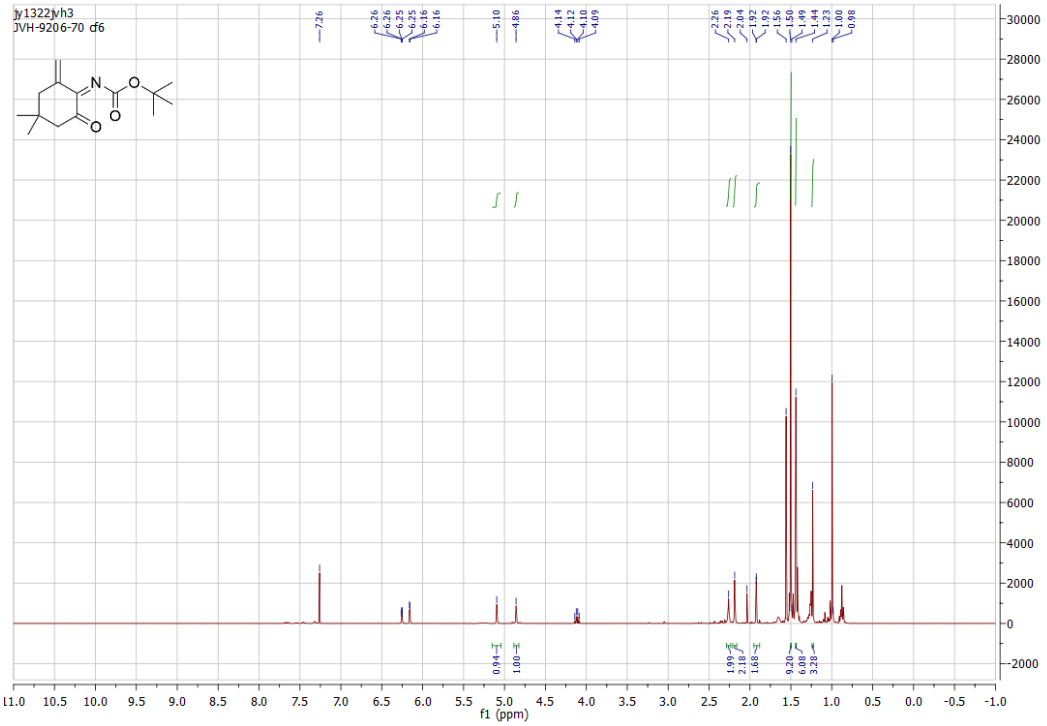

*Appendix 104: [1]H NMR spectrum of the proposed tert-butyl (Z)-(4,4-dimethyl-2-methylene-6-oxocyclohexylidene)carbamate **84**.*

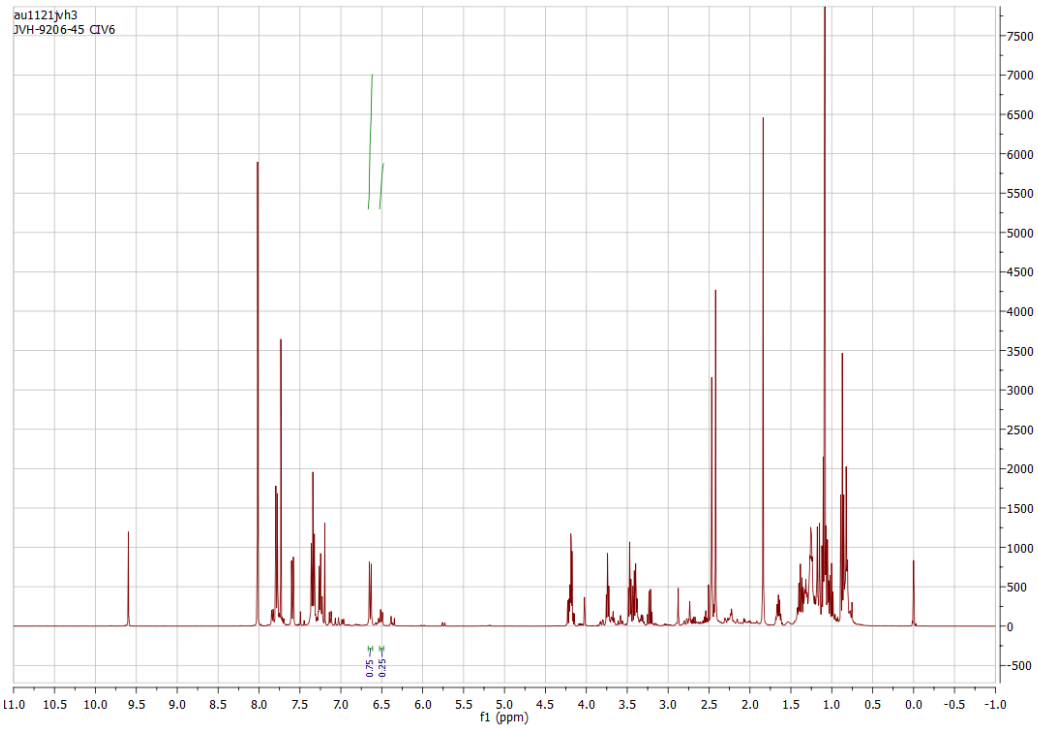

*Appendix 105: Crude [1]H NMR spectrum of the aldol-condensation reaction between 4-(ethyl(2-hydroxyethyl)amino)benzaldehyde **51** and 3,5,5-trimethyl-2-(4-phenyl-1H-1,2,3-triazol-1-yl)cyclohex-2-en-1-one **78**. Conditions **IV**: **78** (1.2 eq.) was dissolved in diethyl ether (35 mg mL^{-1}) to which NaOEt (2.2 eq.) was added and the solution was stirred for 30 minutes. **51** (1.0 eq.) and $LiClO_4$ (1.0 eq.) were added then the reaction mixture was stirred for 16 hours, overnight at 50 °C. 25% conversion to (E)-3-(4-(Ethyl(2-hydroxyethyl)amino)styryl)-5,5-dimethyl-2-(4-phenyl-1H-1,2,3-triazol-1-yl)cyclohex-2-en-1-one **80** is shown by the integration of the Ar(H)-o-N peaks of the starting material and product.*

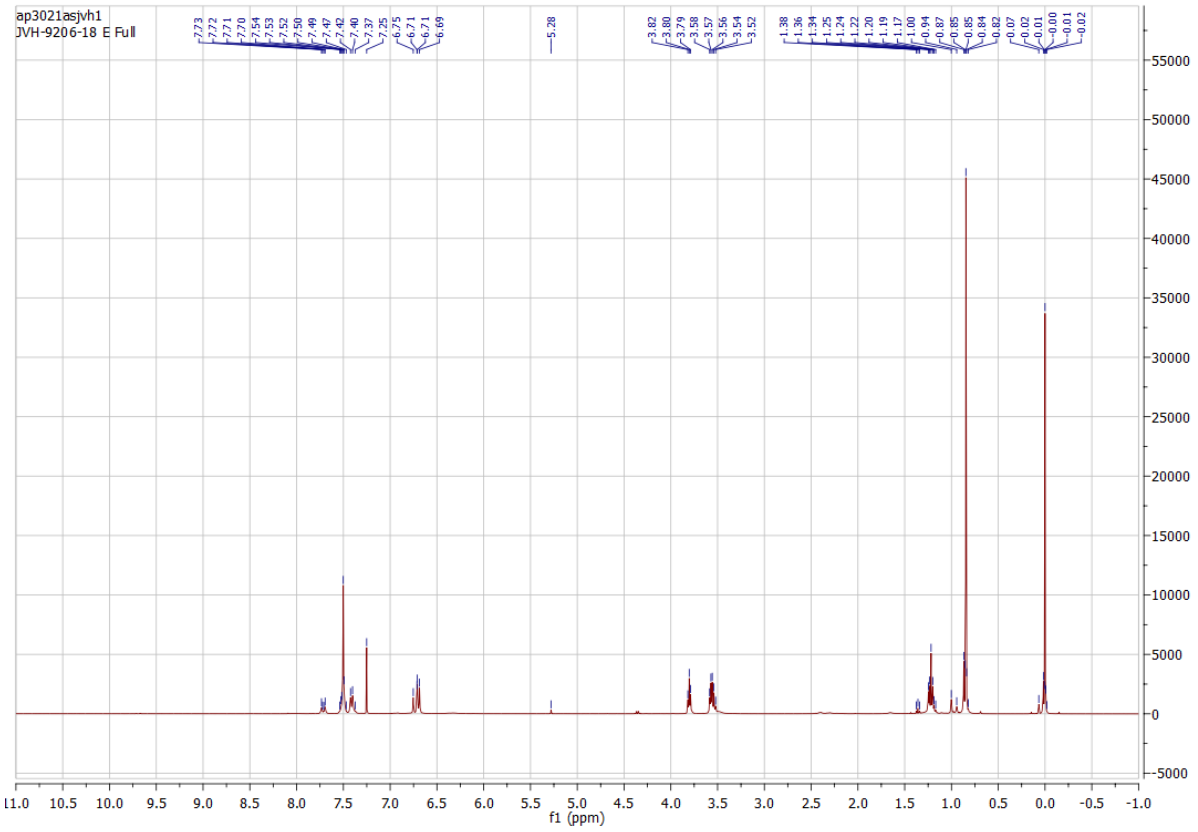

*Appendix 106: ^{1}H NMR spectrum taken of the compound eluting at Rf = 0.2 (0% ethyl acetate in CH_2Cl_2) from the condensation reaction between (E)-2-(3-((E)-4-((2-((tert-butyldimethylsilyl)oxy)ethyl)(ethyl)amino)styryl)-5,5-dimethylcyclohex-2-en-1-ylidene)acetaldehyde **53** and 2-dicyanomethylene-3-cyano-4-methyl-5-phenyl-5-trifluoromethyl-2,5-dihydrofuran **48** dissolved in ethanol at reflux for 1 hour.*